Development of a reverse genetic system for Human enterovirus 71 (HEV71) and the molecular basis of its growth phenotype and adaptation to mice

Patchara Phuektes

DVM, MVSc

This thesis is presented for the degree of Doctor of Philosophy of Murdoch University. 2009

DECLARATION

I declare that this thesis is my own account of my research and contains as its main content work which has not previously been submitted for a degree at any tertiary education institution.

……..

Patchara Phuektes

ACKNOWLEDGMENTS

I would like to give special thanks to my supervisor Professor Peter McMinn for his great support, encouragement and the knowledge he has imparted to me during the period of my study. I wish to sincerely thank my supervisor Associate Professor Stan Fenwick for his continuous support, understanding and invaluable advice. Sincerely thanks also go to Professor John Edwards and Peta Edwards for their encouragement and great advice.

Thanks for great friendship and support from members of the Division of Virology at Telethon Institute for Child Health Research; Beng Hooi, Sharon, Lara, Chee Choy and Kristy. Special thanks to Beng Hooi for your technical assistance and support, and to Sharon for making my time in the lab enjoyable. I appreciate the great assistance from the staff at the Telethon Institute for Child Health Research.

I sincerely thank Murdoch University for providing the scholarship that enables me to undertake this course.

To John Klingler, thank you for your understanding, guidance and encouragement through out the past four years of my PhD. Thanks to my colleagues at National Institute of Animal Health for your support thoughout these years. Thanks also go to Ajarn Tom for making me a better person and giving me invaluable guidance.

Finally, I especially thank to everyone in my family for their continuous love and support throughout my life.

ABSTRACT

Human enterovirus 71 (HEV71) is a member of the Human Enterovirus A species within the Family *Picornaviridae.* Since 1997, HEV71 has emerged as a major cause of epidemics of hand, foot and mouth disease (HFMD) associated with severe neurological disease in the Asia-Pacific region. At the present time, little is known about the pathogenesis of acute neurological disease caused by HEV71. The major aim of this study was to generate infectious cDNA clones of HEV71 and use them as tools for investigating the biology of HEV71 and molecular genetics of HEV71 virulence and pathogenesis.

Two infectious cDNA clones of HEV71 clinical isolates, 26M (genotype B3) and 6F (genotype C2) were successfully constructed using a low copy number plasmid vector and an appropriate bacterial host. Transfection of cDNA clones or RNA transcripts derived from these clones produced infectious viruses. Phenotypic characterisation of clone-derived viruses (CDV-26M and CDV-6F) was performed, and CDV-26M and CDV-6F were found to have indistinguishable phenotypes compared to their wild type viruses.

Strains HEV71-26M and HEV71-6F were found to have distinct cell culture growth phenotypes. To identify the genome regions responsible for the growth phenotypes of the two strains a series of chimeric viruses were constructed by exchanging the 5′ untranslated region (5′ UTR), structural protein (P1), and nonstructural protein (P2 and P3) gene regions using infectious cDNA clones of both virus strains. Analysis of reciprocal virus chimeras revealed that the 5′ UTR of both strains were compatible but not responsible for the observed phenotypes. Both the P1 and P2-P3 genome

regions influence the HEV71 growth phenotype in cell culture, phenotype expression is dependent on specific P1/P2-P3 combinations and is not reciprocal.

In the previous study, in order to investigate the pathogenesis of HEV71 infection, a mouse HEV71 model was developed using a mouse-adapted variant of HEV71-26M. Mouse-adapted strain MP-26M caused fore- and/or hindlimb paralysis in mice, whereas HEV71-26M-infected mice did not develop clinical signs of infection at any virus dose or route of inoculation tested. In this study, the molecular basis of mouse adaptation by HEV71 was identified. Nucleotide sequence analysis of HEV71-26M and MP-26M revealed three point mutations in the open reading frame, each resulting in an amino acid substitution in the VP1, VP2 and 2C proteins; no mutations were identified in the untranslated regions of the genome. To determine which of the three amino acid mutations were responsible for the adaptation and virulence of HEV71-26M in mice, recombinant cDNA clones containing one, or a combination of two or three mutations, were constructed. Mouse virulence assays of the mutated viruses clearly demonstrated that a non-conservative amino acid substitution ($G^{710}\rightarrow E$) in the capsid protein VP1 alone was sufficient to confer the mouse virulence phenotype on HEV71.

In addition, a mouse oral infection model was established in this study. Oral inoculation with the mouse-adapted HEV71 virus, MP-26M, induced fore-or hindlimb paralysis in newborn mice in an age- and dose-dependent manner. As oral transmission is the natural route of HEV71 infection, this murine HEV71 oral infection model will provide a suitable tool for studying HEV71 pathogenesis, for

defining neurological determinants, and for testing vaccine efficacy and immunogenicity in the future.

TABLE OF CONTENTS

CHAPTER TWO: MATERIALS AND METHODS

LIST OF FIGURES

CHAPTER FOUR

CHAPTER FIVE

CHAPTER 6

LIST OF TABLES

CHAPTER THREE

CHAPTER FOUR

CHAPTER FIVE

CHAPTER SIX

PUBLICATIONS AND PRESENTATIONS

PUBLICATIONS

1. Chua, B. H., **P. Phuektes**, S. A. Sanders, P. K. Nicholls, and P. C. McMinn. 2008. The molecular basis of mouse adaptation by human enterovirus 71. Journal of General Virology 89:1622-1632.

PRESENTATIONS

1. Chua, B. H., **P. Phuektes**, S. A. Sanders, and P. C. McMinn. 2007. The molecular basis of mouse adaptation by human enterovirus 71. The 4th Australian Virology Conference, Queensland, Australia

2. **Phuektes, P**., B. H. Chua, Hurrelbrick, R., C. C. Kok, and P. C. McMinn. 2006. Investigating the pathogenesis of enterovirus 71 infection using a reverse genetics approach and a small animal model. The 7th Asia-Pacific Conference for Medical Virology, Delhi, India

3. **Phuektes, P**., B. H. Chua, S. A. Sanders, C. C. Kok, and P. C. McMinn. 2005. Oral infection with enterovirus 71 causes neurological disease mimicking human infection in a mouse model. The 3rd Australian Virology Conference, Melbourne, Australia

ABBREVIATIONS

β-gal	betagalactosidase
µF	microfarad
µg	microgram
µL	microlitre
µM	micromolar
µm	micrometre
Ω	ohm
%	percent
ºC	degree Celsius
3′ UTR	3′ untranslated region
5′ UTR	5′ untranslated region
xg	acceleration due to gravity
aa	amino acid
A	adenine
AFP	acute flaccid virus
AMV	avian myeloblastosis virus
ATCC	American Type Culture Collection
ATP	adenosine triphosphate
bp	base pairs
BEV	bovine enterovirus
BGS	bovine growth serum
BSA	bovine serum albumin
C	cytosine
CAV	Coxsackievirus A
CBV	Coxsackievirus B
cDNA	complementary deoxyribonucleic acid
CDV	clone-derived virus
CHO	Chinese hamster ovarian cells
cm	centimetre
CNS	central nervous system
CMV	cytomegalovirus
COS-7	SV40 transformed African green monkey kidney cells

CPE	cytopathic effects
CSF	cerebrospinal fluid
dH_2O	distilled water
ddH_2O	double deionised water
DEPC	diethyl pyrocarbonate
DMEM	Dulbecco's Modified Eagles Medium
DNA	deoxyribonucleic acid
dNTPs	deoxynucleotide triphosphates
DTT	Dithiothreitol
E	echovirus
E. coli	*Escherichia coli*
EDTA	ethylenediamine tetra-acetic acid
eIF	eukaryotic initiation factor
EMCV	encephalomyocarditis virus
et al.	and others
FCS	foetal calf serum
FITC	fluorescein isothiocyanate
FMDV	foot-and-mouth disease virus
g	gram
G	guanine
h	hour
HBSS	Hank's balance salt solution
HD_{50}	median humane end point
HEV	human enterovirus
HEV71	human enterovirus 71
HEV-A	human enterovirus group A
HEV-B	human enterovirus group B
HEV-C	human enterovirus group C
HEV-D	human enterovirus group D
HFMD	hand, foot and mouth disease
hnRNP C	heterogeneous nuclear ribonucleoprotein C
HRV	human rhinovirus
i.c.	intracerebral
IFA	immunofluorescence assay

IFN	interferon
Ig	immunoglobulin
IL	interleukin
i.m.	intramuscular
i.p.	intraperitoneal
IRES	internal ribosome entry site
i.s.	intraspinal
i.v.	intravenous
IVT	*in vitro* transcription
kb	kilobase pairs
kDa	kiloDalton
kg	kilogram
kV	kilovolt
L	litre
LD_{50}	median lethal dose
M	molar
mAb	monoclonal antibody
mg	milligram
min	minute
mL	millilitre
mM	millimolar
MOI	multiplicity of infection
MOPS	3-N-morpholinopropane sulfonate
mRNA	messenger ribonucleic acid
MVE	Murray Valley encephalitis virus
NB41A3	mouse neuroblastoma cells
ND	not determined
ng	nanogram
NK	natural killer cells
nm	nanometre
nt	nucleotide
NTPase	nucleoside triphosphate hydrolase
OD	optical density
ORF	open reading frame

pAb	polyclonal antibody
PABP	poly (A) binding protein
PBS	phosphate buffered saline
PCBP	poly (C) binding protein
PCR	polymerase chain reaction
PDB	protein databank file
PE	pulmonary edema
PEG	polyethylene glycol
PFU	plaque forming units
pmol	picomole
PTB	polypyrimidine tract-binding protein
PV	poliovirus
PVR	poliovirus receptor
Poly (A)	polyadenylated
RD	rhabdomyosarcoma cells
RE	restriction endonuclease
RNA	ribonucleic acid
RNAse	ribonuclease
rpm	revolutions per minute
RT	reverse transcription
RT	room temperature
SAM	S-adenosylmethionine
s.c.	subcutaneous
SDS	sodium dodecyl sulphate
s	second
T	Thymine
TAE	Tris acetate EDTA buffer
$TCID_{50}$	median tissue culture infectious dose
ts	temperature-sensitive
tr	temperature-resistant
U	Uracil
U	unit
USA	United States of America
UV	ultraviolet

Vero	African green monkey kidney cells
VP	virus protein
VPg	viral protein genome-linked
v/v	volume for volume
w/v	weight for volume
X-gal	5-bromo-4-chloro-3-indolyl-β-D-galactopyranoside

CHAPTER ONE

LITERATURE REVIEW

1.1 The Picornaviridae and the genus enterovirus

1.1.1 Classification

The *Picornaviridae* is a family of small, non-enveloped viruses with a single-strand, positive-sense RNA genome. Based on biological and genetic properties, this virus family is classified into eight genera: enterovirus, apthovirus, cardiovirus, hepatovirus, parechovirus, erbovirus, kobuvirus and teschovirus, four of which contain human pathogens including the Genus Enterovirus, Parechovirus, Kobuvirus and Hepatovirus (Fauquet et al., 2005, Pallansch & Roos, 2007) (http://www.picornaviridae.com). Human enterovirus 71 (HEV71), the subject of this thesis, is classified as a member of the Genus Enterovirus.

Enteroviruses are acid stable, retaining activity at pH 3 or lower, and replicate primarily in the enteric tract (Racaniello, 2007). The Genus Enterovirus consists of more than 100 serotypes (Hyypia et al., 1997, Pallansch & Roos, 2007) (http://www.picornaviridae.com). Of these, approximately 95 serotypes are human pathogens, with a few serotypes infecting cattle, swine and non-human primates (Hyypia et al., 1997, Pallansch & Roos, 2007) (http://www.picornaviridae.com). Human enteroviruses were originally classified as poliovirus (PV), coxsackievirus A (CAV), coxsackievirus B (CBV) and echovirus (E) on the basis of human disease and their pathogenicity in experimental animals (Hyypia et al., 1997, Pallansch & Roos, 2007). Polioviruses 1-3, the first human enteroviruses to be identified, are the causative agents of paralytic poliomyelitis in humans. Polioviruses only infect non-

human primates causing disease resembling human poliomyelitis (Pallansch & Roos, 2007). Coxsackieviruses, first isolated from the faeces of two children with paralysis during a poliomyelitis outbreak, are classified into subgroups A and B based on characteristic diseases produced in newborn mice; CAVs cause flaccid paralysis and CBVs cause spastic paralysis (Hyypia et al., 1997, Pallansch & Roos, 2007). This difference is due to the replication of CAVs in skeletal and heart muscle of infected mice while CBV infections involve a wide range of tissues, including the central nervous system (Hyypia et al., 1997, Pallansch & Roos, 2007). Echoviruses were first isolated after the introduction of cell culture techniques (Robbins et al., 1951). These viruses are unable to infect newborn mice and, at the time of their discovery, the association of the viruses with human diseases was not known (Pallansch & Roos, 2007). The designated name ECHO stands for enteric, cytopathogenic, human, orphan, which refers to the lack of disease association when echoviruses were first identified (Pallansch & Roos, 2007). Individual strains of human enteroviruses were further classified into serotypes by cross-neutralization or cross-complement fixation, and serial numbers were then given according to the order of isolation of serologically distinct isolates (Pallansch & Roos, 2007). There are three serotypes of poliovirus (PV1-3), twenty-one serotypes of coxsackievirus A (CAV 1-14, 16-17, 19-22 and 24), six serotypes of coxsackievirus B (CBV 1-6) and twenty eight serotypes of echovirus (E1-7, 9, 11-21, 24-27, 29-33) (Pallansch & Roos, 2007).

However, there were frequent difficulties in assigning enteroviruses into subgroups based on their pathogenesis in experimental animals and by serotypic differentiation. Thus, the more recent isolates of human enteroviruses have been named with a

system of consecutive numbers: EV68, EV69, EV70 and EV71 (Melnick et al., 1974). Currently, molecular methods have been used for identification of new enterovirus isolates that are untypable using existing neutralizing antisera (Oberste et al., 1999, Oberste et al., 2005, Oberste et al., 2007, Oberste et al., 2001). This method is based on a comparison of nucleotide and deduced amino acid sequences of the complete capsid protein VP1 and/or the capsid P1 region (Oberste et al., 1999, Oberste et al., 2005). VP1 and P1 sequences contain serotype-specific information that can be used for enterovirus identification (Oberste et al., 1999, Oberste et al., 2005). The numbered enteroviruses EV73-EV101 were identified based on this method (Norder et al., 2003, Oberste et al., 2005, Oberste et al., 2007, Oberste et al., 2001).

Human enteroviruses have been classified into four species: Human enteroviruses A-D (HEV-A-D) based primarily on genetic properties (Fauquet et al., 2005, Hyypia et al., 1997, Pallansch & Roos, 2007). Amino acid sequence comparison of the capsid protein P1 and individual proteins spanning the whole coding region leads to grouping of four genetic clusters among human enteroviruses (Pallansch & Roos, 2007). HEV71 is classified as a member of the species HEV-A. The biological significance of the current clustering is still unknown. An overview of the classification of human enteroviruses is outlined in Table 1.1.

1.1.2 Medical significance of human enteroviruses

Enterovirus infections are very common and cause a high total number of cases of disease worldwide, with a billion or more annually, and an estimated 50 million annually in the USA alone (Pallansch & Roos, 2007). Although most enterovirus

Table 1.1 Current genetic classification of human enterovirus

Species	Number of Serotypes	Name of Members
Human enterovirus A	17	Coxsackieviruses A2-A8, A10, A12, A14, A16, Human enteroviruses 71, 76, 89-92
Human enterovirus B	56	Coxsackieviruses A9, Coxsackieviruses B1-B6, Echoviruses 1-7, 9, 11-21, 24-27, 29-33, Human enteroviruses 69, 73-75, 77, 78, 79-88, 93, 97, 98, 100, 101
Human enterovirus C	15	Polioviruses 1-3, Coxsackieviruses A1, 11, 13, 17, 19-22, Human enteroviruses 95, 96, 99
Human enterovirus D	3	Human enteroviruses 68, 70, 94

infections are asymptomatic, enteroviruses can cause a wide range of acute, mild or severe diseases, including mild upper respiratory illness (common cold), non-specific febrile illness, pleurodynia, aseptic meningitis, encephalitis, acute flaccid paralysis (paralytic poliomyelitis), myocarditis, neonatal sepsis-like disease, acute haemorrhagic conjunctivitis, herpangina and febrile rash (hand, foot and mouth disease) (Pallansch & Roos, 2007). Moreover, enteroviruses may cause severe chronic diseases, including myocarditis and dilated cardiomyopathy, type 1 diabetes mellitus and neuromuscular diseases (Pallansch & Roos, 2007). Apart from the especially devastating polioviruses, there are no vaccines available for protection against enteroviruses.

1.1.3 Virion Morphology

Enterovirus virions are small, spherical in shape and have a diameter of about 30 nm (Racaniello, 2007). Virus particles are composed of a protein shell, with no lipid envelope, surrounding the RNA genome (Racaniello, 2007). The viral capsid is icosahedral in symmetry and composed of 60 identical units (protomers). Each protomer consists of one copy of four structural proteins: viral proteins 1 through 4 (VP1-VP4). Three of these proteins, VP1-VP3, form the external surface of the protein shell; VP4, in conjunction with the amino termini of VP1 and VP2, forms an inner surface (Hogle, 2002, Racaniello, 2007). The three external surface proteins have no amino acid sequence homology, but nevertheless share a similar folding pattern of a wedge-shape structure made up of an eight-stranded antiparallel β-barrel with loops connecting the strands (Hogle, 2002, Racaniello, 2007). The carboxyl termini of these proteins are located on the virion surface, and the amino termini are located on the inner surface (Hogle, 2002, Racaniello, 2007). A protein network

formed by the amino termini of these proteins and VP4 contributes significantly to the stability of virions.

The high resolution structures of some picornaviruses, including PV and human rhinovirus type 14 (HRV14) were determined by X-ray crystallography and cryoelectron microscopy (Hogle et al., 1985, Rossmann et al., 1985). It has been shown that the surface of PV has a prominent star-shaped mesa at the 5-fold axis of symmetry, surrounded by a deep canyon and another protrusion at the 3-fold axis (Hogle et al., 1985, Rossmann et al., 1985). The canyon has been identified as the receptor-binding site of PV (Belnap et al., 2000, He et al., 2000). A schematic diagram of the picornavirus virion is shown in Figure 1.1. To date, the high resolution structure of HEV71 remains undetermined.

1.1.4 Genomic structure

The genome of enteroviruses is a single-stranded, polyadenylated, positive-sense RNA of approximately 7-8 kb in size. Genomic RNA is infectious, and the positive-sense RNA directly encodes the viral proteins necessary for RNA replication. The RNA genome is covalently linked to a virally encoded 22-amino acid protein, VPg, at the 5′ terminus of the genome. The viral genome contains a single open reading frame (ORF), encoding a polyprotein of around 2,200 amino acids, which is co- or post-translationally cleaved by viral proteases to yield the mature viral proteins. The polyprotein is divided into three regions, P1, P2 and P3. The P1 region encodes four viral structural proteins, VP1-VP4. The P2 and P3 regions encode seven non-structural proteins, 2A-C and 3A-D, involved in RNA replication, polyprotein processing and shut-down of host cell protein synthesis. A common coding order of

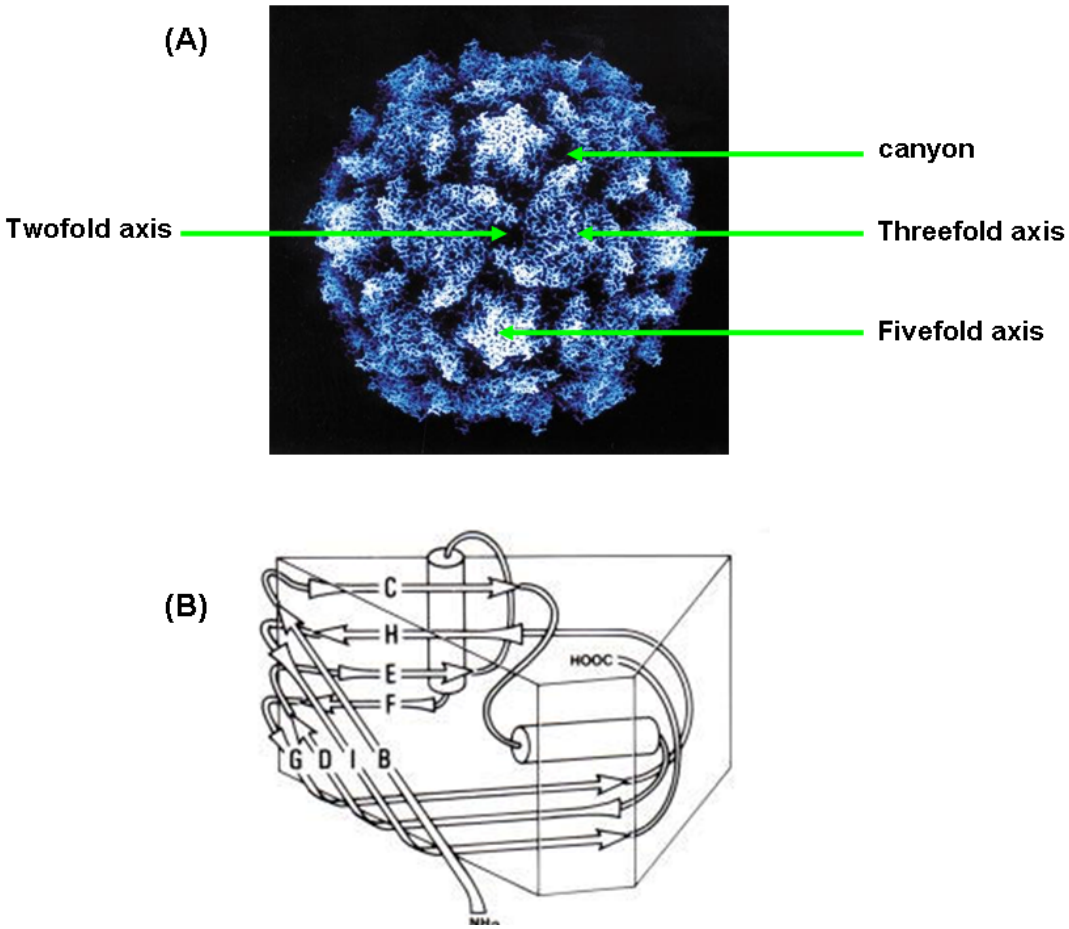

Figure 1.1 Structure of enterovirus. (A) High resolution x-ray crystallographic structure of the Mahoney strain of type 1, poliovirus. The star-shaped mesas at the five-fold axis, the three-bladed propellers at the threefold axis, two-fold axis, and the deep canyon are shown. **(B)** Schematic diagram representation of the core structure eight-stranded beta-sandwich shared by VP1, VP2 and VP3. Adapted from Racaniello 2007.

enterovirus proteins are the structural genes VP4, VP2, VP3 and VP1, followed by the non-structural genes 2A, 2B, 2C, 3A, 3B, 3C and 3D.

The ORF is preceded by a 5′ untranslated region (5′ UTR), and followed by a 3′ untranslated region (3′ UTR), and a poly-A tract. The 5′ UTR of enteroviruses is relatively long, approximately 700-800 nucleotides in length (10% of the genome), and extensively structured. It contains a cloverleaf structure followed by an internal ribosomal entry site (IRES) element. The 5′ cloverleaf plays an essential role in the initiation of negative-strand RNA synthesis (Andino et al., 1990, Parsley et al., 1997), while the IRES element has a role in the initiation of translation (Ehrenfeld & Teterina, 2002). The 3′ UTR is also structured but much shorter than the 5′ UTR and is approximately 50-90 nucleotides in length (1.5% of the genome). The 3′ UTR is required for efficient initiation of negative-strand RNA synthesis (Todd et al., 1997). The genome organization of enteroviruses is shown in Figure 1.2.

1.1.5 Replication cycle

Enterovirus replication takes place in the cytoplasm of the host cell. The first step of virus replication is attachment of the virus to its cell receptor, a molecule on the surface of the cell to which the virus specifically binds and uses for gaining entry into the cell. Binding to the cell receptor leads to capsid structure reorganization, resulting in uncoating and release of the RNA genome into the cytoplasm. The positive-stranded viral RNA genome is then used as a template for translation of viral proteins essential for genome replication and the production of new virus particles. The first step of genome replication is the synthesis of a negative-stranded intermediate from the positive-stranded RNA template, followed by the production

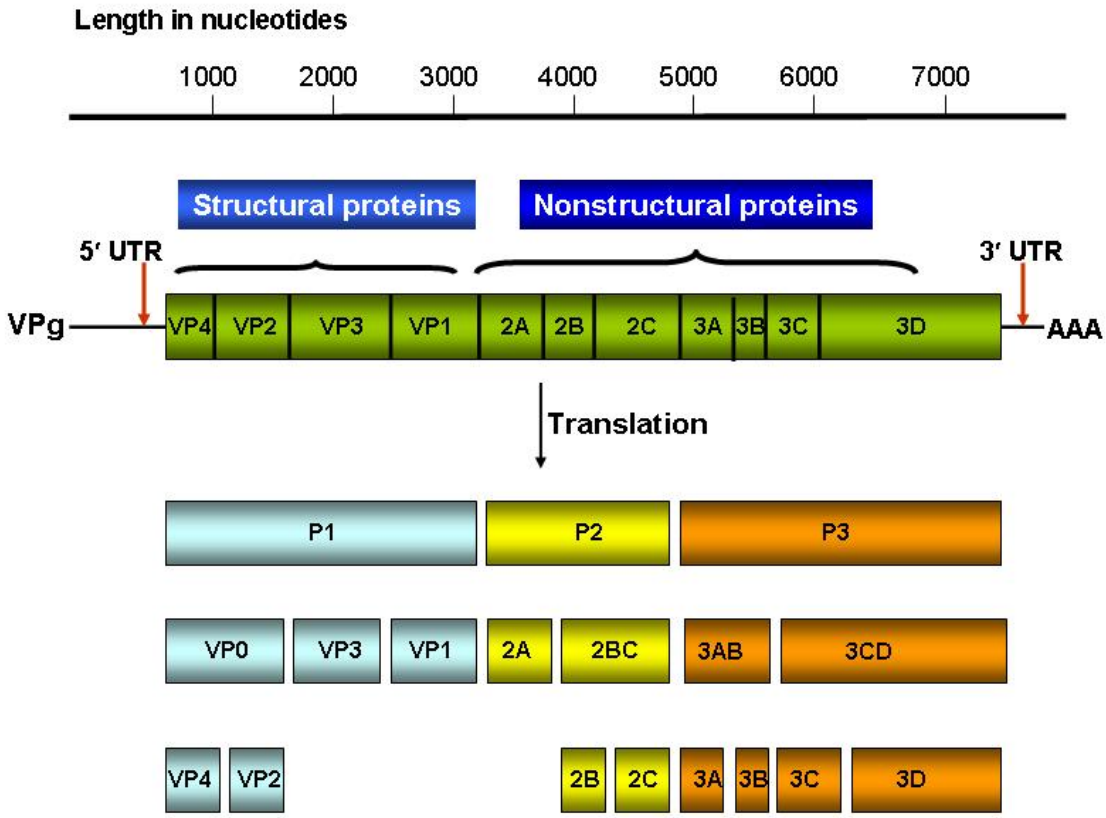

Figure 1.2 Genome structure of enterovirus. The VPg is covalently linked to the 5′ end. A single ORF is preceded by a 5′ untranslated region (5′ UTR), and followed by a 3′ untranslated region (3′ UTR), and a poly-A tract. Following translation into a single polyprotein, the coding region is cleaved into P1, P2 and P3 regions. Intermediate and final cleavage products are shown. (Adapted from Racaniello, 2007).

of a positive-stranded RNA genome. The newly synthesized capsid proteins and positive-stranded RNA are assembled to form the mature virion. The time required for a single replication cycle varies from 5 to 10 h (Racaniello, 2007). Enteroviruses generally generate cytopathic effects and are cytocidal for vertebrate cells (Racaniello, 2007). The replication cycle of enteroviruses is shown in Figure 1.3.

1.1.5.1 Entry of virus into cells

Enterovirus infection is initiated when the virus attaches to a specific receptor on the surface of host cells. The receptors for a number of enteroviruses have been identified (Evans & Almond, 1998, Mendelsohn et al., 1989, Racaniello, 2007, Shafren et al., 1995, Shafren et al., 1997, Triantafilou et al., 2002, Triantafilou et al., 1999). A broad range of cellular receptors are used by members of enteroviruses, and some are shared among the members (summarized in Table 1.2). Some enteroviruses, such as PV, utilize only one receptor for both attachment and entry to the cells (Mendelsohn et al., 1989). By contrast, many enteroviruses, such as CAV12, have been shown to use a cellular receptor only for virus attachment, requiring one or more accessory receptors for entry into cells (Shafren et al., 1997).

After attachment to its respective receptor, the virus undergoes receptor-mediated conformational transition. Binding of PV to the poliovirus receptor (PVR; CD155) at physiological temperature triggers an irreversible conformation change in the native virion (160S particle), resulting in the production of an altered (A) particle (135S particle) (De Sena & Mandel, 1977, Fenwick & Cooper, 1962, Gomez Yafal et al., 1993). The A particle has externalized myristoylated capsid protein VP4 and the N-terminus of the capsid protein VP1 (Fricks & Hogle, 1990). Then, the externalized peptides insert into membranes and form channels and pores that

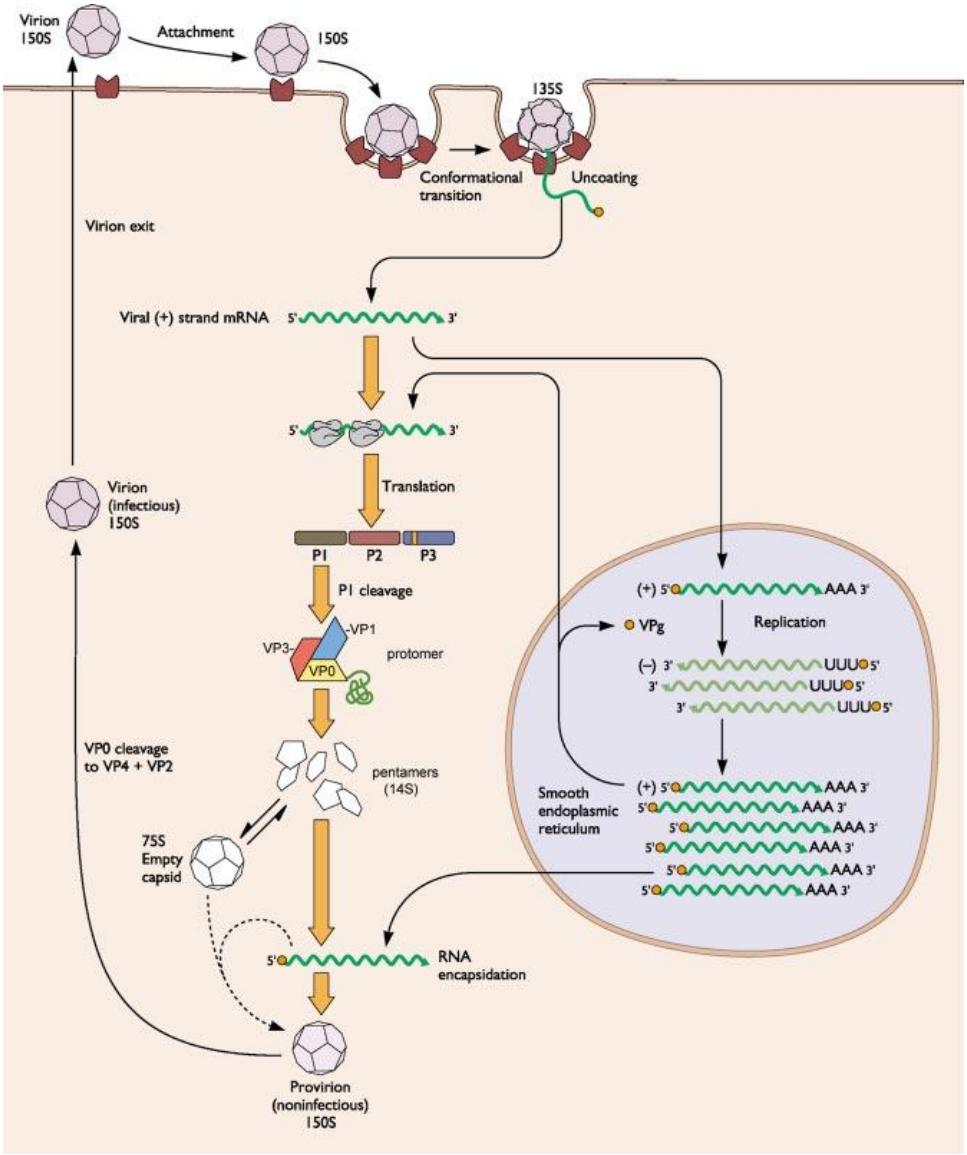

Figure 1.3 Schematic diagram of enterovirus life cycle. Enterovirus infection is initiated when the virus attaches to its cell receptor, leading to conformational changes in the virus that facilitates release of the RNA genome into the cytoplasm and subsequent translation and replication. Taken from Hogle, 2002.

Table 1.2 Cell receptors utilized by members of human enteroviruses[a]

Species	Serotype	Receptor	Type of Receptor	Co-receptor
Human enterovirus A	Coxsackieviruses A2-A8, 10, 12, 14, 16	Unknown		
	Human enteroviruses 71, 76, 89-92	Unknown		
Human enterovirus B	Coxsackievirus A9	$\alpha_v\beta3$, $\alpha_v\beta6$	Integrin	β_2-m, GRP78
	Coxsackieviruses B1-B6	CAR	Ig-like	ND
	Coxsackieviruses B1, 3, 5	DAF(CD55)	SCR-like	$\alpha_v\beta6$-Integrin
	Echoviruses 1, 8	$\alpha_2\beta_1$ (Vla-2)	Integrin	ND
	Echoviruses 3, 6, 7, 11-13, 20, 21, 24, 29, 33	DAF(CD55)	SCR-like	β_2-m, CD59
	Echoviruses 6, 9 (cell culture adapted)	Heparin sulfate	GAG	ND
	Echovirus 22	$\alpha_v\beta3$ (Vibronectin)	Integrin	ND
Human enterovirus C	Polioviruses 1-3	PVR (CD155)	Ig-like	ND
	Coxsackieviruses A13, 18, 21	ICAM-1	Ig-like	ND
	Coxsackievirus A21	DAF(CD55)	SCR-like	ICAM-1
Human enterovirus D	Human enterovirus 70	DAF(CD55)	SCR-like	ND

ND, not determined; β_2-m, β_2-microglobulin; GRP78, glucose related 78kDa protein; CAR, Coxsackievirus-Adenovirus receptor; Ig, immunoglobulin; DAF, Decay-accelerating factor; SCR, short consensus repeat; GAG, glycosaminoglycan; PVR, Poliovirus receptor; ICAM-1, intracellular adhesion molecule 1. [a]Adapted from Racaniello, 2007; Evan and Almond, 1998; Triantafilou *et al*., 1999 and 2002; Shafren *et al*., 1995 and 1997.

facilitate translocation of the viral RNA genome across the plasma or vesicle membrane into the cytoplasm (Fricks & Hogle, 1990, Tosteson & Chow, 1997). An altered form of the virus that has lost its RNA sediments at 80S, called the 80S particle. The trigger for switching from 135S particle to the 80S empty particle is not clearly known.

Although enterovirus cell entry pathways have been studied extensively, particularly in PV, the mechanisms by which enteroviruses gain entry into host cells remains unclear. Earlier studies suggested that PV entered cells via clathrin-mediated endocytosis and the viral uncoating was triggered by acidification of early endosomes (Madshus et al., 1984, Zeichhardt et al., 1987, Zeichhardt et al., 1985). By contrast, subsequent studies showed that blocking the acidification of endosomes with bafilomycin A1 and inhibition of dynamin, a GTPase required for internalization of clathin-coated vesicles, had no effect on PV replication (DeTulleo & Kirchhausen, 1998, Perez & Carrasco, 1993). These findings suggest that clathrin-mediated endocytosis is not essential for poliovirus entry.

Two most recent studies have characterised the PV cell entry pathway using both live-cell imaging and biochemical assays. Brandenburg et al. (2007) found that PV entered the cell by a clatrin-, caveolin-, flotillin-, and microtubule- independent, but tyrosine kinase- and actin-dependent, endocytosis mechanism after binding to receptors on the cell surface. After internalization, viral uncoating occurred rapidly within the cell, and in vesicles located very close (within 100-200 nm) to the plasma membrane. RNA release required energy, an actin skeleton, and the activity of tyrosine kinases. Interestingly, Coyne et al. (2007) found that PV entered human

brain microvascular endothelial cells (HBMECs) by dynamin-dependent caveolar endocytosis. Virus entry was promoted by interaction of PV with PVR that induced intracellular signaling events. PVR-induced signals led to rearrangement of the actin cytoskeleton, and activation of tyrosine kinase and phosphatase essential for dynamin dependent caveolar entry. Taken together, these findings suggest that PV enters different cells by different mechanisms, and utilizes cell's signaling pathways during virus entry.

To date, the cellular receptor of HEV71 has not yet been identified and the mechanisms by which HEV71 enters the cells is for the most part unknown. It has been found that the receptor utilized by HEV71 has a major protein component, and HEV71 possibly enters the cells by a caveolin-mediated endocytosis (Herrero, 2007).

1.1.5.2 RNA replication

After entry into the host cell, the plus stranded RNA genome of enteroviruses must first be translated to provide viral proteins that are necessary for RNA synthesis. The replication strategy involves transcription of the positive-stranded RNA genome into a negative-stranded RNA which is then used as a template for new genomic positive-stranded RNA. The site of synthesis of enterovirus RNA is in the cytoplasm of the host cell (Detjen et al., 1978). Enterovirus RNA replication requires membranous vesicles derived from membranes of endoplasmic reticulum and the Golgi complex (Bienz et al., 1992, Schlegel et al., 1996). These membranous vesicles are induced by nonstructural proteins 2B, 2C, 2BC and 3A (Aldabe & Carrasco, 1995, Cho et al., 1994, Suhy et al., 2000). The function of the membranous vesicles in viral RNA replication is still unclear. It has been hypothesized that the membranous vesicles act as scaffold for assembly of the

replication complex and also protect the viral RNA from nucleases (Fogg et al., 2003). In addition, the membranous vesicles may act to concentrate the viral proteins at the site of RNA synthesis for an efficient RNA replication process (Fogg et al., 2003, Tershak, 1984).

Several viral and cellular factors were found to be involved in enterovirus RNA replication. These include all of the nonstructural proteins, cellular RNA binding proteins (PCBP, PABP and hnRNP C) and the *cis*-acting RNA secondary structures (the cloverleaf of 5′ UTR, *cre* and the 3′ UTR-poly (A) tract) (Paul, 2002, Sean & Semler, 2008). Figure 1.4 shows the current models for negative- and positive-stranded RNA synthesis. The viral RNA-dependent RNA polymerase, $3D^{pol}$, plays a central role in the synthesis of both negative and positive strands (Paul, 2002, Racaniello, 2007). A virus encoded protein, VPg, is essential for protein-primed initiation of the replication of both strands (Paul, 2002, Racaniello, 2007). The initiation of enterovirus RNA replication is regulated predominantly by the interaction between RNA template, $3D^{pol}$, and VPg, with the aid of other viral and host factors (Paul, 2002, Racaniello, 2007).

1.1.5.3 Protein synthesis

Synthesis of enterovirus polyprotein is mediated by an internal ribosomal entry site (IRES) element via a cap-independent mechanism (Ehrenfeld & Teterina, 2002). Enteroviruses have a type I IRES. The translation initiation mediated by the type I IRES involves internal ribosome binding, followed by ribosome scanning of the mRNA to identify a downstream AUG initiation codon (Ehrenfeld & Teterina, 2002). During virus infection, a viral proteinase, 2A, expressed by virus has been

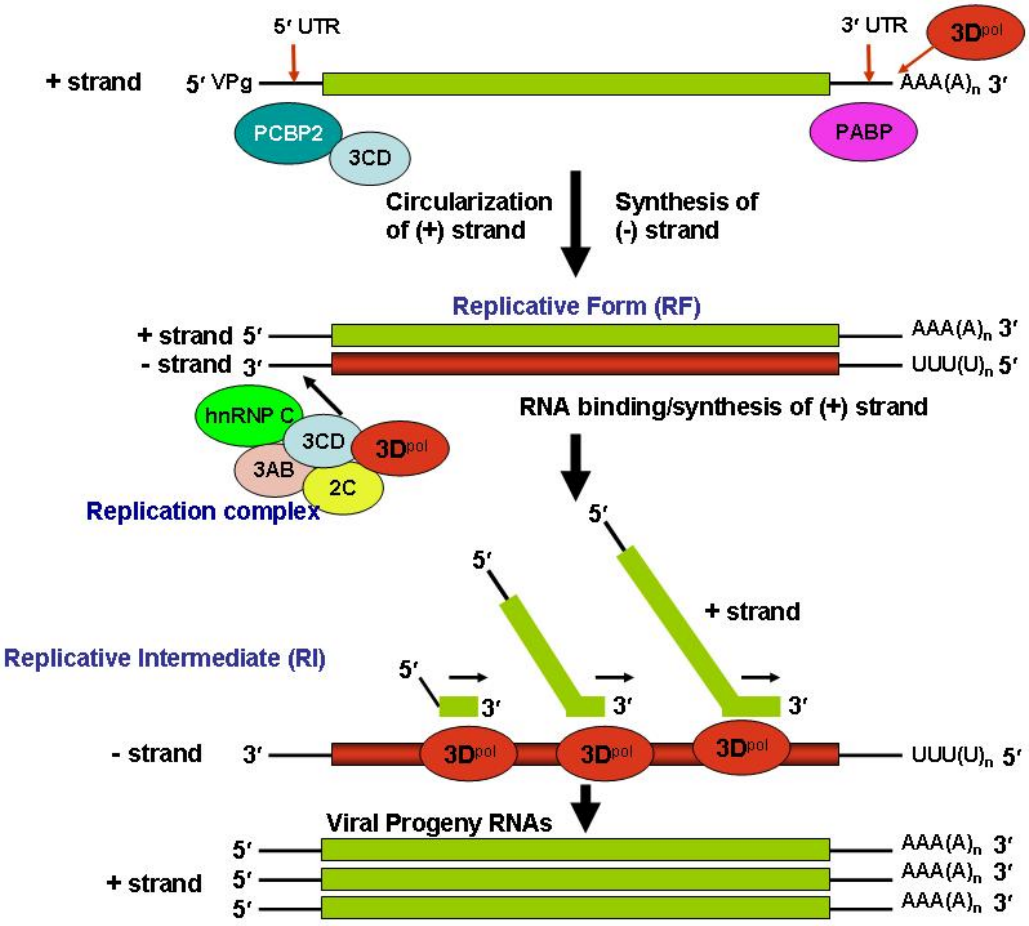

Figure 1.4 Model for the negative- and positive-strand enterovirus RNA synthesis. Initiation of negative-strand RNA synthesis involves the interaction of cellular and viral proteins on the 5′- and 3′- UTRs. A ribonucleoprotein (RNP) complex is formed when PCBP2 and 3CD proteins bind the 5′ cloverleaf. The RNP interacts with the PABP bound to the 3′ poly (A) tract, resulting in a circularised genome. The RNP synthesises the nascent negative-strand RNA beginning at the 3′ poly (A) tract of the genomic RNA. VPg-link precursor (VP-pUpU) synthesised by $3D^{pol}$ using the sequence AAACA of *cre* as template is serve as primer for $3D^{pol}$ during the elongation step. Nascent negative-strand RNA forms heteroduplex with the positive-strand RNA template, called replicative form (RF). Initiation of positive-strand RNA synthesis involves the interaction of cellular and viral proteins on the negative-strand RNA template. VP-pUpU synthesised by $3D^{pol}$ using the 3′-terminal two As of the negative-strand as template is serve as primer for $3D^{pol}$ during the elongation step. Up to six nascent positive-strand RNAs are simultaneously synthesised on one negative-strand RNA template. (Adapted from Sean and Semler, 2008, Paul, 2002).

found to cleave the translation initiation factor, elF4G, required for cap-dependent translation (Gradi et al., 1998, Liebig et al., 2002). Thus, the cap-dependent host cell translation is inhibited while viral protein expression continues via a cap-independent mechanism (Gradi et al., 1998, Liebig et al., 2002).

After translation, the polyprotein precursor is rapidly co or post translationally cleaved by virus-encoded proteinases. High molecular weight precursors do not accumulate in infected cells because they are processed as soon as the viral proteases have been expressed (Racaniello, 2007). Viral proteases, $2A^{pro}$ and $3CD^{pro}$ and its processing product $3C^{pro}$ play a major role in processing of the viral polyprotein (Harris et al., 1990, Lawson & Semler, 1991, Toyoda et al., 1986). The initial cleavage of the polyprotein precursors occurs at the site between the P1 and P2 junction, mediated by $2A^{pro}$, releasing the P1 precursors from the P2-P3 precursors (Harris et al., 1990). Other proteolytic cleavages are largely carried out by $3CD^{pro}$ and/or $3C^{pro}$, including further processing of P1 into VP0, VP3 and VP1, and processing proteins of the P2 and P3 regions (Harris et al., 1990). However, the mechanism of maturation cleavage at the VP4 and VP2 junction is still not known.

1.1.5.4 Virion assembly

The morphogenesis of enteroviruses is a multi-stepped process (Racaniello, 2007). Firstly, the P1 region is released from the polyprotein precursors after being cleaved with 2A protein, and is further processed by proteinase $3CD^{pro}$ into VP0, VP3 and VP1. The 5S protomer consisting one copy each of VP0, VP3 and VP1 is then formed. Five protomers then assemble to form a 14S pentamer which then self-assembles into 80S empty capsids. The final step of morphogenesis is the cleavage of VP0 into VP4 and VP2 by an unknown proteinase. The encapsidation process of

enteroviruses is still poorly defined. Two models of viron assembly have been suggested (Jacobson & Baltimore, 1968, Nugent & Kirkegaard, 1995). One model involves the insertion of newly synthesized viral RNA into the 80S empty capsids to form provirions, in which the VP0 is still not cleaved (Jacobson & Baltimore, 1968). However, an x-ray crystallographic structure of the 80S empty capsid showed no evidence for an opening for viral RNA to gain entry (Basavappa et al., 1994). Another model involves assembly of the 14S pentamers with viral RNA to form the provirions. This model is supported by the finding that the 14S pentamers are stored in 80S empty capsids in infected cells (Nugent & Kirkegaard, 1995).

1.1.6 Mature viral protein

Structural capsid proteins

The structural capsid proteins (VP1, VP2, VP3 and VP4) form the icosahedral structure of virus. The viral protein VP0 is cleaved into VP4 and VP2 in the final stages of virion assembly (Racaniello, 2007). VP1-VP3 proteins are approximately 30 kDa in size (Racaniello, 2007). The amino acid sequences of VP1, VP2 and VP3 are not obviously similar, but all three proteins have similar topology of an eight-stranded, antiparallel β-barrel (Racaniello, 2007). The β-barrel domain is a wedge-shaped structure composed of two antiparallel β-sheets. Packing of the β-barrel units of structural proteins to form a capsid protein shell is strengthened by a network of protein-protein contacts on the interior of the capsid. This network is formed by the N-terminal extensions of VP1 to VP4. VP4 has an extended conformation compared to the other three proteins. It is similar in position and conformation to amino-terminal sequences of VP1 and VP3 and functions as a detached amino-terminal extension of VP2 (Racaniello, 2007).

Nonstructural proteins

2A protein

The enterovirus 2A protein functions primarily as a proteinase. Once the 2A protein gene has been translated, it can adopt a three-dimensional structure component for proteolytic activity (Harris et al., 1990, Toyoda et al., 1986). It then co-translationally cleaves itself at its amino acid terminus to release the P1 structural protein region from the P2 and P3 nonstructural protein regions (Harris et al., 1990, Toyoda et al., 1986). $2A^{pro}$ also plays a role in viral RNA replication and host cell protein synthesis shutoff by cleaving elF4GI to inhibit host cell translation (Gradi et al., 1998, Liebig et al., 2002). $2A^{pro}$ utilizes a cysteine in its active site as the nucleophilic attack group. Amino acid alignment and three-dimensional protein structure data indicated that $2A^{pro}$ adopts a serine protease fold similar to the protease chymotrypsin (Bazan & Fletterick, 1988). It has been reported that 2A protein induced apoptosis and cell death in some members of human enteroviruses including PV and HEV71 (Goldstaub et al., 2000, Kuo et al., 2002). This is because 2A protein induces DNA fragmentation and chromatin condensation in PV, and induces DNA fragmentation and PAR cleavage in HEV71.

2BC protein/2B protein

Protein 2BC is the precursor to 2B and 2C proteins. 2B protein is a small, membrane-associated protein. It has been reported that expression of 2BC and 2B changes membrane permeablilization, inhibits cellular secretory pathways and disrupts the Golgi complex (Cho et al., 1994, Doedens & Kirkegaard, 1995, Sandoval & Carrasco, 1997). Synthesis of 2BC protein also induces the formation of membranous vesicles in infected cells (Cho et al., 1994).

It has been suggested that viral protein 2B is required for viral RNA replication because mutagenesis of the PV 2B causes defects in RNA synthesis (Johnson & Sarnow, 1991). However, the exact role of 2B in RNA synthesis is not clearly known. 2B protein also induces the alteration of cell membrane permeability which is important for releasing of virus from cells (van Kuppeveld et al., 1997). In addition, 2B contributes to the formation of membranous vesicles which are the site of viral replication in infected cells (van Kuppeveld et al., 1997). However, the mechanisms of vesicle formation and regulation are not yet known.

2C protein

Protein 2C is highly conserved and multifunctional. It has been shown to be involved in viral RNA replication (Barton & Flanegan, 1997, Pfister & Wimmer, 1999). Similar to 2BC protein, expression of 2C induces proliferation and rearrangement of membranous vesicles in infected cells (Cho et al., 1994). 2C also binds to membranes and RNA and has nucleoside triphosphatase (NTPase) activity that is inhibited by guanidine (Pfister & Wimmer, 1999, Rodriguez & Carrasco, 1993, Rodriguez & Carrasco, 1995). Mutagenesis of the conserved amino acid within the NTPase domain of 2C results in the loss of viral infectivity (Rodriguez & Carrasco, 1993). Thus, it has been postulated that 2C may have two functions in RNA synthesis: as an NTPase and directing replication complexes to cell membranes (Aldabe & Carrasco, 1995, Cho et al., 1994, Rodriguez & Carrasco, 1995).

3A/3AB protein

3AB is a multifunctional protein. It interacts with membranous vesicles, $3D^{pol}$ and 3CD, and also forms a ribonucleoprotein complex on the 5′ cloverleaf with 3CD

(Xiang et al., 1995). In addition, it has been shown that 3AB stimulates autoproteolysis of 3CD and elongation activity of $3D^{pol}$ ((Molla et al., 1994). It was also found that 3AB can serve as a substrate for VPg uridylylation by $3D^{pol}$ (Richards et al., 2006).

Protein 3A is a mature protein from the 3AB precursor. 3A is associated with membranous vesicles during RNA replication (Towner et al., 1996). It has been shown that 3A is important for homodimerization, inhibition of cellular trafficking and RNA replication (Wessels et al., 2006). Protein 3A also inhibits tumor necrosis factor-induced apoptosis (Neznanov et al., 2001).

3B protein

Protein 3B is also known as VPg or viral protein, genome-linked. It is covalently linked to the 5′ end of the genomic RNA (Flanegan et al., 1977). Protein 3B plays an important role in RNA replication by acting as a protein primer for both negative- and positive-stranded RNA synthesis (Pettersson et al., 1978, Sean & Semler, 2008). VPg is uridylylated by $3D^{pol}$ at a tyrosine residue by using *cre* as a template (Paul et al., 1998, Takegami et al., 1983). The uridylylated VPg then serves as a primer for RNA replication by the RNA-dependent RNA polymerase (Paul et al., 1998).

3C/3CD

Protein 3CD is a fusion between 3C proteinase and 3D polymerase and is the precursor of both mature proteins. Protein 3CD is multifunctional. As a proteinase, 3CD plays a role in proteolytic processing of the structural precursor P1 region of the polyprotein (Lawson & Semler, 1991). Protein 3CD also has a role in RNA

replication. With its RNA-binding activity, 3CD forms ribonucleoprotein complex with the cloverleaf of 5′ UTR either in the presence of 3AB or PCBP (Gamarnik & Andino, 1997, Parsley et al., 1997, Xiang et al., 1995). It has been suggested that the 3CD/PCBP complex mediates a circularization of the positive-stranded RNA genome (Herold & Andino, 2001). The role of 3CD in RNA replication has been further supported by the finding that 3CD stimulates the PV synthesis in *in vitro* translation-RNA replication system (Herold & Andino, 2001). Protein 3CD also influences the uridylylation of VPg by $3D^{pol}$ by an interaction with the *cr*e, an RNA stem-loop element in the 2C coding region (Paul et al., 2000, Rieder et al., 2000).

Protein 3C is the proteinase responsible for proteolytic processing of the P2 and P3 precursor proteins (Lawson & Semler, 1991). Similar to 3CD, 3C has RNA binding activity and is able to bind to the 5′ cloverleaf (Blair et al., 1998, Zell et al., 2002). The role of 3C in viral RNA replication is not clearly demonstrated. Similar to 2A protein, proteinase of 3C cleaves cellular proteins important for host gene expression, including TATA-box binding protein and PABP (Clark et al., 1993, Kuyumcu-Martinez et al., 2002). This cleavage enables the virus to shut down host gene expression. In HEV71, 3C was found to induce apoptosis in human neural cells though a mechanism involving caspase activation (Li et al., 2002).

3D

Protein $3D^{pol}$ is the RNA-dependent RNA polymerase which is responsible for chain elongation during the synthesis of both positive-and negative- stranded RNAs (Flanegan & Baltimore, 1977, Van Dyke & Flanegan, 1980). It has been shown that $3D^{pol}$ activity is enhanced by the 3AB protein (Paul et al., 1994, Plotch & Palant,

1995, Richards & Ehrenfeld, 1998). The interaction of $3D^{pol}$ and 3AB may facilitate localization of the polymerase to membranous vesicles, the sites for RNA replication (Sean & Semler, 2008). Protein $3D^{pol}$ also catalyzes the VPg uridylylation reaction occurring through the precursor 3AB (Lyle et al., 2002, Xiang et al., 1995).

1.1.7 Construction and use of infectious cDNA clones of enteroviruses

An infectious clone is a full-length cDNA copy of the viral genome, carried on a plasmid vector, which serves as a template for the *in vitro* or *in vivo* transcription of infectious RNA. In general, a promoter sequence recognized by *Escherichia coli* or phage DNA-dependent RNA polymerase (such as bacteriophages SP6 or T7) is required for *in vitro* transcription of viral cDNA template, or a eukaryotic promoter sequence, such as cytomegalovirus (CMV) immediate early promoter, is required for *in vivo* transcription of viral cDNA after direct transfection into cells.

The first infectious cDNA clone of an animal virus to be constructed was that of PV, an important member of the human enteroviruses (Racaniello & Baltimore, 1981). This cDNA clone contained no promoter sequence. However, it was able to produce infectious virus after the cDNA transfection into CV-1 cells. The mechanism by which this cDNA clone generates infectious virus is not known. It has been postulated that the cDNA enters the nucleus, where it is transcribed by cellular DNA-dependent RNA polymerase from a cryptic, promoter-like sequence on the plasmid (Flint et al., 2004). Similarly, cDNA of CBV3 virus containing only the bacteriophage T7 promoter sequence without an additional eukaryotic promoter sequence was also found to be infectious *in vivo* (Kandolf & Hofschneider, 1985).

To date, infectious cDNA clones of several members of the human enteroviruses have been constructed using different combinations of plasmid vector and/or bacterial host strains (Arita et al., 2005, Harvala et al., 2002, Kraus et al., 1995, Martino et al., 1999). Most enterovirus infectious clones contain either bacteriophage or eukaryotic promoter sequences for initiation of RNA transcription (Arita et al., 2005, Harvala et al., 2002, Kraus et al., 1995, Martino et al., 1999). Viral cDNA instability in bacterial hosts is the major problem encountered in the construction of infectious cDNA clones for many positive-stranded RNA virus families, particularly flaviviruses and coronaviruses. However, the instability problem has not been well documented in the construction of enterovirus infectious clones. Although HEV71 has become an important pathogen causing large HFMD outbreaks with neurological complications since 1997, the first infectious clone of this virus was only reported in 2005 (Arita et al., 2005). The initial construction of this HEV71 (BrCr) infectious clone in a high copy number plasmid was unsuccessful. However, this group was later able to produce an infectious clone by using a medium-copy number plasmid and the bacterial host strain XL10-gold. Different combinations of plasmid vector and/or bacterial host strains were also found to be major determinants of success or failure in generating an infectious cDNA clone of HEV71 in this study (described in Chapter 3)

With the advance of recombinant DNA technology that enables modification and introduction of mutations in genomic DNA, the establishment of infectious cDNA clones greatly enhances understanding of RNA virus biology. Such clones facilitate genetic manipulation of viral RNA genomes. Thus, infectious clones can serve as useful tools for the investigation of virulence determinants and can also potentially

be used for the design and construction of live-attenuated vaccines. For example, in coxsackievirus B3 (CBV3), the infectious clone has been utilized in various studies, including mutagenesis of a single amino acid in the puff region of the VP2 or mutagenesis in the 5′ UTR for the construction of attenuated myocarditic phenotypes (Dan & Chantler, 2005).

1.2 Human enterovirus 71 (HEV71)

1.2.1 HEV71 infection

HEV71 was first isolated from the stool of an infant with encephalitis in California in 1969 (Schmidt et al., 1974). Since then, HEV71 infections have been found to be associated with a wide range of diseases. It is most often associated with outbreaks of hand, foot and mouth disease (HFMD), a self-limiting childhood disease characterised by a brief febrile illness and vesicular lesions on the hands, feet, mouth and buttocks. In addition to HFMD, HEV71 often causes herpangina, a disease characterised by an abrupt onset of fever and sore throat, associated with small vesicular or ulcerative lesions on the posterior oropharynx. Other members of HEV-A, particularly coxsackievirus A16 (CAV16) and coxsackievirus A10 (CAV10) also cause HFMD and herpangina (Pallansch & Roos, 2007). HFMD and herpangina caused by HEV71 is clinically indistinguishable from HFMD caused by other members of HEV-A (Pallansch & Roos, 2007).

Unlike other causative agents of HFMD and herpangina, HEV71 has been recognised as a highly neurotropic virus causing a range of neurological diseases, including aseptic meningitis, brainstem and/or cerebellar encephalitis, and acute flaccid paralysis (AFP), which may lead to permanent paralysis or death (McMinn,

2002). AFP associated with HEV71 infection is generally milder than PV infection, with a higher rate of complete recovery (Hayward et al., 1989, McMinn et al., 2001b, Samuda et al., 1987). The most severe form of HEV71 neurological disease is brainstem encephalitis, which was found to involve several parts of the brain, including the medulla oblongata, reticular formation, pons and midbrain (Huang et al., 1999, Lum et al., 1998, Wang et al., 1999). Brainstem encephalitis is occasionally associated with neurogenic pulmonary oedema, a clinical manifestation characterised by a rapid onset of cardiopulmonary failure (Huang et al., 1999, Lum et al., 1998, Wang et al., 1999). The mortality rate of brainstem encephalitis associated with neurogenic pulmonary oedema is as high as 80% (Huang et al., 1999, Lum et al., 1998, Wang et al., 1999). Children under 5 years of age are particularly susceptible to HEV71-associated neurological diseases. Recently, a case of acute HEV71 encephalitis in an adult has been reported (Hamaguchi et al., 2008).

Other diseases commonly associated with HEV71 infections include non-specific febrile illness in young children and acute respiratory diseases including pharyngitis, bronchiolitis and pneumonia (Merovitz et al., 2000, Rotbart et al., 1999, Tsai et al., 2001). A case of intrauterine HEV71 infection during pregnancy leading to foetal abnormalities (hepatomegaly, pleural effusion and hydrocephalus) and death has also been reported (Chow et al., 2000).

1.2.2 Epidemiology of HEV71

Since the first isolation in 1969, epidemics of HEV71 infection associated with HFMD and/or neurological diseases have occurred throughout the world including the USA, Brazil, Bulgaria, Hungary, Sweden, and countries in the Asia-Pacific

region (Blomberg et al., 1974, Cardosa et al., 1999, Chumakov et al., 1979, Lin et al., 2006, Melnick, 1984, Nagy et al., 1982, Schmidt et al., 1974, Takimoto et al., 1998, Tu et al., 2007). The earliest large and severe epidemics of HEV71 infection occurred in Bulgaria in 1975 (Chumakov et al., 1979) and Hungary in 1978 (Nagy et al., 1982). Both epidemics were associated with numerous cases of aseptic meningitis (545 cases in Bulgaria, 826 in Hungary), encephalitis or acute flaccid paralysis (149 cases in Bulgaria, 724 cases in Hungary, respectively). Unlike other outbreaks, no cases of HFMD were reported in the Bulgarian epidemic, and only four cases of HEV71-associated HFMD were identified in Hungary (Melnick, 1984, Nagy et al., 1982). Since then, there has been no report of large epidemics of HEV71 infection in European countries.

In the Asia-Pacific region, the first report of HEV71 infection came from Australia, during an epidemic of aseptic meningitis in Melbourne in 1972, in which 39 out of 49 HEV71-infected patients had aseptic meningitis (Kennett et al., 1974). The second outbreak of HEV71 infection in Australia occurred in Victoria in 1986. This outbreak also had a high incidence of neurological involvement, with 6 out of 114 infected patients developing encephalitis and one patient developing poliomyelitis-like paralysis (Gilbert et al., 1988). In addition to Australia, small or large outbreaks of HEV71 associated HFMD or HFMD and acute neurological diseases occurred in several Asian countries including Japan in 1973 and 1978, Hong Kong in 1985, China in 1987 and Singapore in 1987 (McMinn, 2002). These outbreaks were all generally mild and had low mortality.

Since 1997, HEV71 activity has increased significantly in the Asia-Pacific region. Several large epidemics of HEV71 infection have occurred in many countries. The

first large epidemic occurred in Sarawak, Malaysia, in 1997 (Cardosa et al., 1999, Chan et al., 2000). This epidemic was associated with numerous cases of HFMD and herpangina, and was occasionally associated with severe neurological diseases such as aseptic meningitis, acute flaccid paralysis, cerebellar ataxia, and a previously undescribed clinical manifestation, fatal neurogenic pulmonary oedema associated with brainstem encephalitis (Cardosa et al., 1999, Chan et al., 2000). During this epidemic, 889 infected children were hospitalized and 29 died from cardio-respiratory failure. Smaller and less severe epidemics with low mortality rates were later reported in Japan and peninsular Malaysia in the same year and in Singapore in 1998 (Komatsu et al., 1999, Lum et al., 1998, Singh et al., 2000). A large HEV71 epidemic occurred in Taiwan in 1998, with about 130,000 cases of HFMD and herpangina. Of these, 405 cases developed severe neurological diseases and 78 (19%) cases were fatal, mainly due to the development of neurogenic pulmonary edema (Ho, 2000). In 1999, a large outbreak of HEV71 infection occurred in Perth, Western Australia (McMinn et al., 2001b). Approximately 6,000 cases of HFMD were reported, and 29 cases had severe neurological disease. HEV71-associated neurological diseases in Perth included aseptic meningitis, acute cerebellar ataxia, and acute flaccid paralysis.

HEV71 epidemic activity is still high in the Asia-Pacific region, with outbreaks and sporadic cases continuing to occur. Outbreaks of HFMD with a proportion of neurological diseases occurred in Singapore, Korea, Japan and peninsular Malaysia in 2000, Taiwan in 2000 and 2001, Sarawak in 2000, 2003 and 2006, Vietnam in 2005, India, Thailand, Malaysia, Hong Kong and Brunei in 2006 (Cardosa et al., 2003, Fujimoto et al., 2002, Jee et al., 2003, Lin et al., 2006, Lum et al., 2002, Podin et al., 2006, Singh et al., 2002, Tu et al., 2007) (http://www.promedmail.com,

http://www.cdc.gov). The most recent and largest recorded outbreak occurred in China in 2008, with more than 200,000 cases reported (http://www.promedmail.com, http://www.cdc.gov).

Interestingly, similar epidemic patterns were observed following long-term epidemiological studies in Japan and Sarawak. Surveillance data from both countries indicated that HEV71 follows an epidemic mode of transmission, with outbreaks occurring every 3 years (Hosoya et al., 2006, Podin et al., 2006). It has been suggested that quiescent periods between outbreaks could result from the development of population immunity caused by widespread infection in the community during an epidemic (Hosoya et al., 2006, Podin et al., 2006).

Few studies have been performed to investigate the mode of transmission and risk factors associated with HEV71 infections. The primary mode of HEV71 transmission is via the faecal-oral route and, less commonly, via the respiratory route. A study of risk factors for HEV71 infection during the large epidemics of HFMD/herpangina in Taiwan in 1998 showed that significant risk factors for HEV71 infection are a large number of children in the family, attendance at a kindergarten or child care centre, contact with HFMD or herpangina cases, age between 6 months and 5 years of age, and living in a rural area (Chang et al., 2002). The results indicated that efficient spread of HEV71 occurred in families, kindergartens and childcare centres, suggesting that virus transmission is aided by overcrowding and poor sanitation. The faecal-oral route of transmission can occur by direct contact between people or by indirect contact via food, water or objects contaminated with faecal material. Further studies need to be undertaken in order to clarify if the respiratory route is a true mode of transmission of HEV71 infection.

1.2.3 Molecular epidemiology of HEV71

The molecular epidemiology and evolution of HEV71 was originally described by Brown et al. (1999). In this study, the genetic diversity and rate of evolution of HEV71 isolates were determined by comparing the complete nucleotide sequences of the VP1 gene of 113 strains isolated from the USA, and five other countries over a thirty-year period. Three distinct HEV71 genetic lineages (genotypes), designated A, B and C, were identified as shown in Figure 1.5. Genotype A consists of a single virus, the prototype strain BrCr, which was the first HEV71 strain isolated in California in 1969. Genotype B is divided into five subgenotypes, B1 to B5 and genotype C is divided into five subgenotypes, C1 to C5 (Brown et al., 1999, Cardosa et al., 2003, McMinn et al., 2001a, Shimizu et al., 2004, Tu et al., 2007). The nucleotide sequence similarity between the genotypes is 78-83%. Within the B genotype, the strains share at least 87.9% nucleotide sequence identity, and the strains within the C genotype share at least 84.5% identity. Virus isolates within the same subgenotype share more than 90% nucleotide sequence similarity. The nucleotide divergence between genotypes A and the other two genotypes, B and C, is 20-21%, and the divergence between genotypes B and C is 16-25%.

Several regions of the HEV71 genome have been used for phylogenetic analysis, including the 5′ UTR, VP1, VP4 and the VP4-VP2 junction. The VP1 region is the most informative region for molecular epidemiology and evolutionary studies of enteroviruses (McMinn, 2002). This is because the VP1 protein is the most exposed capsid protein and contains the major viral neutralisation epitopes; it is therefore antigenically and genetically distinct, with a strong correlation to virus serotype (Oberste et al., 1999). In addition, no homologous recombination occurs within the

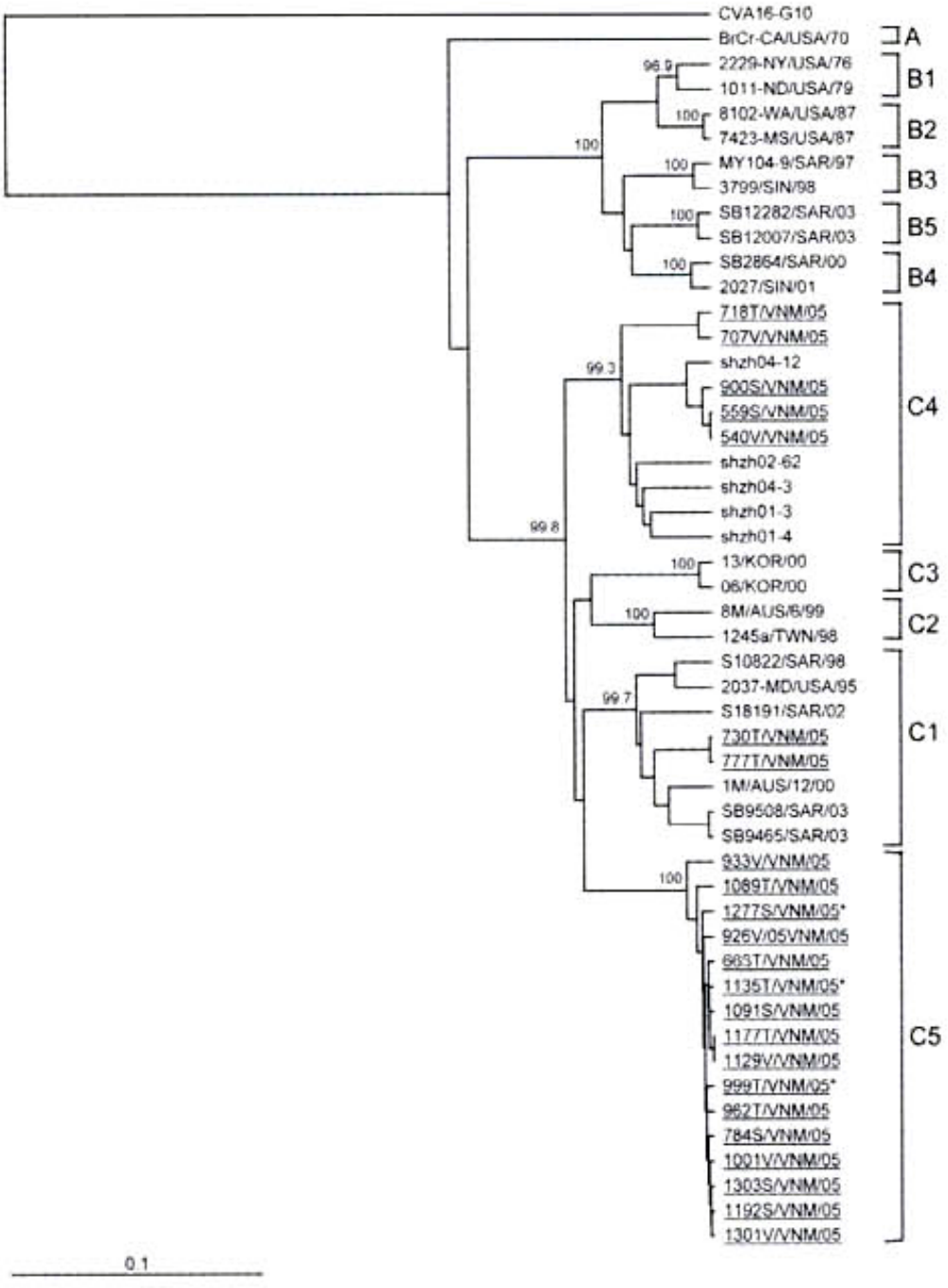

Figure 1.5 An overview of the genetic relationships of human enterovirus 71 (HEV71) strains. Dendrogram showing the genetic relationships among 49 HEV71 strains based on the alignment of complete VP1 gene sequences. The dendrogram shows genogroups A, B and C as identified by Brown et al. (1999). Taken from Tu et al., 2007.

VP1 gene (Oberste et al., 1999). The VP4 gene has been shown to provide similar phylogenetic information to the VP1 gene, and has also been commonly used in molecular epidemiology studies of HEV71 (Cardosa et al., 2003, Chu et al., 2001, Shimizu et al., 1999). However, the VP1-based phylogenetic analysis provides greater statistical confidence than VP4-based analysis (Cardosa et al., 2003).

Studies of molecular epidemiology have improved the understanding of the evolution of HEV71 and the association of genetic diversity of virus strains to pathogenic properties and epidemiologic circulation. Similar to other enteroviruses, such as PV and HEV70, HEV71 is a genetically diverse virus with an estimated evolution rate of 1.35×10^{-2} substitutions per nucleotide per year (Brown et al., 1999). The prototype, BrCr strain, isolated in 1969, is the only strain of genotype A identified. Genotype B was the major strain circulating throughout the world in the 1970s and 1980s, whilst genotype C strains were first isolated from the USA in 1987 (Brown et al., 1999). Strains of genotype B and C have continued to evolve and circulate throughout the world. Co-circulation of different genotypes and the temporal change of dominant genotypes of HEV71 outbreaks have been well documented. For example, four distinct subgenotypes (B3, B4, C1 and C2) co-circulated in Malaysia during 1997-2000 (Herrero et al., 2003). The co-circulation of genotypes B and C was also found in Taiwan in the 1998 HFMD outbreak, with C2 the predominant subgenotype (Lin et al., 2006). The genotype shift occurred during 1999-2003 and genotype B4 was the predominant genotype which was then replaced by genotype C from 2004-2005 (Huang et al., 2008, Lin et al., 2006, Wang et al., 2002).

Recombination has been reported to contribute to genetic diversity and evolution of enteroviruses. Phylogenetic and Simplot analysis of complete genome sequences of HEV-A prototype viruses and also the four newest HEV-A viruses identified has suggested that recombination may play a role in the evolution of viruses in the species (Oberste et al., 1999). The occurrence of intertypic recombinants between HEV71 and several HEV-A virus, including CAV16 has been demonstrated (Chan & AbuBaka, 2006). In addition, intratypic recombination between genotype B and genotype C has also been identified among naturally circulating HEV71 isolates in Taiwan (Huang et al., 2008) and two recombination sites located at the 3′ terminus of protein 2A and 3D has been found. The nonstructural gene region was found to be the recombination hot spot for both intertypic and intratypic recombination in HEV71 and also other HEV-A viruses. Thus, recombinant events may play an important role in the emergence of HEV71 subgenotypes with different potential in disease associations.

1.2.4 Pathogenesis of HEV71

The wide variety of clinical manifestations resulting from HEV71 infection, ranging from mild HFMD to fatal encephalitis, has demonstrated the complexity of HEV71 pathogenesis. Although the pathogenesis of HEV71 associated with neurological diseases has been studied intensively, much remains to be clarified. Initial viral replication probably occurs in the intestine, since virus can be detected in stool for several weeks after infection (Chung et al., 2001). The ability of HEV71 to infiltrate, infect and replicate in cells of the CNS has been clearly demonstrated, as viral antigen was detected in the cytoplasm of neurons (Wong et al., 2008). The

major targets of HEV71 in the CNS are the spinal cord and brainstem (Wong et al., 2008). The distribution of viral lesions in the CNS is wider than PV infection, involving both the pyramidal and extrapyramidal tracts of the CNS (Wong et al., 2008).

The mechanisms of viral entry to the CNS after primary replication are currently unknown. Several studies have shown that viraemia is necessary for the spread of virus, for example, monkeys inoculated intravenously with HEV71 developed neurological syndromes clinically and pathologically similar to human cases of encephalitis (Nagata et al., 2004). Neuroinvasion is most likely preceded by virus replication in extraneural tissue. Wong *et al.* (2008) examined the distribution of inflammatory response in CNS of human HEV71 encephalitis cases. Based on distinct inflammatory responses found in the CNS (spinal cord gray matter, brainstem, hypothalamus, and subthalamic and dentate nuclei), the authors speculated that virus spreads into the CNS via the peripheral nervous system, most likely the motor pathway. However, spread of virus into the CNS via the haematogenous route and subsequent crossing of the blood-brain barrier cannot be ruled out.

Both viral factors such as virulence and tropism, and host factors such as the distribution of host cell receptors and the immune system may contribute to the pathogenesis of HEV71 encephalitis and be responsible for the differences in clinical manifestations of HEV71 infection. It has been postulated that the marked variation in the clinical signs of HEV71 infection are related to dermatotropism or neurotropism of viral strains (McMinn, 2002). The role of host factors on HEV71

encephalitis has been suggested by several findings. Children that developed neurogenic pulmonary oedema (PE) had an abnormal cytokine activation that produces a severe systemic inflammatory response (Wang et al., 2003). Patients with PE were found to have significant higher levels of plasma interleukin-6 (IL-6), IL-10, IL-13, IL-1β and interferon (IFN)-γ, and lower circulating $CD4^+$ T cells, $CD8^+$ T cells, and natural killer (NK) than the other HEV71 cases (Wang et al., 2003). It was also found that children with meningoencephalitis had an altered cellular immune response associated with a high frequency of the G/G genotype of the cytotoxic T lymphocyte antigen-4 polymorphism (Yang et al., 2001). More studies need to be carried out to clarify the role of viral and host factors in the pathogenesis of HEV71 infection.

1.2.5 Molecular determinants of virulence

Like PV, HEV71 is a neurotropic enteric virus. The determinants of HEV71 neurovirulence remain to be elucidated. Molecular genetic analysis of PV virulence has shown that minor sequence variations in the 5′ UTR are sufficient to account for large differences in neurovirulence (Evans et al., 1985, Kawamura et al., 1989, Macadam et al., 1991). An attempt to identify HEV71 neurovirulence determinants by comparing nucleotide sequences of the 5′ UTR and VP1 gene of HEV71 strains isolated from mild HFMD and severe neurological cases has been unsuccessful (AbuBakar et al., 1999, Brown et al., 1999, Shih et al., 2000, Shimizu et al., 1999). During the Perth HEV71 epidemic in 1999, the genotype C2 viruses that have a single amino acid substitute in VP1 (A170V) were exclusively isolated from cases of severe neurological disease (McMinn, 2002). The amino acid substitute in VP1 (A170V) is predicted to affect virus-receptor interactions (McMinn, 2002).

However, the effect of this amino substitution on neurovirulence has not been shown. It has been hypothesized that HEV71 neurovirulence may be determined by more than one genomic region, and host factors may play an important role in limiting the severity of most HEV71 infections (McMinn, 2002).

In the related PV, single-nucleotide changes within the PV IRES greatly alter viral neurovirulence. A point mutation from C to U at nucleotide position 472 in the IRES of PV Sabin type 3 exhibited an attenuated neurovirulence phenotype in both monkey and mouse models (Evans et al., 1985, La Monica & Racaniello, 1989). PV Sabin type 1 and 2 strains also contain mutations in the IRES at position 480 (A to G) and 481 (G to A), respectively. These mutations within IRES stem-loop domain V have been shown to cause impaired growth kinetics in cultured cells of neuronal origin (Haller et al., 1996). The C472U mutation of Sabin type 3 was also found to cause a translation defect in neuronal cells (Svitkin et al., 1990). It has been postulated that the attenuated phenotype associated with the C472U mutation is caused by decreased translation efficiency specific to the brain and spinal cord (La Monica & Racaniello, 1989, Ohka & Nomoto, 2001). In a mouse model, the C472U mutation was found to cause a translation defect in both neuronal and non-neuronal tissues (Kauder & Racaniello, 2004). Mutations within IRES stem-loop domain V were also found to destabilise the secondary structure of the IRES (Macadam et al., 1992, Skinner et al., 1989). The role of the IRES in the determination of PV neurovirulence has been strengthened by the finding that a polio/rhinovirus IRES recombinant (PV backbone with human rhinovirus type 2 IRES) has impaired growth kinetics specific to neuronal cells (Gromeier et al., 1996). The polio/rhinovirus IRES recombinant also exhibited highly attenuated phenotype in

both CD155 transgenic mice and non-human primates (Gromeier et al., 1996, Gromeier et al., 1999).

Mutations within a non-structural protein, RNA-dependent RNA polymerase $3D^{pol}$, of the Sabin PV type 1 vaccine strain were implicated in the temperature-sensitive (*ts*) and low-virulence phenotype of the virus (Christodoulou et al., 1990). Unlike PV, the role of HEV71 IRES, and non-structural proteins in neurovirulence remains poorly defined. Arita et al. (2005) generated HEV71 (BrCr) mutants by introduction of mutations corresponded to *ts* determinants of PV Sabin type 1 into the BrCr infectious clone. It has been demonstrated that a HEV71 (BrCr) variant containing mutations in 5′ UTR (A485G), $3D^{pol}$ (Tyr-73 and Cys-363) and 3′ UTR (A7409G) has attenuated neurovirulent phenotype. Monkeys infected intravenously with this HEV71 mutant showed mild neurological manifestations and histological changes in the CNS compared to monkeys inoculated with the parental BrCr strain (Arita et al., 2005). This group suggested that HEV71 and PV may share common genetic determinants of neurovirulence.

1.2.6 Animal models of HEV71

The development and use of animal models is essential for understanding viral pathogenesis and in the development of therapeutics and vaccines. A number of animal models have been developed to investigate HEV71 infection, including non-human primates and rodents. Non-human primate models are considered the best animal models to study the pathogenesis of HEV71. However, the high cost and restricted availability of monkeys limit their use for pathogenesis studies. Transgenic mice possessing human receptors to HEV71 would serve as a cheaper and more useful animal model. Unfortunately, the receptors of HEV71 are currently

unknown, thus no transgenic mice are available to elucidate pathogenesis. A number of recent studies have developed a mouse model for studies of HEV71 pathogenesis and for vaccine and antiviral efficacy testing (Liu et al., 2005, Tan et al., 2007, Wu et al., 2007). Although a mouse-adapted strain is required for infection of mice, a mouse model is currently the most convenient small animal model that would allow the primary assessment of potential vaccines or antiviral agents against HEV71.

1.2.6.1 Non-human primate model

Old world monkeys including rhesus, green and cynomolgus monkeys were found to be susceptible to HEV71 infection, with cynomolgus monkeys being the most commonly used. Infected cynomolgus monkeys develop neurological manifestations and histopathological features similar to human disease after subcutaneous (s.c.), intraspinal (i.s.), intravenous (i.v.) or oral routes of inoculation (Hashimoto & Hagiwara, 1982a, Hashimoto & Hagiwara, 1982b, Hashimoto et al., 1978, Nagata et al., 2004, Nagata et al., 2002). Subcutaneous inoculation of HEV71 caused complete paralysis or weakness of hind limbs (Hashimoto et al., 1978). Virus-induced lesions found in the CNS of infected monkeys include perivascular cuffings, degeneration and disappearance of the neurons, and meningial lymphocytic infiltration in the grey and/or white matter of the spinal cord, medulla oblongata, cerebral cortex and brainstem (Hashimoto et al., 1978). Most monkeys infected orally with HEV71 do not develop clinical signs of disease, with only one infected monkey showing weakness of the lower extremities (Hashimoto & Hagiwara, 1982a). However, similar lesions in the CNS observed in subcutaneously infected monkeys were also found in orally infected monkeys.

Nagata et al (2002) experimentally infected cynomolgus monkeys with five HEV71 strains isolated from individual patients with fatal encephalitis, meningitis, and HFMD. Following i.s. inoculation with each of the five strains, all monkeys developed neurological manifestations within 1-6 days post-infection regardless of the infecting strain. All the strains of HEV71 appear to be neurotropic and there is no correlation between the neurovirulence and genotype of HEV71. Infected monkeys showed both pyramidal tract signs, such as flaccid paralysis, and extrapyramidal tract signs, such as ataxia and tremor. Histological analysis in the CNS revealed that virus-related lesions occurred in the spinal cord, brainstem, cerebrum and cerebellar cortex and dentate nuclei. The cerebellar nuclei (dentate nuclei) were most severely damaged, with neuron degeneration and necrosis and inflammatory changes being observed. Virus titres in the CNS were high at the acute phase of infection, while the titres dropped to undetectable levels at 3 days after the onset of neurological manifestations. The authors suggested that the clinical course of HEV71 infection in monkeys inoculated via the i.s. route is triphasic involving an incubation period, an acute phase associated with the presence of virus in the CNS, and a subsequent inflammatory response associated with the disappearance of virus.

The neuropathological features of HEV71 were also compared to PV type 1. After i.v. inoculation, HEV71-infected monkeys exhibited extrapyramidal signs including tremor, ataxia and brain oedema, whereas PV-infected monkeys only showed pyramidal signs of flaccid paralysis (Nagata et al., 2004). The distribution of viral lesions in the CNS of HEV71-infected monkeys was spread in both the pyramidal and extrapyramidal tracts of the CNS (Nagata et al., 2004). By contrast, the lesions

induced by PV were mainly restricted to the pyramidal tracts including the spinal motor neurons, thalamus and motor cortex (Nagata et al., 2004).

Pulmonary oedema is a frequent clinical manifestation associated with fatal cases in recent large HFMD outbreaks. The pathogenesis of pulmonary oedema involves virus-induced damage to the brainstem (Chang et al., 1998, Lum et al., 1998). However, no HEV71-infected monkeys with lesions identified in the brainstem developed pulmonary oedema (Hashimoto et al., 1978, Nagata et al., 2004).

1.2.6.2 Small animal model

Newborn and adult cotton rats, Syrian hamsters and newborn mice have been shown to be susceptible to Bulgarian strains of HEV71 (Chumakov et al., 1979). To date, the cotton rat and hamster models have not yet been fully developed and characterised for studies of pathogenesis of HEV71. Mouse models have been extensively used and characterised in recent studies (Chen et al., 2004, Chua et al., 2008, Ong et al., 2008, Wang et al., 2004). The mouse is not the natural host of HEV71. Experimental infections of HEV71 in various strains of adult mice, including random-bred ICR, BALB/c, C3H, nude (BALB/c), C57B/6J, SCID, CD28 knock-out (BALB/c) and TNF-alpha receptor knock-out (C57BL/6J), caused asymptomatic infections (Wu et al., 2002). In newborn ICR mice, unadapted strains of HEV71 produced illnesses leading to hindlimb paralysis and death within two weeks after i.p. inoculation at high viral titres (Yu et al., 2000). However, mouse-adapted strains of HEV71 were required to consistently produce disease in newborn mice at low viral titres (Chen et al., 2007, Chen et al., 2004, Chua et al., 2008).

Chen et al. (2004) first developed a mouse-adapted strain of HEV71 (MP-4643). The original strain of this virus was isolated in 1998 from a patient with fatal encephalitis during the large HFMD outbreak in Taiwan (Yan et al., 2001). It was shown that 1- day-old ICR mice infected with MP-4643 via the i.p. or oral routes developed hindlimb paralysis and death. The mouse oral HEV71 infection model has been further characterised using MP-4643 (Wang et al., 2004). Experimental infection of 7-day-old ICR mice resulted in hindlimb paralysis and death at 5 to 9 days after oral inoculation. The virus first replicated in the intestine, and then in other organs including heart, muscle, skin, liver, spleen, lung, kidney, brain and spinal cord. Neuronal loss and apoptosis were observed in the spinal cord and brain stem. The limb muscles displayed massive necrosis and contained the highest viral titre, indicating that it is a primary site for viral replication in mice. It was also found that anti-HEV71 antibody could protect HEV71-infected mice from developing disease, suggesting that viremia was necessary for the spread of virus to the CNS. The authors suggested that virus could get entry into the CNS through the blood-brain barrier. However, the pattern of spread of virus from the lower to upper segments of the spinal cord also suggested a neural transmission pathway. Potential virulence determinants of the mouse-adapted strain, MP-4643, were located in the 5′ UTR (4 nucleotide changes), the capsid protein VP2 (3 nucleotide, and 1 amino acid changes) and in the protein 2C (8 nucleotide and 4 amino acid changes).

Chen et al. (2007) later demonstrated that retrograde axonal transport was likely to be a major transmission route of HEV71 into the CNS of infected mice. Following i.m. inoculation in the hindlimb, the virus was first detected in the lower segments of the spinal cord, followed by the upper segments and brain. By contrast, a reverse

pattern in which the virus was first detected in the upper segments of spinal cord was observed in mice inoculated in the forelimb. In addition, treatment of HEV71 infected mice with colchicine, a fast axonal transport inhibitor, was found to reduce HEV71 neuroinvasion in a dose-dependent manner.

Chua et al. (2008) also developed a mouse model for studies of HEV71 pathogenesis using a mouse-adapted variant of HEV71 (MP-26M). MP-26M was selected by serial passage of a HEV71 clinical isolate (HEV71-26M) in Chinese hamster ovary (CHO) cells and in newborn BALB/c mice. Infection of newborn BALB/c mice with MP-26M resulted in severe disease of high mortality in age-, dose- and route-of inoculation-dependent manner. By contrast, mice infected with HEV71-26M and CHO-adapted strain (CHO-26M) did not develop clinical signs of infection at any virus dose. Similar to the previous studies (Chen et al., 2007, Chen et al., 2004, Wang et al., 2004), MP-26M infection induced severe necrotizing myositis and skeletal muscle was found to be the primary site of replication in mice, containing the highest viral titre. The molecular basis of mouse adaptation of HEV71 in this model has been identified and described in detail in Chapter 5.

A more recent study by Ong et al. (2008) has characterised the neuropathology of a mouse model of HEV71 encephalomyelitis in more detail. The histopathological changes reported in the CNS were neuropil vacuolation and neuronal damage or loss with no inflammatory response (Ong et al., 2008). Spinal cord and brainstem, particularly the anterior horn cells, brainstem reticular formation and motor trigeminal nucleus, were the most severely affected parts of the CNS. There were no obvious neuronal abnormalities in the cerebral cortex, thalamus, hypothalamus,

cerebellum, dorsal root sensory and autonomic ganglia (Ong et al., 2008). Following i.m. inoculation, viral RNA and antigens were found in ipsilateral lumbar anterior horn cells and adjacent axons at 24-36 h post-infection and in upper cord motor neurons, brainstem, and contralateral motor cortex neurons at 48-72 h post-infection. Similar to the study by Chen et al. (2007), this study strongly suggested that a neural pathway is the primary transmission route of HEV71 into the CNS, with virus gaining entry into the CNS via peripheral motor nerves that innervate skeletal muscles. Similar to the previous studies (Chen et al., 2004, Wang et al., 2004), skeletal muscles were found to be the major sites of viral replication in mice.

1.3 Aim of this study

HEV71 has become an important human pathogen, causing epidemics of HFMD associated with severe neurological complications. However, little is known about the biology and pathogenesis of this virus. Research investigating positive-sense RNA viruses has been considerably advanced by the development of reverse genetic systems. With the introduction of defined genetic changes into full-length infectious-clone constructs, the role of viral specific genetic elements in viral replication and virulence can be determined. This information will provide a genetic basis for the development of a vaccine, and thus could shed light on ways to control this important pathogen.

The specific objectives of this study are:

1. To establish a reverse genetics system for HEV71
2. To identify the genome regions responsible for the growth phenotypes of HEV71

3. To determine the molecular basis of mouse adaptation by HEV71
4. To establish a mouse HEV71 oral infection model for future studies on pathogenesis and vaccine development.

CHAPTER TWO

MATERIALS AND METHODS

2.1 Cells, Viruses and Antibodies

2.1.1 Cell Lines

African green monkey kidney (Vero) cells (ATCC CCL-81), human rhabdomyosarcoma (RD) cells (ATCC CCL-136), SV40 transformed African green monkey kidney (COS-7) cells (ATCC CRL-1651), mouse neuroblastoma (NB41A3) cells (ATCC CCL-147), and Chinese hamster ovary (CHO) cells (ATCC CCL-61) were used in this study. All cell lines were grown at 37ºC in an atmosphere containing 5% CO_2/95% air. Growth medium for Vero, RD, COS-7 and CHO cells consisted of Dulbecco's modified Eagle's media (DMEM; MultiCel^{TM}) supplemented with 5% bovine growth serum (BGS; MultiSer^{TM}) and 2mM L-glutamine. Growth medium for NB41A3 cells contained Ham's F12 media (MultiCel^{TM}) supplement with 2mM L-glutamine, 15% horse serum (MultiSer^{TM}) and 2.5% BGS.

2.1.2 Viruses

HEV71 strain 6F/AUS/6/99 (HEV71-6F, GenBank Accession Number: DQ381846) and strain 26M/AUS/4/99 (HEV71-26M, GenBank Accession number EU364841) were isolated from patients during the 1999 Western Australian HFMD outbreak. Both strains were plaque purified on Vero cells. Isolated plaques were passaged on RD cells to increase the titre for use in subsequent assays. CHO-adapted (CHO-26M, GenBank Accession number EU376004) and mouse-adapted (MP-26M,

GenBank Accession number EU376005) variants of HEV71-26M were obtained from Dr. Beng Hooi Chua, Division of Virology, Telethon Institute for Child Health Research, Perth, Australia.

2.1.3 Antibodies

Rabbit anti-HEV71 polyclonal antibody was kindly provided by Professor Mary Jane Cardosa, Institute of Health & Community Medicine, University Malaysia Sarawak, Sarawak, Malaysia. A mouse anti-HEV71 monoclonal antibody reactive against the VP1 capsid protein of HEV71 was obtained from Chemicon, USA. Both anti-HEV71 polyclonal antibody and a mouse anti-HEV71 monoclonal antibody (Chemicon) were used for immunofluorescence assays.

2.2 Molecular biology

2.2.1 Plasmids

Plasmid vectors used for the construction of sub-genomic and/or full-length clones of HEV71 in this study were pGEM3Z (Promega), pBR322 (New England Biolabs), pMC18 (a derivative of pWSK29 kindly provided by Dr. Andrew Davidson, Monash University, Melbourne, Australia). Plasmid constructs pCMV-T7Pol expressing the T7 RNA polymerase, and pcDNA-lacZ expressing β-galactosidase (β-gal) enzyme, were provided by Dr. Rob Hurrelbrink, Division of Virology, Telethon Institute for Child Health Research, Perth, Australia. Plasmids pCMV-T7Pol and pcDNA-lacZ were used for co-transfection to rescue clone-derived virus, and for determination of transfection efficiency, respectively. Three bi-cistronic constructs, pCRHL, pCR6F and pCR26M were kindly provided by Dr. Chee Choy Kok, Discipline of Infectious

Disease and Immunology, The University of Sydney, Australia. The full-length cDNA clones generated in this study are listed in Table 2.4-2.6.

2.2.2 Bacterial strains

Escherichia coli strains DH5α (Invitrogen), DH10B (Invitrogen), XL1-blue (Stratagene) and XL10-gold (Stratagene) were used for transformations in this study.

2.2.3 Restriction endonuclease (RE) digestion

DNA was digested with appropriate restriction enzymes (Promega or New England Biolabs) according to the manufacturer's instructions. Generally, RE digestions were performed with an excess of enzyme at 37ºC for 1-4 h or overnight when the complete digestion of vector and insert DNA were required for cloning purposes.

2.2.4 Agarose gel electrophoresis

DNA samples for electrophoresis were mixed with dye loading buffer and loaded into wells of preformed agarose gel (Probiogen). DNA samples were separated by electrophoresis through 0.6-2% agarose gels depending on estimated product size. Gels were run at approximately 6 V/cm in 1xTAE buffer (1xTAE = 40mM Tris acetate, 1mM EDTA). A 1 kb ladder (GeneWorks) or 100 kb ladder (GeneWorks) was used as a molecular weight marker. DNA was visualised by exposure to UV light on a transilluminator (Bio-Rad) after staining in 10μg/mL of ethidium bromide solution (Bio-Rad).

2.2.5 Purification of DNA from agarose gels

For cloning or sequencing purposes, DNA samples were mixed with dye loading buffer and SYBR (Molecular Probes) before electrophoresis. DNA was visualised by exposure to visible light on a Dark Reader Transilluminator (Clare Chemical

Research) and the expected DNA band was excised from the gel. Purification of DNA from agarose gels was performed using a Qiaex II Gel Extraction Kit (Qiagen) according to the manufacturer's instructions.

2.2.6 Preparation of plasmid DNA

Small, medium or large scale preparations of plasmid DNA were performed using the Plasmid Mini Kit (Qiagen), Plasmid Midi Kit (Qiagen) or Plasmid Maxi Kit (Qiagen) respectively, according to the manufacturer's instructions.

2.2.7 DNA ligation

The plasmid vectors and insert DNA were digested with appropriate enzymes (Promega or New England Biolabs) according to the manufacturer's instructions. Ligation reactions were performed overnight at either 4ºC or 15ºC. Generally, insert to vector molar ratios of 1:1 or 3:1 were used. Standard ligation reactions contained either 50 or 100 ng of vector DNA, an appropriate amount of insert DNA, 30mM Tris-HCL pH7.8, 10mM $MgCl_2$, 10mM dithiothreitol (DTT), 1mM ATP and 1U of T4 DNA ligase (Promega).

2.2.8 Transformation of DNA into *Escherichia coli* (*E. coli*)

Electro-competent cells were prepared by the method of Siguret *et al.* (1994) and were stored in 15% glycerol at -80ºC until use. A 40 µL volume of cells was thawed on ice and approximately 1-5 µL of the DNA ligation mix was added to the cells. The mixture was then added to a 0.1 cm electroporation cuvette (Astral scientific) previously cooled on ice, and cells were electroporated using a BioRad GenePulsor™ apparatus (Bio-Rad) set at 1.25 kV, 200Ω resistance and 25 µF capacitance. One milliliter of prewarmed 2YT medium [1.6% tryptone (w/v), 0.5%

yeast extract (w/v), 85mM NaCl] or SOC medium [2% tryptone (w/v), 1% yeast extract (w/v), 8.5mM NaCl, 20mM glucose, 2.5mM KCl, 10mM $MgCl_2$] was immediately added to each cuvette and the mixture was transferred to a 1.5 eppendorf tube prior to incubation at 37ºC for 1 h with continuous shaking. The transformation mixture was subsequently plated onto 2YT agar (2YT medium plus 1.5%agar) containing appropriate antibiotics (ampicillin at 100 μg/mL or kanamycin at 50 μg/mL).

2.2.9 Isolation of viral RNA

Virus was propagated in cell culture until required. Cells were subjected to freeze-thaw for three times, and cell debris was separated by centrifugation at 3,000 rpm for 15 min, leaving virus in the supernatant. Viral RNA was then extracted using QIAamp® Viral RNA mini kit (Qiagen) according to the manufacturer's instructions, and eluted in 60 μL of AVE buffer.

2.2.10 Reverse transcription (RT) of viral RNA

(a) RT reaction using SuperScript™ II or SuperScript™ III reverse transcriptase (Invitrogen)

First strand cDNAs of viruses for subsequent cloning and sequencing were synthesised using SuperScript™ II or SuperScript™ III reverse transcriptase (Invitrogen). Reverse transcription reactions were carried out in 0.2 mL tubes in a reaction volume of 20 μL. A sample of 8 μL of viral RNA prepared as described in section 2.2.9 and 3 μL of an appropriate primer (30 pmol) were mixed and heated for 5 min at 65˚C before chilling on ice for 5 min. Five hundred micromoles of dNTPs, 1X concentration of enzyme buffer as supplied by the manufacturer, 10 mM DTT, 40 U of RNasin (Promega) and 200 U of SuperScript™ II or SuperScript™ III

reverse transcriptase were then added. The mixture was incubated at 42ºC for 1 h before inactivation of the enzyme by incubation at 70ºC for 15 min. One microliter of RNaseH (Promega) was added, and the mixture was incubated at 37ºC for 20 min. RT products were stored at -20ºC until required.

(b) RT reaction using M-MLV reverse transciptase (Promega)

First strand cDNAs of strain HEV71-6F and HEV71-26M for subsequent amplification and sequencing of VP1 gene were synthesised using M-MLV reverse transciptase (Promega). Seven microliters of extracted RNA (see section 2.2.9) were mixed with 100 pmol of primer NPIA, heated at 70˚C for 5 min followed by chilling on ice for 5 min. A mixture of 500 μM dNTPs, 1X concentration of enzyme buffer as supplied by the manufacturer, 80 U of RNasin (Promega) and 2 μL of M-MLV reverse transcriptase were then added to a final volume of 50 μL. The mixture was incubated at 42ºC for 1 h before incubation at 70ºC for 15 min. RT products were stored at -20ºC until used.

2.2.11 Polymerase Chain reaction (PCR)

(a) PCR reaction for cloning

Viral DNA fragments used for cloning were amplified by PCR using platinum *Taq* DNA polymerase High Fidelity (Invitrogen). The PCR was carried out in 0.2 mL tubes in a reaction volume of 25 μL. PCR reactions contained 10 pmol each of appropriate forward and reverse primer, 200 μM each of dATP, dTTP, dCTP and dGTP, 2 or 3 mM $MgSO_4$, 1 or 2.5 U of platinum *Taq* DNA polymerase High Fidelity, template first strand cDNA and 1x concentration of enzyme buffer as supplied by the manufacturer. The amplifications were performed in an automated thermocycler, with an initial denaturation at 94˚C for 2 min, followed by 40 cycles of

94˚C for 30 s, 55˚C for 30 s and 68˚C for 5 s, then a final incubation at 68˚C for 10 min.

(b) PCR reaction for sequencing

Viral DNA fragments used for sequencing were amplified using PCR supermix (Invitrogen). The PCR was carried out in 0.2 mL tubes in a reaction volume of 25 μL. PCR reactions contained 10 pmol each of appropriate forward and reverse primers, 22 μL of PCR supermix, and 1 μL of template first strand cDNA. Reactions were incubated for 2 min at 94˚C, then 40 cycles of 94˚C for 30 s, 55˚C for 30 s and 72˚C for 1 min, and finally incubated at 70˚C for 10 min. Primers used for sequencing in this study are listed in Table 2.1 and 2.2.

(c) PCR reaction for sequencing of VP1 gene

The PCR for amplification of VP1 gene was carried in 0.2 mL tube in a final volume of 50 μL. PCR reaction contained 10 pmol each of primers 159 and NPIA (Table 2.3), 200 μM dNTPs, 2 mM $MgSO_4$, 1 unit of Taq DNA polymerase (Invitrogen), 1 x concentration of enzyme buffer and 7 μL of viral cDNA. The PCR mixture was then incubated at 94˚C for 2 min, followed by 35 cycles of 94˚C for 1 min, 50˚C for 45 s and 72˚C for 2.5 min, then a final incubation at 72˚C for 10 min.

2.2.12 DNA sequencing

The nucleotide sequences of the PCR products or cloned DNA fragments were determined by automated DNA sequencing using Big dye-terminator sequencing technology. Sequencing was performed by Australian Genome Research Facility Ltd, University of Queensland, Brisbane, Queensland. Analysis of DNA

Table 2.1 Primers used for sequencing of full-length cDNA clones or clone derived virus of strain HEV71-6F and chimeric recombinant viruses

Primer Name*#	Nucleotide position†	Sequence (5′ - 3′)
EV71-1F	1 – 24	TTA AAA CAG CCT GTG GGT TGC ACC
EV71-488R	464 – 488	GTG CTC CGC AGT TAG GAT TAG CCG C
EV71-509F	510 – 536	GTG TGT CGT AAC GGG CAA CTC TGC AGC
EV71-747R	748 – 772	AGC GTT GTG TGG ACA CCT GTG AGC C
EV71-1258F	1,259 – 1,282	GGT CAG GGT TCT GCA TTC ACG TGC
EV71-1636R	1,613 – 1,639	GCG TCG CAC CTT GGT CAT AAT CTA ACG
EV71-1823F	1,824 – 1,849	CGG TGA AGT TAG AAA CTT GCT AGA GC
EV71-2225F	2,226 – 2,249	GAT CAG CAA CAC TCA CTA CAG AGC
EV71-2248R	2,225 – 2,250	GGA TCA GCA ACA CTC ACT ACA GAG CG
EV71-2490F	2,462 – 2,490	TTG AGA GTT CTA TAG GGG ACA GTG TGA GC
EV71-2717R	2,693 – 2,718	TAT CTC TCC AAC TAA TCC TGC TCT GC
EV71-3208F	3,209 – 3,238	ATG TCA GGG CGT GGA TAC CTC GCC CAA TGC
EV71-3607R	3,608 – 3,632	GCA AGC ATG AGA TGT GAC TGG TAT C
EV71-3783F	3,759 – 3,783	GGA TGA TGA GGC TAT GGA GCA GGG C
EV71-4260F	4,261 – 4,285	AAT CTC GAA CAG TCA GCA GCT TCG C
EV71-4408R	4,409 – 4,433	CGG TGT TTG CTC TTG AAC TGC ATG T
EV71-4867F	4,868 – 4,892	GGA GAG CAG CTA GGC TGT GCT CTG A
EV71-5579R	5,556 – 5,580	ATC TAC TAG CTC CAC AGC ATC TAC G
EV71-5878F	5,879 – 5,903	GCA ACG GTA GGC AAG GTT TCT GCG C
EV71-6020R	6,021 – 6,041	GCC TTC GAA CAC ATC GTG AAA GAC A
EV71-6235F	6,210 – 6,236	GAC CAC CAA GAT GAG CAT GGA GGA TGC
EV71-6656F	6,657 – 6,682	TCT CAG CCC AGT GTG GTT CAG GGC GC
EV71-7260R	7,237 – 7,261	TTG GAA CTG ATC TGA TTG TAC TCA C
Oligo-d$(T)_{24}$		TTT TGT ACA AGC $(T)_{24}$

\# Primers were designed by Dr. Robert Hurrelbrink, except Oligo-d$(T)_{24}$ primer.

* Forward primers are suffixed with "F" and reverse primers are suffixed with "R".

† Nucleotide position is based on HEV71-6F.

Table 2.2 Primers used for sequencing of full-length cDNA clones or clone derived virus strain HEV71-26M and chimeric recombinant viruses

Primer Name∗#	Nucleotide position†	Sequence (5′-3′)
EV71-1F	1 – 24	TTA AAA CAG CCT GTG GGT TGC ACC
26M-533F	536 – 557	CAG CGG AAC CGA CTA CTT TGG G
26M-1386F	1,389 – 1,412	CCC TCC TTA CAT ACA AAC GCA ACC
26M-1576R	1,558 – 1,579	GGT TCA GGG CAG AGT CGA AAG G
26M-1954F	1,957 – 1,990	GAA TTG TGT GCC GTG TTT AGG GCC
26M-2132R	2,112 – 2,135	CCA CCA GGA GGT GTA TAG GCT ATG
26M-2408F	2,411 – 2,436	CTA GTC ACA TAT TAC AGA CAG CCT CC
26M-2622R	2,599 – 2,625	CTC ATC ACT AGT ATT TGA CGA TGC CCC
26M-2806F	2,809 – 2,831	GTG GAG TTG TTC ACC TAC ATG CG
26M-3111R	3,090 – 3,114	CGC TCC ATA TTC AAG GTC TTT CTC C
26M-3451F	3,454 – 3,475	CTA GTG TCG TCT ACC ACT GCC C
26M-3519R	3,496, – 3522,	GTA CAC TCC TGT TTG ACA GTC ACA ACG
26M-3989F	3,992 – 4,013	TAG CTC TGA TAG GGT GCC ACG G
26M-4098R	4,077 – 4,101	CTT TTT AAG CCA GGA CGC ACT TTG C
26M-4591F	4,594 – 4,618	GTC ACG GTC ATG GAT GAC TTA TGT C
26M-4710R	4,689 – 4,713	AAC TCC TTT CTC TTC TAG GGA AGC C
26M-5264F	5,267 – 5,290	CAG TTG TGG CAG TCG TTT CAC TGG
26M-5389R	5,373 – 5,392	CCT GTA CTG TTG CCG TGC GG
26M-5992F	5,995 – 6,016	GGG CCA ACT CGC ACT AAG CTC G
26M-6109R	6,090 – 6,112	AAG CCT GCT CAA AAT CCA CCT CG
26M-6662F	6,665 – 6,688	GCC CTG TCT GGT TCA GAG CAT TGG
26M-6787R	6,768 – 6,790	GCA CAC AGT AAG TTT TGT TGC GG
26M-6787R	6,768 – 6,790	GCA CAC AGT AAG TTT TGT TGC GG

Primers were designed by Dr Beng Hooi Chua

∗ Forward primers are suffixed with “F” and reverse primers are suffixed with “R”.

† Nucleotide position is based on HEV71-26M.

chromatograms was performed using the program Chromas™ version 2.3 (Technelysium Pty Ltd., Australia).

2.2.13 Construction of full-length cDNA clones of HEV71

The strategy for construction of all full-length cDNA clones of HEV71 in this study was similar. Generally, first-strand cDNA fragments covering the full-length genome of HEV71 virus were synthesized from genomic viral RNA with SuperScript™ II or SuperScript™ III reverse transcriptase (Invitrogen), as described in section 2.2.10, plus an appropriate primer. cDNA fragments were then used for PCR amplifications to amplify the 5′ terminus and the 3′ terminus fragments of viral genome. The amplified products were then cloned into plasmid vectors to construct sub-genomic 5′ and 3′ half clones. With the use of unique restriction sites, the 5′ terminus and the 3′ terminus fragments from two sub-genomic clones were assembled into a genome length cDNA clone. Construction procedures of each full-length cDNA clone are described in detail below. A list of HEV71 full-length clones constructed during this study is provided in Table 2.4. Primers used for construction of all full-length cDNA clones of HEV71 are listed and described in Table 2.5.

2.2.13.1 Nucleotide numbering system

The nucleotide numbering in sub-genomic or full-length clones in this study is presented in the form of X^Y. X represents restriction enzyme sites and superscript Y represents the nucleotide position in the viral genome. For example, *Eco*RI^{1400} corresponds to the *Eco*RI restriction enzyme digestion site at nucleotide position 1400 of the viral genome.

2.2.13.2 Construction of a full-length cDNA clone of HEV71 strain 6F in a medium copy number plasmid, pBR322

The full genome sequence of HEV71-6F was obtained from Dr Rob Hurrelbrink (GenBank Accession Number: DQ381846) and is shown in the Appendix A. Primers used for construction of the full-length cDNA clones of HEV71-6F were designed from the published sequence. The numbering of nucleotides in sub-genomic and full-length clones corresponds to the published sequence in the GenBank database. The first-strand cDNA of HEV71-6F was synthesized from viral RNA using primer 6FMluI. Figure 2.1 shows the schematic diagram of the construction of the sub-genomic and full-length cDNA clones of HEV71-6F in pBR322.

(a) Construction of the 5′ half clone, pBR/5′-6F

A cDNA fragment of the 5′ terminus of viral genome spanning nucleotides 1- 4556 was synthesized by PCR using platinum *Taq* DNA polymerase High Fidelity (Invitrogen) and primers 6F01Fh and 6F04R. A unique *Sal*I restriction site, a T7 RNA polymerase promoter and GGG residues were incorporated into the forward primer, 6F01Fh, upstream of the 5′ terminus of the viral genome, and a unique *Aat*II restriction site was incorporated into reverse primer, 6F04R, downstream of nucleotide 4556 of the viral genome to facilitate the cloning. The PCR was carried out as described in section 2.2.11. The resultant PCR product was subsequently digested with *Sal*I and *Aat*II to excise a *Sal*I-*Aat*II fragment and the fragment was cloned into the *Sal*I and *Aat*II sites of predigested plasmid pBR322. The resultant clone, pBR/5′-6F, is 8,214 nucleotides in length.

Table 2.3 Primer pairs used for amplification and sequencing of full VP1 genes of HEV71

Primer Name#	Nucleotide position	Sequence (5′-3′)*
159	2385-2403	ACYATGAAAYTGTGCAAGG
NP1A	3355-3336	GCICCICAYTGITGICCRAA

Primers were designed by Brown et al., 1999.

- Y = C or T, R = A or G, I = inosine

Table 2.4 Full-length cDNA clones of HEV71 strain HEV71-6F and HEV71-26M

Plasmid clone	Derived virus	Description
pBR/HEV71-6F	Not obtained	Contains a T7 RNA polymerase promoter, GGG residues, viral cDNA of the HEV71-6F genome and 25 poly A; cloned into plasmid vector pBR322
pHEV71-6F	CDV-6F	Contains a T7 RNA polymerase promoter, GG residues, viral cDNA of the HEV71-6F genome and 25 poly A; cloned into plasmid vector pMC18
pHEV71-26M	CDV-26M	Contains a T7 RNA polymerase promoter, GG residues, viral cDNA of the HEV71-26M genome and 25 poly A; cloned into plasmid vector pMC18

Table 2.5 Primers used for construction of full-length cDNA clones of HEV71-6F and HEV71-26M

Primer Name	Nucleotide Sequence (5′-3′)	Special features
6F01Fh	AAG CTT GCA TGC **GTC GAC** ***TAA TAC GAC TCA CTA TA*** **GG**T TAA AAC AGC CTG TGG GTT G	Contains a *Sal*I site (GTCGAC), a T7RNA polymerase promoter, GG residues immediately upstream of the 5′ terminus of viral sequence
6F-5′FT7g	GGC TGT **GTC GAC** ***TAA TAC GAC TCA CTA TA*** **G** TTA AAA CAG CCT GTG GGT TGC	Contains a *Sal*I site, a T7RNA polymerase promoter, G residue immediately upstream of the 5′ terminus viral sequence
6F-5′T7GG	GGC TGT **GTC GAC** ***TAA TAC GAC TCA CTA TA*** **G** **G**TT AAA ACA GCC TGT GGG TTG C	Contains a *Sal*I site, a T7RNA polymerase promoter, GG residues immediately upstream of the 5′ terminus viral sequence
6F02R	GGA TCC GAC GTC **ACG CGT** ***TTT TTT TTT TTT TTT TTT TTT TTT*** GCT ATT CTG GTT	Contains *Aat*II (GACGTC) and *Mlu*I (ACGCGT) sites, 25 polyA at the 3′ terminus of viral sequence
6F03F	AAG CTT **GTC GAC** TCC GGA CCC AGA CCA CTT TGA CGG	Contains a *Sal*I site adjacent to viral sequence
6F04R	AAG CTT **GAC GTC** TCC GGA GGT AAG GAA TAC ACA CTG	Contains *Aat*II site adjacent to viral sequence
6FMID	TCT AGA **GAA TTC** TCC GGA GGT AAG GAA TAC ACA CTG	Contains *Eco*RI (GAATTC) site adjacent to viral sequence
6F-MluI	CCG CGG GAA TTC **ACG CGT** *TTT TTT TTT TTT TTT TTT TTT TTT* GCT ATT CTG GTT	Contains *Eco*RI and *Mlu*I sites, 25 polyA at the 3′ terminus of viral sequence
26M-2806F	GTG GAG TTG TTC ACC TAC ATG CG	No special features
26M-3111R	CGC TCC ATA TTC AAG GTC TTT CTC C	No special features
CA16-3′MluI	GAT CCC CGG GGC GGC CGC **ACG CGT** *TTT TTT* TTT *TTT TTT TTT TTT TTT T*GC TAT TCT GG	Contains *Not*I (GCGGCCGC) and *Mlu*I sites, 26 polyA at the 3′ terminus of viral sequence

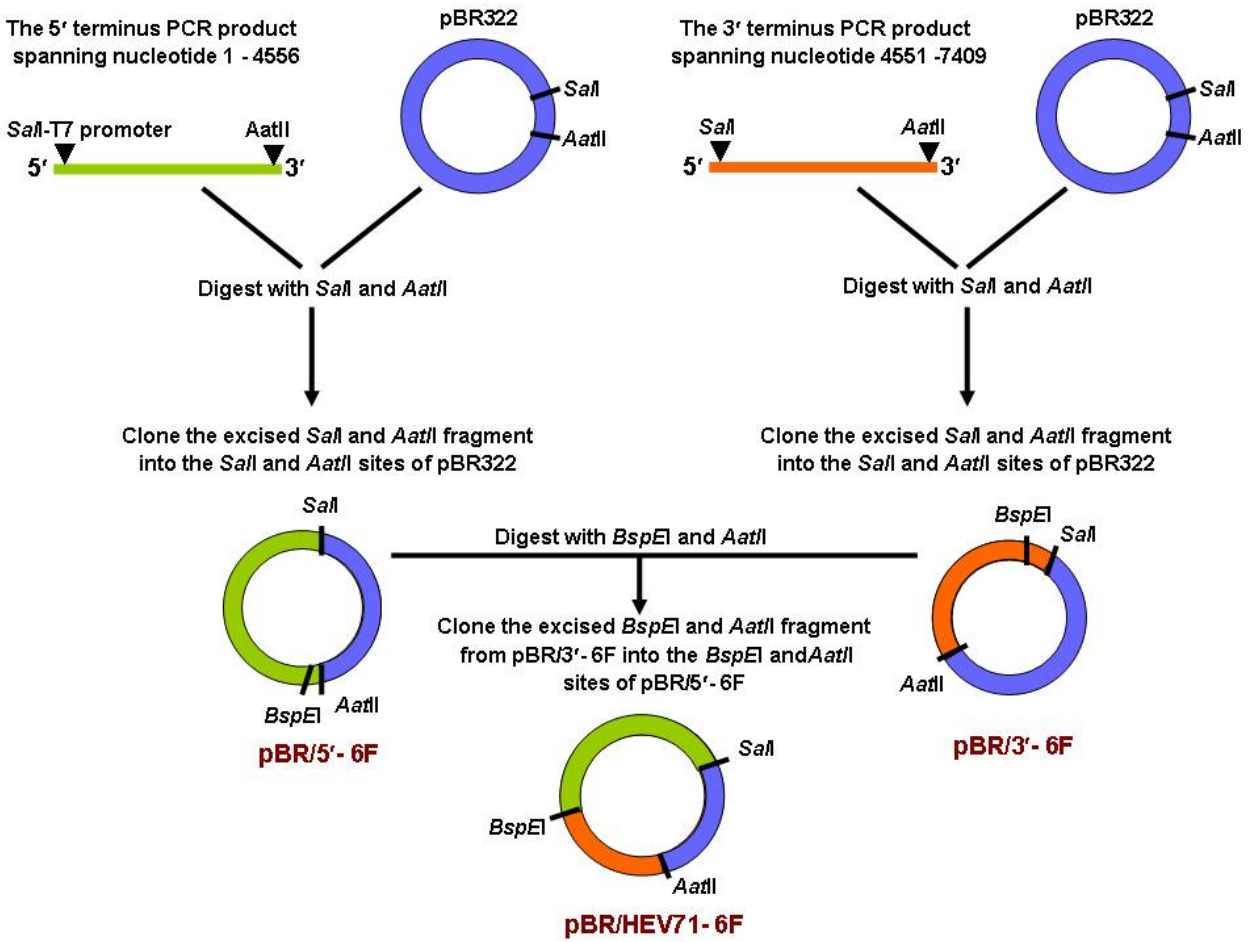

Figure 2.1 The schematic diagram of the construction of the sub-genomic and full-length cDNA clones of HEV71-6F in pBR322.

(b) Construction of the 3′ half clone, pBR/3′-6F

A 3′ terminus fragment spanning nucleotides 4551-7409 of the viral genome and 25 poly A tail was amplified by PCR using primers 6F03F and 6F02R. A unique *Sal*I site was incorporated into the forward primer, 6F03F, upstream of nucleotide 4551, and *Mlu*I and *Aat*II sites were incorporated into the reverse primer, 6F02R, downstream of the poly A tail. The PCR was performed using the conditions described in section 2.2.11. The PCR product was then digested with *Sal*I and *Aat*II. The excised *Sal*I-*Aat*II fragment was subsequently cloned into *Sal*I and *Aat*II sites of plasmid pBR322. The resultant clone, pBR/3′-6F, is 6,528 nucleotides in length.

(c) Construction of the full-length cDNA clone, pBR/HEV71-6F

The full-length clone pBR/HEV71-6F was constructed by excising a *BspE*I^{4551}-*Aat*II fragment from clone pBR/3′-6F and then the fragment was cloned into the *BspE*I^{4551}-*Aat*II sites of clone pBR/5′-6F. The resultant clone was 11,097 nucleotides in length and contained a T7 RNA polymerase promoter and additional G residues (2G or 3G) upstream of the viral cDNA and 25 poly A tail.

2.2.13.3 Construction of a full-length cDNA clone of HEV71 strain 6F in a low copy number plasmid, pMC18

The steps involved in the construction of sub-genomic and full-length cDNA clones of HEV71-6F in pMC18 are shown in Figure 2.2.

(a) Construction of the 5′ half clone, pMC/5′-6F

A 5′ terminus fragment of the viral genome spanning nucleotides 1-4551 was generated by PCR as described in section 2.2.11. Forward primers, 6F-5′ T7GG or 6F-5′ T7G, and reverse primer, 6F-MID, were used in the PCR reaction. *Sal*I

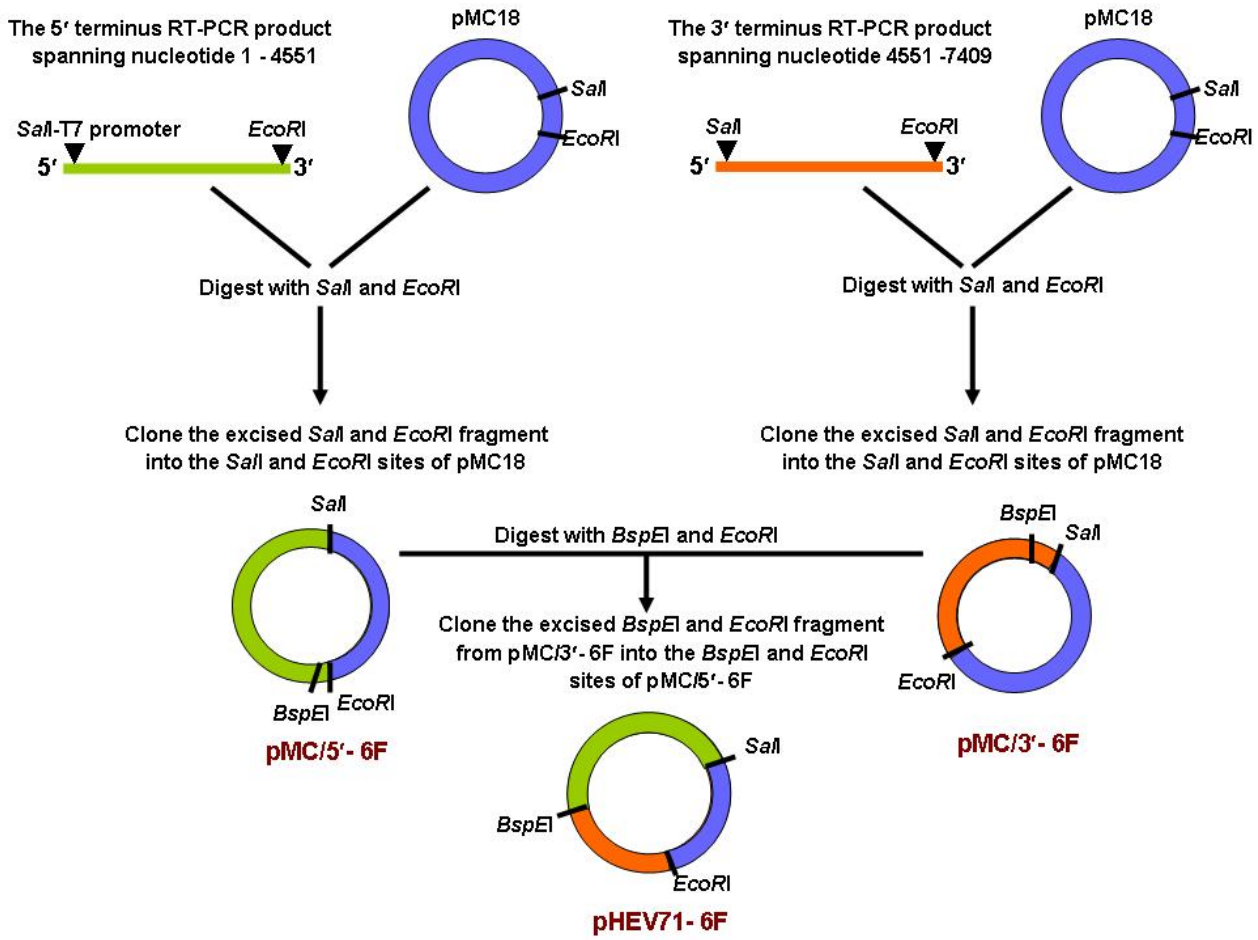

Figure 2.2 The schematic diagram of the construction of the sub-genomic and full-length cDNA clones of HEV71-6F in pMC18.

restriction site, T7 RNA polymerase promoter and G residues (1G or 2G) were incorporated into the forward primer upstream of the viral genome, and *EcoR*I site was added into the reverse primer downstream of nucleotide 4551. The PCR product was digested with *Sal*I and *EcoR*I, and the fragment cloned into plasmid pMC18 at the *Sal*I and *EcoR*I sites. The resultant clone, pMC/5′-6F, is 9,952 nucleotides in length.

(b) Construction of the 3′ half clone, pMC/3′-6F

A 3′ terminal covering nucleotides 4551-7409 of the viral genome and 25 poly A tail was amplified using primers 6F03F and 6FMluI, with *Sal*I and *EcoR*I sites were incorporated into forward and reverse primers, respectively. PCR conditions were as described in 2.2.11. The PCR product was digested with *Sal*I and *EcoR*I, and the excised fragment was then cloned into *Sal*I- and *EcoR*I-predigested pMC18. The resultant clone, pMC/3′-6F, is 8,272 nucleotides in length.

(c) Construction of the full-length clone, pHEV71-6F

The genome-length clone pHEV71-6F was constructed by excising a *BspE*I^{4551}-*EcoR*I fragment from clone pMC/3′-6F and then cloned into the *BspE*I^{4551}-*EcoR*I sites of clone pMC/5′-6F. The resultant clone was 12,835 nucleotides in length and contained a T7 RNA polymerase promoter and additional GG or G residues upstream of the viral cDNA.

2.2.13.4 Construction of a full-length cDNA clone of HEV71 strain 26M in low copy number plasmid, pMC18

The full genome sequence of HEV71-26M was kindly provided by Beng Hooi Chua, Division of Virology, Telethon Institute for Child Health Research, Perth, Australia

(GenBank Accession number EU364841). The numbering of nucleotides in sub-genomic and full-length clones corresponds to the viral genome sequence as shown in the Appendix A. Figure 2.3 is a schematic diagram of the construction of the sub-genomic and full-length cDNA clones of HEV71-26M in pMC18.

(a) Construction of the 5′ half clone, pMC/5′-26M

A cDNA copy of the 5′ terminus spanning nucleotides 1-3114 was generated by PCR. PCR reactions were similar to the conditions described in 2.2.11, except that the primers 6F-5′ T7GG, and 26M-3111R were used in amplification. Restriction enzymes *Sal*I and *EcoR*I were then used to digest the PCR product, and then a *Sal*I-*EcoR*I^{2842} fragment was cloned into *Sal*I- and *EcoR*I-predigested pMC18. The resultant clone, pMC/5′-26M, is 8,237 nucleotides in length.

(b) Construction of the 3′ half clone, pMC/3′-26M

A cDNA fragment covering nucleotides 2809-7409 of the viral genome and 25 poly A tail was amplified by PCR using primers 26M-2806F and CA16-3′MluI. A unique *Not*I restriction enzyme site was incorporated into the reverse primer downstream of the polyA tail for cloning. The fragment PCR was cut by *EcoR*I and *Not*I restriction enzymes, and a *EcoR*I^{2842}-NotI fragment was cloned into pMC18 at the *EcoR*I and *Not*I sites. The resultant clone, pMC/3′-26M, is 9,964 nucleotides in length.

(c) Construction of the full-length clone, pHEV71-26M

The full-length cDNA clone, pHEV71-26M was constructed by excising a *Sal*I-*EcoR*I^{2842} fragment from clone pMC/5′-26M and then cloned into the *Sal*I-*EcoR*I^{2842} sites of clone pMC/3′-26M. The resultant clone is 12,803 nucleotides in length and

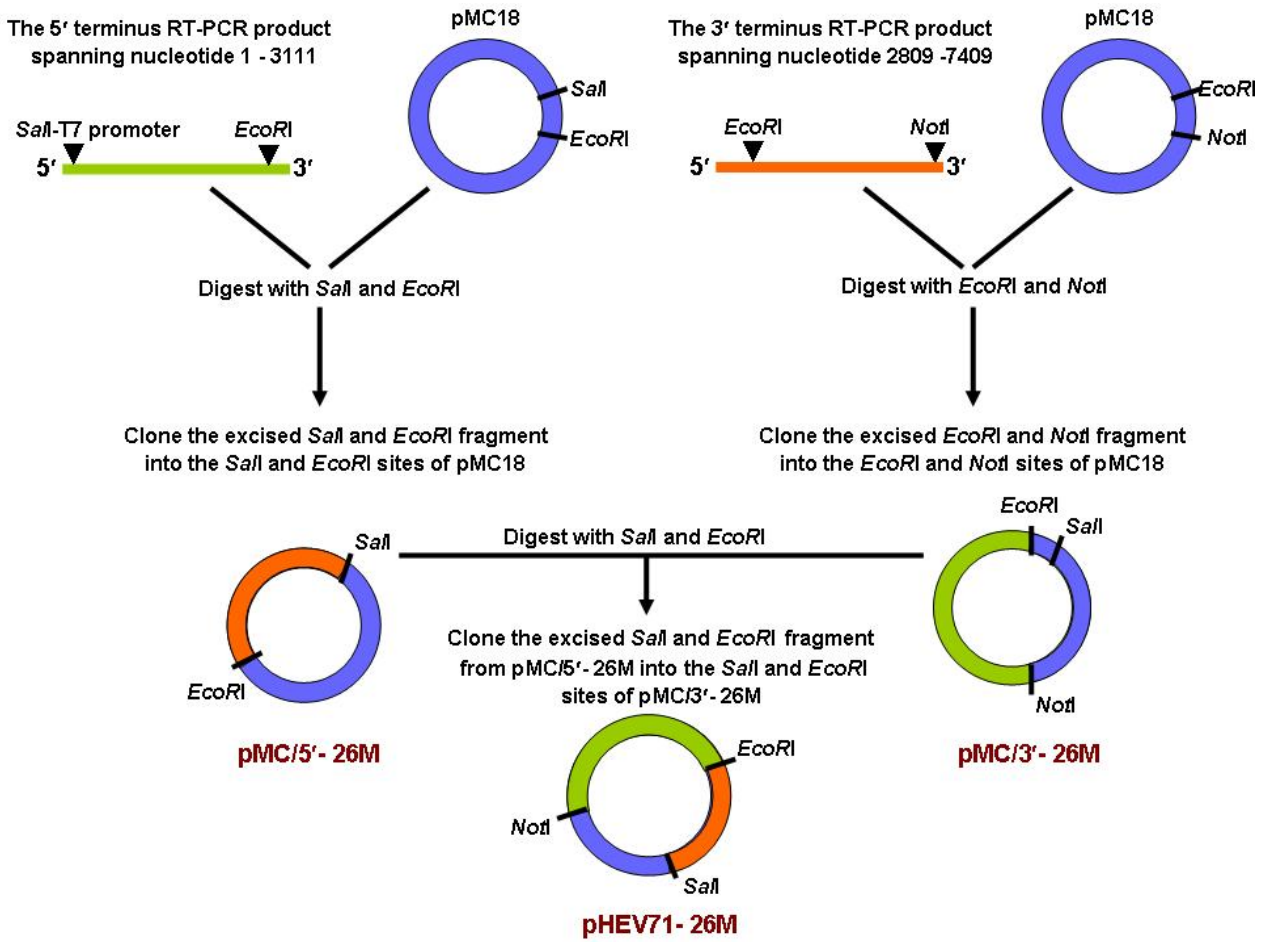

Figure 2.3 The schematic diagram of the construction of the sub-genomic and full-length cDNA clones of HEV71-26M in pMC18.

contains a T7 RNA polymerase promoter and additional GG residues upstream of the viral cDNA.

2.2.14 Construction of chimeric recombinant viruses between HEV71-6F and HEV71-26M

To identify the molecular determinants affecting phenotypic differences between strains HEV71-6F and HEV71-26M, a collection of chimeric recombinant viruses, exchanging the corresponding 5′ UTR, structural protein genes (P1 region), and non-structural protein genes (P2 and P3 regions) between these two strains, were constructed. In order to design the constructs, the full genome sequences of both strains were compared and found to have 80% nucleotide sequence identity. All chimeric recombinant viruses were constructed using fusion PCR and/or site-directed mutagenesis, and plasmids pHEV71-6F and pHEV71-26M were used as the templates. The list of chimeric recombinant constructs is shown in Table 2.6. The construction procedures of each clone are described in detail below. Primers used for construction of all chimeric recombinant clones are listed and described in Table 2.7.

2.2.14.1 Naming system

The name of the recombinant constructs is presented in the form pA/B/C, where A is a backbone virus, B is the exchanged genomic region, and C is the name of virus providing the exchanged genomic region. For example**,** plasmid p6F/5′UTR/26M contains 5′ UTR from HEV-26M, while the rest of the viral cDNA genome is from HEV71-6F.

Table 2.6 Chimeric recombinant clones between HEV71-6F and HEV71-26M

Plasmid clone	Derived virus	Description*
p6F/5′UTR/26M	CDV-6F/5′UTR/26M	Contains **5′UTR of 26M**, P1 of 6F, P2 and P3 of 6F
p26M/5′UTR/6F	CDV-26M/5′UTR/6F	Contains **5′UTR of 6F**, P1 of 26M, P2 and P3 of 26M
p6F/P1/26M	CDV-6F/P1/26M	Contains 5′UTR of 6F, **P1 of 26M**, P2 and P3 of 6F
p26M/P1/6F	CDV-26M/P1/6F	Contains 5′UTR of 26M, **P1 of 6F**, P2 and P3 of 26M
p6F/NS/26M	CDV-6F/NS/26M	Contains 5′UTR of 6F, P1 of 6F, **P2 and P3 of 26M**
p26M/NS/6F	CDV-26M/NS/6F	Contains 5′UTR of 26M, P1 of 26M, **P2 and P3 of 6F**

*****All plasmid clones contain a T7 RNA polymerase promoter, GG residues, 25 poly A; cloned into plasmid vector pMC18

Table 2.7 Primers used for construction of chimeric recombinant viruses between HEV71-6F and HEV71-26M

Primer Name	Nucleotide Sequence (5´-3´)*	Special features
6FIRES26MF	ACA GTC AAA CAT GGG CTC ACA GGT GTC CAC	No special features
6FIRES26MR	TAC CCG ATC GCT GTA ACC AC	No special features
6F-5′T7GG	GGC TGT **GTC GAC** ***TAA TAC GAC TCA CTA TAG*** **G** GTT AAA ACA GCC TGT GGG TTG C	Contains a *Sal*I site, a T7RNA polymerase promoter, GG residues immediately upstream of the 5′ terminus viral sequence
26MIRES6FF	CACAACCAAAT ATGGGCTCACAAGTGTCTAC	No special features
26M-1576R	GGT TCA GGG CAG AGT CGA AAG G	No special features
6FBlnIF	CGC ACA GCT ATC ACC ACC CT***A*** GGG AAA TTT G	Contains a single point mutation A to introduce *Bln*I site (CCTAGG)
6FBlnIR	AGG GTG GTG ATA GCT GTG CGA CTG GCA CCA	No special features
26MBlnIF	GTA CTG CCA TTA CTA CCC T***A***G GAA AGT TCG	Contains a single point mutation A to introduce *Bln*I site (CCTAGG)
26MBlnIR	AGG GTA GTA ATG GCA GTA CGG CTA GTG CCG	No special features
6FP126MR	GTA GAC ACT TGT GAG CCC ATA TTT GGT TGT G	No special features
6FP126MR2	CCA AAT TTC **CCT AGG** GTA GTA ATG GCA	Contains *Bln*I site
26MP16FR	GTG GAC ACC TGT GAG CCC ATG TTT GAC TGT A	No special features
26MP16FR2	TGT CCA AAT TTC **CCT AGG** GTG GTG ATA GCT G	Contains *Bln*I site

*26M sequences are underlined. Restriction sites are in bold font.

2.2.14.2 Nucleotide numbering system

The numbering of nucleotides in sub-genomic and full-length clones corresponds to the viral genome sequences as shown in the Appendix A. Nucleotide numbering is presented in the form X^{YZ}, where X is the restriction enzyme site, and superscript Y is the name of the virus, and superscript Z is the nucleotide position.

2.2.14.3 Construction of the chimeric virus cDNA clone, p6F/5′UTR/26M

Chimeric virus cDNA clone p6F/5′UTR/26M was constructed using fusion PCR and molecular cloning. A fragment containing part of the 5′ UTR of 26M (10 nt) and part of the 6F P1 region (246 nt) was amplified by PCR, as described in section 2.2.11, using pHEV71-6F as template DNA. Forward primer, 6FIRES26MF, contained 10 bp of the 3′ end of 26M 5′ UTR adjacent to 20 bp of the 5′ end of 6F P1 region, and the reverse primer, 6FIRES26MR, contained 6F P1 region that has a *BbvC*I^{6F961} restriction site for cloning. The resultant PCR product was purified and used as a reverse primer for a second round PCR, in which primer 6F-5′ T7GG was used as a forward primer to amplify the whole 26M 5′ UTR from pHEV71-26M template. Fusion PCR product was digested with *Sal*I and *BbvC*I^{6F961}, and a *Sal*I-*BbvC*I^{6F961} fragment was cloned into *Sal*I- and *BbvC*I^{6F961}-predigested plasmid pHEV71-6F in a three-fragment ligation reaction.

2.2.14.4 Construction of the chimeric virus cDNA clone p26M/5′UTR/6F

Chimeric virus cDNA clone p26M/5′UTR/6F was constructed using a similar strategy to p6F/5′UTR/26M. The first round PCR was performed using primers

26MIRES6FF and 26M-1576R. PCR conditions were as described in 2.2.11, with pHEV71-26M used as template DNA. Forward primer, 26MIRES6FF, contained 11 bp of the 3′ end of 6F 5′ UTR and 20 bp of the 5′ end of 26M P1 region. The reverse primer, 26M-1569R was part of 26M P1 region. The second round PCR to amplify a full 5′ UTR of 6F from pHEV71-6F template was performed using forward primer, 6F-5′ T7GG, and gel-purified first round PCR product as a reverse primer. The fusion PCR product was digested with *Sal*I and *Bsiw*I^{26M1442}, and a *Sal*I-*Bsiw*I^{26M1442} fragment was cloned into *Sal*I- and *Bsiw*I^{26M1442}-predigested plasmid pHEV71-26M.

2.2.14.5 Construction of pHEV71-6FBlnI and pHEV71-26MBlnI

To facilitate the construction of other chimeric recombinant viruses, a *Bln*I restriction site was introduced into the parental clones, pHEV71-6F and pHEV71-26M at the P1/P2 junction by site-directed mutagenesis. Briefly, a *Pst*I^{6F530}-*BamH*I^{6F5864} fragment of pHEV71-6F was excised and then sub-cloned into pGEM3Z. The resultant clone, pGEM3Z-6F was 8,059 nucleotides in length. An *EcoR*I^{26M2842} - *EcoR*V^{26M4819} fragment of pHEV71-26M, spanning the 26M P1 and P2 regions, was sub-cloned into pBR322. The resultant clone, pBR-26M, was 6,151 nucleotides in length. Both sub-genomic clones, pGEM3Z-6F and pBR-26M, were then methylated using *Hpa*I methylase enzyme. The methylation reaction contained plasmid DNA (100 ng), 1XSAM, 1X methylation buffer as supplied by the manufacturer and 4 units *Hpa*I methylase. The reaction was incubated at 37˚C for 4 h before incubation at 65˚C for 15 min to inactivate the enzyme. Methylated plasmids were then used for subsequent PCR mutagenesis reactions.

Mutagenesis was achieved by designing a forward primer for PCR containing a single C to A transition mutation at nucleotide position 3,330 for HEV71-6F and T

to A mutation at nucleotide position 3,333 for HEV71-26M. This mutation did not change the encoded amino acid sequence of either strain. PCR conditions are described below.

DNA template (100 ng of methylated pGEM3Z-6F or pBR-26M), 10 μM each of primers (primers 6FBlnIF and 6FBlnIR or primer 26MBlnIF and 26MBlnIR), 200 μM of dNTP's, 2.5 U of platinum *Taq* DNA polymerase High Fidelity, and 1x concentration of enzyme buffer (as supplied by the manufacturer) were combined in a final volume of 50 μL. The amplifications were performed in an automated thermocycler, with an initial denaturation at 94˚C for 2 min, followed by 20 cycles of 94˚C for 30 s, 55˚C for 30 s and 68˚C for 5 s, then a final incubation at 68˚C for 10 min. One hundred nanograms of PCR products were then transformed into *E. coli* strain XL1-blue. Plasmids pGEM3Z-6F and pBR-26M with an introduced *Bln*I site were screened by restriction enzyme digestion and sequencing and positive clones selected. Plasmid pGEM3Z-6F+*Bln*I site was digested with *Stu*I and *BspE*I to excise a *Stu*I^{6F1689}-*BspE*I^{6F4551} fragment. This fragment was then cloned back into pHEV71-6F to generate pEV71-6FBlnI. Plasmid pBR-26M+*Bln*I was digested with *Kpn*I and *EcoR*V. The excised *Kpn*I^{26M3062}-*EcoR*V^{26M4819} fragment was cloned back into pHEV71-26M to create pHEV71-26MBlnI.

2.2.14.6 Construction of the chimeric virus cDNA clone p6F/P1/26M

Construction of the chimeric virus cDNA clone p6F/P1/26M was performed using fusion PCR. The 796 nt fragment containing 6F 5′ UTR adjacent to the 5′ terminus (20 nt) of 26M P1 was amplified by PCR using primer 6F-5′ T7GG and a reverse

primer 6FP126MR. This gel purified fragment was then used in the second round PCR as a forward primer and 6FP126MR2 (containing a *Bln*I site) was used as a reverse primer. Both PCR reactions were performed in the conditions described in 2.2.11. The fusion PCR product was 3,362 nt in length and contained 6F 5′UTR and 26M P1. The PCR product was digested with *Sal*I and *Bln*I^{26M3333}, and a gel purified *Sal*I-*Bln*I fragment cloned into pHEV71-6FBlnI to generate p6F/P1/26M.

2.2.14.7 Construction of the chimeric virus cDNA clone p26M/P1/6F

Chimeric virus cDNA clone p26M/P1/6F was constructed using a similar procedure to the construction of p6F/P1/26M. Primers 6F-5′ T7GG and 26MP16FR were used in the first round PCR. The 799 nt PCR product containing 26M 5′ UTR adjacent to the 5′ terminus (20 nt) of 6F P1 was used for a second round PCR with a reverse primer, 26MP16FR2. The fusion PCR product was 3,365 nt in length and contained 26M 5′ UTR and 6F P1. The product was digested with *Sal*I and *Bln*I, and a gel purified *Sal*I-*Bln*I^{6F3330} fragment was then cloned into pHEV71-26MBlnI to generate p26M/P1/6F.

2.2.14.8 Construction of the chimeric virus cDNA clone p6F/NS/26M

Chimeric virus cDNA clone p6F/NS/26M was constructed by digestion of plasmid pHEV71-26MBlnI with *Bln*I and *Mlu*I. The excised *Bln*I^{26M3333}-*Mlu*I fragment was then cloned into *Bln*I6F^{3330}-and *Mlu*I-predigested plasmid pHEV71-6FBlnI to produce p6F/NS/26M.

2.2.14.9 Construction of the chimeric virus cDNA clone p26M/NS/6F

Chimeric virus cDNA clone p26M/NS/26M was constructed by digestion of plasmid pHEV71-6FBlnI with *Bln*I and *Mlu*I. The excised *Bln*I^{6F3330}-*Mlu*I fragment was then cloned into *Bln*I^{26M3333}-and *Mlu*I-predigested pHEV71-26MBlnI to produce p26M/NS/6F.

2.2.15 Construction of the chimeric recombinant viruses between the parental strain HEV71-26M and its mouse-adapted strain (MP-26M)

To identify genetic determinants of mouse adaptation and virulence, chimeric recombinant viruses between the parental strain 26M and its mouse-adapted strain, MP-26M were constructed. pHEV71-26M was used as a backbone plasmid, and one, two or three mutations of MP-26M were introduced into the clone at the corresponding sites to produce mutant viruses. The list of recombinant clones is shown in Table 2.8. The clone construction methods included RT-PCR of mouse-adapted virus, restriction enzyme digestion and cloning, as described in detail below. Primers used for construction of all chimeric recombinant viruses between HEV71-26M and MP-26M are listed and described in Table 2.9.

2.2.15.1 Naming system

The name of the recombinant constructs is presented in the form pA-Bm (one mutation) or pA-B-Cm (two mutations) where A is a backbone virus HEV71-26M, and B and C are the genomic regions containing amino acid substitutions of MP-26M. For example**,** plasmid p26M-VP2m contains an amino acid substitution of

Table 2.8 Chimeric recombinant clones between HEV71-26M and MP-26M

Plasmid clone	Derived virus	Description*#
p26M-VP2m	CDV-26-VP2m	Contains viral cDNA of the 26M genome with a mutation in the VP2 protein
p26M-VP1m	CDV-26M-VP1m	Contains viral cDNA of the 26M genome with a mutation in the VP1 protein
p26M-2Cm	CDV-26M-2Cm	Contains viral cDNA of the 26M genome with a mutation in the 2C protein
p26M-VP1-2Cm	CDV-26M-VP1-2Cm	Contains viral cDNA of the 26M genome with mutations in the VP1 and 2C proteins
p26M-VP2-2Cm	CDV-26M-VP2-2Cm	Contains viral cDNA of the 26M genome with mutations in the VP2 and 2C proteins
p26M-VP2-VP1m	CDV-26M-VP2-VP1m	Contains viral cDNA of the 26M genome with mutations in the VP2 and VP1 proteins
pMP-26M	CDV-MP-26M	Contains viral cDNA of the 26M genome with mutations in the VP2, VP1 and 2C proteins

*****All plasmid clones contain a T7 RNA polymerase promoter, GG residues, 25 poly A; cloned into plasmid vector pMC18

VP2 mutation is at nucleotide A1400→T or amino acid K218→I.
VP1 mutation is at nucleotide G2876→A or amino acid G710→E.
2C mutation is at nucleotide A4727→G or amino acid K1327→R.

Table 2.9 Primers used for construction of chimeric recombinant viruses between HEV71-26M and MP-26M

Primer Name	Nucleotide Sequence (5´-3´)	Special features
26M-553F	CAG CGG AAC CGA CTA CTT TGG G	No special features
26M-2806F	GTG GAG TTG TTC ACC TAC ATG CG	No special features
26M-3111R	CGC TCC ATA TTC AAG GTC TTT CTC C	No special features
CA16-3′MluI	GAT CCC CGG GGC GGC CGC **ACG CGT** *TTT TTT* TTT *TTT TTT TTT TTT TTT T*GC TAT TCT GG	Contains *Not*I and *Mlu*I sites, 26 polyA at the 3′ terminus of the viral sequence

MP-26M in the VP2 protein. The full-length cDNA clone of MP-26M (three mutations) was named pMP-26M.

2.2.15.2 Nucleotide numbering system

The numbering of nucleotides in sub-genomic and full-length clones corresponds to the viral genome sequences, as shown in the Appendix A. Nucleotide numbering is present in the form X^Y, where X is the restriction enzyme site, and superscript Y is the nucleotide position that is identical between these two strains.

2.2.15.3 Construction of the chimeric virus cDNA clone p26M-VP2m

The first strand cDNA of the mouse-adapted strain, MP-26M, was generated using SuperScript^{TM} III reverse transcriptase (Invitrogen) as described in 2.2.10 with primer CA16-*Mlu*I. A fragment of nucleotide 533-3111 was then amplified by PCR using primers 26M-533F and 26M-3111R. The PCR fragment was digested with *Hind*III and *Eco*RI, and a *Hind*III^{968}-*Eco*RI^{2842} digested fragment was then sub-cloned into *Hind*III- and *Eco*RI- predigested pBR322. The resultant plasmids, pBRMP-VP2, were screened by restriction enzyme digestion and sequencing. A positive clone, pBRMP-VP2, was digested with *Hind*III and *Bsiw*I, and then the excised *Hind*III^{968}-*Bsiw*I^{1442} fragment cloned into the corresponding fragment of pHEV71-26M to produceHEV71-26M with the VP2 mutation (nt A1400→T or aa K218→I).

2.2.15.4 Construction of the chimeric virus cDNA clone p26M-VP1m

Clone p26M-VP1m was constructed by PCR amplification of a 4,654 fragment of MP-26M using primers 26M-2806F and CA16-3′*Mlu*I. An *EcoR*I^{2842} - *EcoR*V^{4819} digested PCR fragment was sub-cloned into pBR322. The resultant clones, pBRMP were screened by restriction enzyme digestion and sequencing. Clone pBRMP was digested with *EcoR*I and *Kpn*I, and the excised *EcoR*I^{2842}- *Kpn*I^{3062} fragment cloned into the corresponding fragment of pHEV71-26M to produce HEV71-26M with the VP1 mutation (nt G2876→A, aa G710→E).

2.2.15.5 Construction of the chimeric virus cDNA clone p26M-2Cm

Clone p26M-2Cm was constructed from plasmids pBRMP and pEV71-26M. Both plasmids were digested with *Kpn*I and *EcoR*V. An excised *Kpn*I^{3062}- *EcoR*V^{4819} fragment from pBRMP was cloned into *Kpn*I^{3062}- and *EcoR*V^{4819}- predigested plasmid pHEV71-26M to produce HEV71-26M with the 2C mutation (nt A4727→G, aa K1327→R).

2.2.15.6 Construction of the chimeric virus cDNA clone p26M-VP1-2Cm

To construct clone p26M-VP1-2Cm, plasmids pBRMP and pHEV71-26M were digested with *EcoR*I and *EcoR*V. An excised *EcoR*I^{2842}-*EcoR*V^{4819} fragment from pBRMP was cloned into *EcoR*I^{2842}- and *EcoR*V^{4819}-predigested plasmid pHEV71-26M to generate mutant HEV71-26M with the VP1 and 2C mutations.

2.2.15.7 Construction of the chimeric virus cDNA clone p26M-VP2-2Cm

Clone p26M-VP2-2Cm was constructed from plasmids pBRMP and p26M-VP2m. Both plasmids were digested with *Kpn*I and *EcoR*V. An excised *Kpn*I^{3062}-*EcoR*V^{4819} fragment from pBRMP was cloned into *Kpn*I^{3062}- and *EcoR*V^{4819}-predigested plasmid p26M-VP2m.

2.2.15.8 Construction of the chimeric virus cDNA clone p26M-VP2-VP1m

Clone p26M-VP2-VP1m was constructed from plasmids pBRMP and p26M-VP2m. Plasmid pBRMP was digested *EcoR*I and *Kpn*I, and the excised *EcoR*I^{2842}- *Kpn*I^{3062} fragment was cloned into the corresponding fragment of p26M-VP2m to produce mutant HEV71-26M with the VP2 and VP1 mutations.

2.2.15.9 Construction of the chimeric virus cDNA clone pMP-26M

A full-length clone of MP-26M was constructed from plasmids pBRMP-VP2 and p26M-VP1-2Cm. Both plasmids were digested with *Hind*III and *Bsiw*I. An excised *Hind*III^{968}-*Bsiw*I^{1442} fragment from pBRMP-VP2 was cloned into *Hind*III^{968}- and *Bsiw*I^{1442} –predigested plasmid p26M-VP1-2Cm.

2.2.16 *In vitro* transcription (IVT) of viral RNA from a cDNA template

Plasmids containing full-length HEV71 cDNA were linearlised with *Mlu*I for at least 4 h, followed by incubation at 50ºC with proteinase K (200 μg/mL) and SDS (0.5%). Approximately 1 μg of linearlised plasmid was purified by phenol/chloroform extraction and ethanol precipitation and resuspended in 8 μL of nuclease-free water.

The MEGAscript T7 kit (Ambion) was used to *in vitro* transcribe RNA in a 20 μL reaction mixture according to manufacturer's instruction. The reaction mixture was incubated at 37ºC for 4 h, followed by the addition of 1 μL DNaseI to remove the DNA template. RNA products were precipitated by adding 2.5 M Lithium chloride at -20ºC for 1 h, and then pelleted by centrifugation for 15 m at 13,200 rpm, washed with 70% ethanol, and resuspended in nuclease-free water. The concentration of RNA was quantified using spectrophotometry or by running RNA samples on a denaturing formaldehyde-agarose gel.

2.2.17 Transfection

(a) Transfection of RNA and DNA to rescue clone-derived virus

Transfections of *in vitro* transcribed RNA or plasmid full-length cDNA clones were performed on COS-7 cells using Lipofectamine™ 2000 (Invitrogen) according to manufacturer's protocols. Briefly, COS-7 cells were seeded into 12-well tissue culture trays (Cellstar) at a density of $3x10^5$ cells/well. Cells were grown in DMEM supplemented with 2 mM L-glutamine and 5% BGS. After incubation for 18-24 h, cells were washed once with PBS and replaced with serum-free medium, Optimem (Invitrogen), prior to transfection. For transfection of RNA, the lipid-nucleic acid complex containing 1 or 3 μg of transcribed RNA and 3 μL of Lipofectamine™ 2000 was added to the cells. For DNA transfection, 1.6 μg of each full-length cDNA clone construct, 1.6 μg pCMV-T7Pol and 4 μL of Lipofectamine™ 2000 was added to the cells. Transfected cells were incubated for 4 h, after which the transfection medium was removed and replaced with DMEM supplemented with 2 mM L-glutamine and 2% FCS, and the cells incubated for a further 72 h. Transfected cells were then subjected to three cycles of freeze-thawing and the virus supernatant

clarified by centrifugation at 3,000 rpm for 15 min. The recovered clone-derived viruses (CDV) were then passaged to increase the titre for subsequent assays or were stored at -80 ºC until required.

(b) Transfection of DNA to determine transfection efficiency

Plasmid pcDNA-lacZ expressing β-gal was used to transfect cell lines used in this study to determine transfection efficiency. RD, Vero or COS-7 cells were seeded in a 24-well tissue culture tray (Cellstar). The seeding density was such that the cells were approximately 90% confluent at the time of transfection. Cells were transfected with pcDNA-lacZ (0.8-1.6 μg) and Lipofectamine^{TM} 2000 (1-3 μL), following the protocol as described above. Transfected cells were incubated for 24 h, and *in situ* staining was then performed to detect β-gal expression. Briefly, transfected cells were washed with D-PBS (2.7 mM KCl, 1.1mM KH_2PO_4, 0.41 M NaCl, 8.1 mM Na_2HPO_4.7H2O), and then fixed for 5 min at RT with fixative (D-PBS, 2% formaldehyde, 0.05% glutaraldehyde). Cells were then washed twice with D-PBS, followed by staining with substrate/stain solution (D-PBS, 5 mM potassium ferricyanide, 5mM potassium ferrocyanide, 2 mM $MgCl_2$, 1mg/mL X-gal). After incubation for at least 2 h, the cells were observed and evaluated for the proportion of β-gal-positive (blue) cells.

2.2.18 Stability testing of full-length infectious cDNA clones of HEV71-6F and HEV71-26M

The instability of the viral cDNA during passage in bacteria is a common problem encountered in the construction of full-length infectious cDNA clones. Therefore, the genetic structure and functional integrity of full-length infectious cDNA clones

of HEV71-6F and HEV71-26M were examined by serial passage in 2YT media containing 100 μg/mL ampicillin at two different incubation temperatures, 37˚C or 30˚C, for five passages. Briefly, plasmids pHEV71-6F or pHEV71-26M were transformed into *E. coli* XL10-gold. Two clones of each construct were subsequently selected and grown in 6 mL of 2YT at 37˚C or 30˚C for 16 h, then plated onto 2YT agar. The inoculated plates were incubated at 37˚C or 30˚C for about 18-24 h. Two isolated colonies were picked from each plate, and grown in 6 ml of 2YT at 37˚C or 30˚C for 16 h, then plated onto 2YT agar. Colonies were picked after 18-24 h of incubation. The passages were repeated ten times, and plasmid mini-preparations were performed from 2YT culture media at passages 1 and 5. The genetic structure of the clones was examined by restriction endonuclease digestion with *Bgl*I or *Pvu*II for pHEV71-6F and pHEV71-26M, respectively.

The functional integrity of these clones was assessed by infectivity testing. Briefly, COS-7 cells were seeded in a 24-well tissue culture tray (Cellstar) at a density of $1.6x10^5$ cells/well. After incubation for 24 h, 0.8 μg of plasmids pHEV71-6F or pHEV71-26M and 0.8 μg of pCMV-T7 were co-transfected into COS-7 cells using 3 μL of Lipofectamine™ 2000 (Invitrogen), following the protocol described in section 2.2.17. Viral RNA was transcribed in the transfected cells by T7 RNA polymerase. Transfected cells were freeze-thawed three times, and clarified by centrifugation. Virus supernatants were then determined for viral titre by $TCID_{50}$.

2.2.19 *In vivo* translation efficiency and luciferase assays

The IRES translation efficiencies of strains HEV71-6F and HEV71-26M were compared using bi-cistronic constructs and luciferase assays. Each bi-cistronic

construct contained two luciferase genes; renilla luciferase (LucR) and firefly luciferase (LucF). LucR is controlled by the cytomegalovirus immediate-early promoter (IE) and LucF was controlled by a hairpin structure, HEV71-6F IRES or HEV71-26M IRES for pCRHL, pCR6F and pCR26M, respectively. RD or COS-7 cells were seeded onto 24-well plates and incubated for 24 h to reach about 90% confluency at the time of transfection. One microgram of each bi-cistronic construct and 3 μL of Lipofectamine^{TM} 2000 were transfected into the cells using the protocol described in 2.2.17. Cells were assayed for luciferase activity at 24 h post-transfection using dual luciferase reagents (Promega), following the manufacturer's protocol, and were quantitated using a Luminometer (Ascent).

2.2.20 Stability testing of mouse-adapted virus *in vitro* and *in vivo*

Mutations in the VP2, VP1, and 2C genes of the mouse-adapted strain MP-26M were examined for genetic stability by serial passage of MP-26M in RD, Vero or CHO cells for five passages. Virus stocks from each passage were collected and viral RNA extracted. A part of the VP2, VP1, and 2C genes covering the mutation sites were amplified by RT-PCR, and the amplified products sequenced.

The stability of the VP2, VP1 and 2C mutations in MP-26M was also tested by five serial passages in mice. Briefly, a group of seven day-old mice were inoculated with MP-26M by the intramuscular (i.m.) route. Mice were observed twice daily for clinical signs of infection. At 4 and 5 days post-infection, brain and muscle tissues were aseptically collected from infected mice after perfusion with PBS. The tissue samples were immediately frozen in liquid nitrogen and stored at -80˚C until used.

Tissue samples were thawed on ice, homogenised in 10% (w/v) Hank's balance salt solution (HBSS, pH8), freeze-thawed three times and centrifuged. Five microliters of clarified virus supernatant from muscle tissue was then used to inoculate a further group of seven day-old mice; the passage was repeated five times.

2.3 Virus Assays

2.3.1 Plaque assays

Vero cell monolayers in 12-well tissue culture trays (Cellstar) at a density of $2.2x10^5$ cells/well or RD cells at $3x10^5$ cells/well, were used for plaque assays. Ten-fold serial dilutions of virus were inoculated at 100 µL per well. After incubation for 30 min at 37ºC, virus was removed and the cells washed with PBS. Cells were then overlaid with 1 mL of 0.5% agarose (ICN) in DMEM supplement with 2 mM L-glutamine and 2.5% FCS. After incubation for four days, 0.5% agarose in 2.5%FCS/DMEM was overlaid onto the first layer of agarose gel and further incubated for three days. The cells were then fixed and stained with crystal violet solution (1% crystal violet (w/v), 10% formaldehyde in PBS) to visualise plaques.

2.3.2 Median tissue culture infectious dose ($TCID_{50}$)

$TCID_{50}$ assays were used to determine virus titres. Monolayers of Vero cells in 96-well tissue culture trays at a density of $1x10^4$ cells/well (Cellstar) were inoculated with 100 µL of ten-fold serial dilutions of virus solution per well and then incubated at 37ºC with 5% CO_2 for 5 days before observing for CPE. $TCID_{50}$ titres were determined by the method of Reed and Muench (1938).

2.3.3 Single-step growth analysis

Monolayers of Vero, RD, CHO or NB41A3 cells were cultured in 12- or 48-well tissue culture trays (Cellstar). Virus was inoculated onto the cells at a multiplicity of infection (MOI) of 5 or 10$TCID_{50}$ per well and then incubated for 1 h at 37ºC. Inoculated cells were then washed three times with PBS and overlaid with 200 µL DMEM supplemented with 2 mM L-glutamine and 2% FCS per well. The cells and supernatants were collected every 4 h over 24 h, with the first time point (time=0) being collected immediately after cell inoculation. Samples at each time point were freeze-thawed three times and clarified by centrifugation at 8,000x*g* for 10 min prior to determination of virus titre by $TCID_{50}$ assay.

2.3.4 Immunofluorescence assays (IFA)

Vero or RD cells on glass coverslips in 96-well tissue culture trays (Cellstar) were seeded at confluent density and incubated overnight at 37ºC, prior to inoculation with virus. Cells that showed CPE were fixed in 50:50 acetone/methanol for 10 min, then air dried. Cells were then overlaid with mouse anti-HEV71 monoclonal antibody (Chemicon) or rabbit anti-HEV71 polyclonal antibody and incubated for 30 min at 37ºC in a moist chamber. Cells were subsequently washed in PBS for 30 min and air dried before being overlaid with FITC conjugate goat anti-mouse IgG or FITC conjugate goat anti-rabbit IgG (Sigma). Both secondary antibodies contained 0.2% Evans blue as a counter stain. Cells were incubated for a further 30 min at 37ºC in a moist chamber, then washed in PBS for 15 min and air dried. Mounting fluid was added prior to visualisation under a UV light microscope (Leica BX-210) for fluorescence.

2.3.5 Temperature sensitivity assay

Temperature sensitivity testing of cloned-derived viruses was performed by plaque assay on Vero cells, as described in section 2.3.1. Infected cells were incubated at 33ºC, 37ºC, or 39ºC. Plaque numbers and morphologies were compared in cells incubated at the different temperatures.

2.3.6 Polyethylene glycol concentration of virus

Virus from tissue culture supernatants was concentrated using polyethylene glycol 6000 (PEG) to increase viral titre for oral inoculation of mice. RD cell monolayers in 175 cm^2 tissue culture flasks were infected with HEV71-6F, HEV71-26M or MP-26M at MOI of 0.1-5. After 16 to 24 hours incubation, cells were freeze-thawed three times and clarified by centrifugation at 3,000 x*g* for 15 min. NaCl was then slowly added to the virus supernatant to a final concentration of 2.2% with constant stirring at 4°C, followed by adding PEG to a final concentration of 7% with constant stirring at 4°C overnight. Virus was collected by centrifugation for 20 min at 10,000 x*g*, and the precipitated pellets were drained and resuspended in PBS with 2%BSA. The suspension was then centrifuged twice at 10,000 x*g* for 1 min, and virus supernatant stored at -80°C. The infectivity and the titre of virus supernatant were determined using plaque and $TCID_{50}$ assays.

2.4 Mouse experiments

All animal procedures were approved by the Animal Experimentation Ethics Committee of the Telethon Institute for Child Health Research, Perth, Australia. Animal care and observation were performed in accordance to the guidelines of the committee. Animal were provided with food and water *ad libitum*. Specific

pathogen free advanced pregnant BALB/c mice were obtained from the Animal Resources Centre, Murdoch University, Perth, Australia.

2.4.1 Oral inoculation

(a) Determination of gastrointestinal transit time

In order to define a suitable fasting time before oral infection of suckling mice, gastrointestinal transit time was determined in newborn mice. One-day-old BALB/c mice were separated from their mothers for 6 h. They were then fed with 20-30 µL milk (30 mL/kg body weight) containing phenol red using a 24 gauge plastic feeding tube. Mice were sacrificed at 1, 2, or 4 h after feeding and the stomach contents collected. Gastric emptying at specific times were determined following the method described by Scarpignato et al. (1980), with slight modifications. Briefly, the stomach was immersed in 100 mL of 0.1 N NaOH and homogenised. The suspension was allowed to settle for 60 min at RT. Five millilitres of supernatant was then added to 0.5 mL 20% w/v trichloroacetic acid (TCA). The mixture was centrifuged at 3,000 x*g* for 20 min at 4°C, and the supernatant was added to 4 mL of 0.5 N NaOH. The absorbance of samples was read at a wavelength of 560 nm. The gastric emptying was calculated from the presence of residual phenol red using the following formula;

$$\text{Percent gastric emptying} = 1 - \frac{\text{absorbance of sample}}{\text{absorbance of standard}} \times 100$$

Phenol red recovered from stomach immediately after the administration of meal was normalised to 100%.

(b) Oral infection with HEV71

Mice were infected orally after fasting for 2 h, using 24 gauge plastic feeding tubes. Virus was PEG precipitated to increase the titre, as described in section 2.3.7. Blue food dye (1%v/v) tracer was added to each virus dilution prior to inoculation to allow the virus inoculum be visualised in the stomach through the translucent abdominal wall.

2.4.2 Virulence assays in mice

The mouse virulence phenotype of wild-type HEV71 strains 6F and 26M, the mouse-adapted strain MP-26M and other mutant viruses were determined by intraperitoneal (i.p.), intracranial (i.c.), intramuscular (i.m.) or oral inoculation of one-or seven- day old BALB/c mice. The inoculation volume was 50 μL for i.p., 10 μL for i.c., 5 μL for i.m. and 50 μL for oral inoculation. In all experiments, infected animals were observed twice daily for clinical signs of illness for up to 14 days post-inoculation and animals that succumbed to infection were euthanised by overdose of pentobarbitone sodium.

In order to minimise distress in experimental animals, the 50% humane end-points (HD_{50}) were utilized instead of 50% lethal doses (LD_{50}). Humane endpoints have been found to be almost identical to lethal endpoints in several animal models of viral virulence (Wright & Phillpotts, 1998). Determination of the HD_{50} was performed by infecting groups of 8 to10 one-or seven-day-old mice with ten-fold serial dilutions of virus via i.p., i.m. or oral routes. HD_{50}s were calculated by the method of Reed and Muench (1938).

For determination of average survival times, groups of 8 to12 seven-day-old mice were infected with virus at an appropriate dose by the i.p. or i.m. routes. Deaths of infected mice were recorded over a period of 14 days.

2.4.3 Viral RNA extraction from mouse brain and muscle

Brain and muscle tissues were collected after perfusion with PBS and immediately frozen in liquid nitrogen. Tissues were then stored at -80˚C until used. Tissue samples were thawed on ice, homogenised in 10% (w/v) HBSS (pH 8)**,** followed by freeze-thawing three times. Virus supernatant was clarified by centrifugation at 3,000 x*g* for 15 min, and then at 10,000 x*g* for 1 min. Virus in clarified supernatants was used for RNA extraction using the QIAamp® Viral RNA mini kit (Qiagen) according to the manufacturer's instructions.

2.5 Statistical analysis

Statistic significance was statistically calculated using unpaired Student's *t*-test (Elwood, 1988). P values of less than 0.05 were considered significant

2.6 Bioinformatics

2.6.1 RNA secondary structure prediction

All secondary structures were predicted using MFOLD (version 3.2) software program (Mathews et al., 1999, Zuker, 2003). The parameters used are as followed; folding temperature at 37°C, linear RNA sequence, percent suboptimality number of 5, upper bound on the number of computed foldings of 50, default window parameter, maximum interior/bulge loop size of 30, maximum asymmetry of an

interior/bulge loop of 30, no limit to maximum distance between paired bases, structure draw mode of untangle with loop fix and no base numbering.

2.6.2 Protein homology modeling

The complete amino acid sequences of the capsid proteins VP2 and VP1 from HEV71-26M, CHO-26M and MP-26M were individually submitted to an online automated protein homology modeling program, ESyPred3D (Lambert et al., 2002); available on line at http://www.fundp.ac.be/sciences/biologie/urbm/bioinfo/esypred/. The predicted three-dimensional structure of each of the proteins were then viewed in RasMol 2.7 (http://rasmol.org/).

CHAPTER THREE

CONSTRUCTION OF GENOME LENGTH INFECTIOUS cDNA CLONES OF HEV71 GENOTYPE B3 AND C2 STRAINS AND PHENOTYPIC CHARACTERISATION OF CLONED-DERIVED VIRUSES

3.1 Introduction

The development of reverse genetic systems has greatly enhanced the understanding of RNA virus biology. Here, infectious cDNA clones, a double-stranded copy of the viral genome carried on a plasmid vector, are constructed and become templates for producing synthetic viruses (Racaniello, 2007). Clone-derived viruses are generated by transfecting either plasmid cDNA clones or RNA transcripts derived by *in vitro* transcription into susceptible cells (Racaniello, 2007). The first infectious cDNA clone of an animal RNA virus was that of poliovirus (Racaniello & Baltimore, 1981). Such clones facilitate genetic manipulation of RNA viral genomes and thus the role of specific viral genetic elements in viral replication, transcription, translation or virulence can be investigated.

The construction of infectious cDNA clones of RNA viruses can be technically difficult and require extensive optimisation. In general, the first step is reverse transcription of the viral RNA into a single-stranded cDNA. A double-stranded copy of the viral genome is generated by PCR amplification using a single-stranded cDNA as a template, and the double-stranded cDNA copy cloned into a plasmid vector followed by transformation into a bacterial host to multiply. The full-length cDNA clone is *in vitro* transcribed into RNA, and the RNA transcript is transfected into

cells to rescue clone-derived virus. Alternatively, the plasmid cDNA clone is transfected into cells directly.

The recent increase in the distribution of HEV71 represents an emerging disease problem in the Asia-Pacific region. In order to develop effective vaccines and control strategies, it is essential to understand the biology of this virus. A reverse genetic system will help in investigating the molecular mechanisms of HEV71 replication, transcription and translation, and assist in identifying the genetic determinants of virulence and pathogenesis. In this study, we established a reverse genetic system for representative strains of HEV71 genotype B and C, the two genotypes associated with recent outbreaks. The construction and characterisation of infectious cDNA clones of HEV71 is reported in this chapter.

3.2 Results

3.2.1 Design and construction of full-length cDNA clones of HEV71

HEV71 strain 6F/AUS/6/99 (HEV71-6F) and strain 26M/AUS/4/99 (HEV71-26M), belonging to genotype C2 and B3, respectively, were used as parental strains for developing a reverse genetic system for HEV71. Both strains were isolated from clinical cases during the 1999 Western Australian HFMD outbreak. Both strains have been fully sequenced in our laboratory. In order to produce infectious RNA from full-length cDNA clones *in vitro* or *in vivo*, the RNA polymerase promoter of bacteriophage T7, and an additional one, two or three G residues were positioned immediately upstream of the 5′ terminus of viral cDNA in order to facilitate transcription and to improve transcription efficiency, respectively. A poly (A) tail of

25 nucleotides and a *Mlu*I restriction site (A/CGCGT) was incorporated immediately downstream of the viral cDNA in order to generate synthetic virus with an authentic 3′ terminus.

Selection of appropriate plasmid vectors and bacterial host strains has been found to be critical for construction of infectious cDNA clones of several RNA viruses (Hurrelbrink et al., 1999, Lai et al., 1991, Rice et al., 1989). The full-length cDNA clone of HEV71-6F was previously constructed using a high copy number plasmid vector, pDONR201, and amplified in *E. coli* strain DH5α (Beng Hooi Chua, unpublished data), but the clone was found to be non-infectious. In this study, the full-length cDNA clone of HEV71-6F was initially constructed using a medium copy number plasmid, pBR322, and *E. coli* strain DH5α. Plasmid pBR322 contains a pMB1 origin of replication (*ori*) and has an intermediate copy number of 40 per cell. pBR322 and DH5α were chosen because they have been used successfully for construction of infectious cDNA clones of several other enteroviruses and flaviviruses (Cello et al., 2002, Kapoor et al., 1995, Khromykh & Westaway, 1994, Mandl et al., 1997, Martino et al., 1999).

Initially, the construction strategy involved amplification of the complete viral genome by RT-PCR and the amplified product was cloned into a plasmid vector to generate a full-length cDNA clone. However, several attempts to amplify the whole genome of HEV71-6F from the first strand cDNA template by PCR were unsuccessful. Thus, the 5′ and 3′ terminal fragments of 5,000 and 2,907 nucleotides in length were amplified and the resulting PCR products cloned into pBR322 to produce two sub-genomic clones, pBR/5′-6F and pBR/3′-6F. The full-length

HEV71-6F cDNA clone (pBR/HEV71-6F) was successfully constructed from these two overlapping fragments using appropriate unique restriction sites. As noted above, these clones contained an additional one, two or three G residues at the 5′ terminus. Cloning and assembly of sub-genomic and full-length clones was assisted by use of the computer program SECentral. The cloning procedures are described in detail in section 2.2.13 and the schematic diagram of the construction of the sub-genomic and full-length cDNA clones are shown in Figure 2.1-2.3.

Sub-genomic and full-length clones of HEV71-6F were propagated in *E. coli* strain DH5α at 37˚C, and the clones were screened by restriction enzyme digestion with appropriate enzymes. Of 20 full-length pBR/HEV71-6F clones screened, none were found to be infectious. In order to identify the problem, one of the clones was fully sequenced and compared to the HEV71-6F sequence. Sequencing results revealed that there were 17 nucleotide differences between HEV71-6F and pBR/HEV71-6F sequences (Table 3.1). These mutations resulted in 8 deduced amino acid changes, located in both structural and non-structural proteins, and 2 stop codons, located in the viral capsid protein VP3 and in the non-structural protein 2A.

The mutations found in pBR/HEV71-6F are likely to be introduced by the bacterial host. It has been suggested that the instability of full-length viral cDNA clones in bacterial cells could be improved by changing the *E. coli* strain and/or the plasmid vector (Boyer & Haenni, 1994). We attempted to solve this problem by changing the *E. coli* strain from DH5α to DH10B and by propagating the cells at 37˚C or at a reduced temperature of 30˚C. The bacterial host strain, DH10B, has the ability to

Table 3.1 Differences between the sequences of HEV71-6F and full-length clone pBR/HEV71-6F

Position in viral genome	Nucleotide position	Nucleotide substitution	Amino acid substitution
5′ UTR	477	A→G	-
VP2	1694	T→C	L→P
VP3	2197	C→T	Stop codon (CAA→TAA)
VP3	2202	G→A	
VP1	2462	T→C	I→T
VP1	2772	A→G	I→M
2A	3476	G→A	G→D
2A	3679	C→T	Stop codon (CAA→TGA)
2A	3680	A→G	Stop codon (CAA→TGA)
2B	3849	A→G	none
2B	3947	T→A	V→D
3C	5631	A→G	none
3C	5808	T→C	none
3D	6131	A→G	N→S
3D	6508	T→C	F→L
3D	6904	A→G	N→D
3D	7056	T→C	none

propagate large cloned DNA such as BAC constructs and allows stable replication of high-copy number plasmids (Raleigh et al., 1988). Previous studies (Shi et al., 2002, Sriburi et al., 2001) have shown that full-length cDNA clones with medium or high copy number plasmids are more stable when propagated at reduced temperature.

However, no infectious clone-derived virus was obtained from clone pBR/HEV71-6F (24 clones) propagated in DH10B at either 30˚C or 37˚C. In order to solve the problem, another plasmid vector, pMC18, with a seven-fold lower copy number to pBR322 and an additional *E. coli* strain, XL10-gold, were also tested. The pMC18 vector has been used successfully for construction an infectious cDNA clone of the flavivirus Murray Valley Encephalitis Virus (MVE) (Hurrelbrink et al., 1999) and is a modified version of the pWSK29, containing a pSC10 *ori* and a low copy number of six per cell. Similar to *E. coli* strain DH10B, XL10-gold allows propagation of large DNA molecules and is recombinant deficient (*rec*A), helping to ensure insert stability (http://www.stratagene.com).

Sub-genomic (pMC/5′-6F and pMC/3′-6F) and full-length cDNA clones of HEV71-6F (pHEV71-6F) were successfully constructed in pMC18 using different restriction sites for cloning according to the unique restriction sites in the viral genome and the pMC18 vector. These pHEV71-6F clones contain an additional one or two extra G residues at the 5′ terminus. All sub-genomic and full-length clones were grown in *E. coli* strain DH10B or XL10-gold at 30˚C. No infectious clone-derived virus of HEV71-6F (CDV-6F) was recovered from pHEV71-6F (24 clones) propagated in DH10B. However, CDV-6F was obtained from two of 18 pHEV71-6F clones

propagated in XL10-gold. These infectious pHEV71-6F clones have an additional two G residues at the 5′ terminus.

By the use of a similar clone construction strategy, an infectious cDNA clone of HEV71 strain 26M (pHEV71-26M) was also successfully constructed. Plasmid vector pMC18 and the bacterial host XL10-gold were used. Clone-derived virus 26M (CDV-26M) was recovered from 10 of 16 pHEV71-26M clones screened. The use of different plasmid vectors, bacterial host strains, incubation temperatures, and number of additional 5′ terminal G residues in construction of full-length cDNA clones of HEV71 and infectivity of clone-derived virus is summarised in Table 3.2.

3.2.2 Recovery of infectious clone-derived viruses

For *in vitro* RNA synthesis, full-length cDNA plasmids were linearised with *Mlu*I and the linearised plasmids were transcribed using MEGAscript T7 kit (Ambion), as described in section 2.2.16. RNA transcripts had an authentic 3′ end of the HEV71 genomic RNA and two additional 5′ nonviral G residues, which is the transcription start site of T7 RNA polymerase. Analysis of RNA transcripts on formaldehyde-denatured agarose gels showed a single band with a mobility identical to that of genomic RNA extracted from HEV71 (Figure 3.1).

Table 3.2 Summary of the use of different plasmid vectors, bacterial host strains, incubation temperatures, and number of G residues in construction of full-length HEV71 cDNA clones and infectivity of clone-derived virus.

Virus (strain)	Plasmid vector	Bacterial host strain	Incubation Temperature	Number of G residues	Recovery of clone-derived virus
HEV71-6F	pBR322	DH5α	37˚C	1, 2 or 3G	No
	pBR322	DH5α	30˚C	1, 2 or 3G	No
	pBR322	DH10B	37˚C	1, 2 or 3G	No
	pBR322	DH10B	30˚C	1, 2 or 3G	No
	pMC18	DH10B	30˚C	1G or 2G	No
	pMC18	XL10-Gold	30˚C	1G	No
	pMC18	XL10-Gold	30˚C	2G	Yes
HEV71-26M	pMC18	XL10-Gold	30˚C	2G	Yes

Transfection of RNA or DNA into mammalian cells has been achieved by calcium phosphate, DEAE-dextran, electroporation and cationic lipid reagents (liposomes) (Sambrook & Russell, 2000). Most of the recent studies used electroporation or liposomes to transfect clone-derived RNA or cDNA clones into susceptible cells (Boot et al., 2001, Bredenbeek et al., 2003, Hurrelbrink et al., 1999, Shi et al., 2002). Initial attempts to transfect Vero cells with RNA transcripts by electroporation resulted in approximately 50-60% cell death. Transfection of RNA and DNA using liposomes (Lipofactamine^{TM} 2000, invitrogen) was found to be simpler, easier to optimise, required fewer cells, and caused less cell death than electroporation. Thus, this method was chosen and fully optimised for use in our experiments.

The transfection efficiency of Lipofactamine^{TM} 2000 in different HEV71-susceptible cell lines was determined using plasmid pcDNA-lacZ expressing β-gal. RD, Vero or COS-7 cells were seeded in 24-well tissue culture trays and were approximately 90% confluent at the time of transfection. These cells were transfected with the same amount of Lipofactamine^{TM} 2000-pcDNA-lacZ complex: 3 μL of Lipofactamine^{TM} 2000 and 0.8 μg of pcDNA-lacZ. Transfection and *in situ* staining protocols are described in section 2.2.17 (b). COS-7 cells had the highest transfection efficiency, with the highest number of β-gal-positive cells, as shown in Figure 3.2. Therefore COS-7 cells were chosen for subsequent transfection experiments in order to rescue clone-derived viruses.

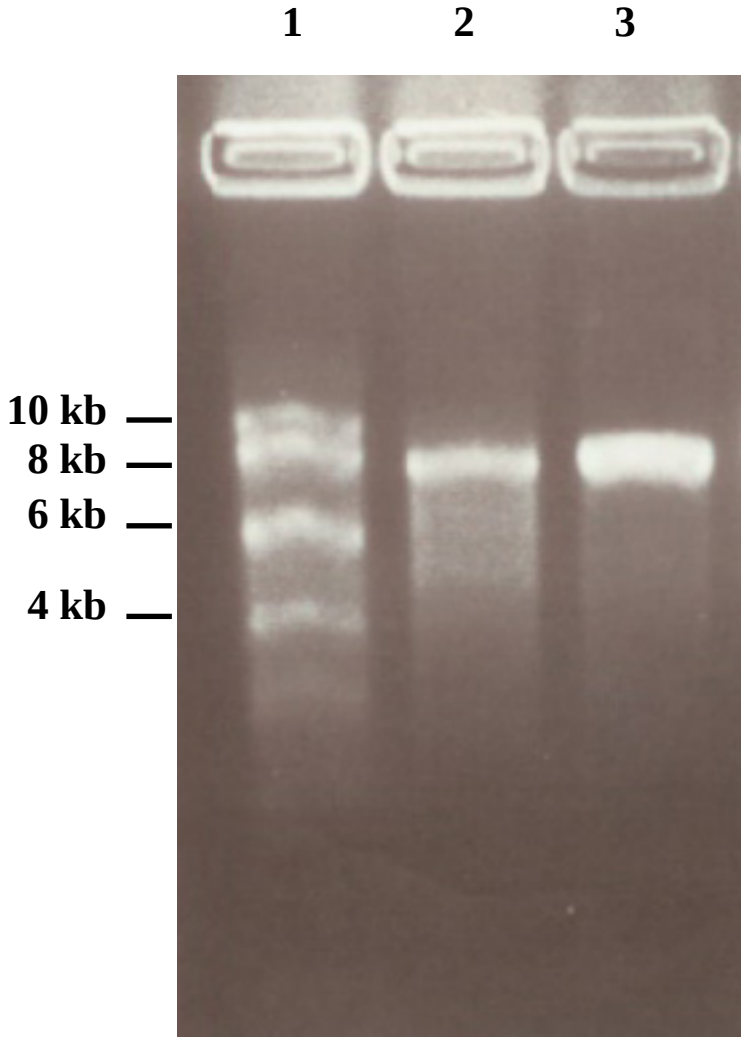

Figure 3.1 Formaldehyde-denatured agarose gel showing identical mobility between extracted genomic RNA of HEV71 (Lane 2) and RNA transcripts from a full-length cDNA clone of HEV71 (Lane 3). Molecular size standards (0.5-10 kb RNA ladder, Invitrogen) are shown in base pairs on the left for comparison (Lane 1)

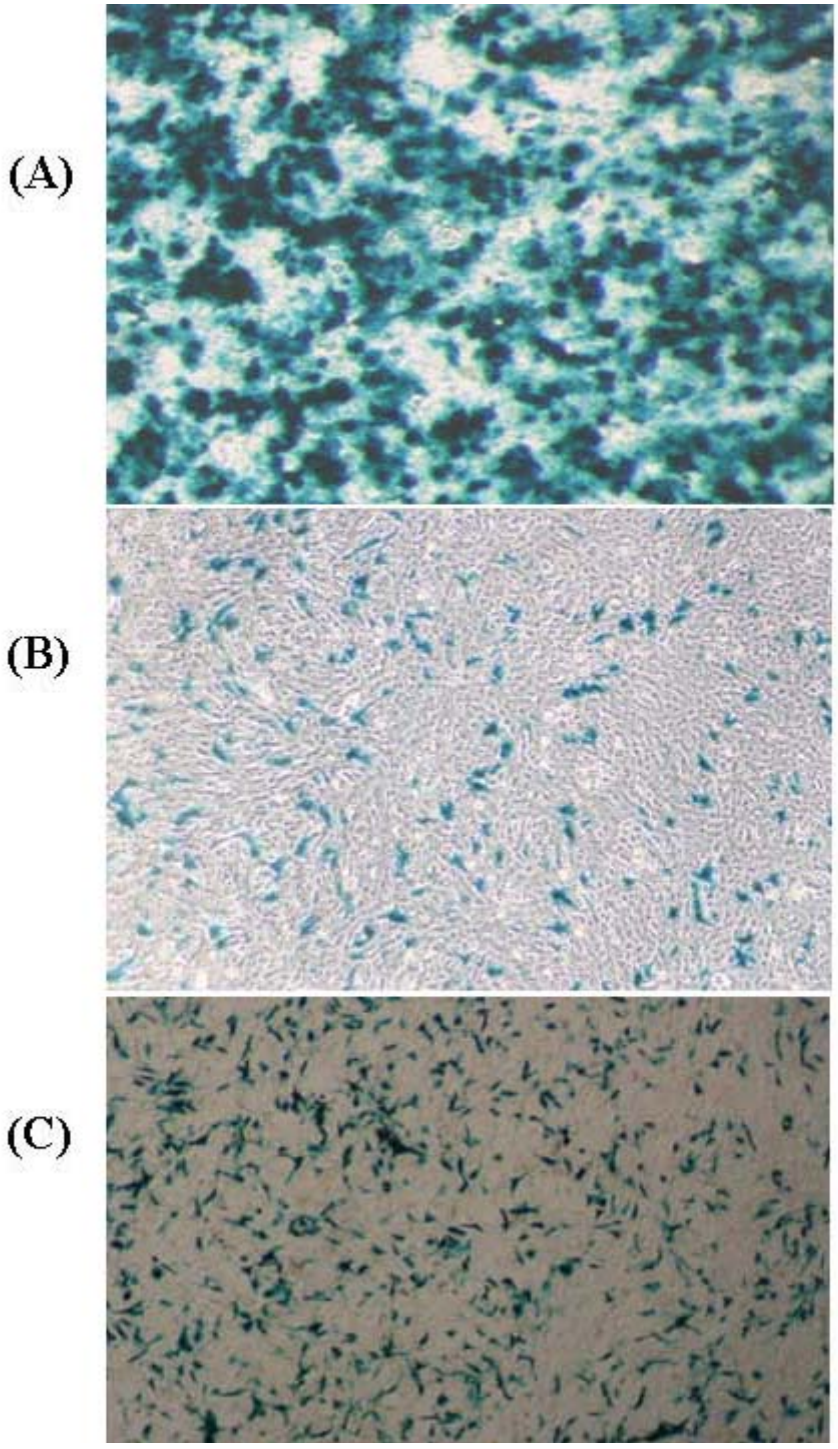

Figure 3.2 Comparison of transfection efficiency in different cell lines. COS-7 (A), Vero (B) or RD cells (C) were transfected with pcDNA-lacZ (0.8 μg) and Lipofectamine^{TM}2000 (3 μL). Transfected cells were incubated for 24 h and the cells were stained with X-gal to detect β-gal expression.

The optimal conditions for transfection of COS-7 cells with Lipofactamine^{TM} 2000 were determined using pcDNA-lacZ. COS-7 cells were seeded in 12-well tissue culture trays at a density of $3.2x10^5$ cells/well. Cells were subsequently transfected with different combinations of mixtures of the pcDNA-lacZ (0.8, 1.6, 3.2, 6.4 μg) and Lipofactamine^{TM} 2000 (2, 4, 6, 12 μL). Optimal conditions were obtained when COS-7 cells were transfected with 3.2 μg of pcDNA-lacZ and 4 μL of Lipofactamine^{TM} 2000, with approximately 15% cell death and 80% transfection efficiency.

Initially, both RNA transcripts and plasmid full-length cDNA clones were used to transfect COS-7 cells in order to rescue clone-derived virus populations. For DNA transfection, the full-length cDNA clone was co-transfected with plasmid pCMV-T7Pol. pCMV-T7Pol, which expresses T7 RNA polymerase, provides the T7 RNA polymerase for transcription of full-length viral cDNA in the cells. Transfection of DNA was undertaken by mixing 1.6 μg of full-length viral cDNA and 1.6 μg of pCMV-T7Pol with 4 μL of Lipofactamine^{TM} 2000, and the mixture added to the cells. For RNA transfection, 3 μg of RNA transcript was mixed with 3 μL of Lipofactamine^{TM} 2000, and the mixture added to the cells. Transfection protocols are described in detail in section 2.2.17. Clone-derived viruses were obtained from both RNA and DNA transfection. CPE was observed from secondary infected Vero and RD cells within 24-48 h. However, the specific infectivity of these two methods was not compared. As the DNA transfection method is simpler, with no *in vitro* transcription step required, this method was chosen for the rescue of clone-derived viruses in all subsequent studies.

3.2.3 Confirming the presence of clone-derived viruses 6F and 26M

The presence of clone-derived viruses was confirmed by immunofluorescence assays. Clone-derived viruses 6F and 26M harvested from transfected COS-7 cells were passed into Vero and RD cell monolayers on glass cover slips. Infected cells were fixed in 50:50 acetone/methanol and labelled with mouse anti-HEV71 monoclonal antibody, as described in section 2.3.4. Cells infected with wild-type viruses HEV71-6F and HEV71-26M, and mock-infected cells were used as positive and negative controls, respectively. Cells infected with CDV-6F or CDV-26M showed immunofluorescence similar to the wild-type virus infected cells, indicating that HEV71 clone-derived viruses had been rescued from the cDNA clones (Figure 3.3 and 3.4). Furthermore, the presence of CDV-6F and CDV-26M was confirmed by extracting viral RNA from the culture supernatant of RD passage 1, and performing RT-PCR to amplify the full VP1 gene, as described in section 2.2.10 (b) and 2.2.11 (b). The VP1 PCR products were sequenced and compared to the sequences of wild-type HEV71-6F and HEV71-26M. Nucleotide sequences of clone-derived viruses were found to be identical to that of their respective wild-type viruses.

3.2.4 Stability of clones in *E.coli*

Instability of the full-length clones pBR/HEV71-6F during passage in *E. coli*, prompted an investigation into the stability of pHEV71-6F and pHEV71-26M. *E.coli* strain XL10-gold was transformed with pHEV71-6F or pHEV71-26M. Two colonies from each transformation were propagated for five cycles consisting of

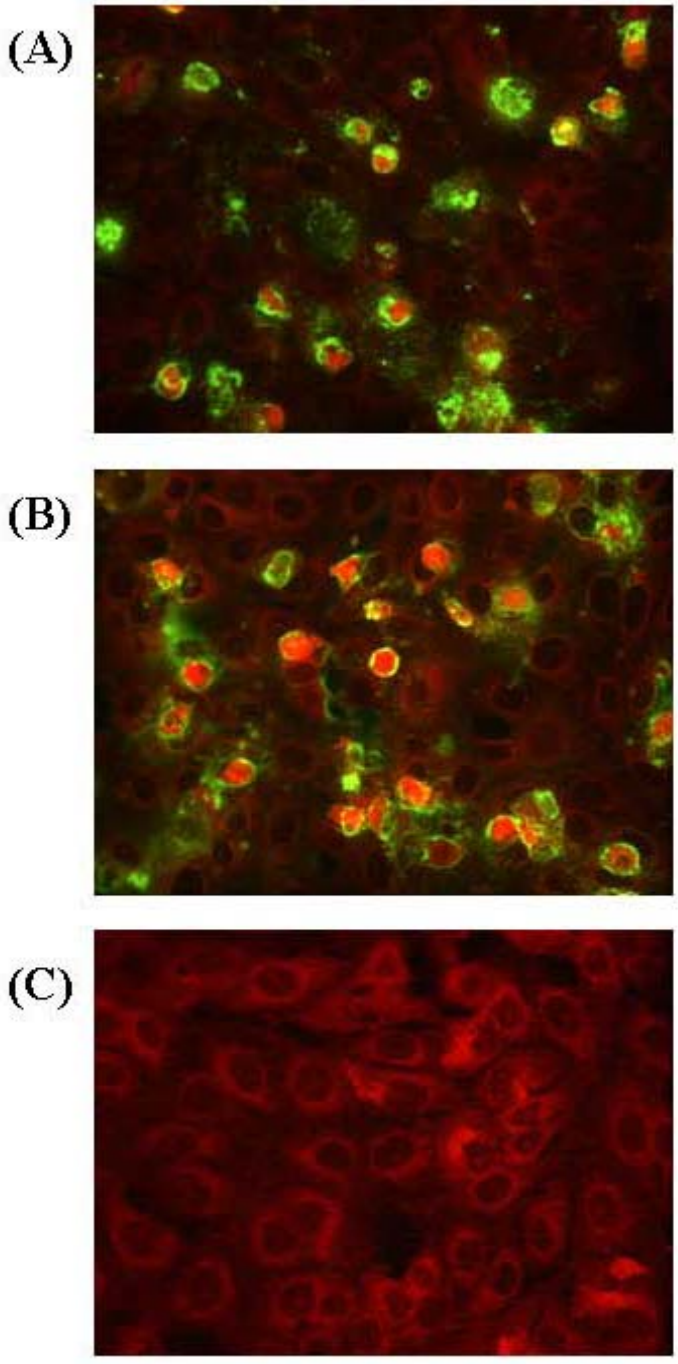

Figure 3.3 Immunofluorescence assay of Vero cells infected with HEV71-6F (A) or CDV-6F (B) Cells were infected with virus and incubated for 24 h prior to staining with mouse anti-HEV71 monoclonal antibody and FITC conjugated goat anti-mouse IgG. (C) Mock infected cells were included as negative controls. Both infected and non-infected cells were counterstained with Evans blue showing a dull red fluorescence.

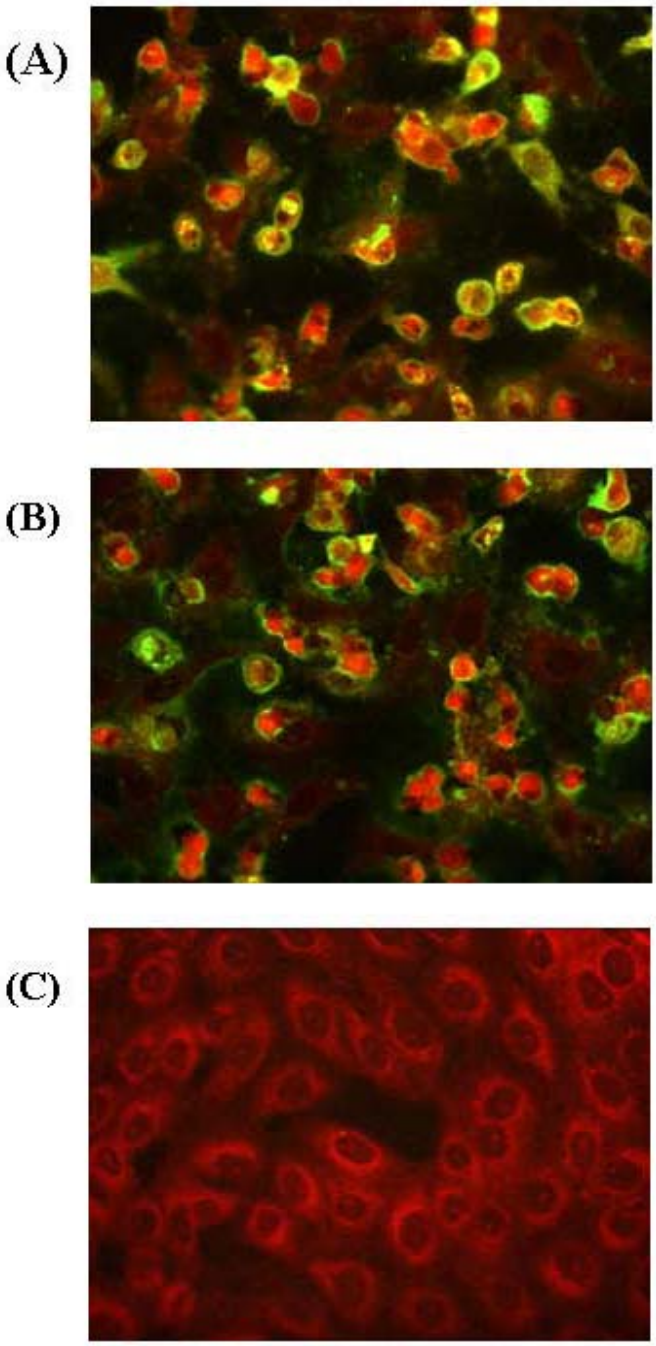

Figure 3.4 Immunofluorescence assay of Vero cells infected with HEV71-26M (A) or CDV-26M (B). Cells were infected with virus and incubated for 24 h prior to staining with mouse anti-HEV71 monoclonal antibody and FITC conjugated goat anti-mouse IgG. (C) Mock-infected cells were included as negative controls. Both infected and non-infected cells were counterstained with Evans blue showing a dull red fluorescence.

alternating growth in liquid and solid media at two different incubation temperatures, 30˚C or 37˚C, as described in section 2.2.18. The functional integrity of the full-length clones was examined by restriction endonuclease digestion with appropriate enzymes and by infectivity testing. Digestion of pHEV71-6F (12,835 nucleotides) with *Bgl*I was predicted to generate fragments of 4265, 3642, 2906, 1267, 290, 234 and 231 nucleotides. Plasmid pHEV71-26M (12,803 nucleotides) digested with *Pvu*I was predicted to generate fragments of 4986, 2928, 2731 and 2158 nucleotides. Restriction enzyme digestions of plasmid DNA purified after 1 and 5 passages at 30˚C or 37˚C incubation generated the expected patterns, as shown in Figure 3.5. The specific infectivity of purified plasmids from passage 1 and 5 at both temperatures of incubation was assessed by co-transfection of 0.8 μg of purified plasmids and 0.8 μg of pCMV-T7 into COS-7 cells. Viral RNA was transcribed in the transfected cells by T7 RNA polymerase. The specificity of these plasmids did not differ significantly (Table 3.3). These data indicate that the full-length clones were genetically stable during passage in bacterial cells.

3.2.5 Genotypic characterisation of infectious clones and clone-derived viruses

The sequence of HEV71-6F cDNA within the plasmid full-length clone, pHEV71-6F was determined using Big-dye-terminator sequencing technology. Primers used for sequencing pHEV71-6F are shown in Table 2.1. The HEV71-6F cDNA sequence was compared to the published sequence of HEV71-6F (DQ381846). One nucleotide difference was identified in the 3D gene ($T^{7056}\rightarrow C$). However, this nucleotide substitution does not lead to an amino acid change. Clone-derived virus CDV-6F at RD stock passage 3 was also sequenced. Similar to sequencing results of

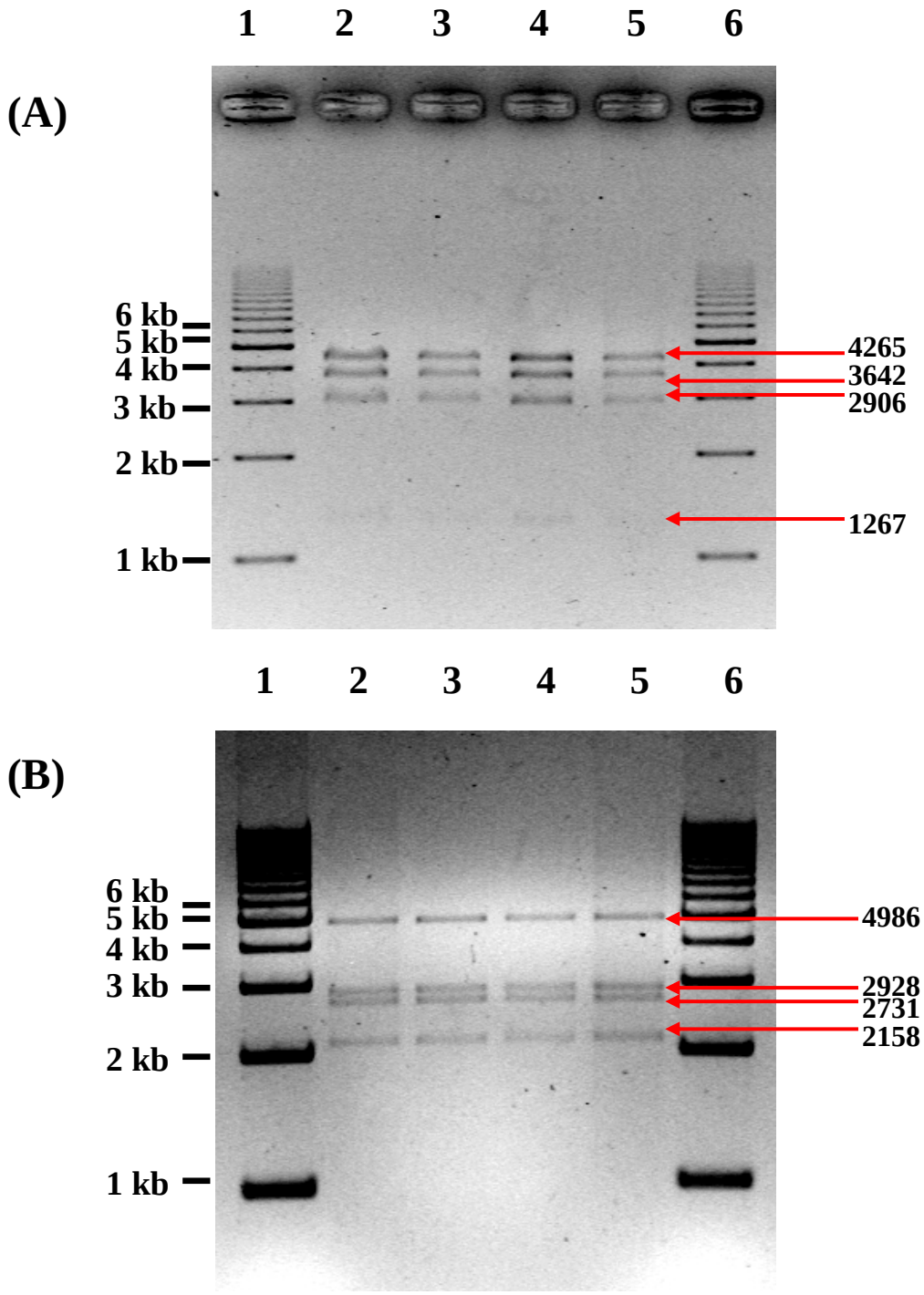

Figure 3.5 Stability of full-length cDNA clones, pHEV71-6F and pHEV71-26M during five passages in *E. coli* at 30˚C or 37˚C. Plasmids pHEV71-6F and pEV71-26M were digested *Bgl*I and *Pvu*I, respectively. (A) The expected banding pattern was observed in pHEV71-6F at passage 1 at 30˚C and 37˚C (Lanes 2 and 3), and at passage 5 at 30˚C and 37˚C (Lanes 4 and 5). (B) The expected banding pattern was observed in pHEV71-26M at passage 1 at 30˚C and 37˚C (Lanes 2 and 3), and at passage 5 at 30˚C and 37˚C (Lanes 4 and 5).

Table 3.3 Specific infectivity of the RNA derived from pHEV71-6F and pHEV71-26M after 1 and 5 passages in *E. coli*

Incubation temperature (˚C)	Viral titre (log_{10} $TCID_{50}$/mL)			
	CDV-6F passage 1	CDV-6F passage 5	CDV-26M passage 1	CDV-26M passage 5
30	2.72 (± 0.19)	2.61 (± 0.2)	7.83 (± 0.47)	7.76 (± 0.12)
37	2.61 (± 0.19)	2.65 (± 0.17)	7.54 (± 0.07)	7.57 (±0.29)

HEV71-6F cDNA, the nucleotide substitute, $T^{7056}\rightarrow C$, was identified in CDV-6F. This nucleotide change can be used as a genetic marker to differentiate between clone-derived virus and the wild-type HEV71-6F virus. Viral cDNA of HEV71-26M was also sequenced and compared to the sequence of the parental HEV71-26M (EU364841); no nucleotide differences were identified.

3.2.6 Phenotypic characterisation of clone-derived virus

Clone-derived viruses CDV-6F and CDV-26M were compared phenotypically to their parental viruses by plaque morphology and by determining growth kinetics in susceptible cell lines.

The plaque size and morphology of CDV-6F and CDV-26M were compared to their parental viruses on Vero and RD cells. Both HEV71-6F and HEV71-26M produced clearer plaques in Vero-infected cells than in RD cells. CDV-6F and HEV71-6F displayed an identical small plaque phenotype (Figure 3.6). CDV-26M and HEV71-26M also had an indistinguishable large plaque phenotype (Figure 3.6).

The growth kinetics of clone-derived viruses and their parental viruses were compared using RD cells. RD cell monolayers in 24-well tissue culture trays were infected with CDV-26M or HEV71-26M at an MOI of 10. Since both CDV-6F and HEV71-6F produced low viral titres, the growth kinetics of CDV-6F and HEV71-6F were examined by infecting monolayers of RD cells in 24-well tissue culture trays at an MOI of 1. Viruses were harvested at 4 h intervals for 24 h and the yields quantified by $TCID_{50}$ assay. As shown in Figure 3.7, the replication kinetics of CDV-6F and HEV71-6F were nearly identical. The growth kinetics of CDV-26M

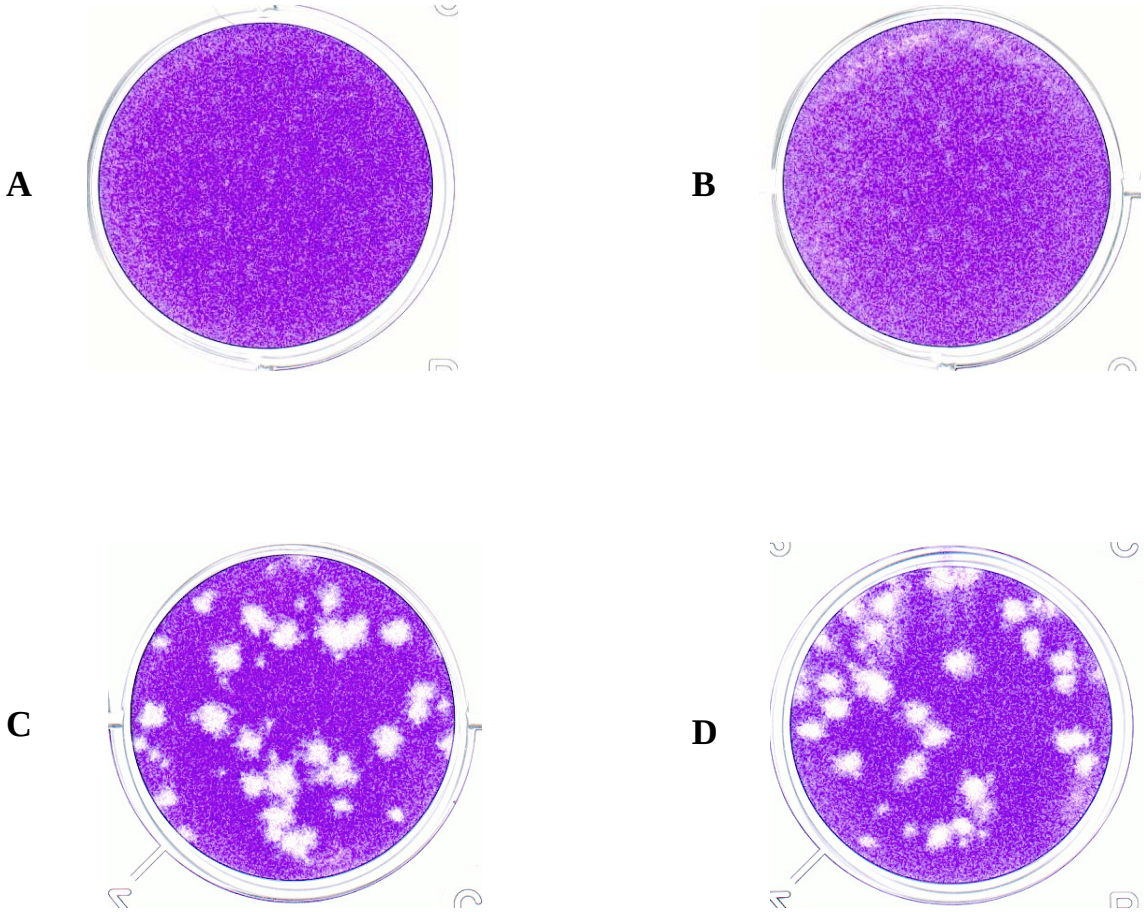

Figure 3.6 Plaque morphology of parental and clone-derived HEV71-6F and HEV71-26M in Vero cells. Vero cells in 12-well tissue culture trays were infected with the indicated viruses. Plaques were visualised 7 days post-infection by staining with crystal violet. (A) HEV71-6F (B) CDV-6F (C) HEV71-26M (D) CDV-26M

A

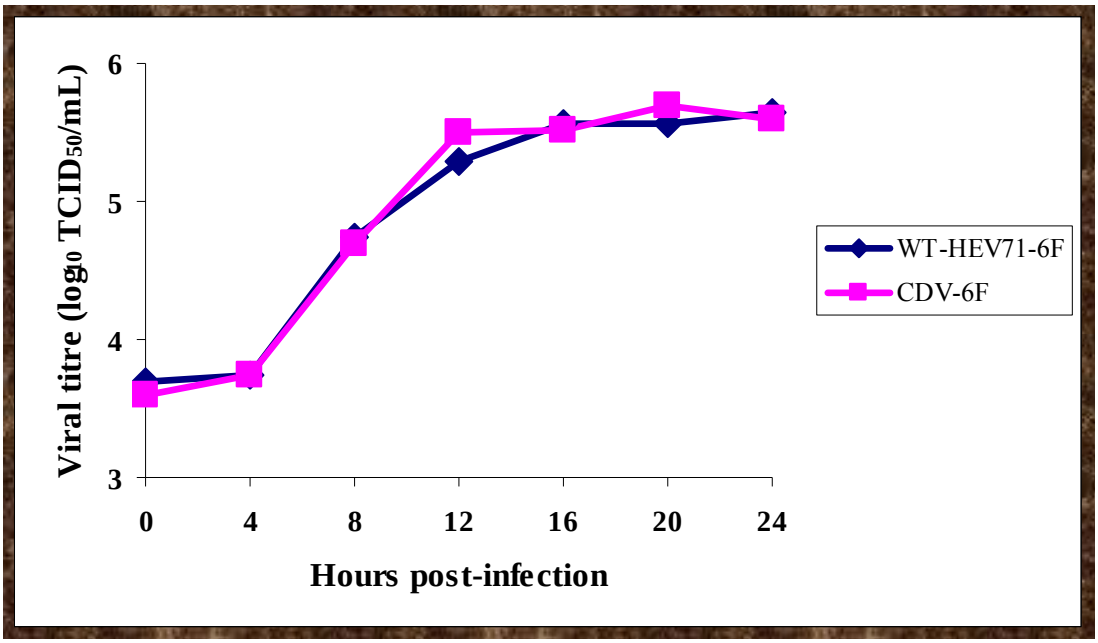

B

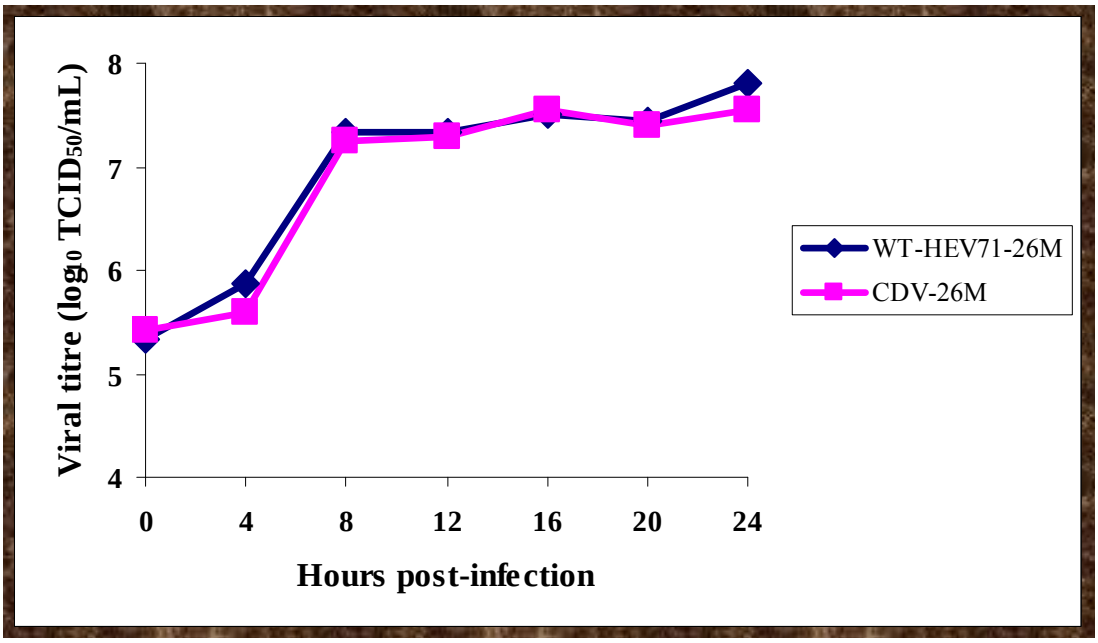

Figure 3.7 Growth kinetics of the parental and clone-derived HEV71-6F and HEV71-26M on RD cells. RD cell monolayers were infected with viruses at an MOI of 1x$TCID_{50}$/cell (HEV71-6F) or MOI of 10x$TCID_{50}$/cell (HEV71-26M). Samples of cell culture supernatant were collected at the times indicated and viral titres were determined by $TCID_{50}$ assay. All assays were performed in duplicate. (A) HEV71-6F and CDV-6F (B) HEV71-26M and CDV-26M

and HEV71-26M were also very similar (Figure 3.7). These data suggest that the parental and clone-derived viruses of both HEV71 strains are indistinguishable in their replication and spread in susceptible cells.

3.3 Discussion

Infectious cDNA clones provide a valuable tool for studying the molecular biology of RNA viruses. This approach is based on the infectious nature of the viral RNA genome in permissive host cells. In this study, full-length cDNA clones of two recent clinical isolates of HEV71 were successfully generated. RNA transcripts from plasmid DNA were infectious upon transfection into susceptible COS-7 cells. The clone-derived viruses exhibited biological properties indistinguishable from their parental viruses, including identical plaque morphology and growth kinetics.

A common problem encountered in the construction of infectious cDNA clones is the instability of the viral cDNA insert during passage in bacteria. This problem has been reported for several positive-stranded RNA viruses, including coronavirus and flavivirus (Masters, 1999, Mishin et al., 2001, Rice et al., 1989, Sumiyoshi et al., 1992). It has been hypothesized that genetic instability results from the expression of viral cDNA fragments encoding products that are potentially toxic to the bacterial host (Boyer & Haenni, 1994). Multiplication of clones containing toxic fragments in bacteria leads to the selection of mutations, deletions or gene rearrangements in the viral sequence (Boyer & Haenni, 1994).

Several strategies have been used to overcome this problem: (1) The cloning and propagating of full-length cDNA clones in bacteria was avoided. Full-length

infectious cDNA clones of several viruses were successfully obtained using sub-genomic clones and *in vitro* ligation approach in which the full-length *in vitro*-ligated fragments were directly used as a template for *in vitro* transcription (Kapoor et al., 1995, Rice et al., 1989, Sumiyoshi et al., 1992). In addition, high fidelity RT-PCR has been employed to generate full-length cDNA containing an upstream promoter for direct *in vitro* transcription. This approach was used to generate infectious RNA transcripts in tick-borne encephalitis virus (TBEV) (Gritsun & Gould, 1995). (2) Use of nonbacterial cloning systems, for example, the construction of full-length infectious cDNA clones of dengue virus type 1 and 2 in yeast cells (Polo et al., 1997). (3) Infectious cDNA clones designed to contain eukaryotic promoters for direct transfection of cell culture. The insertion of an intron into a toxic region in the viral genome prohibits the expression of toxic products, thus allowing stable amplification of the plasmid in bacteria (Yamshchikov et al., 2001). Infectious RNA was generated in the cell nucleus and the intron was removed by splicing during RNA translocation from the nucleus to the cytoplasm (Yamshchikov et al., 2001). Using this approach, infectious cDNA clones of Japanese encephalitis virus (JEV) and transmissible gastroenteritis coronavirus (TGEV) were successfully obtained (Gonzalez et al., 2002, Yamshchikov et al., 2001). (4) Full-length cDNA clones in high copy number plasmids were propagated in bacteria at low temperature and under a low level of antibiotic selection. This approach was reported in the construction of infectious dengue virus type 2 (Sriburi et al., 2001). (5) Full-length infectious cDNA clones were constructed by the use of medium- or low-copy number plasmid vectors and appropriate bacterial host strains. This approach has been reported for several positive-stranded RNA viruses (Hurrelbrink et al., 1999, Lai et al., 1991). (6) Bacterial artificial chromosomes

(BACs) have been employed. Genetic instability of JEV cDNA was overcome by cloning into a BAC plasmid (Yun et al., 2003).

There has been no report on the instability of enterovirus full-length cDNA clones. In a previous study by Arita et al. (2005), an infectious cDNA clone of the prototype HEV71 strain BrCr was initially constructed in a high copy number plasmid pCR-XL-TOPO which was found to be infectious. The authors did not comment on any genetic instability problems. However, this infectious cDNA clone was later cloned into a medium copy number plasmid P/Hd40 (Arita et al., 2005). In our study, attempts to generate an infectious cDNA clone of HEV71 strain 6F using the medium copy plasmid pBR322 were unsuccessful. The full-length cDNA clone, pBR/HEV71-6F propagated in DH5α at 37˚C was found to be non-infectious. Sequencing one of the pBR/HEV71-6F clones revealed that there were two stop codons, one located in the viral capsid protein VP3 and another in the non-structural protein 2A. It is likely that the bacterial host introduces these mutations into the viral genome in order to decrease the expression of HEV71 proteins that are toxic to bacterial host cell. Although less likely, the introduction of these mutations during PCR amplification cannot be ruled out.

Approaches to overcoming genetic instability of the full-length HEV71-6F in pBR322 by propagating bacterial host at a lower temperature of 30˚C and changing the bacterial host strain to DH10B was also not successful. Interestingly, pBR322 has been used successfully in the construction of infectious cDNA clones of some enteroviruses and flaviviruses such as PV and dengue virus type 2 and 4 (Cello et al., 2002, Kapoor et al., 1995, Lai et al., 1991). By contrast, infectious clones of JEV

(Sumiyoshi et al., 1992), TBE (Mandl et al., 1997), yellow fever virus (Rice et al., 1989) and MVE (Hurrelbrink et al., 1999) virus could not be constructed with this plasmid. These results indicate that the intermediate copy number of plasmid pBR322 may have exceeded the tolerance of bacterial cells to the toxic products derived from full length cDNA clones of these viruses.

In order to solve the problem of genetic instability, the low copy number plasmid pMC18 (approximately 6 copies per cell; Wang and Kushner, 1991) was tested. This plasmid has been used successfully for construction of an MVE infectious clone (Hurrelbrink et al., 1999). Sub-genomic and full-length cDNA clones of HEV71-6F were constructed in pMC18 and the clones propagated in two bacterial strains; DH10B and XL10-gold. Two full-length clones amplified in XL10-gold were found to be infectious whilst none of the clones propagated in DH10B were infectious. Using pMC18 and XL10-gold, an infectious cDNA clone of HEV71 strain 26M was also successfully constructed. These results clearly demonstrate that a fortuitous combination of plasmid vector and bacterial host was critical for generating infectious cDNA clones of HEV71. It remains unclear why XL10-gold was more suitable for propagating cDNA clones of HEV71 than DH5α and DH10B. The influence of bacterial host strain on infectivity of full-length cDNA clones has also been reported for several viruses, including dengue virus type 4 (Lai et al., 1991).

The inclusion of non-viral nucleotide sequences at the 5′ end of viral cDNA has been reported to have an adverse effect on the infectivity of some infectious clones, particularly in plant RNA viruses (Boyer & Haenni, 1994). In animal viruses, the influence of the number of non-viral nucleotides at the 5′ end on infectivity was assessed in Sindbis virus clones (Rice et al., 1987). Clones containing 8 to 198 non-

viral nucleotides were not infectious while only clones containing one additional G residue were infectious. These results indicated that large numbers of non-viral nucleotides at the 5′ end are deleterious to infectivity. In addition to length, the sequence of 5′ end non-viral nucleotides has also been found to have an effect on infectivity (Duechler et al., 1989). It has been hypothesized that the extra non-viral nucleotides at the 5′ end interfere with initiation of positive strand RNA synthesis from the 3′ end of the negative strand (Boyer & Haenni, 1994).

The effect of 5′ extension on clone-derived viral RNA infectivity has been reported for PV infectious clones (Kaplan et al., 1985). Similar to a Sindbis virus clone, the specific infectivity of a PV clone containing 60 non-viral nucleotides including 18 G residues was much lower than that of viral RNA, while the infectivity of clone-derived RNA with two additional G residues was similar to that of parental virus (van der Werf et al., 1986). Most enterovirus infectious cDNA clones contain an additional 1, 2 or 3 G residues at the 5′ end of the viral cDNA and these non-viral nucleotides have not been shown to alter infectivity (Arita et al., 2005, Kraus et al., 1995, Martino et al., 1999). It has been shown that one extra G residue at the end of the T7 promoter sequence is important for *in vitro* transcription efficiency (Janda et al., 1987). In this study, only HEV71-6F clones containing two G residues at the 5′ terminus were found to be infectious. The earlier report of HEV71 infectious clone of strain BrCr also contains two G residues. It is possible that the inclusion of two G residues in HEV71 clones provide the optimal conditions for efficient transcription and RNA synthesis.

The inclusion of non-viral nucleotide sequences at the 3′ end of viral cDNA has less effect on infectivity than at the 5′ end, the inclusion of 1 to 7 non-viral nucleotides at the 3′ end appears to be well tolerated (Boyer & Haenni, 1994). Similar to most animal viruses, the presence of four non-viral nucleotides in enterovirus cDNA clones as a result of linearisation at a unique restriction site has no apparent effect on infectivity (Kraus et al., 1995, Sarnow, 1989). By comparing the sequences of *in vitro* transcribed RNA with viral RNA of clone-derived virus, several studies found that non-viral nucleotide at the 5′ and 3′ end are removed, presumably during transfection and replication of the RNA templates in infected cells. (Khromykh & Westaway, 1994, Klump et al., 1990). It has been hypothesized that host cell nucleases may eliminate non-viral nucleotides or, alternatively, viral RdRps may be able to initiate replication of extended transcripts by recognizing their cognate binding site internally, leading to elimination of non-viral nucleotides in the daughter strand (Boyer & Haenni, 1994).

The poly (A) tail at the 3′ end may play an important role in the infectivity of enterovirus cDNA clones. It has been reported that PV RNAs with poly (A) tails less than 8 nucleotides in length were much less efficient in negative-strand RNA synthesis than those with 80 nucleotides (Herold & Andino, 2001). Silvestri *et al*. (2005) showed that PV RNAs with poly $(A)_{11}$ and poly$(A)_{12}$ had negative-strand RNA synthesis at 1-3% of the level observed with poly $(A)_{80}$ RNA, and increasing the length of the poly (A) tail from 12 to 20 residues resulted in an increase in negative strand synthesis by 30-fold or more. PV RNA with poly $(A)_{20}$ had a similar level of negative-strand RNA synthesis to poly$(A)_{80}$. These results indicate that the length of poly (A) tail plays an important role in viral RNA replication and

infectivity, possibly by assisting the binding of poly (A) binding protein. The HEV71 clones reported in this study and by Arita et al. (2005) were designed to contain a 25-mer poly (A) tail. Further studies are necessary to determine the minimum size of the poly (A) tail required for infectivity of HEV71 RNAs and to elucidate the role of the poly (A) tail in HEV71 RNA infection.

Either the cDNA clone or RNA transcripts have been used for transfection to recover clone-derived virus populations in most infectious clone systems (Boot et al., 1999, Hurrelbrink et al., 1999, Yun et al., 2003). Transfection of plasmid cDNA has been reported to have several advantages (Boot et al., 2001). *In vitro* transcription, which is an expensive and laborious process, is not required and infectivity is less affected by RNA degradation. In addition, Boot et al. (2001) compared RNA and cDNA transfection methods for rescue of infectious bursal disease virus (IBDV) and found that cDNA transfection gave rise to a much higher level of protein expression than RNA transfection, and was more efficient in recovering a crippled variant of IBDV. By contrast, porcine enteric calicivirus (PEC) could not be recovered by transfecting the plasmid cDNA clone, but only by transfecting of RNA transcripts (Chang et al., 2005). In this study, clone-derived HEV71 was obtained by transfection of either plasmid cDNA or RNA transcripts into susceptible cells. However, the recovery efficiencies between these two transfection methods were not compared. Since transfection of cDNA is simpler and less expensive, this method is preferable for recovering of clone-derived HEV71 populations.

Genotypic and phenotypic characterisation of clone-derived virus by comparison with parental virus is required to confirm the authenticity of the clone-derived virus.

Genetic characterisation of the HEV71-6F cDNA clone and its clone-derived virus population by complete nucleotide sequencing revealed one nucleotide difference compared to parental virus (GenBank). This mutation may have been introduced either during RT-PCR amplification or during cloning. Alternatively, this mutation may reflect the quasispecies nature of the parental virus stock. This silent mutation in the pHEV71-6F clone has no effect on infectivity and was still present in clone-derived virus. Complete sequencing of clone-derived CDV-26M showed no nucleotide difference compared to parental virus. Clone-derived CDV-6F and CDV-26M were compared to their parental virus in several aspects of viral replication, including plaque morphology and growth kinetics in cell culture. These clone-derived viruses showed in vitro growth properties indistinguishable from their parental viruses.

In conclusion, we have successfully constructed full-length infectious cDNA clones of two recent clinical isolates of HEV71. The availability of these infectious cDNA clones will make a significant contribution to the future study of viral replication and disease pathogenesis. Due to the distinct growth characteristics of these two strains, further studies were undertaken to determine the genomic regions responsible for their growth phenotypes, by constructing chimeric constructs between these two infectious clones. This work is described in Chapter 4.

CHAPTER FOUR

MAPPING GENETIC DETERMINANTS OF THE CELL CULTURE GROWTH PHENOTYPE OF HUMAN ENTEROVIRUS 71

4.1 Introduction

Human enterovirus 71 (HEV71) is a genetically diverse virus with an estimated evolution rate of 1.35×10^{-2} substitutions per nucleotide per year in the VP1 gene (Brown et al., 1999). Three distinct HEV71 genotypes, designated A, B and C were identified by Brown *et al*. (1999). The prototype strain BrCr is the sole member of genotype A. Most HEV71 isolates belong to either genotype B or C, which are further divided into subgenotypes B1-B5 and C1-C5, respectively (Brown et al., 1999, Cardosa et al., 2003, McMinn et al., 2001a, Shimizu et al., 2004, Tu et al., 2007). Co-circulation of these two distinct genotypes, B and C, in the same region has been well documented (Herrero et al., 2003, Lin et al., 2006, McMinn et al., 2001a). During an HEV71 outbreak in the USA in 1987, strains of both genotypes were isolated (Brown et al., 1999). Viruses belonging to both genotypes were also identified during the large HFMD epidemic in Taiwan in 1998 and several outbreaks in Malaysia from 1997 to 2000 and in Perth in 1999 (Herrero et al., 2003, Lin et al., 2006, McMinn et al., 2001a).

During the 1999 HFMD epidemic in Western Australia, HEV71 belonging to genotypes B3 and C2 were isolated, indicating the co-circulation of both genotypes. Genotype C2 viruses were isolated mainly from cases of severe neurological disease, while viruses belonging to genotype B3 were isolated mainly from uncomplicated HFMD cases and aseptic meningitis (McMinn et al., 2001a). Interestingly, we have

found that two HEV71 strains isolated during the Western Australian epidemic, 26M/AUS/99 (genotype B3) and 6F/AUS/99 (genotype C2) had distinct cell culture growth phenotypes. The studies in this chapter aim to identify genome regions responsible for the growth phenotypes of the two strains. Chimeric recombinant viruses carrying reciprocal exchanges of HEV71-6F and HEV71-26M 5′ UTR, structural protein genes (P1 region) and non-structural protein genes (P2 and P3 regions) were generated and biological properties of the parental and chimeric viruses in tissue culture were compared.

4.2 Results

4.2.1 Phenotypic differences of HEV71-6F and HEV71-26M

Both HEV71-6F and HEV71-26M are able to grow on human and monkey cell lines (RD and Vero cells). However, during the propagation of both wild-type and clone-derived viruses of these two strains, we were unable to generate high titre stocks of HEV71-6F; the maximal titre was approximately 10^6 $TCID_{50}$/mL, whilst HEV71-26M grew to high titres of $\geq 10^7$ $TCID_{50}$/mL. This prompted us to investigate the phenotypic differences of these two strains, including the use of plaque morphology, growth kinetics, virulence in mice and adaptation to rodent cells. Infectious clone-derived viruses, CDV-6F and CDV-26M, were used throughout the studies. Plaque size and morphology of HEV71-6F and HEV71-26M were examined on RD and Vero cells. HEV71-6F displayed a pinpoint plaque phenotype while HEV71-26M exhibited a large plaque phenotype (Figure 3.6). Both strains produced clearer plaques on Vero than on RD cells. The growth properties of HEV71-6F and HEV71-26M were compared by infecting monolayers of RD cells in 24-well tissue

culture trays at an MOI of 1 $TCID_{50}$/cell. HEV71-6F grew to approximately 100-fold lower titres than HEV71-26M (data not shown).

It has been reported that newborn mice are susceptible to HEV71 infection after intraperitoneal (i.p.) inoculation at a high viral titre (Yu et al., 2000). To determine if HEV71-6F and HEV71-26M are able to infect newborn mice and if there is an observable difference in virulence phenotype between these two strains, groups of five one-day-old BALB/c mice were inoculated by intracranial (i.c.) or i.p infection. with the highest doses possible, at 10^4 and $5x10^4$ $TCID_{50}$, for i.c. and i.p. inoculation, respectively. Similar to most HEV71 strains, both HEV71-6F and HEV71-26M caused no observable signs of infection in newborn mice (data not shown).

In order to determine if HEV71-6F and HEV71-26M are able to adapt and grow in cells of rodent origin, confluent CHO cells were infected with each virus at MOI = 1. Both viruses were then blind passaged five times in CHO cells and the viral titre at each passage was determined by $TCID_{50}$ assay. HEV71-6F was not able to adapt to CHO cells; the viral titres decreased at approximately one log in each subsequent passage and no virus was detected at passages four and five (Figure 4.1). By contrast, HEV71-26M adapted to grow well in CHO cells after passage two, with the titre increasing by approximately one log at each passage (Figure 4.1).

(A)

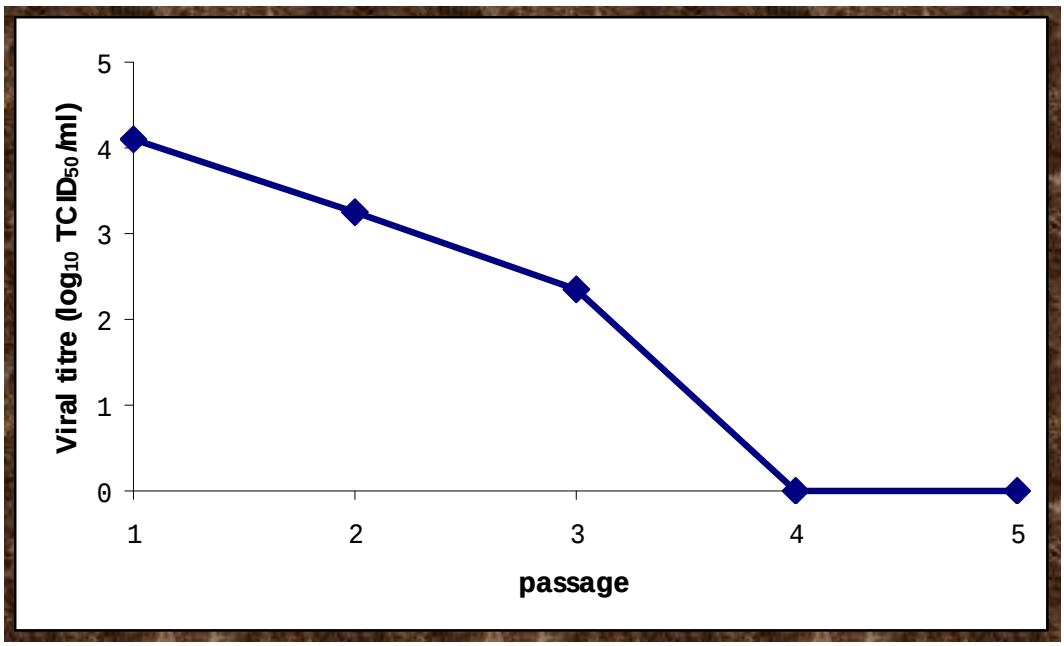

(B)

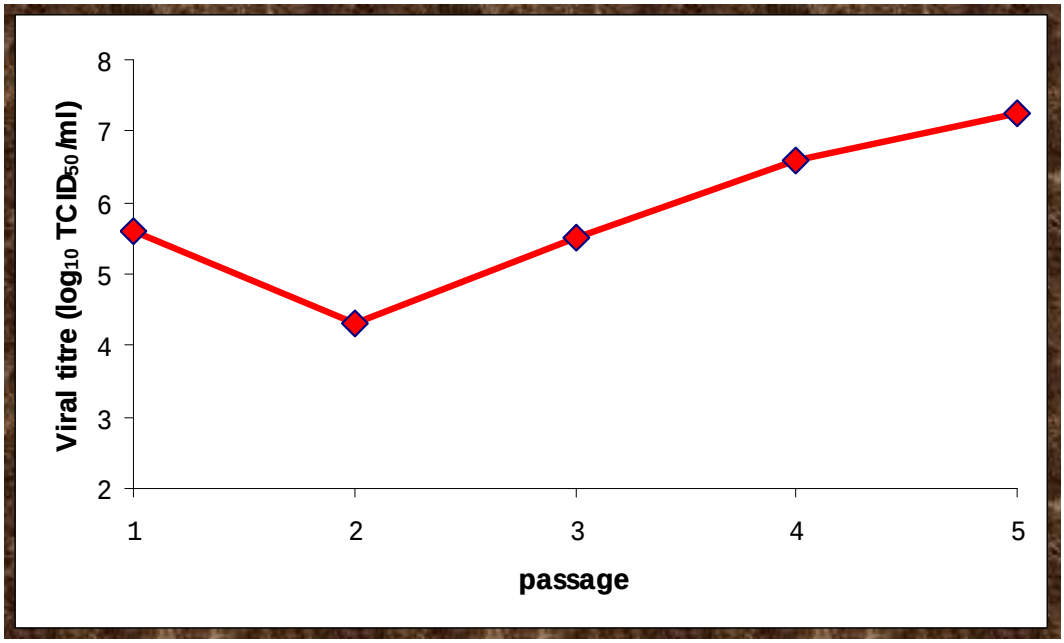

Figure 4.1 Adaptation of HEV71-6F and HEV71-26M to growth in CHO cells. CHO cells monolayers were infected with each virus at an MOI of 1. Virus was then blind passaged five times and the viral titre at each passage determined by $TCID_{50}$ assay on Vero cells. At each passage, virus was harvested after 72 h of incubation. (A) HEV71-6F (B) HEV71-26M

4.2.2 Comparison of nucleotide and deduced amino acid sequences of HEV71-6F and HEV71-26M

Whole genome sequencing of strains HEV71-6F and HEV71-26M was performed by Robert Hurrelbrink and Beng Hooi Chua (Division of Virology, Telethon Institute for Child Health Research). The complete nucleotide and deduced amino acid sequences of HEV71-6F and HEV71-26M were compared by pair-wise alignment using global parameters of the Clone Manager 5/Align Plus 4 software program. The nucleotide and amino acid sequence similarities between HEV71-6F and HEV71-26M are shown in Table 4.1.

The HEV71-26M genome is three nucleotides longer than that of HEV71-6F, with the three nucleotide difference located in the 5′ UTR. Overall, the nucleotide and amino acid identity between these two strains are 80% and 95%, respectively. The non-coding regions, 5′- and 3′- UTRs of HEV71-6F and HEV71-26M had a similar degree of nucleotide sequence identity at 85% and 84%, respectively. The capsid region, P1, has the highest nucleotide and amino acid sequence identity at 82% and 96%, respectively, while the P3 region has the lowest sequence identity at 77% and 93%, respectively. For each individual protein cleavage product, VP4 is the most conserved protein (100% amino acid identity) and 3C and 3D proteins appear the least conserved (93% amino acid identity).

Table 4.1 Nucleotide and deduced amino acid sequence identity of HEV71-6F and HEV71-26M

Genetic region	Length (nt)	Sequence identity (%)	
		Nucleotide	Amino acid
Genome	7409/7412	80	95
5′ UTR	744/747	85	-
P1	2586	82	96
VP4	207	81	100
VP2	762	83	97
VP3	726	80	96
VP1	891	82	95
P2	1734	78	96
2A	450	81	96
2B	297	76	94
2C	987	78	96
P3	2259	77	93
3A	258	76	94
3B	66	80	95
3C	549	74	93
3D	1386	78	93
3′ UTR	86	84	-

4.2.3 Secondary structure analysis of HEV71-6F and HEV71-26M

Complex RNA secondary structures have been identified both in the non-coding and coding regions of the enterovirus genome (Goodfellow et al., 2000, Le et al., 1996, Pilipenko et al., 1989, Pilipenko et al., 1992b). The non-coding regions, 5′- and 3′-UTRs, contain RNA structural motifs that are important for viral replication and/or translation (Andino et al., 1993, Andino et al., 1990, Le et al., 1996, Pilipenko et al., 1989, Pilipenko et al., 1992a). An internal structural element, termed the *cis*-acting replication element or *cre* has been identified within the 2C coding region of several enteroviruses (Goodfellow et al., 2000, Paul et al., 2000, Van Ooij et al., 2006). Enteroviruses employ both stem-loops and bulges within these RNA secondary structures as a contact point for cellular and viral protein binding (Andino et al., 1993, Andino et al., 1990, Paul et al., 2000, Pilipenko et al., 1996). The protein-RNA interactions on the secondary structures are required during RNA replication and translation processes.

As RNA secondary structures are involved in important viral replication activity, such as RNA replication and translation, we predicted and compared secondary structures of 5′- and 3′- UTRs and *cre* between HEV71-6F and HEV71-26M in order to identify potential molecular determinants of growth phenotype. All secondary structures were predicted using the MFOLD (version 3.2) software program (Mathews et al., 1999, Zuker, 2003). Computer predictions of RNA secondary structures of HEV71-6F and HEV71-26M were performed based on the cognate structures of poliovirus type 1 (PV1) Mahoney strain and CBV3 Nancy strain. The

predicted secondary structures of these viruses have been validated by chemical and enzymatic probing for nucleotides involved in base pairing and mutagenesis analysis (Bailey & Tapprich, 2007, Pilipenko et al., 1992a).

4.2.3.1 5′ UTR and 3′ UTR

The 5′ UTR of enteroviruses contains two highly conserved elements, the 5′ cloverleaf (stem loop I) and the internal ribosomal entry site (IRES). Stem-loop structures II to VI form the IRES (Pilipenko et al., 1989, Skinner et al., 1989). The 5′ UTR sequences of PV1, CBV3, HEV71-6F and HEV71-26M were aligned, and the nucleotide sequence and boundary of each domain of HEV71 5′ UTR identified (Figure 4.2). The structure of each domain of HEV71 5′ UTR was then predicted using MFOLD software (Mathews et al., 1999, Zuker, 2003). The predicted structures of each virus are shown in Figure 4.3. The 5′ UTR secondary structures of HEV71-6F and HEV71-26M were found to be highly similar to one another.

In addition to structural elements, three common sequence motifs that have been identified as key elements in the function of enterovirus IRES were also compared. The first motif is located in the region linking domains V and VI. This motif is described as Yn-Xm-AUG, where Yn is a pyrimidine-rich sequence, Xm is a 15- to 25- nt spacer, and AUG is the 3′ boundary of the IRES (Pilipenko et al., 1992b). The second motif, GNRA tetra-loops, is located at the terminal loop of domain IV (Ehrenfeld & Teterina, 2002). The third motif are two A/C rich loops located at domain IV and V (Lopez de Quinto & Martinez- Salas, 1997). Similar to PV1 and CBV3, these three IRES motifs were identified in both HEV71-6F and HEV71-26M (Figure 4.3).

Domain I

```
PV1          uuaaaacagcucugggguuguacccacccagaggcccacguggcggcuaguacuccgguauugcgguacccuuguacgccuguuuuauacucccuuccc 100
HEV71-6F     .........cugu......c......-...c...g..uac...gc.....c....u..c.c..a......u....g..........gacu.........  99
HEV71-26M    .........cugu......c......u.acag...........-.....c....u.a.uc.a...a.u.u....g...........c.ac...cc...  99
CBV3-Nancy   .........cugu......au.....-...c.......-u...gc.....c....u.....ca.......u....g...............c....c...  98
```

Domain II

```
PV1          -------gu-----a------acuuagacgc---a---caaaaccaa-guucaa----uagaagg----ggguacaaaccaguaccaccacgaacaagca 167
HEV71-6F     cgaa---..-----.------.......a..---u---gu...u...c.a....----...u.....-u.ug...c......cau.u.uu..u...... 171
HEV71-26M    aauuu--.c-----.------.......a..----.aua..c...acu-.a.....---c..c.....-caugg.gc.....ccaugu.uu..u...... 174
CBV3-Nancy   caacu--..-----.------.......a.u---.---ac.c..acc-.a.....---c..uca.----c.ugg..c.....cca.guuuu..u...... 170
```

Domain III

```
PV1          cuucuguuucccggu--u--gaugucguauagacugcuugcgugguugaaagcgacgga-uccguuauccgcuuauguacuucgagaagcccaguaccac 262
HEV71-6F     ..............ac.--..guauca....g.....c...c..c....g.a..aaacg.u.....c...acc.ac.............uu........ 269
HEV71-26M    ..............ac.--..guauca..........ca..c.......g.a..aa.cg.....gc..ac...........a..u....g... 272
CBV3-Nancy   .......a....ac.--..guauca..........ca..c.......g.a..aa.cg.u.....gcc.ac........a..a..u....a... 268
```

Domain IV

```
PV1          cucggaaucuucgaugcguugcgcucagcacucaaccccagaguguagcuuaggcugaugagucuggacaucccucaccggugacggugguccaggcugc 362
HEV71-6F     .au.a.cgagg.aga.u...u..u.......-.......-.......a.c...........c.acug..a...c..ug..c...ca...cagu...... 365
HEV71-26M    .auu...g..g..ga.u...u.....g.....ucc...----.....a.c....c........acug..au..c...g..c...c....cagu...... 368
CBV3-Nancy   .gu....gu.g.aga.u...u..........-.....-.......a.c...uc........accg...u..c...g..c...c....cggu...... 364
```

```
PV1          guuggcggccuaccuauggcuaacgccaugggacgcu--agu-uguga-acaaggugugaagagccuauugagcuacauaagaauccuccggccccugaa 458
HEV71-6F     ..........g..c....ag..au...........cu.a.-.c..-...u.....................gc.ggu.g.....------------ 462
HEV71-26M    .c.........g......ggc.ac....a.......--cuaa....g-...u....c......u..........gu..gu.g.....------------ 465
CBV3-Nancy   ..........g..c....gg..ac...........--cua-auac.g...u....c......u..........gu.ggu.g.....------------ 461
```

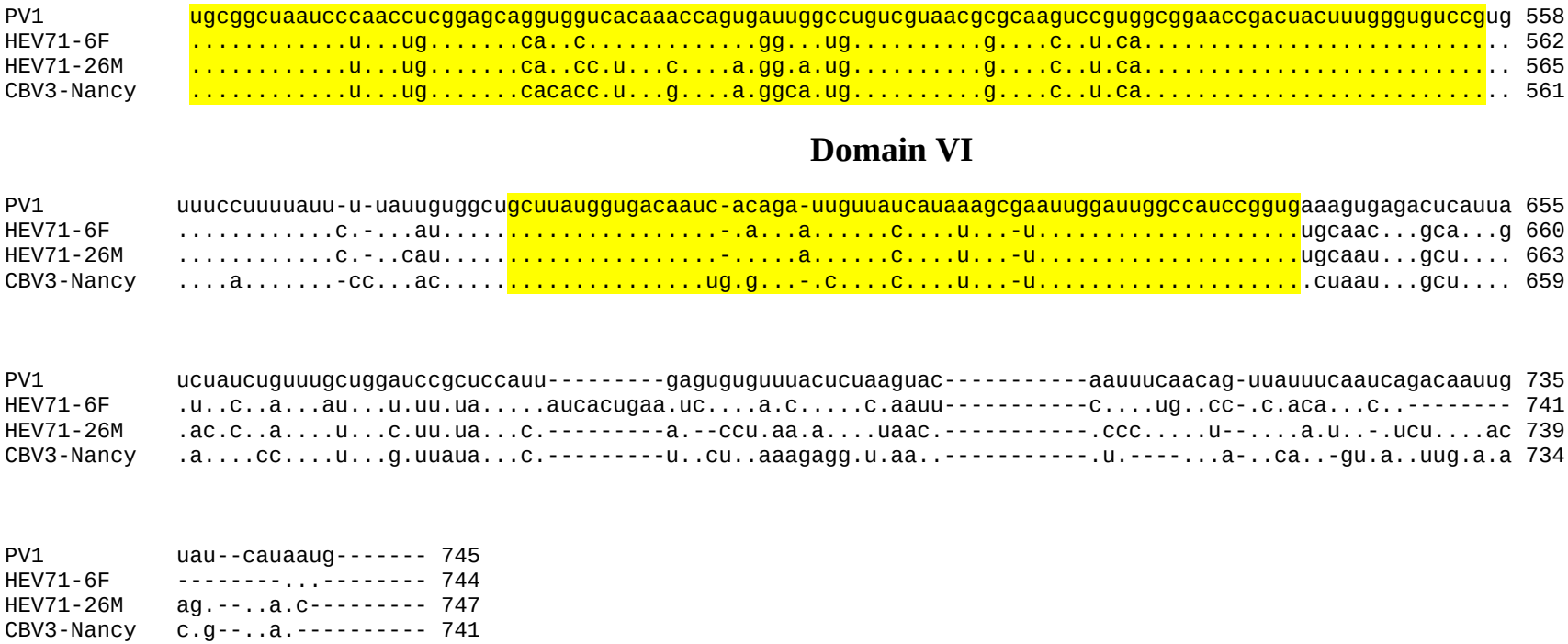

Figure 4.2 Sequence alignments of the cloverleaf and IRES elements of HEV71-6F, HEV71-26M, CBV3 and PV1 based on known PV1M and CBV3 5′UTR secondary structure sequences (Andino et al., 1990, Bailey & Tapprich, 2007, Pilipenko et al., 1989, Skinner et al., 1989). Corresponding domains are indicated. Consensus sequence is represented as (•) and gap sequence is represented as (-).

Figure 4.3 Comparison of the predicted 5′ UTR secondary structures of HEV71-6F and HEV26M. The 5′ UTR structures of HEV71-6F and HEV71-26M were predicted based on the structures of PV1 **(A)** and CBV3 **(B)**. The structure of each domain was predicted using MFOLD (Version 3.2) software. **(C)** HEV71-6F, **(D)** HEV71-26M. Three common sequence motifs are shown in different colours, Yn-Xm-AUG motif in blue, GNRA motif in red and A/C rich sequence motif in yellow.

(A) PV1 Mahoney

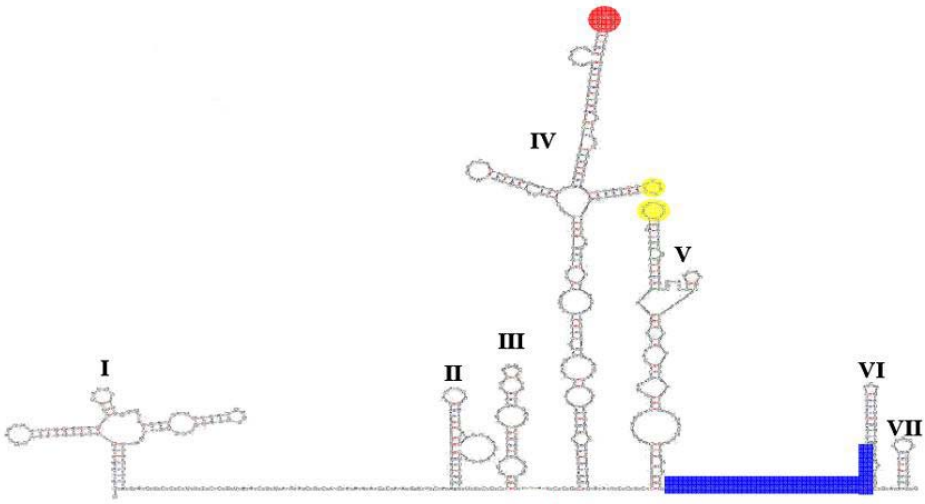

(B) CBV3

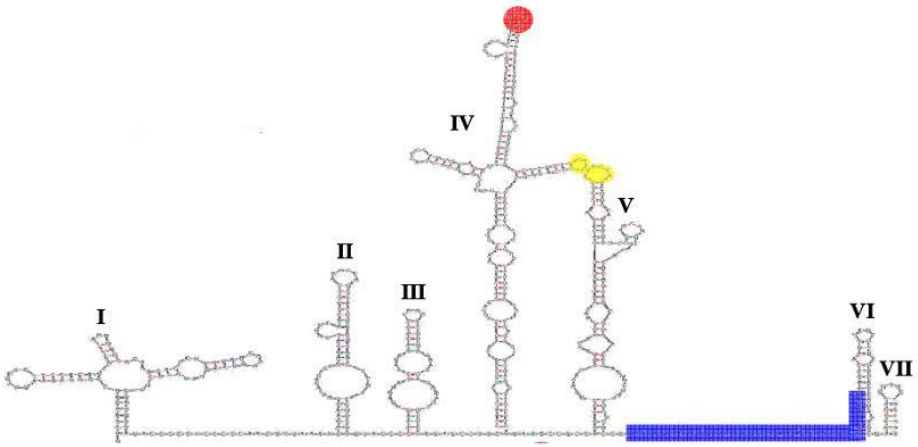

(C) HEV71-6F

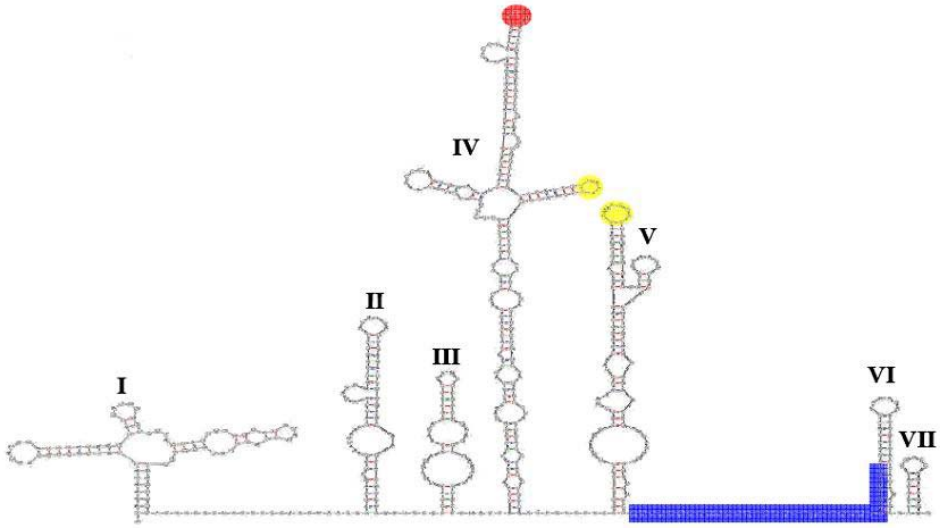

(D) HEV71-26M

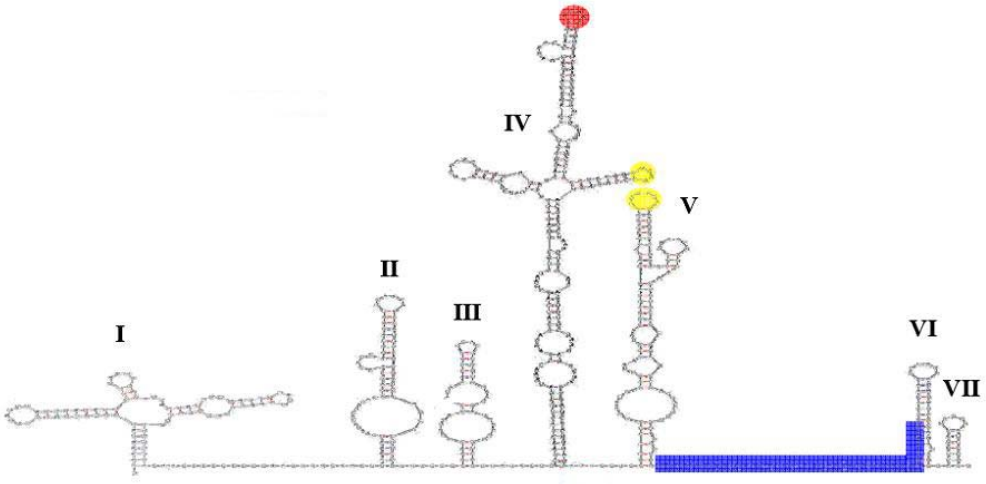

The 3′ UTR of enteroviruses encodes a stem-loop structure that is not universally conserved. Two forms of the 3′ UTR secondary structure of enteroviruses have been identified (Pilipenko et al., 1992b). Two stem-loops, X and Y, were predicted to form within the 3′ UTR of PV (Pilipenko et al., 1992b), while the 3′ UTR of CBV3 was predicted to contain three stem-loops, X, Y and Z (Pilipenko et al., 1992b). Similar to the 3′ UTR of CBV3, the 3′ UTR secondary structures of HEV71-6F and HEV71-26M were predicted to contain three stem-loops, X, Y and Z, and are similar to one another (Figure 4.4).

4.2.3.2 Cis-acting replication element (cre)

Cre functions as a template for $3D^{pol}$ during the uridylylation of VPg in RNA synthesis. *Cre* elements have been identified within the 2C protein gene of PV (Goodfellow et al., 2000, Paul et al., 2000) and CBV3 (Van Ooij et al., 2006). The *cre* elements identified thus far share similar stem-loop structures (Goodfellow et al., 2000, McKnight & Lemon, 1998, Paul et al., 2000, Van Ooij et al., 2006). A common motif, $R^1NNNA^1A^2R^2NNNNNNR^3$, has been proposed for the loop segment. The *cre* sequences of HEV71-6F and 26M were identified by nucleotide sequence comparison with the PV1 and CBV3 *cre* sequences (Figure 4.5), and the *cre* structures predicted by MFOLD software. The predicted *cre* structures of HEV71-6F and HEV71-26M were found to be different (Figure 4.5), in which *cre* structures of HEV71-6F and HEV71-26M were similar to that of PV1 and CBV3, respectively. The predicted *cre* structure of HEV71-6F contained 9 nucleotides of terminal loop and 7 nucleotides internal loop. For HEV71-26M, a difference at the nucleotide position 13 of the core *cre* consensus sequence from HEV71-6F resulted in the formation of a larger terminal loop of 16 nucleotides.

Figure 4.4 The predicted 3′ UTR secondary structures of HEV71-6F and HEV71-26M based on the 3′ UTR sequences and structures of PV1 and CBV3 (Pilipenko et al., 1992b). **(A)** nucleotide sequence alignments of 3′ UTR of PV1, CBV3, HEV71-6F and HEV71-26M. **(B)** The 3′ UTR secondary structures of each virus were predicted using MFOLD (Version 3.2) software. Stem-loop structures X, Y and Z of the 3′ UTR are indicated.

(A)

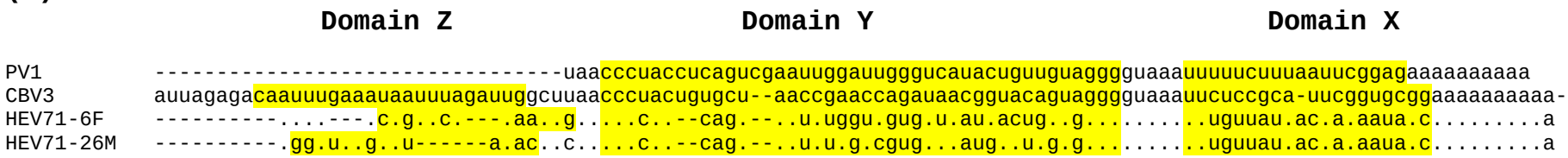
Domain Z
Domain Y
Domain X
PV1 ----------uaacccuaccucagucgaauuggauugggucauacuguuguaggggguaaauuuuucuuuaauucggagaaaaaaaaaa
CBV3 auuagagacaauuugaaauaauuuagauuggcuuaacccuacugugcu--aaccgaaccagauaacgguacaguaggggguaaauucuccgca-uucggugcggaaaaaaaaaa-
HEV71-6F ----------.....---.c.g..c.---.aa..g.....c..--cag.--..u.uggu.gug.u.au.acug..g.....uguuau.ac.a.aaua.c.....a
HEV71-26M ----------.gg.u..g..u-----a.ac..c.....c..--cag.--..u.u.g.cgug...aug..u.g.g.....uguuau.ac.a.aaua.c.....a

(B)

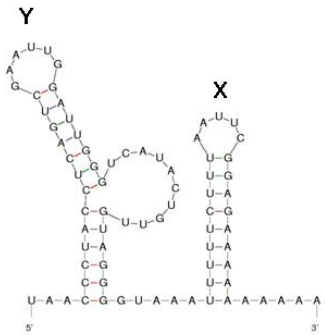

PV1

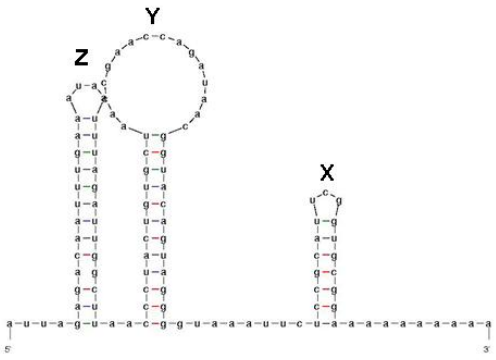

CBV3

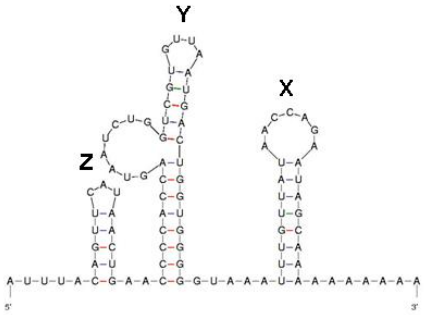

HEV1-6F

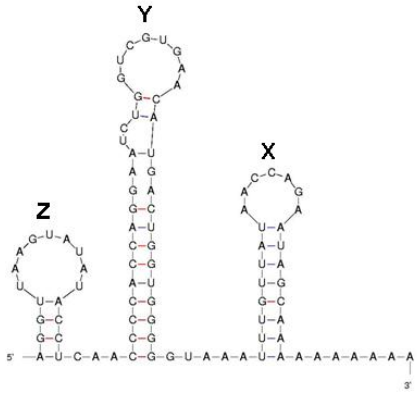

HEV71-26M

(A)

```
PV1     uauuaacaacuacauacaguucaagagcaaacaccguauugaaccaguauguuugcuagua-- 4504
CBV3    g..g.g...u.............uc....ug.....u..........cc.g-- 4421
6F      a..g..u..u.....g.....................u.....cc.aa.ca.u-- 4458
26M     a..g..........g.....................a.....u......c.--..u..uu 4461
```

(B)

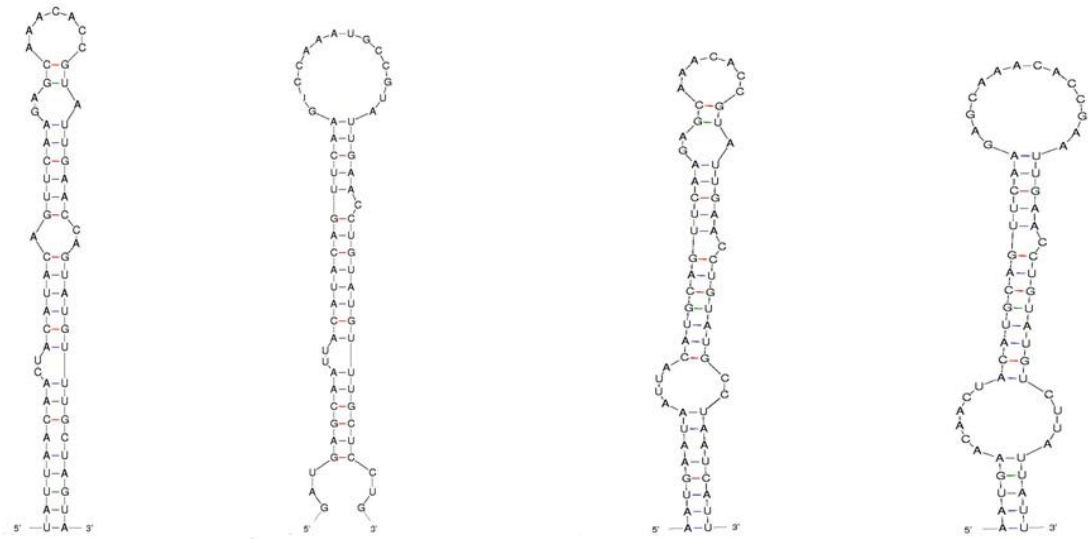

Figure 4.5 The predicted *cre* structures of HEV71-6F and HEV71-26M based on the *cre* sequences and structures of PV1 and CBV3 (Goodfellow et al., 2000, Paul et al., 2000, Van Ooij et al., 2006). **(A)** nucleotide sequence alignments of *cre* of PV1, CBV3, HEV71-6F and HEV71-26M; the consensus sequence is highlighted in yellow. **(B)** The *cre* secondary structures of each virus were predicted using MFOLD (Version 3.2) software.

4.2.4 Construction and recovery of chimeric recombinant viruses

To identify the genome regions responsible for the growth phenotype of HEV71-6F and HEV71-26M, six chimeric recombinant cDNA constructs (p6F/5′UTR/26M, p26M/5′UTR/6F, p6F/P1/26M, p26M/P1/6F, p6F/NS/26M and p26M/NS/6F) were generated by exchanging corresponding 5′ UTR, structural protein gene (P1 region) and non-structural protein gene (P2 and P3) regions between these two strains, resulting in three reciprocal pairs of chimeric genomes (Figure 4.6). Chimeras are identified in the form of pA/B/C, where A is a backbone virus, B is the exchanged genomic region, C is the name of the virus providing the exchange genomic region. Chimeric recombinant clones were constructed using fusion PCR and site-directed mutagenesis; the full-length infectious cDNA clones of HEV71-6F and HEV71-26M were used as backbone templates. Construction procedures are described in detail in section 2.2.14.

Six chimeric cDNA clones were co-transfected with pCMV-T7Pol into COS-7 cells, as described in section 2.2.17, in order to rescue chimeric recombinant viruses. Viable virus populations were recovered from all six cDNAs. Recovered viruses were passaged five times in RD cells to increase the titre for use in subsequent assays. In order to verify that the recovered viruses contained the expected genetic composition, RNA extracted from each recovered virus population at RD passage 5 was sequenced. Analysis of the sequence data obtained from the junction sites of each virus revealed that all recovered viruses had the expected genotype (data not shown).

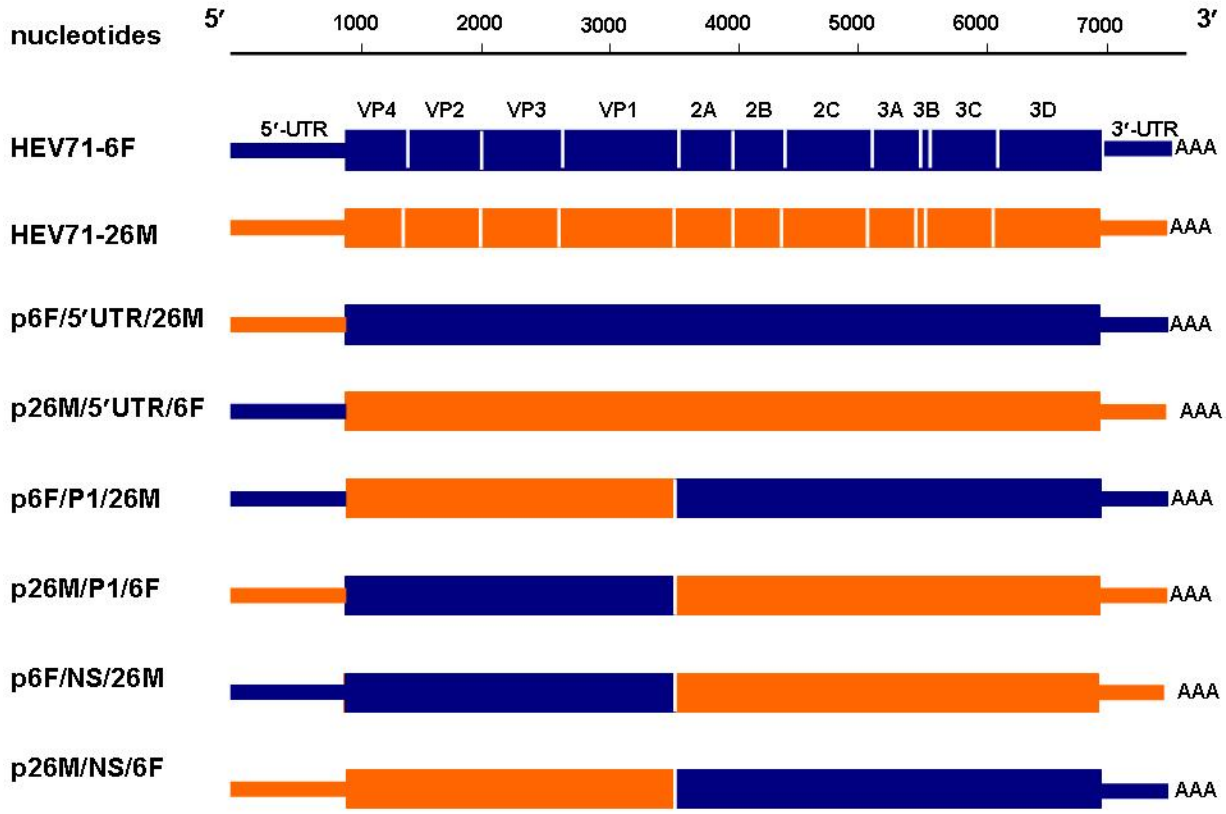

Figure 4.6 Schematic diagram of the intratypic chimera recombinant constructs between HEV71-6F and HEV71-26M. Chimeras are identified by using the following nomenclature; pA/B/C where A is the backbone virus, B is the exchange genomic region, C is the the name of virus providing the exchanged genomic region.

4.2.5 Characterisation of chimeric recombinant viruses in vitro

In order to map genetic determinants of the cell culture growth phenotype of HEV71-6F and HEV71-26M, plaque morphology and growth kinetics of the parental CDV-6F, CDV-26M and all chimeric recombinant viruses were compared.

4.2.5.1 Plaque morphology

Plaque morphologies of the parental and recombinant viruses were examined on Vero and RD cell monolayers. Although the parental and recombinant viruses produced a clearer plaque morphology on Vero cells, similar patterns of plaque morphology were observed on both Vero and RD cells (Figure 4.7). Average plaque size was determined on Vero cells from samples of 9 to 13 plaques. Results are shown in Table 4.2. Parental viruses and reciprocal chimeras with a replacement in the 5′ UTR displayed similar plaque morphology: HEV71-6F and 6F/5′UTR/26M had extremely small plaque phenotypes (less than 0.5 mm diameter), whereas HEV71-26M and 26M/5′UTR/6F had large plaque phenotypes (average sizes of more than 2 mm diameter). Interestingly, compatibility between capsid (P1) and non-structural proteins (P2 and P3) of HEV71-6F and HEV71-26M were found to be nonreciprocal. The HEV71-26M-based chimera with a derived 6F P1 region, 26M/P1/6F, had a small plaque phenotype similar to that of HEV71-6F (less than 0.5 mm). However, the HEV71-6F-based chimera with the 26M P1 region, 6F/P1/26M, was also found to display a small plaque phenotype, with an average size of 0.9 (±0.5) mm. The HEV71-6F-based chimera with 26M P2- P3 regions, 6F/NS/26M, exhibited a large plaque size of 1.4 (±0.46) mm. The plaque size of 6F/NS/26M

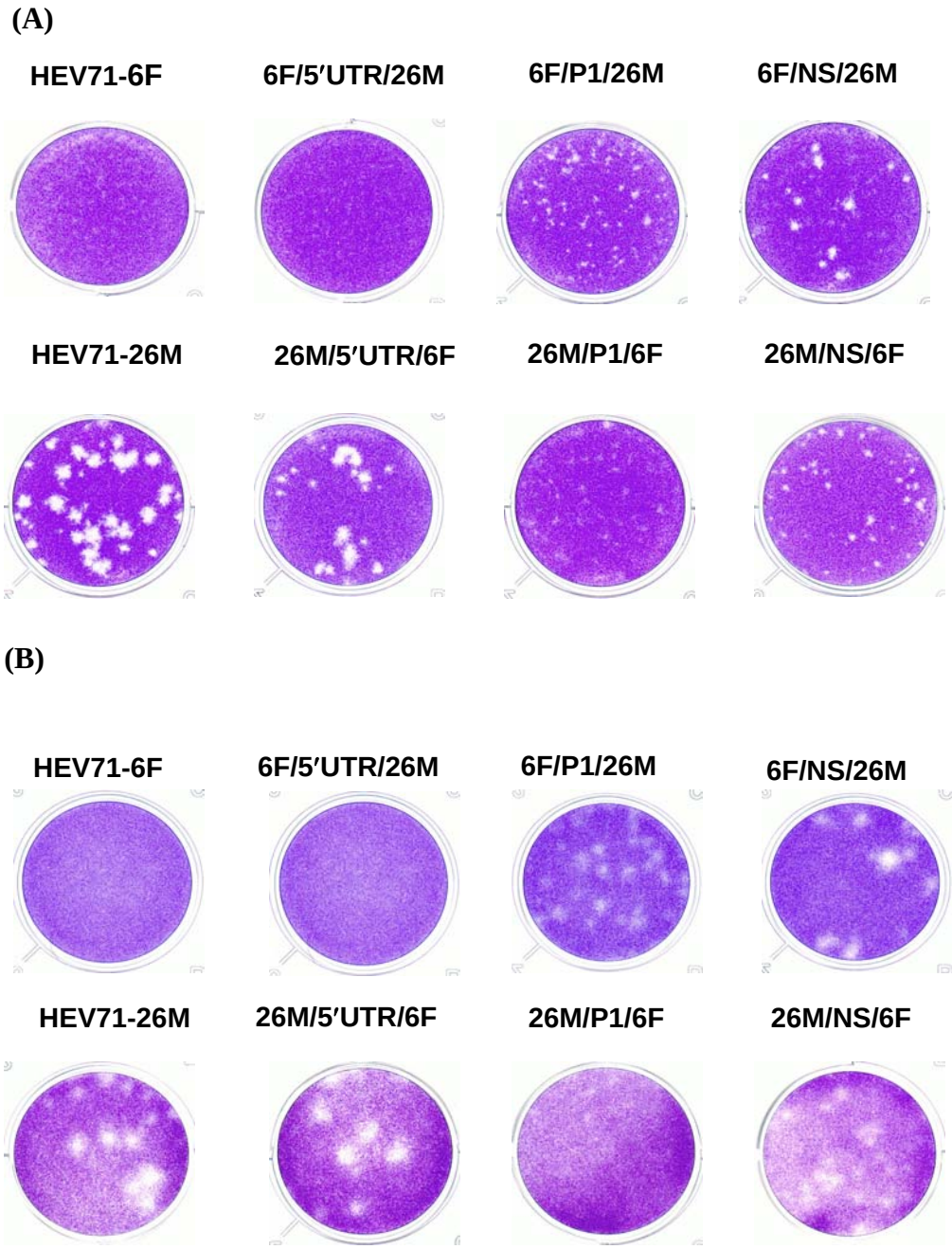

Figure 4.7 Plaque phenotype of parental HEV71-6F and HEV71-6F based chimera viruses on Vero **(A)** and RD **(B)** cells. Ten-fold serial dilutions of virus were inoculated at 100 μL per well in 12-well tissue culture trays. Infected cells were incubated for seven days before staining with crystal violet solution.

Table 4.2 Plaque phenotypes of parental and chimeric recombinant viruses on Vero cells

Parental backbone virus	Viruses	Average diameter of plaques (mm)[#]
HEV71-6F	HEV71-6F	<0.5
	6F/5′UTR/26M	<0.5
	6F/P1/26M	0.9 (0.5)
	6F/NS/26M	1.4 (0.46)
HEV71-26M	HEV71-26M	2.29 (0.78)
	26M/5′UTR/6F	2.09 (0.76)
	26M/P1/6F	<0.5
	26M/NS/6F	1 (0.47)

Numbers in brackets = standard deviation.

was, however, smaller than that of HEV71-26M. In addition, HEV71-26M-based chimera with 6F P2-P3 regions, 26M/NS/6F, produced a larger plaque size than HEV71-6F. The average plaque size of 26M/NS/6F is 1 (±0.47) mm.

4.2.5.2 Growth kinetics

The growth characteristics of parental and chimeric viruses were compared in Vero and RD cells. Both Vero and RD cells were infected at a MOI of 5 $TCID_{50}$/cell. All assays were performed in triplicate and results are shown in Figure 4.8.

Overall, similar growth characteristics were observed on Vero and RD cells. In general, all viruses exhibited similar growth patterns, with titres rising from 4 h post-infection and peaking between 10^6-$10^{7.7}$ $TCID_{50}$/mL at about 12 to 16 h post-infection. Similar to plaque morphology results, reciprocal 5′ UTR chimeras, 6F/5′UTR/26M and 26M/5′UTR/6F had similar growth to their parental backbone viruses. HEV71-6F and 6F/5′UTR/26M produced a peak titre of 10^6 $TCID_{50}$/mL in both Vero and RD cells, whilst HEV71-26M and 26M/5′UTR/6F replicated more efficiently, with peak titres of 10^7 and $10^{7.7}$ $TCID_{50}$/mL in Vero and RD cells, respectively.

Reciprocal P1 and P2-P3 chimeras were found to display growth characteristics in between that of the parental backbone viruses. In HEV71-6F-based chimera viruses, 6F/NS/26M replicated most efficiently, with titres of $10^{6.5}$ and $10^{7.2}$ $TCID_{50}$/mL at 12 h post-infection in Vero and RD cells, respectively. Chimeric virus, 6F/P1/26M, grew slower than that observed for 6F/NS/26M during initial stages of infection.

(A)

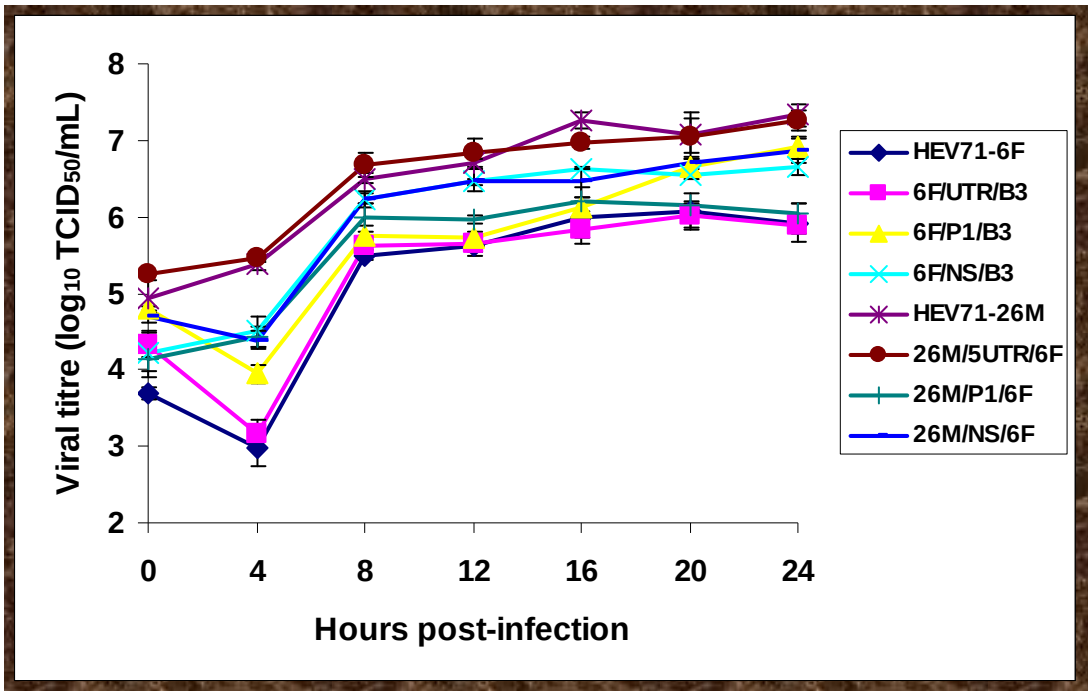

(B)

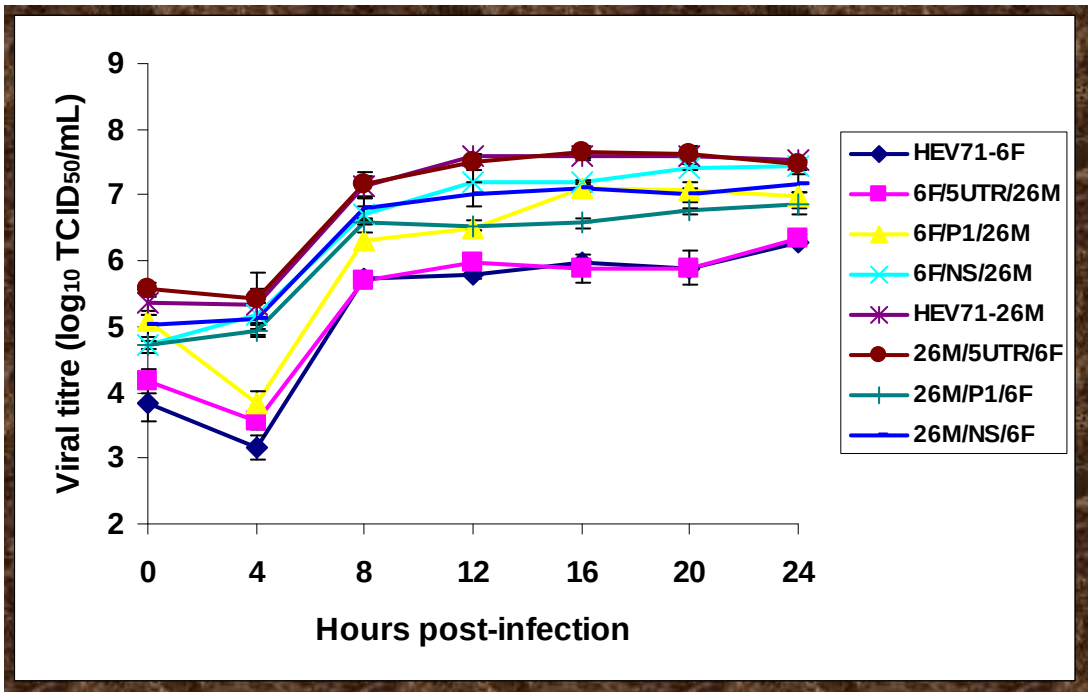

Figure 4.8 Single step growth kinetics of parental and chimeric viruses on Vero **(A)** and RD cells **(B).** Cell monolayers were infected with at an MOI of 5xTCID/cell. Cell culture supernatants were collected at the times indicated and titrated by $TCID_{50}$ assay. All assays were performed in triplicate. At each time point, titres are the average of three samples; error bars represent the standard error of the mean.

The growth rate of 6F/P1/26M at 12 h post-infection was comparable to HEV71-6F, with titres of $10^{5.7}$ and $10^{6.5}$ $TCID_{50}$/mL in Vero and RD cells, respectively. However, this virus produced high peak titres of $10^{6.7}$ $TCID_{50}$/mL at 20 h post-infection in Vero cells and $10^{7.1}$ $TCID_{50}$/mL at 16 h post-infection in RD cells. In summary, the peak titres obtained for 6F/NS/26M were about threefold lower than HEV71-26M in both Vero and RD cells, and 6F/P1/26M produced two- and fourfold lower titres than HEV71-26M in Vero and RD cells, respectively. Both 6F/NS/26M and 6F/P1/26M replicated to higher titres than the parental HEV71-6F.

In HEV71-26M based chimera viruses, the titres obtained at 12 h post-infection for 26M/NS/6F were $10^{6.5}$ and 10^{7} $TCID_{50}$/mL in Vero and RD cells, respectively. These titres were three- and fivefold lower than the titre produced by HEV71-26M. Chimeric 26M/P1/6F replicated less efficiently than 26M/NS/6F, with titres at $10^{6.2}$ and $10^{6.6}$ $TCID_{50}$/mL in Vero and RD cells, respectively. These titres correspond to six- and thirteen-fold lower than the titres observed for HEV71-26M. Both 26M/NS/6F and 26M/P1/6F replicated to higher titres than the parental HEV71-6F.

Taken together, the results of plaque morphology and growth kinetics indicated the 5′ UTR of both strains were compatible but not responsible for the observed phenotypes. Both the P1 and P2-P3 genome regions were found to influence the HEV71 growth phenotype in cell culture.

4.2.6 Translation efficiency of HEV71-6F and HEV71-26M 5′ UTR

In order to verify the compatibility of the 5′ UTR between HEV71-6F and HEV71-26M, the translation efficiencies of 5′ UTR of these two strains were compared using bi-cistronic constructs and luciferase assays. Each bi-cistronic construct contained two luciferase genes; renilla luciferase (LucR) and firefly luciferase (LucF). LucR is controlled by the cytomegalovirus immediate-early promoter (IE) and LucF was controlled by a hairpin, HEV71-6F 5′ UTR or HEV71-26M 5′ UTR for pCRHL, pCR6F and pCR26M, respectively. (Three bi-cistronic constructs were kindly provided by Dr. Chee Choy Kok, Discipline of Infectious Diseases and Immunology, The University of Sydney, Australia). *In vivo* translation efficiencies of these three constructs were measured in both RD and COS-7 cells. RD and COS-7 cells were seeded onto 24-well plates and incubated for 24 h on order to reach about 90% confluency at the time of transfection. One microgram of each bi-cistronic construct and 3 μL of Lipofectamine^{TM} 2000 were transfected into the cells using the protocol described in 2.2.17. Cells were assayed for luciferase activity at 24 h post-transfection. The resulting translation efficiencies are shown in Figure 4.9. The translation efficiency of HEV71-6F 5′ UTR or HEV71-26M 5′ UTR was not significantly different in both RD and COS-7 cells ($p>0.05$).

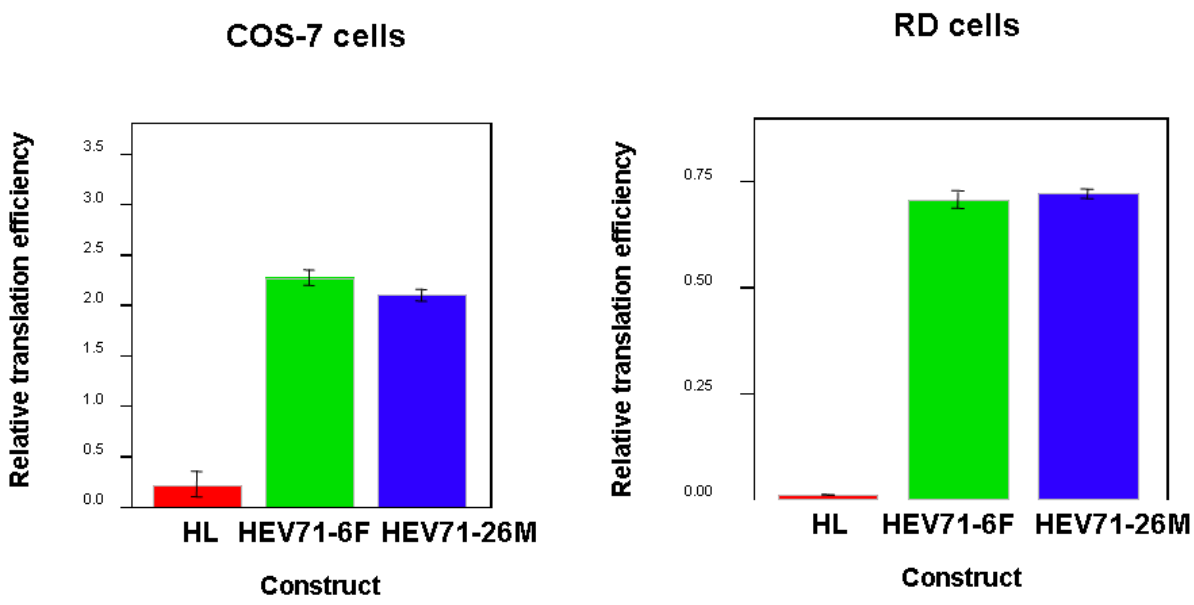

Figure 4.9 Comparative translation efficiency of 5′ UTR HEV71-6F and HEV71-26M in COS-7 and RD cells. Bi-cistronic constructs, pCRHL, pCR6F and pCR26M , were transfected into COS-7 and RD cells using Lipofectamine^{TM} 2000. The luciferase expression was measured by luciferase assay. Results presented represent the means of triplicate samples; error bars represent the standard error of the mean.

4.3 Discussion

HEV71 is a genetically diverse virus that is continuously evolving. Most HEV71 isolates belong to the two genotypes, B and C, which have a nucleotide similarity of 75-84%. We have previously observed that two HEV71 strains (HEV71-26M and HEV71-6F), isolated during the 1999 HFMD epidemic in Perth, Western Australia, displayed distinct replication kinetics during virus propagation. These two isolates belong to different genetic lineages (B3 and C2) that co-circulated during the Perth epidemic. To date, there has been no report on phenotypic differences between strains belonging to different genotypes. In this study, we describe the distinct growth phenotypes of these two strains. Genotypic and RNA secondary structure differences between these two strains were also investigated. In addition, we created a series of chimeric viruses in order to identify the genome regions responsible for their respective growth phenotypes.

Growth phenotypes of HEV71-6F and HEV71-26M were initially compared in terms of plaque morphology and growth kinetics in human (RD) and monkey kidney (Vero) cells. Plaque size correlates well with viral growth kinetics. HEV71-26M, which has a large-plaque phenotype, replicated to a significantly higher titre in both RD and Vero cells than HEV71-6F, which has a small-plaque phenotype. In this study, however, the growth phenotypes at different temperatures of these two viruses have not yet been identified. Further studies are needed in order to fully characterise growth properties of these two HEV71 strains, particularly their growth at different temperatures and in other human non-neuronal and neuronal cells. Differences in temperature sensitivity and replication efficiency in human cell lines between two HEV71 strains (genotypes C) isolated from the 1998 HFMD outbreak in Taiwan

have been reported (Kung et al., 2007). The HEV71 strain TW98NTU2078 isolated from a patient with encephalitis, was found to be temperature-resistant and to replicate more efficiently in human astrocytoma (HTB-14) and human peripheral blood mononuclear (PBMCs) cells than the strain TW98NTU1186, isolated from a patient with herpangina (Kung et al., 2007). Genetic determinants underlying different growth phenotypes of these two strains have not yet been identified.

Interestingly, HEV71-26M was able to adapt to grow in CHO cells, while HEV71-6F failed to adapt to CHO cells. Further investigation is needed to understand the differences of CHO cell adaptation between the two strains. It could be due to differences in an early event in virus replication, such as virus binding and entry, or in viral translation and RNA replication within the cells. Virus binding assays and entry studies of these two viruses in CHO cells would help to clarify this issue. Additionally, HEV71-26M may have more efficient translation and replication mechanisms in the cellular environment of CHO cells than HEV71-6F. In order to verify this hypothesis, further studies can be undertaken by transfection of viral RNAs of these two viruses into CHO cells and by determination of their specific-infectivity. In addition, HEV71 luciferase replicons, in which the P1 regions of 6F and 26M are replaced by the firefly luciferase gene, can be used in CHO cell transfection experiments. Luciferase activity is then measured in order to determine replication efficiency of the viruses.

We later describe how a single amino acid mutation, $K^{218}\rightarrow I$, located in the EF loop of capsid protein VP2 is responsible for the CHO cell-adapted phenotype of HEV71-26M (described in Chapter 5). HEV71-6F also has the positive charged polar lysine

(K) at this position. A neutral non-polar isoleucine (I) mutation identified in CHO-adapted HEV71-26M can be introduced into VP2 protein of HEV71-6F using the infectious cDNA clone in order to investigate if the $K^{218}\rightarrow I$ mutation confers CHO cell adaptation of HEV71-6F.

The 5′ UTR cloverleaf structure and the stem-loop elements in 3′ region of enteroviruses, are highly conserved. The cloverleaf is involved in RNA replication, by interacting with cellular proteins PCBP and 3CD, resulting in the formation of an RNA-protein (RNP) complex ((Parsley et al., 1997). This complex functionally circularises the viral RNA template though its interaction with PABP on the 3′ poly (A) tract for the initiation of negative-strand RNA synthesis. The IRES structure is essential for initiation of cap-independent translation of viral protein (Ehrenfeld & Teterina, 2002). It has been suggested that the RNA secondary structures of the 3′ UTR are not essential for enterovirus RNA replication, but may allow for efficient RNA synthesis through arrangement of the enterovirus RNA on membranous vesicles (Todd et al., 1997). Investigation of the predicted RNA structural folding of the 5′- and 3′- UTRs of HEV71-6F and HEV71-26M revealed strong similarity in the structures, suggesting that the 5′- and 3′- UTRs stem-loop structure may not influence the observed replication phenotype of HEV71-6F and 26M. In addition, the translation efficiencies of these two strains were found to be similar. Reciprocal 5′ UTR chimeras displayed parental virus phenotypes, suggesting that the 5′ UTR of both strains are compatible and not responsible for the observed phenotypes. The role of 3′ UTR on growth phenotype of the two viruses will need to be confirmed by construction of reciprocal 3′ UTR chimeras between HEV71-6F and HEV71-26M.

The *cre* element was first discovered within the VP1 gene of human rhinovirus 14 (Ref). Similar *cre* structures have since been found within the 2C gene sequence of several enteroviruses, including PV and CBV3 (Goodfellow et al., 2000, Paul et al., 2000, Van Ooij et al., 2006). *Cre* plays a role in VPg uridylylation, which is the first step in viral RNA synthesis. *Cre* contains a conserved loop motif, $R^1NNNA^1A^2R^2NNNNNNR^3$, with two adenylate residues within the consensus sequence 5′-AAACA-3′ being required for VPg uridylylation by $3D^{pol}$ ((Paul et al., 2003). It has been shown that disruption of the PV *cre* sequence resulted in a defect in positive-stranded RNA synthesis, but not in negative-stranded RNA synthesis (Goodfellow et al., 2003, Murray & Barton, 2003). However, Van OoiJ *et al*. (2006) found that the CBV3 *cre* plays an essential role in both positive- and negative-stranded RNA synthesis. Putative *cre* elements were identified within the 2C gene of HEV71 by MFOLD software (Mathews et al., 1999, Zuker, 2003). Interestingly, the predicted *cre* structure of HEV71-6F is similar to the PV *cre* (Goodfellow et al., 2003), while the HEV71-26M *cre* structure more closely resembles the predicted structure of CBV3 *cre* (Van Ooij et al., 2006). This structural difference is due to nucleotide variablility at position 13 of the conserved motif; U in HEV71-6F and A in HEV71-26M. Further studies need to be undertaken in order to determine the effect of the structural differences in *cre* on replication efficiency and to determine if *cre* plays a role in the growth phenotype of these two strains. This could be done by construction of reciprocal *cre* chimeras between HEV71-6F and HEV71-26M and by characterisation of the growth properties of the chimeric *cre* viruses. Alternatively, as the *cre* function has been found to be position-independent (Yin et al., 2003), by using full-length cDNA clones, the *cre* of each virus can be disrupted and the *cre* from another virus can be inserted between the 5′ UTR and P1 region or the P1 and

P2 regions. These constructs will enable a functional analysis of HEV71-6F *cre* and HEV71-26M *cre* on viral RNA replication, without changing the amino acid sequence of the 2C protein of each virus. In addition, the difference in VPg uridylylation efficiency between the predicted *cre* of these two viruses can also be determined by using an *in vitro* uridylylation assay.

Evaluation of the cell culture growth properties of the parental (HEV71-26M and HEV71-6F) and chimeric recombinant viruses suggest that both the structural region (P1) and non-structural regions (P2 and P3) contribute to the growth phenotype of HEV71. Phenotype expression is dependent on specific P1/P2-P3 combinations and is not reciprocal. The underlying mechanisms of this finding require further investigation. It is possible that there are differences at the early and the later stages of the virus replication cycle between these two HEV71 strains. Experiments to define virus binding and cell entry into different cell lines, including neuronal and rodent cell lines, could provide evidence for the role of the capsid region (P1) in phenotypic differences. A cell-free translation-RNA replication system could be a useful tool for investigating the role of P2 and P3 in replication efficiencies of the two strains, since this system allows the study of individual steps in the virus life cycle, except the early steps of virus attachment and entry. Alternatively, luciferase replicons containing the firefly luciferase gene in place of the P1 region can also be used. These systems have been used successfully in determination of PV translation and RNA replication (Franco et al., 2005, Toyoda et al., 2007). More detailed mapping will need to be undertaken in order to define the role of the P2 and P3 regions more fully.

CHAPTER FIVE

IDENTIFICATION OF GENETIC DETERMINANTS OF MOUSE ADAPTATION AND VIRULENCE OF HEV71

5.1 Introduction

Human enterovirus 71 (HEV71), similar to the related poliovirus (PV), has a limited host range, with humans the only known natural host. Although old world monkeys such as cynomolgous, rhesus and African green monkeys can be experimentally infected, other animal species including rodents are not susceptible to HEV71. Thus, old world monkeys have provided the only useful animal model to elucidate HEV71 pathogenesis; the high cost of monkeys and their maintenance precludes their widespread use for studies of viral pathogenesis. A small animal model would provide a more economical and practical tool for studies of HEV71 pathogenesis and vaccine development.

A recent study has reported the development of a mouse-adapted HEV71 strain. Seven-day-old mice infected with mouse-adapted HEV71 by oral, intramuscular (i.m.), intraperitoneal (i.p.) or intracerebral (i.c.) routes developed acute flaccid paralysis mimicking HEV71 infection in humans and monkeys, suggesting that a mouse model could be an alternative animal model for HEV71 study (Chen et al., 2004, Wang et al., 2004). Mouse-adapted HEV71 was more virulent in mice, exhibited larger plaque size and grew more rapidly in cell culture than the parental virus (Wang et al., 2004). Potential virulence determinants of this mouse-adapted strain were identified; the 5′ untranslated region (four nucleotide changes), the capsid proteins VP2 (3 nucleotide and 1 amino acid changes), and the non-structural

protein 2C (8 nucleotide and 4 amino acid changes) (Wang et al., 2004). However, the role of these mutations in the virulence phenotype of the mouse-adapted strain was not determined.

In order to establish a small animal model for studies of pathogenesis and for vaccine efficacy and immunogenicity testing, we have developed a HEV71 infection model using a mouse-adapted variant of strain HEV71-26M (Chua et al., 2008; see Appendix B). To create a mouse-adapted strain, HEV71-26M virus was passaged six times in CHO cells. A CHO-adapted variant of HEV71-26M (CHO-26M) was then passaged six times by i.c. inoculation of one-day-old BALB/c mice. The mouse-adapted variant, MP-26M, was observed to have markedly increased virulence in newborn BALB/c mice compared to the parental HEV71-26M and CHO-26M. Newborn mice infected with MP-26M by i.m., i.p. and i.c. routes developed fore- and/or hindlimb paralysis in an age- and dose-dependent manner, whereas HEV71-26M and CHO-26M infected mice did not develop clinical signs of infection at any virus dose or route of inoculation. Tissue distribution studies using CHO-26M as a parental strain and MP-26M revealed that skeletal muscle was the primary site of replication in newborn mice for both viruses (Chua et al., 2008).

Adaptation of HEV71-26M to CHO cells and mice has resulted in a number of nucleotide and deduced amino acid changes in the viral genome. In order to understand the molecular mechanisms of mouse adaptation and virulence of HEV71-26M, reverse genetics was used to generate mutant viruses processing specific amino acid alterations. The construction and characterisation of mutant viruses *in vitro* and

in vivo is outlined in this chapter and the critical mutations that occur during CHO cell and mouse adaptation are identified.

5.2 Results

5.2.1 Comparison of nucleotide and deduced amino acid sequences of the mouse-adapted strain (MP-26M) and the CHO-adapted strain (CHO-26M) to their parental strain HEV71-26M and other HEV71 strains

The whole genome sequencing of strains HEV71-26M, CHO-26M and MP-26M was performed by Beng Hooi Chua (Division of Virology, Telethon Institute for Child Health Research). To identify molecular determinants of CHO cell and mouse adaptation, the complete nucleotide and deduced amino acid sequences of strains HEV71-26M, CHO-26M and MP-26M were compared. Results obtained are presented in Table 5.1. Comparison of HEV71-26M and CHO-26M sequences revealed four nucleotide differences, located in the VP2 ($A^{1400}\rightarrow T$), VP1 ($T^{2739}\rightarrow C$), 2A ($T^{3531}\rightarrow C$) and 3D ($G^{6981}\rightarrow A$) genes. Only one of these mutations resulted in a deduced amino acid change - in VP2 ($K^{218}\rightarrow I$). Three nucleotide sequence differences were identified between CHO-26M and MP-26M in VP1 ($G^{2876}\rightarrow A$), 2C ($A^{4644}\rightarrow G$, $A^{4727}\rightarrow G$) and 3D ($C^{6429}\rightarrow A$), which resulted in two deduced amino acid changes (VP1, $G^{710}\rightarrow E$) and (2C, $K^{1327}\rightarrow R$). The amino acid changes $K^{218}\rightarrow I$ in VP2 and $K^{1327}\rightarrow R$ in 2C are unique to all HEV71 complete sequences available in GenBank, whereas the VP1 change ($G^{710}\rightarrow E$) is not unique. No nucleotide sequence changes were observed in the 5′ and 3′ UTRs.

Table 5.1 Comparison of nucleotide and amino acid sequences of the wild-type HEV71-26M, CHO-adapted variant, CHO-26M, mouse-adapted variant, MP-26M and other HEV71 strains

Viral Proteins	Nucleotide position	Nucleotide				Amino acid position	Amino acid			
		HEV71-26M	CHO-26M	MP-26M	Other HEV71 strains		HEV71-26M	CHO-26M	MP-26M	Other HEV71 strains
VP2	1400	A	T	T	A	218	K	I	I	K
VP1	2739	T	C	C	C, T	664	G	G	G	G
2A	2876	G	G	A	A, G	710	G	G	E	E,G,Q,R,A
2A	3531	T	C	C	C, T	928	N	N	N	N,S
2C	4644	A	A	G	A, C, T	1299	S	S	S	S
2C	4727	A	A	G	A	1327	K	K	R	K
3D	6429	C	C	A	A,C,G,T	1894	R	R	R	R,S
3D	6981	G	A	A	A,G,T	2078	T	T	T	T

5.2.2 Construction of recombinant viruses

To determine which of the three amino acid mutations were responsible for the adaptation and virulence of HEV71-26M in mice, seven recombinant cDNA clones containing one, or a combination of two or three mutations (Figure 5.1 and Table 2.8) were constructed by exchanging corresponding genomic regions of CHO-26M and MP-26M into the full-length clone of HEV71-26M using RT-PCR amplification and molecular cloning, as described in detail in section 2.2.15. Two separate clones of each mutant were selected, and purified plasmid DNA was prepared for sequencing analysis. Partial VP2, VP1 and 2C genes were sequenced to confirm the presence of appropriate mutations of each construct.

To generate each of the mutant viruses, purified plasmid DNA from each of the seven clone constructs were co-transfected with pCMV-T7Pol into COS-7 cells using Lipofectamine^{TM}2000 (Invitrogen) as described in section 2.2.17. Infectious clone-derived viruses were recovered from the transfected cells at three days post-transfection and were passaged once on RD cells to generate working stocks for mouse virulence assays and for cell culture characterisation. Clone-derived viruses are designated by the prefix CDV. Partial VP2, VP1 and 2C gene RT-PCR and nucleotide sequencing was undertaken to ensure that the site-specific change/s remained present in the rescued virus populations. Nucleotide sequencing showed that all mutant viruses, except CDV-26M-VP1m, retained the introduced mutation/s. Several attempts to rescue a CDV-26M-VP1m population that retained the VP1 mutation (nt $G^{2876}\rightarrow A$) were unsuccessful. These included transfection of the full length clone, p26M-VP1m and passage of the rescued virus in Vero and CHO cells.

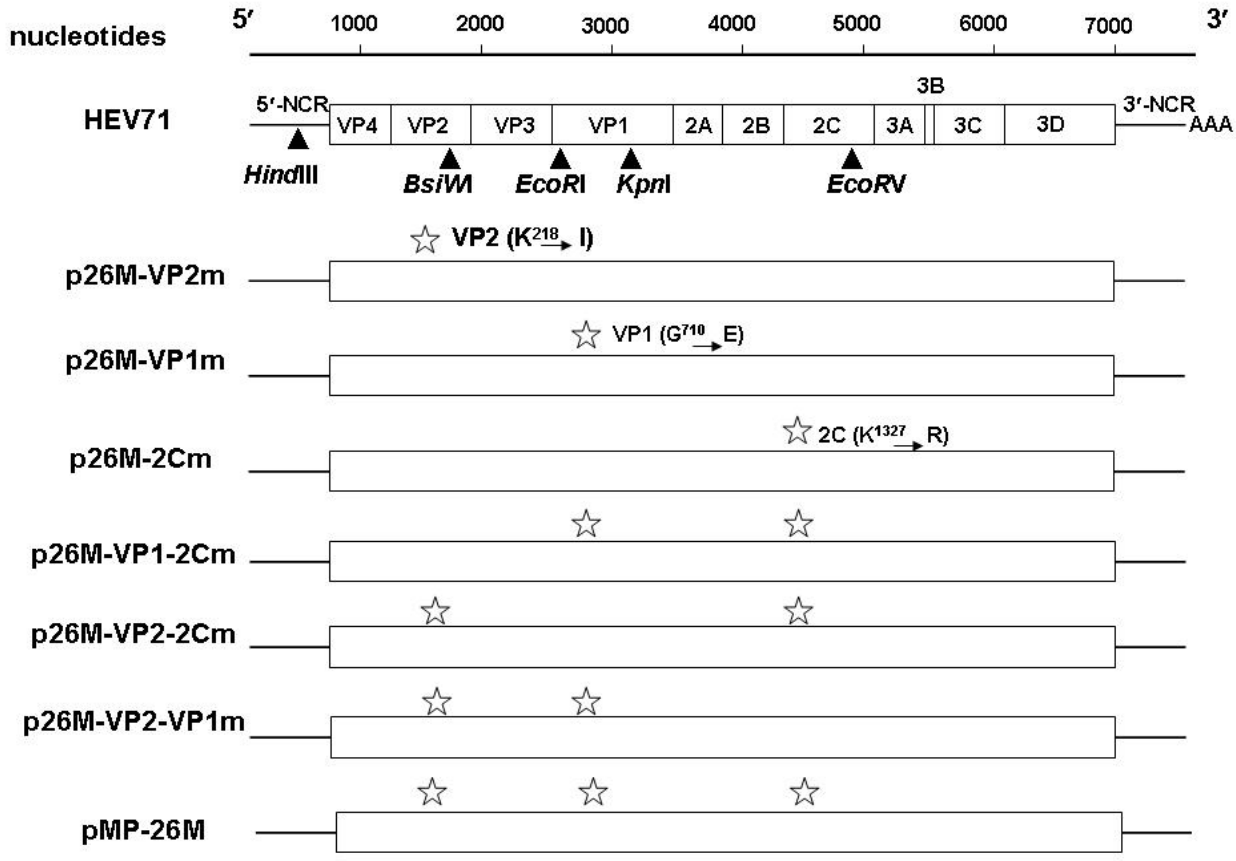

Figure 5.1 Schematic representation of recombinant cDNA clones containing one, or a combination of two or three mutations. Genome maps of HEV71-26M and its variants are represented as an open box, with individual genes and non-coding regions indicated for HEV71-26M. Amino acid mutations observed in CHO-26M (VP2, K^{218}→I) and MP-26M (VP2, K^{218}→I, VP1, G^{710}→ E, 2C, K^{1327}→R) are shown as open stars. The approximate positions of the restriction enzyme sites used in clone construction are indicated on the HEV71-26M genome.

Stocks of all recombinant viruses were found to be at titres of $\geq 10^6$ $TCID_{50}$/mL, except CDV-26M-VP1-2Cm, which had a titre at approximately 10^4 $TCID_{50}$/mL. Similar to CDV-26M-VP1m, it was not possible to produce a high titre stock of CDV-26M-VP1-2Cm that had retained the VP1 mutation (nt $G^{2876} \rightarrow A$). Therefore, CDV-26M-VP1m and CDV-26M-VP1-2Cm were omitted from all subsequent analyses.

5.2.3 Stability of introduced mutations during passage in mice and cell culture

It is possible that the amino acid substitutions introduced during mouse adaptation may revert to that of the parental virus during cell culture passage (Jia et al., 2001). To determine if the amino acid substitutions in VP2, VP1 and/or 2C of mouse-adapted virus revert to the wild-type sequence during passage in cell culture, the stability of these mutations was determined by examining the VP2, VP1 and 2C nucleotide sequences of MP-26M at increasing passage levels in cell culture. Infectious clone-derived MP-26M (CDV-MP-26M) was passaged five times in RD cells and viral RNA extracted from culture supernatants was collected at each passage level. The VP2, VP1 and 2C genes were amplified by RT-PCR and their nucleotide sequences determined. The VP2 ($A^{1400} \rightarrow T$; $K^{218} \rightarrow I$) and 2C ($A^{4727} \rightarrow G$; $K^{1327} \rightarrow R$) gene mutations were retained during the five passages on RD cells (Figure 5.2). By contrast, the VP1 ($G^{2876} \rightarrow A$; $G^{710} \rightarrow E$) gene mutation had reverted to the wild-type HEV71-26M/CHO-26M sequence by the second RD cell passage (Figure 5.3). Similar results were obtained after passaging CDV-MP-26M in Vero and CHO cells (data not shown). These results indicated that there is a strong selective pressure being applied at this codon. Due to instability of the VP1 mutation, only

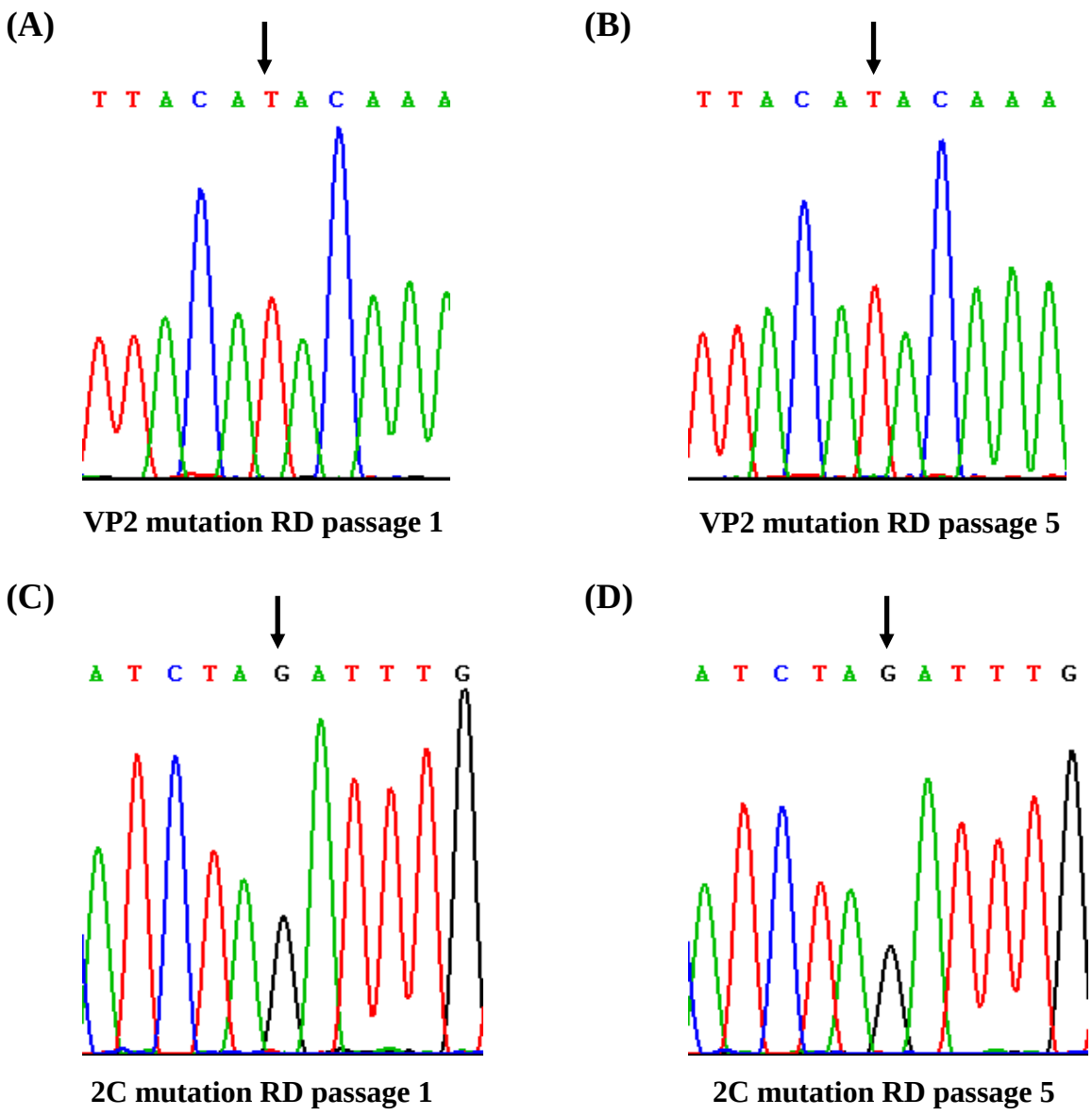

Figure 5.2 Stability of a mutation (A^{1400}→T; K^{218}→I) in the capsid protein VP2 and a mutation (A^{4727}→G; K^{1327}→R) in the non-structural protein 2C during cell culture passage. Infectious clone-derived MP-26M was passaged five times in RD cells and viral RNA extracted from culture supernatants collected at each passage level. The VP2 and 2C genes were amplified by RT-PCR and their nucleotide sequences determined. (A) and (B) Sequence analysis of RT-PCR products of VP2 gene from virus stock RD cell passage 1 and 5. (C) and (D) Sequence analysis of RT-PCR products of 2C gene from virus stock RD cell passage 1 and 5.

virus stocks of the first RD cell passage were used for all *in vitro* and *in vivo* analysis.

As the VP1 ($G^{710}\rightarrow E$) mutation rapidly reverts to wild-type during passage in RD cells, it is possible that the VP2, VP1 and 2C mutations would also revert to wild-type HEV71-26M/CHO-26M during passage in mice. To examine the stability of these mutations in mice, CDV-MP-26M was serially passaged five times in seven-day-old BALB/c mice by i.m. inoculation (10^4 $TCID_{50}$) as described in section 2.2.21. Brain and limb muscle specimens were collected from mice showing clinical signs of HEV71 disease between four and five days post-infection. RNA was extracted from brain and muscle homogenates obtained at each mouse passage, the VP1 and 2C genes were amplified by RT-PCR, and the amplicons sequenced. Similar to RD cell passage, the VP2 ($K^{218}\rightarrow I$) and 2C ($K^{1327}\rightarrow R$) mutations persisted during five passages in mice (data not shown). Interestingly, the VP1 ($G^{710}\rightarrow E$) mutation also persisted during mouse passage (Figure 5.4). Viruses isolated from both brain and limb muscles retained these mutations.

5.2.4 Identification of genetic determinants of CHO cell adaptation of HEV71

It has been found that both HEV71-6F and HEV71-26M, cannot replicate well in CHO cells (data not shown). After two passages in CHO cells, HEV71-26M titres had increased and after six passages in CHO cells had reached titres similar to those observed for HEV71-26M in primate (Vero, RD) cells. In order to determine if the VP2 ($K^{218}\rightarrow I$) mutation was responsible for the improved growth of virus in CHO cells, single-step growth analysis was undertaken in RD and CHO cells using

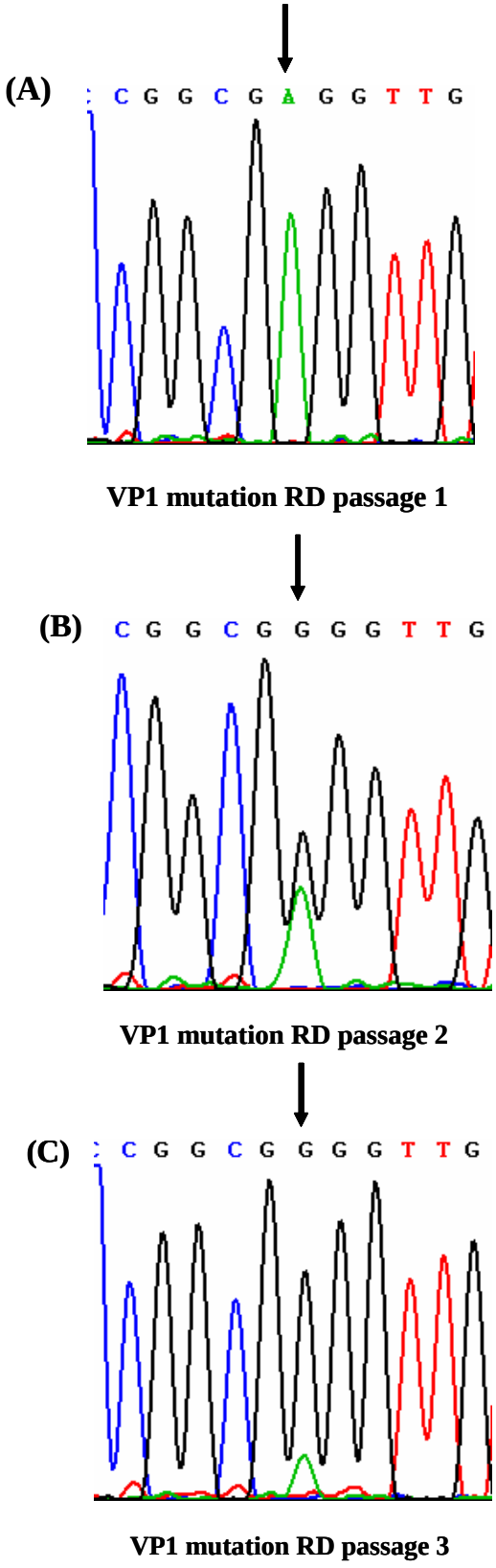

Figure 5.3 Stability of a mutation (G^{2876}→A; G^{710}→E) in the capsid protein VP1 during passage in RD cells. Sequence analysis of RT-PCR products of VP1 gene from virus stock RD cell passage 1 (A), passage 2 (B), and passage 3 (C).

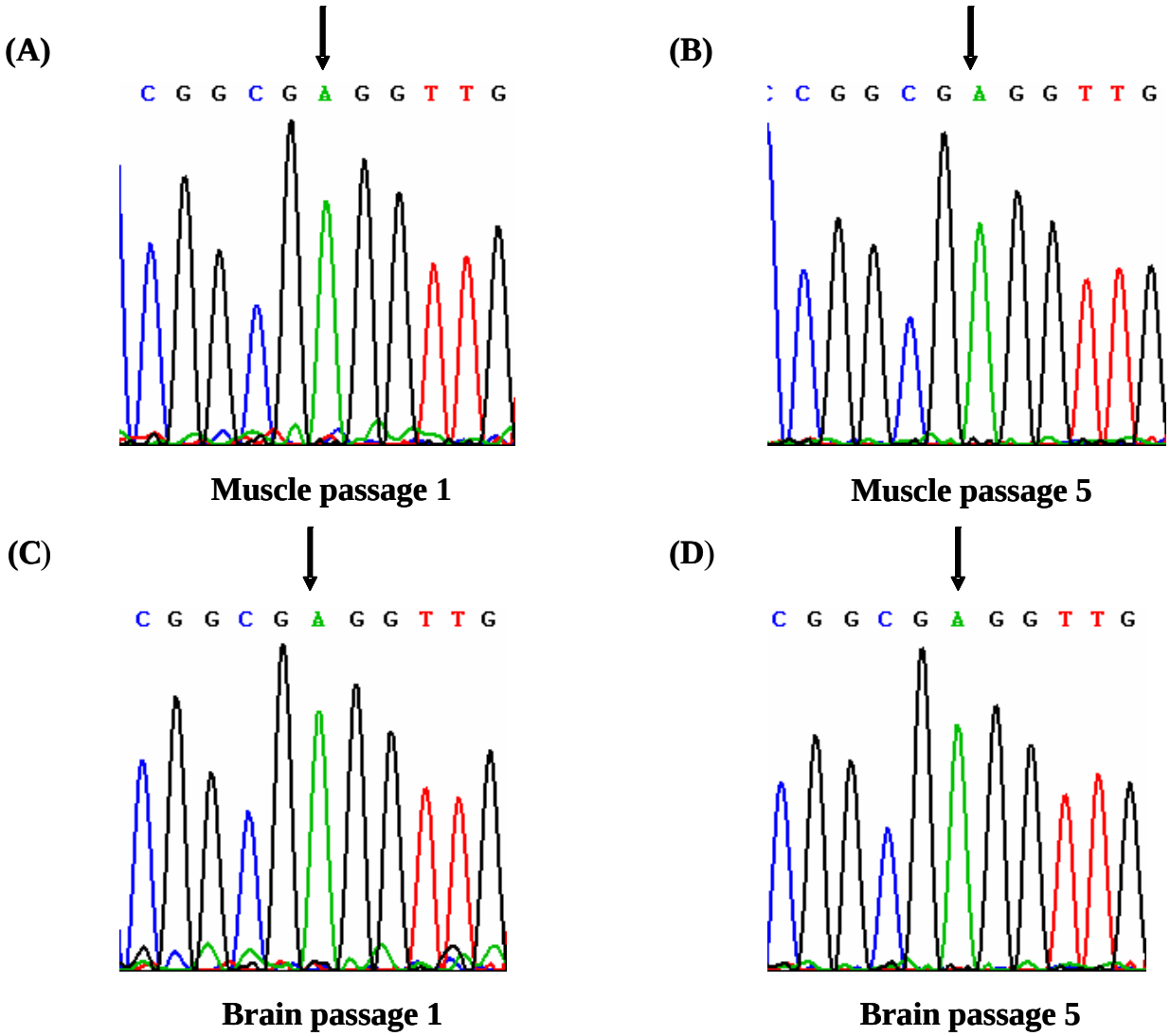

Figure 5.4 Stability of a mutation (G^{2876}→A; G^{710}→E) in the capsid protein VP1 during passage in mice. CDV-MP-26M, was serially passaged five times in seven-day-old BALB/c mice by intramuscular inoculation at a dosage of 10^4 $TCID_{50}$. Brain and limb muscle specimens were collected from mice showing clinical signs of HEV71 disease between four and five days post-infection. RNA was extracted from brain and muscle homogenates obtained at each mouse passage, the VP1 gene was amplified by by RT-PCR, and the amplicons sequenced. (A) and (B) Sequence analysis of RT-PCR products of VP1 gene from muscle homogenates at mouse passage 1 and 5. (C) and (D) Sequence analysis of RT-PCR products of VP1 gene from brain homogenates at mouse passage 1 and 5.

infectious clone-derived HEV71-26M and CHO-26M (CDV-26M-VP2m). The results are shown in Figure 5.5. The replication kinetics and virus yields of both viruses in RD cells are nearly identical. By contrast, HEV71-26M replicates poorly in CHO cells, whereas CDV-26M-VP2m replicates efficiently, with maximum titers >100-fold higher than parental virus. These results demonstrate that the amino acid substitution $K^{218}\rightarrow I$ in VP2 conferred the CHO cell-adapted phenotype on HEV71.

5.2.5 Identification of genetic determinants of HEV71 mouse adaptation

In order to determine which of the three amino acid changes is responsible for the mouse-adapted phenotype, mouse virulence assays of the parental and mutant viruses were undertaken by determination of the HD_{50} values and average survival times after i.m. and i.p. inoculation. It was previously shown that newborn BALB/c mice were susceptible to the mouse-adapted strain, MP-26M, by three routes of inoculation; i.p., i.m. and i.c. in an age- and dose-dependent manner (Chua et al., 2008). HD_{50} values for MP-26M in seven-day-old BALB/cmice were $3.4x10^3$, $1.5x10^2$, and $5x10^2$ $TCID_{50}$, after i.p., i.m. and i.c. inoculation, respectively (Chua et al., 2008). Newborn mice remained susceptible to MP-26M infection until 14 days of age. Seven-day-old BALB/c mice were chosen in all mouse virulence assays.

(A)

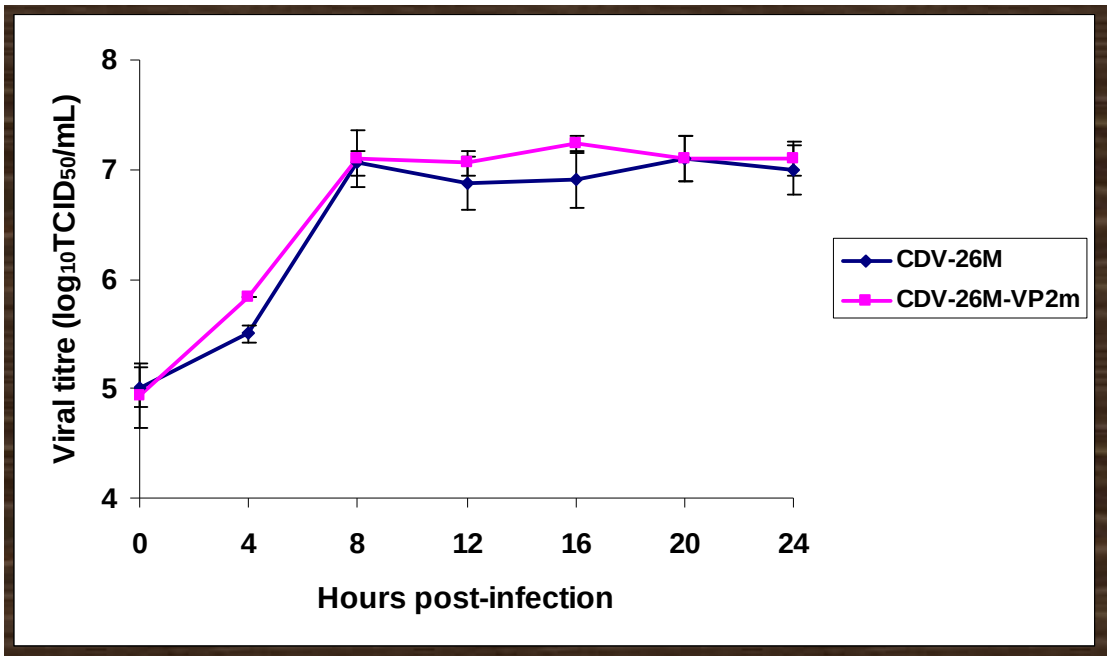

(B)

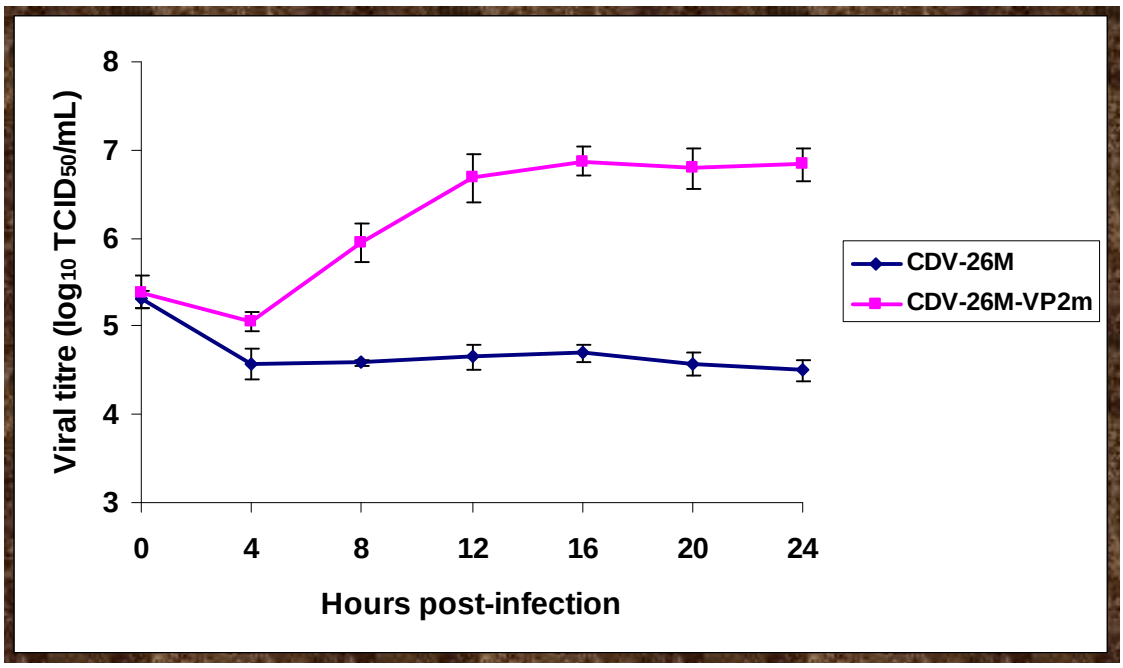

Figure 5.5 Growth kinetics of CDV-26M and CDV-26M-VP2m in RD **(A)** and CHO **(B)** cells. Cell monolayers were infected at MOI of 5x$TCID_{50}$/cell. Cell culture supernatants were collected at the times indicated. Samples at each time point were freeze-thawed three times and clarified by centrifugation prior to determination of virus titre by $TCID_{50}$ assay. All assays were performed in triplicate. At each time point, titres are the average of three samples, with error bars representing the standard error of the mean.

5.2.5.1 Mortality profile and average survival time

Groups of 8 or 12 BALB/c mice were inoculated intraperitoneally with $2x10^5$ $TCID_{50}$ or intramuscularly with $1x10^4$ $TCID_{50}$ of each clone-derived virus population, including CDV-26M, CDV-26M-VP2m (CHO-26M), CDV-MP-26M, and three other mutant viruses, CDV-26M-2Cm, CDV-26M-VP2-2Cm, CDV-26M-VP2-VP1m. The dosages of $2x10^5$ $TCID_{50}$ and $1x10^4$ $TCID_{50}$ corresponded to approximately $60xHD_{50}$ of the i.p. route and $100xHD_{50}$ of the i.m. route for the wild-type MP-26M (Chua et al., 2008). Mice were observed daily and scored for the presence of clinical signs of infection, including ruffled fur, hunched body posture, fore-or hind-limb paralysis and failure to thrive, and the results are shown in Table 5.2.

As expected, the parental CDV-26M caused no detectable morbidity or mortality in infected mice, while the clone-derived mouse-adapted virus, CDV-MP-26M, caused 100% mortality with a mean time to death 4 (±0) days by the i.p. route and 5 (±0) days by the i.m. route. Clone-derived CHO-adapted virus, CDV-26M-VP2m, and CDV-26M-2Cm exhibited a non-virulent phenotype in mice compared to CDV-MP-26M. Neither virus caused observable clinical signs of infection and mortality in mice infected by the i.m. route, and only in 1 of 12 mice infected with CDV-26M-VP2m by the i.p. route developed fore limb paralysis and succumbed to the infection, with a delayed time to death by six days compared to CDV-MP-26M.

Two mutant viruses containing combinations of two amino acid substitutions, CDV-26M-VP2-2Cm and CDV-26M-VP2-VP1m had markedly different mouse virulence phenotypes. Mice infected with CDV-26M-VP2-2Cm by either the i.p. or i.m.

Table 5.2 Mortality profile, average survival time and HD_{50} of the parental and mutant viruses

Virus	Mortality		Average survival time (SD)# (days)		HD_{50} i.m. ($TCID_{50}$)
	i.p.	i.m.	i.p.	i.m.	
CDV-26M	0% (0/8)	0% (0/8)	>14	>14	$>10^4$
CDV-26M-VP2m	8.3 (1/12)*	0% (0/8)	>14*	>14	$>10^4$
CDV-26M-2Cm	0% (0/8)	0% (0/8)	>14	>14	$>10^4$
CDV-26M-VP2-VP1m	100% (8/8)	100% (8/8)	4.0±(0.0)	4.9 (0.35)	1.6
CDV-26M-VP2-2Cm	0% (0/8)	0% (8/8)	>14	>14	$>10^4$
CDV-MP-26M	100% (8/8)	100% (8/8)	4.0±(0.0)	5±(0.0)	5

*One mouse developed hindlimb paralysis and was sacrificed on day 10 post-infection.

Average survival time = number of days ± standard deviation

routes showed no clinical signs of infection. By contrast, CDV-26M-VP2-VP1m exhibited a mouse virulence phenotype similar to CDV-MP-26M, causing 100% morbidity and mortality with a mean time to death of 4 (±0) days by the i.p. route and 4.9 (±0.35) days by the i.m. route.

5.2.5.2 50% Humane end point (HD_{50})

Due to similar mortality profiles and average survival times after i.p. and i.m. inoculation, HD_{50} values of each virus were determined only by the i.m. route. Groups of 8 to 10 BALB/c mice were inoculated intramuscularly with serial ten-fold dilutions of virus. Mice were observed daily and scored for clinical signs of infection as described above and HD_{50} values calculated as described in section 2.4.2. The results are shown in Table 5.2.

The HD_{50} value of the parental CDV-26M was greater than 10^4 $TCID_{50}$ with no observed mortality at the lowest dilution of virus tested. Virus populations without the VP1 ($G^{710}\rightarrow E$) mutation; CDV-26M-VP2m, CDV-26M-2Cm, CDV-26M-VP2-2Cm, had similar HD_{50} values (at $>10^4$ $TCID_{50}$) to CDV-26M. By contrast, the two virus populations that contained the VP1 mutation, CDV-26M-VP2-VP1m and CDV-MP-26M, had HD_{50} values of 1.6 and 5.0 $TCID_{50}$, respectively. The results of mouse virulence assays clearly demonstrated that a non-conservative amino acid substitution ($G^{710}\rightarrow E$) in the capsid protein VP1 was alone sufficient to confer the mouse virulence phenotype on CDV-26M.

5.2.6 Other phenotypic characterisation of clone-derived viruses

In an attempt to identify potential cell culture correlates of the difference in mouse virulence phenotype observed between clone-derived viruses containing the MP-26M- VP1 mutation and other clone-derived viruses, the plaque morphology, growth kinetics in RD and NB41A3 (mouse neuroblastoma) cells and temperature sensitivity of CDV-26M, CDV-26M-VP2m, CDV-26M-VP2-2Cm, CDV-26M-VP2-VP1m and CDV-MP-26M in Vero and RD cells were compared. Since CDV-26M-2Cm and CDV-26M-VP2-2Cm exhibited identical mouse virulence phenotypes, CDV-26M-2Cm was omitted in the following experiments.

5.2.6.1 Plaque morphology and temperature sensitivity

Plaque size, which is considered a good indicator of the rate of viral replication (Flint et al., 2004), was determined on RD and Vero cells at 32˚C, 37˚C and 39˚C incubation. The results are presented in Figure 5.6. All viruses were observed to produce clearer plaques on Vero than on RD cells. At 32˚C and 37˚C incubation, the parental CDV-26M, CHO-adapted CDV-26M-VP2m and CDV-26M-VP2-2Cm displayed a similar large plaque phenotype on both cell types. Mean values of plaque diameter (in mm) of CDV-26M, CDV-26M-VP2m and CDV-26M-VP2-2Cm at 33˚C incubation were at 2.86 (±0.56), 3.28 (±0.83), 3.35 (±1.09), respectively, and were at 2.56 (±0.62), 3 (±0.75), 3.05 (±0.79), respectively, at 37˚C incubation. By contrast, viruses containing VP1 mutation, including CDV-26M-VP2-VP1m and CDV-MP-26M, demonstrated a smaller plaque phenotype. Mean values of plaque diameter of CDV-26M-VP2-VP1m and CDV-MP-26M at 33˚C incubation were at

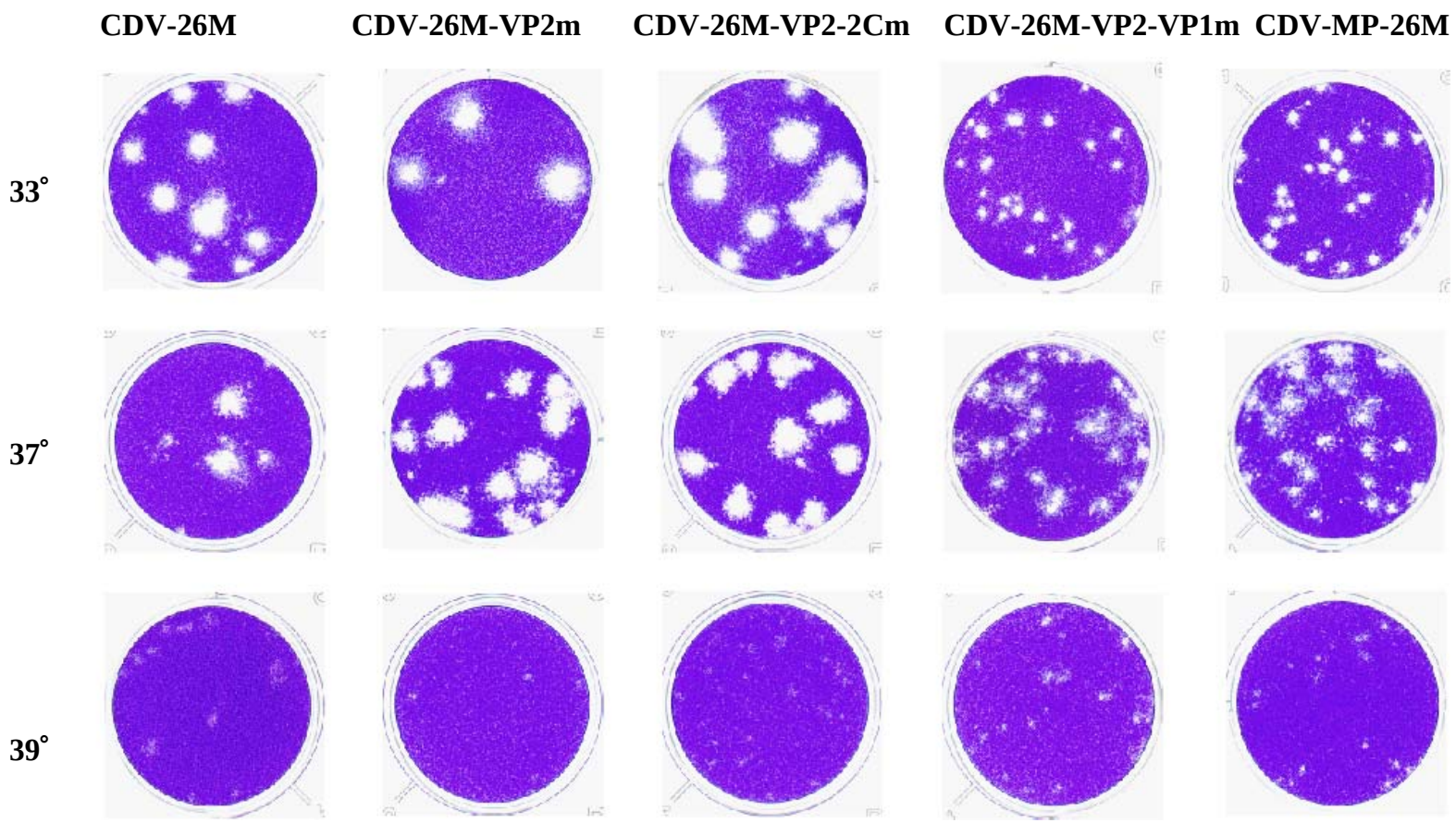

Figure 5.6 Plaque morphology of clone-derived viruses in Vero cells. Ten-fold serial dilutions of virus were inoculated at 100 µL per well into 12-well tissue culture trays. Infected cells were incubated for seven days at 33˚C, 37˚C or 39˚C before staining with crystal violet solution.

1.06 (±0.32) and 1.13 (±0.43), respectively and were at 1.3 (±0.42) and 1.33 (±0.44), respectively, at 32˚C incubation. All viruses exhibited a small plaque phenotype at 39˚C incubation.

The temperature sensitivity of the wild-type CDV-26M, CDV-26M-VP2m, CDV-26M-VP2-2Cm, CDV-26M-VP2-VP1m, CDV-MP-26M was determined by comparing virus yields at 32˚C, 37˚C and 39˚C. Temperature sensitivity was defined as logarithmic difference of the $TCID_{50}$ values at 37˚C and 39˚C (Arita et al., 2005). The Δ37/39˚C values from 2 to 2.75 are defined as slight temperature sensitive phenotype and more than 2.75 as strong temperature sensitive phenotype. All of the viruses grew to similar titres at 32˚C and 37˚C (Table 5.3); growth impairment was detected in all virus populations when cultured at 39˚C. However, none of the viruses exhibited a temperature sensitive phenotype.

5.2.6.2 Single-step growth analysis in RD and NB41A3 cells

The single-step growth kinetics of CDV-26M, CDV-26M-VP2m, CDV-26M-VP2-2Cm, CDV-26M-VP2-VP1m, CDV-MP-26M were examined in RD and NB41A3 cells over a 24 hour period. Both RD and NB41A3 cells were infected at MOI of 5x$TCID_{50}$/cell. In RD cells, CDV-26M, CDV-26M-VP2m and CDV-26M-VP2-2Cm grew identically and produced maximum titres of approximately $10^{7.5}$ $TCID_{50}$/mL at 12 hours post-infection (Figure 5.7). Two viruses containing the VP1 ($G^{710}\rightarrow E$) mutation, CDV-26M-VP2- VP1m and CDV-MP-26M, grew poorly compared to the other viruses; peak titres were approximately 100-fold lower than for CDV-26M, CDV-26M-VP2m and CDV-26M- VP2-2Cm. However, the maximal titres were also achieved at 12 h post-infection. In NB41A3 cells (Figure

Table 5.3 Temperature sensitivity of virus yields of clone-derived viruses on Vero cells

Virus	Virus Titre (log_{10} PFU/mL)			Δ37/39˚C [#]
	33˚C	37˚C	39˚C	
CDV-26M	6.9	6.8	6.4	1.06
CDV-26M-VP2m	7.1	7.15	6.7	1.07
CDV-26M-VP2-2Cm	7.1	7.0	6.4	1.1
CDV-26M-VP2-VP1m	6.4	6.36	6.1	1.04
CDV-MP-26M	6.5	6.5	6.1	1.07

[#]Δ37/39˚C at 2.0-2.75 = slight temperature sensitive phenotype, at ≥ 2.75 = strong temperature sensitive phenotype (Arita et al., 2005)

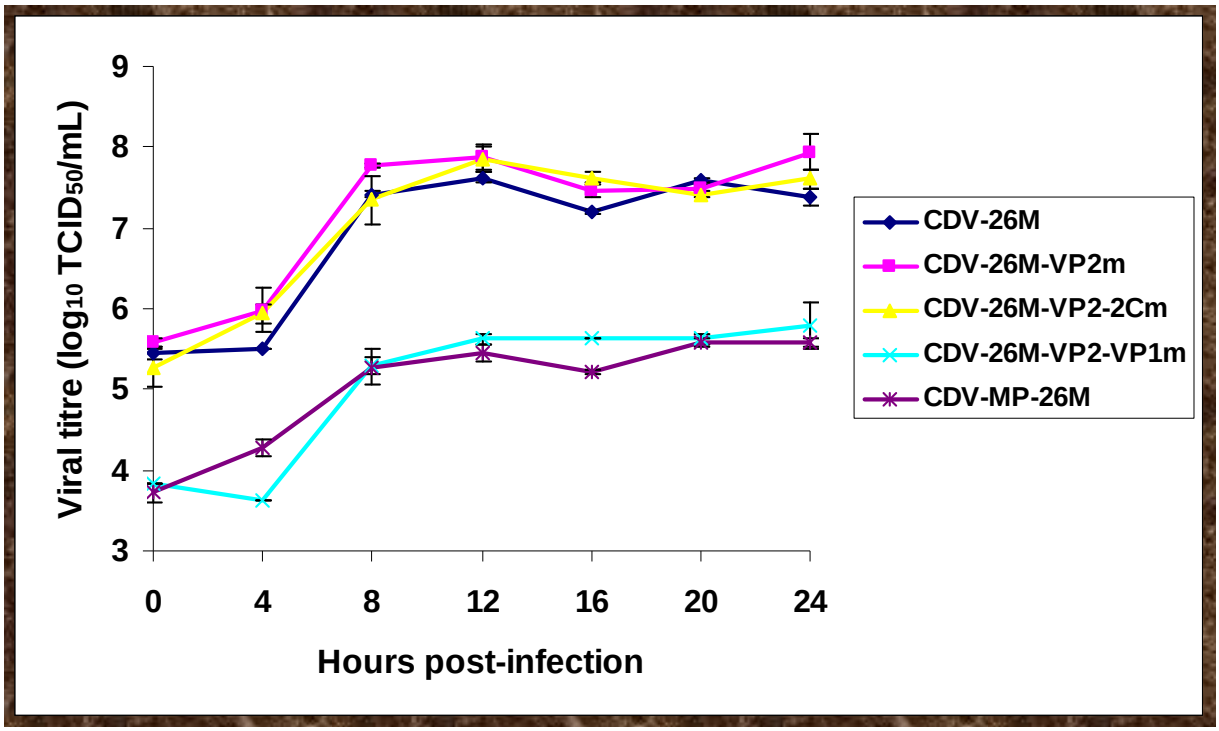

Figure 5.7 Single step growth kinetics of clone-derived viruses in RD cells. Cell monolayers were infected at a MOI of 5x$TCID_{50}$/cell. Cell culture supernatants were collected at the times indicated and titrated by $TCID_{50}$ assay. All assays were performed in triplicate. At each time point, titres are the average of three samples; error bars represent the standard error of the mean.

5.8), similar growth kinetics was observed for viruses containing VP2 and 2C mutations, CDV-26M-VP2m and CDV-26M-VP2-2Cm, and for viruses containing VP1 mutations, CDV-26M-VP2-VP1m and CDV-MP-26M, while CDV-26M had a distinct growth pattern. CDV-26M-VP2m and CDV-26M-VP2-2Cm viruses grew at approximately $10^{6.5}$ $TCID_{50}$/mL at 12 h post-infection, which was 10-fold higher than CDV-26M and 100-fold higher than CDV-26M-VP2-VP1m and CDV-26M-MP at the same time. Maximum titres of all viruses occurred at approximately 20 h post-infection.

5.2.7 Predicted protein structure

In order to locate the amino acid substitutions found in the capsid proteins VP2 and VP1 of CHO-26M and MP-26M, three-dimensional structures of VP2 and VP1 proteins were predicted. The virus most closely related to HEV71 by primary sequence, for which there are structural data, is bovine enterovirus (BEV). The amino acid identity between HEV71 and BEV are 58% for VP2 and 41% for VP1, respectively. The known crystallographic structure of bovine enterovirus capsid proteins (PDB number: 1BEV_2 for VP2 and 1BEV_1 for VP1) was therefore used to predict the location of the mutations found in VP2 and VP1 of CHO-26M and MP-26M. The complete amino acid sequences of VP2 and VP1 from HEV71-26M, CHO-26M and MP-26M were individually submitted to an online automated protein homology modelling program, ESyPred3D (http://www.fundp.ac.be/sciences/biologie/urbm/bioinfo/esypred/), and the predicted three-dimensional structure of each of the proteins were viewed in RasMol 2.7 (http://rasmol.org/). The $K^{218}\rightarrow I$ mutation in VP2 was predicted to be located in the

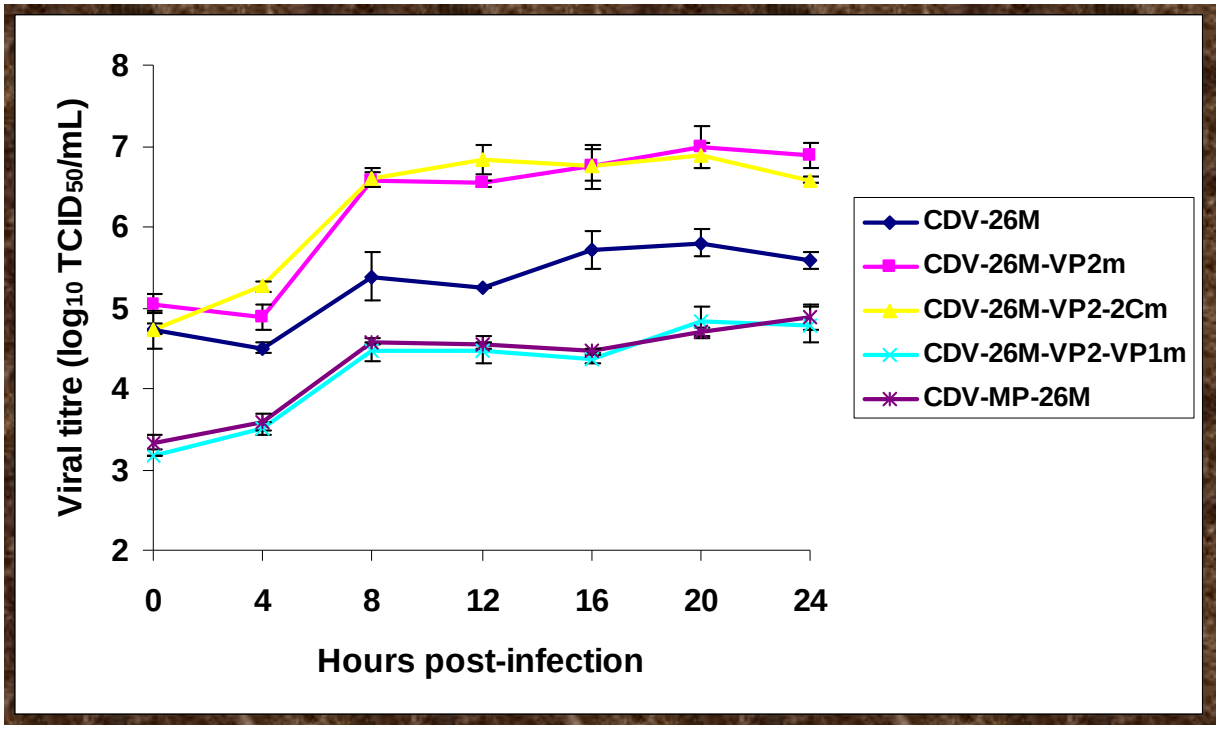

Figure 5.8 Single step growth kinetics of clone-derived viruses in mouse neuroblastoma (NB41A3) cells. Monolayers were infected with viruses at MOI of 5x $TCID_{50}$/cell. Cell culture supernatants were collected at the times indicated and titrated by $TCID_{50}$ assay. All assays were performed in triplicate. At each time point, titres are the average of three samples; error bars represent the standard error of the mean.

surfaced-exposed region of the EF loop and the VP1 ($G^{710}\rightarrow E$) mutation was predicted to be located in the surface-exposed of the DE loop (Figure 5.9 and 5.10).

5.3 Discussion

Most HEV71 strains infect only primates and do not cause disease in mice. However, mouse-adapted strains of HEV71 can be selected by passage of virus in mouse brain (Arita et al., 2005, Chen et al., 2004, Chua et al., 2008, Ong et al., 2008). Adaptation has been described as the modification of an organism to make it more fit for existence within a certain environment (Domingo & Holland, 1997, Domingo et al., 1997). RNA virus populations are complex and contain heterogeneous mixtures of related viral genomes called quasispecies (Domingo & Holland, 1997, Domingo et al., 1997). This is due to high replicative error rates in RNA genomes, with mutation frequencies of 10^{-3} and 10^{-5} per nucleotide (Domingo & Holland, 1997, Domingo et al., 1997). Quasispecies are thought to aid the survival of RNA virus populations in the presence of selective pressures (Domingo & Holland, 1997, Domingo et al., 1997). Viruses with beneficial mutations are able to survive and adapt to a new environment, thus generating new quasispecies (Domingo & Holland, 1997, Domingo et al., 1997). This explains why HEV71 rapidly adapts to growth under the strong selective pressure of mouse passage. Nevertheless, the molecular mechanisms of host range adaptation by HEV71 have not been clarified.

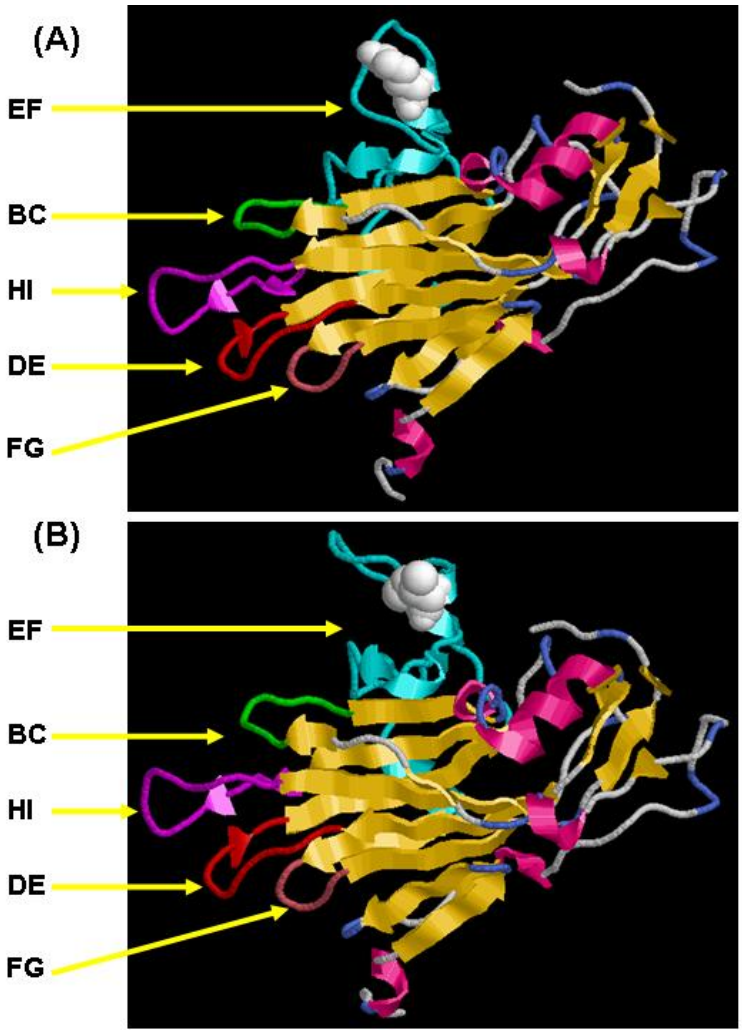

Figure 5.9 Predicted three-dimentional structure of VP2 protein based on the known crystallographic structure of BEV (PDB no: 1BEV_2). The structures were predicted using ESyPred3D program. Amino acid residue 218 of VP2 was displayed as a spacefill model. Each individual loop is shown in different colour; BC loop in green, DE loop in red, EF loop in cyan, FG loop in pink and HI loop in magenta. **(A)** the predicted HEV71-26M VP2 protein with lysine (polar and basic) at residue 218 (K-218) **(B)** the predicted CHO-26M VP2 protein with isoleucine (nonpolar and neutral) at residue 218 (I-218). .

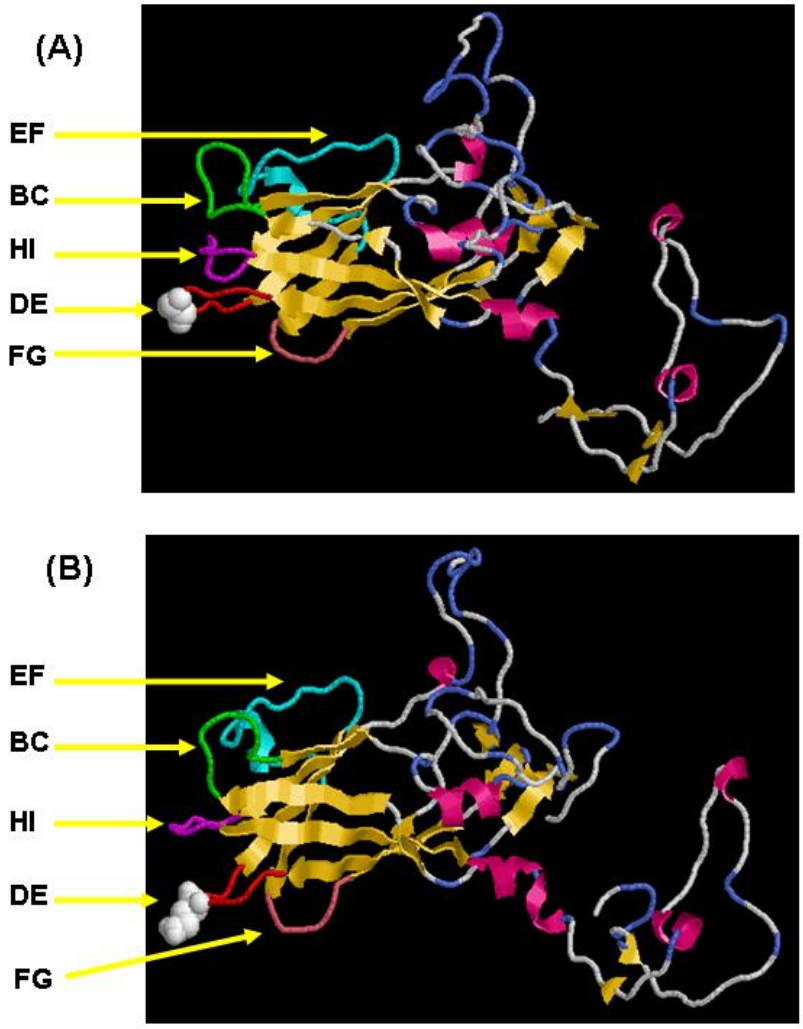

Figure 5.10 Predicted three-dimentional structure of VP1 protein based on the known crystallographic structure of BEV (PDB no: 1BEV_1). The structures were predicted using ESyPred3D program. Amino acid residue 710 of VP1 was displayed as a spacefill model. Each individual loop is shown in different colour; BC loop in green, DE loop in red, EF loop in cyan, FG loop in pink and HI loop in magenta. **(A)** the predicted HEV71-26M VP1 protein with glycine (nonpolar and neutral) at residue 710 (G-710) **(B)** the predicted MP-26M VP1 protein with glutamic acid (polar and acidic) at residue 710 (E-710).

In this study, the molecular basis of mouse- and CHO cell-adaptation by HEV71 was identified by the use of a reverse genetic approach, a mouse HEV71 infection model and by *in vitro* characterisation. A single amino acid change in VP2 ($K^{218}\rightarrow I$) was identified between HEV71 strain 26M and its CHO-adapted variant, CHO-26M, and two additional amino acid changes in VP1 ($G^{710}\rightarrow E$) and 2C ($K^{1327}\rightarrow R$) were identified between HEV71-26M and its mouse-adapted variant, MP-26M. In an attempt to specify genetic determinants of mouse adaptation and CHO cell adaptation of HEV71, recombinant cDNA clones containing one or a combination of two or three mutations were constructed by exchanging corresponding genomic regions of CHO-26M or MP-26M into the full-length infectious cDNA clone of HEV71-26M. Clone-derived viruses were passaged once on RD cells prior to characterisation. The use of clone-derived viruses with limited cell culture passage is likely to provide more homogenous virus population than wild-type virus. Furthermore, specific mutation/s can be introduced into the infectious cDNA clone.

HEV71-26M is unable to replicate in CHO cells. A CHO-adapted variant of HEV71-26M, CHO-26M, was selected after six passages in CHO cells. Single-step growth analysis of clone-derived viruses HEV71-26M (CDV-26M) and CHO-26M (CDV-26M-VP2m) in CHO cells clearly demonstrated that the VP2 ($K^{218}\rightarrow I$) mutation is responsible for the improved growth of HEV71-26M in this cell line. The VP2 protein of enteroviruses forms part of a deep cleft on the virion surface that may function as the site of virion attachment to the cellular receptor (Hogle et al., 1985). In the related PV, amino acid residues in VP2 located in the EF loop, a major neutralizing antigenic site, and residues on the inner surface of the N-terminus of VP2 have been shown to be responsible for mouse adaptation and virulence

(Couderc et al., 1996, Couderc et al., 1994, Couderc et al., 1993). The residue located in the EF loop of VP2 confers a mouse-adapted phenotype of PV by allowing more efficient receptor-mediated conformation changes during viral uncoating and internalisation (Couderc et al., 1996).

In this study, the amino acid substitution $K^{218}\rightarrow I$ of CHO-26M is predicted to be located in the surface exposed of EF loop of the VP2 protein. Interestingly, this unique amino acid change was also identified in a mouse-adapted variant of HEV71 (strain 4643) reported by Wang et al. (2004), in which the positively charged polar lysine was substituted by a non-polar leucine residue. However, data from mouse virulence assays demonstrated that the $K^{218}\rightarrow I$ mutation in VP2 was not sufficient to confer the mouse virulent phenotype of HEV71-26M, but only conferred adaptation to improved growth in CHO cells. Further investigation is needed to understand the mechanism by which the $K^{218}\rightarrow I$ mutation confers CHO cell adaptation. Transfection of viral RNA or cDNA of the parental HEV71-26M and CHO-26M (CDV-26M-VP2m) into CHO cells, virus binding assays and internalisation kinetics of these two viruses in CHO cells would help to clarify the mechanism by which this mutation confers CHO cell adaptation.

A single amino acid substitution in protein 2C ($K^{1327}\rightarrow R$) was also identified in MP-26M (Chen et al., 2004). This mutation is in a different location to the four amino acid substitutions identified in protein 2C of the mouse-adapted strain MP-4643 (Wang et al., 2004). Protein 2C is required for viral RNA synthesis. It functions as a nucleotide triphosphatase (NTPase), as a director of viral replication complexes to cell membranes (Pfister & Wimmer, 1999, Teterina et al., 2001) and may also play a

role in virion assembly (Li & Baltimore, 1990, Vance et al., 1997). A temperature-sensitive PV mutant with a mutation in 2C has been shown to have a defect in uncoating. In addition, a single amino acid change was identified in 2C of a PV strain resistant to hydantoin, a drug known to block virion assembly. In our studies, mouse virulence assays clearly demonstrated that the 2C ($K^{1327}\rightarrow R$) mutation was not responsible for the mouse virulence phenotype of HEV71-26M. No differences in cell culture growth properties, plaque morphology or thermostability were identified between viruses expressing the wild-type (lysine) or mutant (arginine) residue at position 1327 in 2C, suggesting that this amino acid change does not affect viral RNA replication or virion assembly of HEV71. In addition, the 2C ($K^{1327}\rightarrow R$) is the conservative amino acid substitution. Taken together, these data indicated that 2C $K^{1327}\rightarrow R$ mutation did not play an important role in mouse adaptation of HEV71.

In our study, only clone-derived viruses, CDV-26M-VP2-VP1m and CDV-MP-26M, containing the VP1 ($G^{710}\rightarrow E$) mutation were virulent in seven-day-old BALB/c mice, indicating that the VP1 ($G^{710}\rightarrow E$) change is a major genetic determinant of mouse virulence in our model. Arita *et al.* (2008) recently demonstrated an identical mutation responsible for adaptation of HEV71 to growth in SCID/NOD mice. This non-conservative ($G^{710}\rightarrow E$) amino acid substitution is predicted to be located on the surface-exposed DE loop of capsid protein VP1. In the related poliovirus, the DE loop of VP1 is located adjacent to the capsid canyon at the fivefold axis of symmetry (Hogle et al., 1985). Amino acid mutations in the DE loop of the PV VP1 protein display altered heat-induced and receptor-mediated capsid conformation changes (Colston & Racaniello, 1995, Martin et al., 1991, Martin et al., 1988, Wien et al., 1997). In our study, a residue located in the DE loop of capsid protein VP1 appears

to be solely responsible for the mouse virulence phenotype of HEV71. Taken together, these data suggest that mouse adaptation by HEV71 may involve an early step in virus replication, in particular, a change in the specificity of receptor binding. It is likely that parental HEV71-26M is unable to infect mice due to an inability to bind or to enter mouse cells in order to initiate infection. The VP1 ($G^{710}\rightarrow E$) mutation may act directly by affecting interactions with mouse cellular receptor/s or a murine homologue of the human receptor. Alternatively, this mutation may allow HEV71 to undergo mouse cell-specific post-binding capsid conformational changes or cell penetration, and thus enable HEV71 to overcome the host range restriction. Further investigation is needed to understand the mechanism by which this mutation confers mouse adaptation.

Interestingly, the VP1 ($G^{710}\rightarrow E$) mutation is not unique among HEV71 strains. It is the most variable position in VP1, containing amino acids with different polarity and charge, positive charge (L-Arginine, L-Alanine), negative charge (L-glutamic acid), neutral polar (L-glutamine) and neutral non-polar (Glycine), and is not genotype-specific. HEV71 strain 6F has amino acid E at this position, but is not virulent in mice. The nature of the amino acid at this position suggests that the VP1 ($G^{710}\rightarrow E$) mutation may interact with other capsid proteins resulting in the change of the surface structure of the virion. Moreover, it was not possible to obtain a stable HEV1-26M clone-derived virus population that contained only VP1 ($G^{710}\rightarrow E$) mutation or VP1 ($G^{710}\rightarrow E$) and 2C ($K^{1327}\rightarrow R$) mutations due to reversion of VP1 mutation to that of wild type HEV1-26M virus. This suggests capsid protein interactions in which the VP2 ($K^{218}\rightarrow I$) mutation may help to stabilize VP1 mutation via an as yet unknown interaction between these two capsid proteins. The VP2 and

VP1 interaction may cooperate to introduce structural change in the virion that allows the recognition of a mouse cell receptor. Alternatively, this interaction may facilitate a receptor-mediated conformational change during cell entry and virus uncoating. The EF, DE, HI and BC loops interact with one another to form part of neutralisation-antigenic site 1 (Moss & Racaniello, 1991). It has been hypothesised that interactions at this interface play a significant role in the dynamics of capsid-associated receptor attachment and cell entry (Moss & Racaniello, 1991). Thus, the mutations predicted in the EF loop of VP2 and the DE loop of VP1 of MP-26M may interact and regulate conformational transition of the virion during receptor attachment and cell entry.

Clone-derived viruses containing the VP1 mutation, CDV-26M-VP2-VP1m and CDV-MP-26M, had a small plaque phenotype and grew to lower titres in cell culture compared to the other viruses and these defects appears to be linked to the effect on mouse virulence. This differs from mouse-adapted HEV71 strain MP-4643 reported previously, which was shown to have larger plaque size and grew more rapidly in cell culture than the parental virus (Wang et al., 2004). However, no mutation was identified in the VP1 protein of MP-4643 and there was only one mutation identified in VP2, indicating that the molecular basis of mouse adaptation and virulence of strains MP-4643 and MP-26M differ considerably.

The small plaque phenotype and growth defects in cell culture of CDV-26M-VP2-VP1m and CDV-MP-26M could possibly be due to low stability of the capsid. The VP1 mutation was also found to be unstable during cell passage in primate (RD and Vero) and hamster (CHO) cells, but is stable during mouse passage. These data

suggest that the VP1 ($G^{710}\rightarrow E$) mutation has effects on conformational stability, and thus HEV71 is intolerant to this mutation, and under high selection pressure to revert to wild-type in RD, Vero and CHO cells. The stability of the VP1 mutation in mouse cell lines needs to be further investigated.

Interestingly, CDV-26M-VP2-VP1m and CDV-MP-26M also replicated to lower titres compared to other viruses in the mouse neuronal cell line, NB41A3. By contrast, clone-derived viruses containing the VP2 mutation replicated more efficiently than the other viruses. Studies in mice showed that skeletal muscle and/or connective tissue were the primary sites of replication for both CHO-26M and MP-26M (Chua et al., 2008). However, MP-26M replicated more efficiently than CHO-26M in mouse limb muscle with approximatly 10-fold higher titres being detected in limb muscle of MP-26M-infected mice than CHO-26M-infected mice (Chua et al., 2008). CHO-26M caused mild pathological changes in muscles of infected mice whereas MP-26M induced severe myositis (Chua et al., 2008). It has been suggested that the flaccid paralysis in MP-26M-infected mice is due to myositis, as inconsistent pathological changes were observed in the central nervous system (Chua et al., 2008). The VP2 and VP1 mutations of MP-26M have opposite affects on viral growth characteristics in the mouse neuronal cell line, NB41A3. It is possible that the VP1 mutation enhances replication of MP-26M in muscle cells but not neuronal cells. Single step growth analysis of clone-derived viruses in primary mouse muscle and neuronal cells would help clarify this issue.

In conclusion, the molecular basis of CHO cell adaptation and mouse adaptation of HEV71 was characterised. An amino acid substitution ($K^{218}\rightarrow I$) located in the

surface- exposed EF loop of VP2 was associated with CHO cell adaptation and a non-conservative amino acid substitution ($G^{710}\rightarrow E$) located in the surface exposed DE loop of VP1 was found to be a critical determinant of mouse adaptation and virulence of HEV71. CHO cell and mouse adaptation determinants are likely to involve an early event in virus replication cycle; ie virus binding and entry into cells. Identification of viral genomic regions responsible for expanded host range and virulence greatly enhances our understanding of the biology of HEV71, and thus can advance research on viral pathogenesis and vaccine development for prevention and control of this important pathogen.

CHAPTER SIX

DEVELOPMENT OF A MOUSE HEV71 ORAL INFECTION MODEL

6.1 Introduction

The development of an animal model that mimics human disease is essential for the study of viral pathogenesis and the development of effective therapeutics and vaccines. The first animal models for HEV71 infection were established in non-human primates. Cynomolgus, rhesus and green monkeys were found to be susceptible to HEV71 infection after subcutaneous (s.c.), intraspinal (i.s.), intracerebral (i.c.), intravenous (i.v.) or oral inoculation (Chumakov et al., 1979, Hashimoto & Hagiwara, 1982a, Hashimoto & Hagiwara, 1982b, Hashimoto et al., 1978, Nagata et al., 2004). HEV71 infection of monkeys induced neurological manifestations such as flaccid paralysis, tremor, ataxia and brain oedema similar to that seen in human cases. Detailed pathological studies of infected cynomolgus monkeys revealed a widespread distribution of virus-induced lesions in both the pyramidal and extrapyramidal tracts of the CNS (Nagata et al., 2004). The virus was found to replicate in the spinal cord, brainstem, cerebral cortex, dentate nuclei and cerebrum (Nagata et al., 2004). However, the monkeys with brainstem lesions did not develop fatal neurogenic pulmonary oedema, a new clinical manifestation associated with brainstem encephalitis observed in human cases during recent large HFMD epidemics in Southeast Asia.

Due to the prohibitive cost of primate experiments, several research groups have developed mouse models as an alternative tool for HEV71 pathogenesis studies, and

for antiviral and vaccine testing. The mouse is not a natural host of HEV71 and adult mice are not susceptible to HEV71 infection (Wu et al., 2002, Yu et al., 2000). However, newborn mice were found to be susceptible to infection with an unadapted HEV71 strain after i.p. inoculation at a high viral titre (Yu et al., 2000). In all studies, a mouse-adapted HEV71 strain was required to consistently produce disease in newborn mice. Mouse-adapted HEV71 strains have been reported to cause similar clinical signs of infection in mice up to 2 weeks old regardless of the route of inoculation (Chen et al., 2007, Chua et al., 2008, Ong et al., 2008). The virus induced acute flaccid paralysis in an age-, dose-, and route-of-inoculation-dependent manner (Chen et al., 2007, Chua et al., 2008, Ong et al., 2008). The amount of virus that constituted a 50% lethal dose (LD_{50}) was lowest for i.m., followed by i.c., i.p. and oral inoculation, respectively (Chen et al., 2007, Chua et al., 2008). The route of inoculation also affected disease course (Chen et al., 2007). Mice infected intracranially developed flaccid paralysis in both fore and hind limbs and died one to two days after the onset of disease (Chen et al., 2007). By contrast, intramuscular and orally infected mice always developed paralysis in the hind limbs and had longer lag times between the onset of paralysis and death (Chen et al., 2007). Although mice were found to be resistant to infection with mouse-adapted strains beyond the age of 14 days, the mouse model was successfully used for testing vaccine candidates by passive immunization and determination of protective efficacy against lethal HEV71 challenge in susceptible newborn mice (Wu et al., 2002).

We have developed a HEV71 infection model in newborn BALB/c mice by i.c., i.m. and i.p. inoculation with a mouse-adapted variant of HEV71-26M (MP-26M) (Chua et al., 2008). Consistent with the studies reviewed above, our mouse-adapted strain

caused fore- and/or hindlimb paralysis, hunched back and eventual death in newborn BALB/c mice. Infectivity studies established skeletal muscle as the primary site of replication. Histological studies showed intense inflammation within infected muscle groups. Virus was isolated from the brain although there was no obvious virus-induced lesion in the CNS. More detailed pathological studies, including immunohistochemistry and *in situ* hybridization assays will need to be carried out in order to provide more insight into the involvement of the CNS and the mechanism of virus spread.

As the oral route is a natural route of HEV71 infection in human beings, a mouse HEV71 oral infection model would serve as the valuable tool for studying HEV71 pathogenesis, and for vaccine or antiviral efficacy testing. We aimed to establish a mouse HEV71 oral infection model for future studies, particularly for defining virulence determinants, and for testing of vaccine efficacy and immunogenicity. The preliminary results are described in this chapter.

6.2 Results

6.2.1 Determination of stomach emptying time

To optimise the duration of fasting prior to oral infection of suckling mice with virus we determined gastrointestinal transit time in newborn mice. Stomach emptying in adult mice has an exponential decay constant of 74 min and gastric emptying time is within 6 h (Schwarz et al., 2002). In newborn mice, however, this information is not known.

One-day old mice were separated from their mothers for 6 h and were then fed with milk containing phenol red at about 20-30 μL (30 mL/kg body weight) using plastic feeding tubes. Groups of two mice were sacrificed immediately (time = 0 h) and at 1, 2, and 4 h after feeding. Stomach and intestinal contents were observed, and gastric emptying time was determined using the method described in section 2.4.2. The extent of gastric emptying was 27%, 40% and 52% after feeding for 1, 2, and 4 h respectively. A fasting time of 2 hours was chosen for subsequent experiments to minimize physiological stress, which could affect clinical observation of HEV71 infection in newborn mice.

6.2.2 Effect of blue food dye on HEV71 infectivity

To ensure that mice were cleanly inoculated via the stomach, blue food dye was used to visualise the virus inoculum in the stomach and to allow monitoring of virus deposits in other regions. It was first necessary to detect if blue food dye inhibited HEV71 infectivity. Serial virus dilutions were mixed with blue food dye at a final concentration of 0%, 0.1%, 0.5%, 1% or 2% (v/v), and the suspensions incubated at 37°C for 1 h prior to determination of virus titre by $TCID_{50}$ assay (see section 2.3.2). Blue food dye was observed to have no adverse effect on HEV71 infectivity (Table 6.1). Hence, blue food dye was added to each virus dilution at a final concentration of 1% (v/v) prior to oral inoculation of mice in all subsequent experiments. At this concentration, virus inoculum could be readily observed in the stomach of mice after each inoculation.

Table 6.1 Effect of blue food dye on HEV71 infectivity

Concentration of blue food dye in virus dilution (% v/v)	Viral titre * ($TCID_{50}$/mL)
0	$6.8x10^6$
0.1	$4.7x10^6$
0.2	$5.6x10^6$
1	$1.0x10^7$
2	$6.8x10^6$

*Determined by $TCID_{50}$ assay on Vero cells.

6.2.3 Infectivity of a mouse-adapted variant of HEV71-26M (MP-26M) in one-day old BALB/c mice after oral infection

Experimental infection with MP-26M via i.c., i.p. and i.m. routes caused lethal illness in one-day old BALB/c mice. Infected mice developed fore- and/or hindlimb paralysis, hunched back, dehydration and eventual death (Chua et al., 2008). The 50% humane end-points (HD_{50}) for the i.c., i.p. and i.m. routes of infection were 5.0×10^2, 3.4×10^3 and 1.5×10^2 $TCID_{50}$, respectively (Chua et al., 2008). In order to develop a HEV71 oral infection model, groups of 5-6 one-day-old BALB/c mice were orally infected with MP-26M virus at increasing doses, ranging from 5×10^3 to 5×10^6 $TCID_{50}$ per dose, after fasting for 2 h. Mice were observed daily for clinical signs of HEV71 infection; control animals were inoculated with phosphate-buffered saline (PBS). Similar to other routes of inoculation, MP-26M-infected mice displayed fore-and/or hindlimb paralysis, hunched back, and dehydration. Mice succumbed to infection 5 to 11 days after inoculation. Oral inoculation with MP-26M also resulted in dose-dependent mortality (Figure 6.1). The HD_{50} value for the oral route was 5×10^5 $TCID_{50}$, which was higher than the HD_{50} values for other routes of inoculation. Experimental infection of one-day- old BALB/c mice with parental (unadapted) HEV71 (5×10^6 $TCID_{50}$) by the oral route produced no clinical signs of infection.

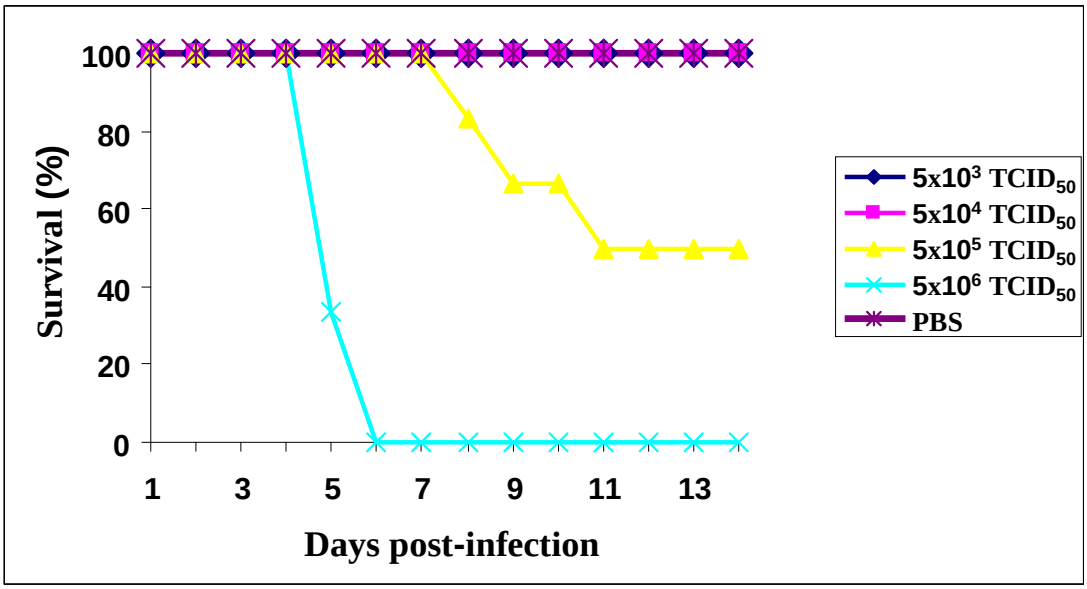

Figure 6.1. **Percentage survival of one-day-old BALB/c mice after oral infection with MP-26M.** Groups of 5-6 one-day-old BALB/c mice were orally infected with MP-26M virus at increasing doses (from $5x10^3$ to $5x10^6$ $TCID_{50}$). Control animals were inoculated with phosphate-buffered saline (PBS). Mice were observed for 14 days post-infection and the percentage survival calculated.

6.2.4 Age dependence of mouse susceptibility to HEV71 after oral infection

In order to determine whether susceptibility of newborn mice to HEV71 infection after oral inoculation is age-dependent, groups of 5-8 newborn mice were infected orally with MP-26M at 5×10^6 $TCID_{50}$ (ten times the HD_{50} value) at increasing ages (day 1, 2, 3, 5, 7, 9 and 14). Mice were observed daily for clinical signs of infection and survival and mortality rates for the different age groups were recorded. The results are shown in Figure 6.2. Mice were susceptible to oral infection with MP-26M until 14 days of age. Similar mortality profiles were observed in mice of 1, 3 and 5 days of age. The first deaths occurred at 5 days post-infection, and 100% mortality was reached by day 6. In mice inoculated at 9 and 11 days of age, the first deaths occurred on days 6 and 7 post-infection and the groups had 66.7% and 50% mortality, respectively.

6.3 Discussion

In this study, an oral inoculation model for HEV71 infection in mice was established. Similar to previous studies (Chen et al., 2007, Chen et al., 2004, Chua et al., 2008, Wang et al., 2004), BALB/c mice were susceptible to MP-26M infection via the oral route in an age- and dose-dependent manner. Mice orally infected with the parental strain HEV71-26M developed no clinically overt disease, whereas MP-26M infected mice developed fore and/or hind limb paralysis. Chen et al. (2004) found that newborn ICR mice infected orally with an unadapted HEV71 strain (HEV71-4643) developed skin lesions characterised as desquamation and cicatrisation. However, we did not observe skin lesions in mice infected orally with

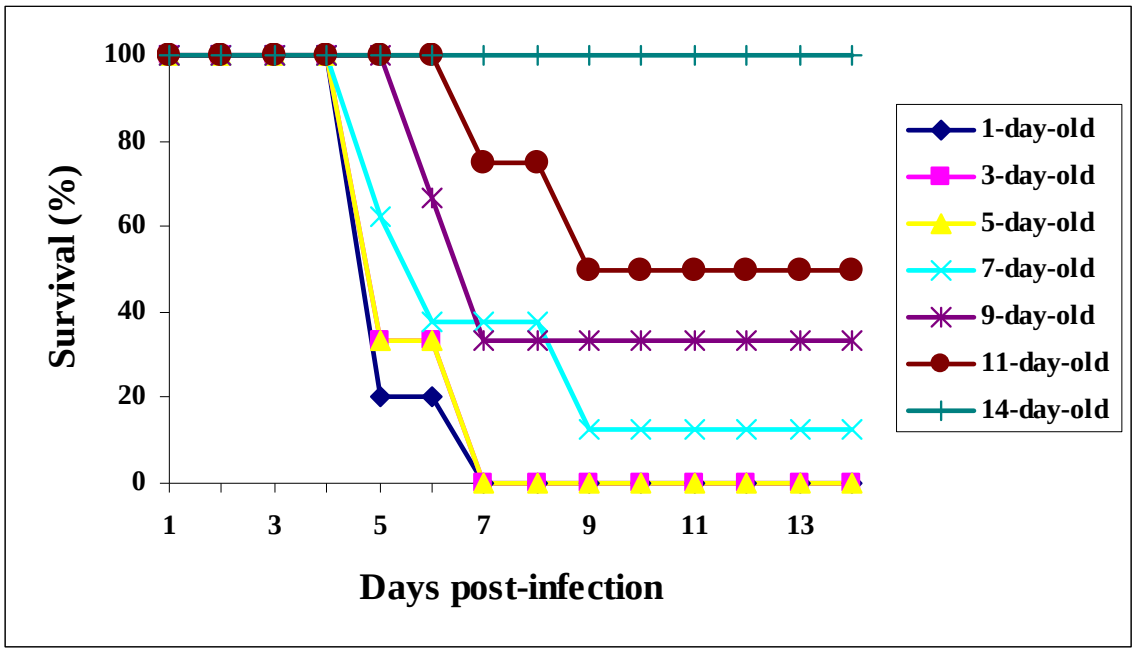

Figure 6.2 Age-related survival of BALB/c mice orally infected with MP-26M. Groups of 5-8 BALB/c mice were infected orally at the indicated ages with ten HD_{50} ($5x10^6$ $TCID_{50}$) of MP-26M. Mice were observed for 14 days post-infection and the percentage survival calculated.

HEV71-26M. This discrepancy may be due to the different virus and/or host strains used in this study. Generally, however, the clinical manifestations of the mouse-adapted strain MP-26M infection we observed were consistent with previous studies (Chen et al., 2007, Chen et al., 2004, Chua et al., 2008, Wang et al., 2004).

The HD_{50} for oral inoculation is much higher than that observed for other routes of inoculation. This may be explained by the fact that the virus has to overcome unique physical barriers in the alimentary tract. By using poliovirus receptor (PVR)-expressing mice lacking the interferon α and β receptor (PVR-IFNAR$^{-/-}$) and artificial quasispecies pool of ten distinct genetically marked viruses, Kuss et al. (2008) demonstrated that physical barriers play a major role in limiting the spread of poliovirus (PV) in orally infected mice. Three major bottleneck barriers that affect virus trafficking inside the host were identified, including mouth to gut, mouth to blood and mouth to brain. Following oral inoculation of PVR-IFNAR$^{-/-}$ with ten genetically marked viruses, only 16% and 19% of input viruses were present in the stomach, and small intestine and colon, respectively, indicating physical barriers in gut tissues. In addition, only 9% and 21% of input viruses were detected in blood and brain, respectively. These two bottlenecks, mouth to gut and mouth to blood, could be partially overcome by physical disruption of colon epithelium. Interestingly, the bottleneck barriers were largely absent in the PVR-IFNAR$^{-/-}$ mice inoculated via i.m. and i.p. routes. The physical barriers that the HEV71 virus must overcome in the alimentary tract might explain the high HD_{50} observed for oral inoculation compared to other routes of inoculation. The age-related resistance to oral inoculation may be due to cell maturation in tissues and/or development of the

immune system in mice (Griffin et al., 1974, Hirsch et al., 1970, Johnson, 1964, Roos et al., 1978).

The mechanism of CNS penetration by enteroviruses remains to be elucidated. Virus could gain entry to the CNS via the peripheral nerves that innervate the wall of the alimentary tract and/or secondary infected muscles and visceral organs (Blinzinger & Anzil, 1974, Sabin, 1956). Alternatively, virus could enter the bloodstream and then penetrate the CNS by passage across the blood-brain barrier (Blinzinger et al., 1969, Bodian, 1955). Both PV and HEV71 are neurotropic enteroviruses and are spread by fecal-oral transmission. In humans, PV infection is initiated by ingestion of the virus (Sabin, 1956). The virus first infects and multiplies in the oropharyngeal and alimentary mucosa (Bodian & Horstmann, 1965, Sabin, 1956). The virus then enters the deep cervical and mesenteric lymph nodes from where it is released into the blood, causing a transient viremia (Bodian & Horstmann, 1965). Replication at extraneural sites, including brown fat, reticuloendothelial tissues and muscle is thought to sustain viremia (Bodian & Horstmann, 1965, Ren & Racaniello, 1992, Wenner & Kamitsuka, 1957). Serum neutralizing antibody to PV prevents the development of poliomyelitis, suggesting that viremia is necessary for the spread of virus into the CNS (Bodian & Horstmann, 1965). Thus, the blood-brain barrier pathway is considered the primary route by which poliovirus disseminates to the CNS. However, dissemination via a neural pathway has also been reported in several studies in humans, primates, and in the transgenic mouse model (Nathanson & Bodian, 1961, Nathanson & Langmuir, 1995, Ohka et al., 1998). Furthermore, another neurotropic enteric virus, Reovirus serotype 3, spreads from the intestinal tract directly to regional nerves innervating

the intestine and then through parasympathetic fibers to the CNS of infected mice (Morrison et al., 1991).

The pathway for HEV71 entry into the CNS remains unknown. Using a murine oral infection model, Wang et al. (2004) showed that the virus first replicates in the intestine. Virus replication was then observed in the limb muscles and spinal cord, followed by the brain. Limb muscles were found to be a major site for viral replication and maintenance of viremia. The authors suggested that viremia was necessary for the spread of virus into the CNS, because anti-HEV71 antibodies could protect HEV71-infected mice from developing disease. Neuroinvasion was probably preceded by virus replication in extraneural tissues. However, the pattern of spread of the virus from the lower to upper segments of the spinal cord also suggested a neural transmission pathway, such as retrograde axonal transport. A recent study of a mouse model has shown that HEV71 entered the CNS via peripheral motor nerves after i.m. inoculation, and its spread in the CNS involved motor and other neural pathways (Ong et al., 2008). To date, the route of entry into the CNS and the neuropathology of HEV71 infection has not been clearly defined. More detailed histopathological studies will help provide more information on the pathogenesis of HEV71 infection. A well-characterised mouse oral infection model could enhance antiviral and vaccine efficacy testing.

CHAPTER SEVEN

GENERAL DISCUSSION

Since its first discovery in 1969, Human Enterovirus 71 (HEV71) has been associated with several large outbreaks of hand, foot and mouth disease in young children. While hand, foot and mouth disease is a common clinical manifestation, HEV71 occasionally causes severe neurological diseases during acute infection, including aseptic meningitis, brainstem and/or cerebellar encephalitis, and acute flaccid paralysis, which may lead to permanent paralysis or death (McMinn, 2002). Since 1997, several large epidemics of HEV71 infection have continued to occur in many countries in the Asia-Pacific region including Malaysia, Taiwan, Australia, Vietnam, Singapore, Thailand, India, Brunei, Hong Kong and China (Cardosa et al., 2003, Ho, 2000, Lin et al., 2006, McMinn et al., 2001b, Tu et al., 2007)(http://www.promedmail.org, http://www.cdc.gov). Interestingly, these recent outbreaks have been associated with an increasing incidence of cases with neurological complications. A new severe clinical manifestation of HEV71 infection, a fatal neurogenic pulmonary oedema associated with brainstem encephalitis, has also been identified (Ho, 2000, Lum et al., 1998). HEV71 is now considered the leading cause of acute neurological infection in children in the Asia-Pacific region (Daley & Dwyer, 2002, Palacios & Oberste, 2005, Wong et al., 2000). Due to the increase in prevalence and the severe nature of HEV71-associated neurological disease, investigations into the molecular genetics of virulence have become important areas of research. This knowledge is essential for the development of vaccines for prevention and control of HEV71 infection.

Studies on the molecular biology and genetics of virulence of RNA viruses have been considerably advanced by the development of infectious cDNA clones. Infectious cDNA clones have been produced for a number of enteroviruses, including poliovirus (PV), CAV9, CBV3 and Echovirus 7 (Cello et al., 2002, Chua, 2007, Harvala et al., 2002, Martino et al., 1999). Such clones serve as useful tools for the analysis of molecular basis of enterovirus replication and virulence (Dan & Chantler, 2005, Harvala et al., 2002, Johnson & Sarnow, 1991), and will continue to provide much insight into the molecular biology of enteroviruses and the nature of enterovirus attenuation. Infectious clones have also been used as the basis for the design and production of live-attenuated vaccines in several studies (Dan & Chantler, 2005, Gromeier et al., 1996, Haller et al., 1996).

In this study, infectious cDNA clones of HEV71-6F (genotype C2) and HEV71-26M (genotype B3), two strains isolated during the 1999 Western Australian HFMD outbreak, were successfully constructed. Selection of appropriate plasmid vectors and bacterial host strains was found to be the most critical for the construction of infectious cDNA clones of HEV71. All full-length cDNA clones of HEV71-6F, constructed in a medium copy number plasmid pBR322 and propagated in *E. coli* strain DH5α, were found to be non-infectious. One of the clones was fully sequenced and compared to the HEV71-6F sequence in order to identify the problem. Sequencing revealed eight amino acid mutations located in both structural and non-structural proteins, and two stop codons, located in the VP3 and 2A proteins. These mutations are likely to have been introduced into the viral genome by the bacterial host in order to decrease the expression of HEV71 proteins toxic to the host cell. The medium copy number of pBR322 may have exceeded the

tolerance of bacterial host cells to the toxic products expressed from the viral cDNA. Genetic instability of the cloned cDNA has been described for several RNA viruses, particularly flaviviruses and coronaviruses (Masters, 1999, Mishin et al., 2001, Rice et al., 1989, Sumiyoshi et al., 1992), but has not been well documented for enteroviruses. The instability problem encountered in the construction of HEV71-6F infectious cDNA clones was overcome by using a combination of low copy number plasmid pMC18 and bacterial host strain XL10-gold. This protocol was also successfully used for generating infectious cDNA clone of HEV71-26M. The reason why XL10-gold is more suitable for propagating cDNA clones of HEV71 than the other two strains, DH5α and DH10B, remains unclear. Clone-derived viruses (CDV) of HEV71-6F and HEV71-26M were successfully obtained by transfection of plasmid cDNA into susceptible cells. Analysis of the *in vitro* phenotype of both clone-derived viruses illustrates the integrity of the infectious clone system. CDV-6F and CDV-26M were found to display *in vitro* growth properties indistinguishable from their respective parental viruses.

Interestingly, the two HEV71 strains, HEV71-6F and HEV71-26M, were found to have distinct cell culture growth phenotypes. HEV71-26M replicated more efficiently than HEV71-6F in both human (RD) and monkey (Vero) cell lines. HEV71-26M exhibited a large plaque phenotype and was able to adapt to grow in rodent (CHO) cells. By contrast, HEV71-6F displayed a pinpoint plaque phenotype and failed to adapt to grow in CHO cells. Further study will need to be undertaken in order to determine temperature sensitivity and growth phenotype of these two strains in other cells of human origin.

In Chapter 4, we aimed to identify the genome regions responsible for the growth phenotypes of the two strains. Chimeric recombinant viruses carrying reciprocal exchanges of HEV71-6F and HEV71-26M 5′ UTR, structural protein genes (P1 region) and non-structural protein genes (P2 and P3 regions) were generated and growth properties of the parental and chimeric viruses in cell culture were compared. Reciprocal 5′ UTR chimeras (6F/5′ UTR/26M and 26M/5′ UTR/6F) exhibited similar growth patterns to their parental backbone virus. Secondary structures of 5′ UTR of these two strains were also highly similar. In addition, the translation efficiencies of 5′ UTR of these two strains were not significantly different in both human (RD) and monkey (COS-7) cells. Taken together, these data indicate that the 5′ UTR is not responsible for distinct growth phenotypes between these two strains. Reciprocal P1 and P2-P3 chimeras displayed growth phenotypes in between that of the parental backbone virus, indicating that both P1 and P2-P3 genome regions influence the HEV71 growth phenotype in cell culture. These results suggest that differences in growth characteristics between HEV71-6F and HEV71-26M may involve both early (binding and entry) and RNA replication steps. Further investigations will need to be undertaken in order to verify this hypothesis. A cell binding and viral cell entry assays may help to clarify the role of the capsid protein P1 in phenotypic differences. Experiments to define viral RNA synthesis, such as the use of a cell-free translation-RNA replication system, the HEV71 luciferase replicons or quantitative real-time PCR, would help to determine the role of P2 and P3 in growth phenotype of these two strains. In addition, the role of *cre* and 3′ UTR on phenotypic differences will need to be confirmed by construction of reciprocal *cre* or 3′ UTR chimeras between HEV71-6F and HEV71-26M. This work will provide much insight into the molecular basis of HEV71 replication.

Similar to the related PV, HEV71 has a limited host range, with humans the only known natural host. Non-human primate models have long been the most suitable animal models to study the pathogenesis of both PV and HEV71. Since the identification of the cell receptor for PV, PVR (CD155), transgenic mice possessing the PVR have been developed (Koike et al., 1994, Ren et al., 1990). PVR transgenic mice have eliminated the need for primates, and have become the definitive small animal model for most experimental procedures, providing new information on PV pathogenesis and serving as tool for vaccine testing (Koike et al., 1994, Koike et al., 1991, Ren & Racaniello, 1992, WHO, 1998). Unfortunately, the HEV71 cellular receptor has not been identified, thus no HEV71-receptor-expessing-transgenic-mice are available. With limited resource of monkeys, several recent studies have developed a mouse model as an alternative animal model for HEV71 infection by using mouse-adapted variants of HEV71 (Arita et al., 2008, Chen et al., 2004, Chua et al., 2008, Ong et al., 2008). A previous study by our group (Chua et al., 2008), has established a mouse HEV71 infection model using a mouse-adapted variant of HEV71-26M (MP-26M). MP-26M was created by serial passage of HEV71-26M in CHO cells, and CHO-adapted virus (CHO-26M) was then serially passaged for six times by intracerebral inoculation of one-day-old BALB/c mice. Despite improved growth in CHO cells, CHO-26M did not cause any clinical signs of infection in newborn BALB/c mice. By contrast, infection of newborn mice with MP-26M resulted in severe disease and death in an age-, dosage- and route-dependent manner.

In Chapter 5, the molecular basis of CHO cell- and mouse- adaptation was determined. A single amino acid substitution within the VP2 capsid protein ($K^{218}\rightarrow I$) was identified in CHO-26M. Two further amino acid mutations were

identified in MP-26M, located within the VP1 capsid protein ($G^{710}\rightarrow E$) and the 2C protein ($K^{1327}\rightarrow R$). No nucleotide sequence changes were observed in the 5′- and 3′-UTRs. By comparison with amino acid sequences of other HEV71 strains, the amino acid changes $K^{218}\rightarrow I$ in VP2 and $K^{1327}\rightarrow R$ in 2C are found to be unique, whereas the $G^{710}\rightarrow E$ in VP1 is not unique. In order to study the molecular basis of CHO cell- and mouse- adaptation, infectious cDNA clone-derived mutant virus populations containing the mutations identified in CHO-26M and MP-26M were generated, and these clone-derived viruses (CDV) were characterised in cell culture and in the mouse model. Data obtained from our study clearly demonstrated that the VP2 ($K^{218}\rightarrow I$) mutation is responsible for the improved growth of HEV71-26M in CHO cells, and the VP1 ($G^{710}\rightarrow E$) is a major genetic determinant of mouse adaptation. Interestingly, the only capsid protein mutation identified in the mouse-adapted virus selected by Chen et al. (2004) was located at the same position in VP2, with the positively charged lysine residue substituted by a non-polar leucine. Moreover, an identical mutation in VP1 ($G^{710}\rightarrow E$) was identified in the mouse-adapted virus selected by Arita *et al*. (2008). Repeated selection at these amino acid positions in VP2 and VP1 strongly indicates that these amino acid residues play an essential role in the infection cycle of HEV71 in rodent cells, expanding host range of HEV71.

Both amino acid substitutions in VP2 ($K^{218}\rightarrow I$) and VP1 ($G^{710}\rightarrow E$) are predicted to be located in surface exposed loops; $K^{218}\rightarrow I$ in the EF loop of VP2 and $G^{710}\rightarrow E$ in the DE loop of VP1. The finding that a CDV population that contains only the $G^{710}\rightarrow E$ mutation is unstable due to reversion to the wild-type sequence after a single passage in RD cells suggests that the VP2 residue I^{218} may help to stabilize the

VP1 residue E^{710} via an as yet unknown interaction between these two capsid proteins. The VP2 and VP1 interaction may cooperate to introduce structural change in the virion that either allows the recognition of a mouse cell receptor or may facilitate receptor-mediated conformational changes after attachment.

Taken together, these data suggested that CHO cell- and mouse- adaptation determinants are likely to involve an early step in virus replication, particularly a change in the specificity of receptor binding. Further study is needed to understand the mechanisms by which the amino acid mutations, VP2 ($K^{218}\rightarrow I$) and VP1 ($G^{710}\rightarrow E$), confer CHO cell- and mouse- adaptation. Cell binding assays and internalization kinetics of the parent HEV71-26M and CHO-26M (CDV-26M-VP2) in CHO cells would help to clarify the mechanism by which the VP2 ($K^{218}\rightarrow I$) confers CHO cell adaptation. Similarly, virus cell binding assays and internalization kinetics of HEV71-26M, and viruses expressing the VP1 ($G^{710}\rightarrow E$) mutation in cell lines of mouse origin, in particular, mouse muscle and neuronal cells will need to be undertaken in order to determine the mechanism by which this mutation confers mouse adaptation.

In a previous study by our research group (Herrero, 2007), identification of the HEV71 cell surface receptor was attempted by using Virus Overlay Protein Binding Assays (VOPBA) and MALDI-TOF MS. This approach has been used successfully for the identification of cellular receptor for a number of viruses, such as dengue virus (Tio et al., 2005). Preliminary VOPBA results showed that HEV71 bound to a 55kDa/pI 5, 40kDa/pI 6 and 32kDa/pI 7 proteins expressed on the plasma membrane of RD cells (Herrero, 2007). This method is being optimised in our research group.

Preliminary analysis of these proteins by MALDI-TOF MS did not result in matches to any characterised proteins in the MASCOT or MS fit seach engines. These data are being analysed against other search engines. If this approach is successful in the identification of the HEV71 cellular receptor, it will be useful to identify mouse homologue receptors of HEV71 in future studies. Experiments can be carried out by performing VOPBA and MALDI-TOF MS using mouse cell lines, particularly muscle and neuronal cells, and mouse-adapted virus MP-26M.

Although a mouse model is not as good as a monkey model for studying HEV71 pathogenesis due to the need to select mouse-adapted strains for infection of mice, it is, however, currently the most convenient animal model and has served as a useful tool for testing of vaccine efficacy and immunogenicity. For example, Yu et al. (2000) has shown that passive immunization with inactivated HEV71 was able to protect newborn mice against HEV71 infection. In addition, Wu et al. (2007) demonstrated that active immunization with avirulent HEV71 or CAV16 by the oral route could protect newborn mice against infection with virulent HEV71. Furthermore, a recent study by Ong et al. (2008) has shown that a model of HEV71 infection in 2 week-old mice can be used to study pathogenesis of HEV71 infection, particularly in viral transmission pathways and mechanisms of neuronal damage.

The natural route of HEV71 infection in human is the oral route. Given that a well-characterised mouse infection model will provide more information on the pathogenesis of HEV71 infection and provide a useful tool for development of vaccines, we thus aimed to establish a mouse HEV71 oral infection model and the preliminary results are described in Chapter 6. BALB/c mice orally infected with a

mouse-adapted strain, MP-26M, developed fore- and/or hindlimb paralysis similar to other routes of inoculation. Mice were also susceptible to MP-26M infection via an oral route in an age- and dose-dependent manner. This mouse oral infection model will need to be thoroughly characterised pathologically in a future study.

In summary, the work described in this thesis has contributed to the understanding of the molecular biology of HEV71. A reverse genetic system developed in this study has proven to be an invaluable tool for the study of molecular mechanisms of replication and virulence. Infectious cDNA clones can be used for further study on viral genetic elements that control viral translation and replication processes. The impact of these processes and the role of viral genetic elements on determination of viral neurovirulence can therefore be determined. This information will provide a genetic basis for the development of a live, attenuated vaccines for control of this important neurotropic virus.

REFERENCES

AbuBakar, S., Chee, H. Y., Al-Kobaisi, M. F., Xiaoshan, J., Chua, K. B. & Lam, S. K. (1999). Identification of enterovirus 71 isolates from an outbreak of hand, foot and mouth disease (HFMD) with fatal cases of encephalomyelitis in Malaysia. *Virus Res* **61**, 1-9.

Aldabe, R. & Carrasco, L. (1995). Induction of membrane proliferation by poliovirus proteins 2C and 2BC. *Biochem Biophys Res Commun* **206**, 64-76.

Andino, R., Rieckhof, G. E., Achacoso, P. L. & Baltimore, D. (1993). Poliovirus RNA synthesis utilizes an RNP complex formed around the 5′-end of viral RNA. *EMBO Journal* **12**, 3587-98.

Andino, R., Rieckhof, G. E. & Baltimore, D. (1990). A functional ribonucleoprotein complex forms around the 5′ end of poliovirus RNA. *Cell* **63**, 369-80.

Arita, M., Ami, Y., Wakita, T. & Shimizu, H. (2008). Cooperative effect of the attenuation determinants derived from poliovirus sabin 1 strain is essential for attenuation of enterovirus 71 in the NOD/SCID mouse infection model. *J Virol* **82**, 1787-97.

Arita, M., Shimizu, H., Nagata, N., Ami, Y., Suzaki, Y., Sata, T., Iwasaki, T. & Miyamura, T. (2005). Temperature-sensitive mutants of enterovirus 71 show attenuation in cynomolgus monkeys. *J Gen Virol* **86**, 1391-401.

Bailey, J. M. & Tapprich, W. E. (2007). Structure of the 5′ nontranslated region of the Coxsackievirus B3 genome: Chemical modification and comparative sequence analysis. *J Virol* **81**, 650-68.

Barton, D. J. & Flanegan, J. B. (1997). Synchronous replication of poliovirus RNA: initiation of negative-strand RNA synthesis requires the guanidine-inhibited activity of protein 2C. *J Virol* **71**, 8482-9.

Basavappa, R., Syed, R., Flore, O., Icenogle, J. P., Filman, D. J. & Hogle, J. M. (1994). Role and mechanism of the maturation cleavage of VP0 in poliovirus assembly: structure of the empty capsid assembly intermediate at 2.9 A resolution. *Protein Sci* **3**, 1651-69.

Bazan, J. F. & Fletterick, R. J. (1988). Viral cysteine proteases are homologous to the trypsin-like family of serine proteases: structural and functional implications. *Proc Natl Acad Sci U S A* **85**, 7872-6.

Belnap, D. M., McDermott, B. M., Jr., Filman, D. J., Cheng, N., Trus, B. L., Zuccola, H. J., Racaniello, V. R., Hogle, J. M. & Steven, A. C. (2000). Three-dimensional structure of poliovirus receptor bound to poliovirus. *Proc Natl Acad Sci U S A* **97**, 73-8.

Bienz, K., Egger, D., Pfister, T. & Troxler, M. (1992). Structural and functional characterization of the poliovirus replication complex. *J Virol* **66**, 2740-7.

Blair, W. S., Parsley, T. B., Bogerd, H. P., Towner, J. S., Semler, B. L. & Cullen, B. R. (1998). Utilization of a mammalian cell-based RNA binding assay to characterize the RNA binding properties of picornavirus 3C proteinases. *RNA* **4**, 215-25.

Blinzinger, K. & Anzil, A. P. (1974). Neural route of infection in viral diseases of the central nervous system. *Lancet* **2**, 1374-5.

Blinzinger, K., Simon, J., Magrath, D. & Boulger, L. (1969). Poliovirus crystals within the endoplasmic reticulum of endothelial and mononuclear cells in the monkey spinal cord. *Science* **163**, 1336-7.

Blomberg, J., Lycke, E., Ahlfors, K., Johnsson, T., Wolontis, S. & von Zeipel, G. (1974). Letter: New enterovirus type associated with epidemic of aseptic meningitis and-or hand, foot, and mouth disease. *Lancet* **2**, 112.

Bodian, D. (1955). Emerging concept of poliomyelitis infection. *Science* **122**, 105-8.

Bodian, D. & Horstmann, D. H. (1965). Polioviruses. In *Viral and Rickettsial Infections of Man*, pp. 430-73. Edited by F. L. Horsfall & I. Tamm. Philadelphia: Lippincott.

Boot, H. J., ter Huurne, A. A., Peeters, B. P. & Gielkens, A. L. (1999). Efficient rescue of infectious bursal disease virus from cloned cDNA: evidence for involvement of the 3′-terminal sequence in genome replication. *Virology* **265**, 330-41.

Boot, H. J., ter Huurne, A. A., Vastenhouw, S. A., Kant, A., Peeters, B. P. & Gielkens, A. L. (2001). Rescue of infectious bursal disease virus from mosaic full-length clones composed of serotype I and II cDNA. *Arch Virol* **146**, 1991-2007.

Boyer, J. C. & Haenni, A. L. (1994). Infectious transcripts and cDNA clones of RNA viruses. *Virology* **198**, 415-26.

Bredenbeek, P. J., Kooi, E. A., Lindenbach, B., Huijkman, N., Rice, C. M. & Spaan, W. J. (2003). A stable full-length yellow fever virus cDNA clone and the role of conserved RNA elements in flavivirus replication. *J Gen Virol* **84**, 1261-8.

Brandenburg, B., Lee, L. Y., Lakadamyali, M., Rust, M. J., Zhuang, X. & Hogle, J. M. (2007). Imaging Poliovirus Entry in Live Cells. *PLoS Biol* **5**, e183.

Brown, B. A., Oberste, M. S., Alexander, J. P., Jr., Kennett, M. L. & Pallansch, M. A. (1999). Molecular epidemiology and evolution of enterovirus 71 strains isolated from 1970 to 1998. *J Virol* **73**, 9969-75.

Cardosa, M. J., Krishnan, S., Tio, P. H., Perera, D. & Wong, S. C. (1999). Isolation of subgenus B adenovirus during a fatal outbreak of enterovirus 71-associated hand, foot, and mouth disease in Sibu, Sarawak. *Lancet* **354**, 987-91.

Cardosa, M. J., Perera, D., Brown, B. A., Cheon, D., Chan, H. M., Chan, K. P., Cho, H. & McMinn, P. (2003). Molecular epidemiology of human enterovirus 71 strains and recent outbreaks in the Asia-Pacific region: comparative analysis of the VP1 and VP4 genes. *Emerg Infect Dis* **9**, 461-8.

Cello, J., Paul, A. V. & Wimmer, E. (2002). Chemical synthesis of poliovirus cDNA: generation of infectious virus in the absence of natural template. *Science* **297**, 1016-8.

Chan, Y.F. & AbuBakar, S. (2006). Phylogenetic evidence for inter-typic recombination in the emergence of human enterovirus 71 subgenotypes. *BMC Microbiol* **6**, 74-84.

Chan, L. G., Parashar, U. D., Lye, M. S., Ong, F. G., Zaki, S. R., Alexander, J. P., Ho, K. K., Han, L. L., Pallansch, M. A., Suleiman, A. B., Jegathesan, M. & Anderson, L. J. (2000). Deaths of children during an outbreak of hand, foot, and mouth disease in Sarawak, Malaysia: clinical and pathological characteristics of the disease. for the outbreak study group. *Clin Infect Dis* **31**, 678-83.

Chang, K. O., Sosnovtsev, S. S., Belliot, G., Wang, Q., Saif, L. J. & Green, K. Y. (2005). Reverse genetics system for porcine enteric calicivirus, a prototype sapovirus in the Caliciviridae. *J Virol* **79**, 1409-16.

Chang, L. Y., Huang, Y. C. & Lin, T. Y. (1998). Fulminant neurogenic pulmonary oedema with hand, foot, and mouth disease. *Lancet* **352**, 367-368.

Chang, L. Y., King, C. C., Hsu, K. H., Ning, H. C., Tsao, K. C., Li, C. C., Huang, Y. C., Shih, S. R., Chiou, S. T., Chen, P. Y., Chang, H. J. & Lin, T. Y. (2002). Risk factors of enterovirus 71 infection and associated hand, foot, and mouth disease/herpangina in children during an epidemic in Taiwan. *Pediatrics* **109**, e88.

Chen, C. S., Yao, Y. C., Lin, S. C., Lee, Y. P., Wang, Y. F., Wang, J. R., Liu, C. C., Lei, H. Y. & Yu, C. K. (2007). Retrograde axonal transport: a major transmission route of enterovirus 71 in mice. *J Virol* **81**, 8996-9003.

Chen, Y. C., Yu, C. K., Wang, Y. F., Liu, C. C., Su, I. J. & Lei, H. Y. (2004). A murine oral enterovirus 71 infection model with central nervous system involvement. *J Gen Virol* **85**, 69-77.

Cho, M. W., Teterina, N., Egger, D., Bienz, K. & Ehrenfeld, E. (1994). Membrane rearrangement and vesicle induction by recombinant poliovirus 2C and 2BC in human cells. *Virology* **202**, 129-45.

Chow, K. C., Lee, C. C., Lin, T. Y., Shen, W. C., Wang, J. H. & Peng, C. T. (2000). Congenital enterovirus 71 infection: a case study with virology and immunohistochemistry. *Clin Infect Dis* **31**, 509-12.

Christodoulou, C., Colbere-Garapin, F., Macadam, A., Taffs, L. F., Marsden, S., Minor, P. & Horaud, F. (1990). Mapping of mutations associated with

neurovirulence in monkeys infected with Sabin 1 poliovirus revertants selected at high temperature. *J Virol* **64**, 4922-9.

Chu, P. Y., Lin, K. H., Hwang, K. P., Chou, L. C., Wang, C. F., Shih, S. R., Wang, J. R., Shimada, Y. & Ishiko, H. (2001). Molecular epidemiology of enterovirus 71 in Taiwan. *Arch Virol* **146**, 589-600.

Chua, B. H. (2007). The molecular pathogenesis of human enteroviruses: construction of infectious cDNA clones of enteroviruses and development of a mouse model to study the pathogenesis of enterovirus 71. In *Discipline of Microbiology and Immunology*, pp. 260. Perth: The University of Western Australia.

Chua, B. H., Phuektes, P., Sanders, S. A., Nicholls, P. K. & McMinn, P. C. (2008). The molecular basis of mouse adaptation by human enterovirus 71. *J Gen Virol* **89**, 1622-32.

Chumakov, M., Voroshilova, M., Shindarov, L., Lavrova, I., Gracheva, L., Koroleva, G., Vasilenko, S., Brodvarova, I., Nikolova, M., Gyurova, S., Gacheva, M., Mitov, G., Ninov, N., Tsylka, E., Robinson, I., Frolova, M., Bashkirtsev, V., Martiyanova, L. & Rodin, V. (1979). Enterovirus 71 isolated from cases of epidemic poliomyelitis-like disease in Bulgaria. *Arch Virol* **60**, 329-40.

Chung, P. W., Huang, Y. C., Chang, L. Y., Lin, T. Y. & Ning, H. C. (2001). Duration of enterovirus shedding in stool. *J Microbiol Immunol Infect* **34**, 167-70.

Clark, M. E., Lieberman, P. M., Berk, A. J. & Dasgupta, A. (1993). Direct cleavage of human TATA-binding protein by poliovirus protease 3C in vivo and in vitro. *Mol Cell Biol* **13**, 1232-7.

Colston, E. M. & Racaniello, V. R. (1995). Poliovirus variants selected on mutant receptor-expressing cells identify capsid residues that expand receptor recognition. *J Virol* **69**, 4823-9.

Couderc, T., Delpeyroux, F., Le Blay, H. & Blondel, B. (1996). Mouse adaptation determinants of poliovirus type 1 enhance viral uncoating. *J Virol* **70**, 305-12.

Couderc, T., Guedo, N., Calvez, V., Pelletier, I., Hogle, J., Colbere-Garapin, F. & Blondel, B. (1994). Substitutions in the capsids of poliovirus mutants selected in human neuroblastoma cells confer on the Mahoney type 1 strain a phenotype neurovirulent in mice. *J Virol* **68**, 8386-91.

Couderc, T., Hogle, J., Le Blay, H., Horaud, F. & Blondel, B. (1993). Molecular characterization of mouse-virulent poliovirus type 1 Mahoney mutants: involvement of residues of polypeptides VP1 and VP2 located on the inner surface of the capsid protein shell. *J Virol* **67**, 3808-17.

Coyne, C. B., Kim, K. S. & Bergelson, J. M. (2007). Poliovirus entry into human brain microvascular cells requires receptor-induced activation of SHP-2. *EMBO J* **26**, 4016-28.

Daley, A. J. & Dwyer, D. E. (2002). Emerging viral infections in Australia. *J Paediatr Child Health* **38**, 1-3.

Dan, M. & Chantler, J. K. (2005). A genetically engineered attenuated coxsackievirus B3 strain protects mice against lethal infection. *J Virol* **79**, 9285-95.

De Sena, J. & Mandel, B. (1977). Studies on the in vitro uncoating of poliovirus. II. Characteristics of the membrane-modified particle. *Virology* **78**, 554-66.

Detjen, B. M., Lucas, J. & Wimmer, E. (1978). Poliovirus single-stranded RNA and double-stranded RNA: differential infectivity in enucleate cells. *J Virol* **27**, 582-6.

DeTulleo, L. & Kirchhausen, T. (1998). The clathrin endocytic pathway in viral infection. *EMBO J* **17**, 4585-93.

Doedens, J. R. & Kirkegaard, K. (1995). Inhibition of cellular protein secretion by poliovirus proteins 2B and 3A. *EMBO J* **14**, 894-907.

Domingo, E. & Holland, J. J. (1997). RNA virus mutations and fitness for survival. *Annu Rev Microbiol* **51**, 151-78.

Domingo, E., Menendez-Arias, L. & Holland, J. J. (1997). RNA virus fitness. *Rev Med Virol* **7**, 87-96.

Duechler, M., Skern, T., Blaas, D., Berger, B., Sommergruber, W. & Kuechler, E. (1989). Human rhinovirus serotype 2: in vitro synthesis of an infectious RNA. *Virology* **168**, 159-61.

Ehrenfeld, E. & Teterina, N. L. (2002). Initiation of Translation of Picornavirus RNAs: Structure and Function of the Internal Ribosome Entry Site. In *Molecular Biology of Picornaviruses*, pp. 159-169. Edited by B. L. Semler & E. Wimmer. Washington, DC: ASM Press.

Elwood, J. M. (1988). Causal relationships in medicine: A practical system for critical appraisal. New York: Oxford University Press.

Evans, D. J. & Almond, J. W. (1998). Cell receptors for picornaviruses as determinants of cell tropism and pathogenesis. *Trends Microbiol* **6**, 198-202.

Evans, D. M., Dunn, G., Minor, P. D., Schild, G. C., Cann, A. J., Stanway, G., Almond, J. W., Currey, K. & Maizel, J. V., Jr. (1985). Increased neurovirulence associated with a single nucleotide change in a noncoding region of the Sabin type 3 poliovaccine genome. *Nature* **314**, 548-50.

Fauquet, C. M., Mayo, M. A., Maniloff, J., Desselberger, U. & Ball, L. A. (2005). Virus Taxonomy: VIIIth Report of the International Committee on Taxonomy of Viruses, 2nd edn, pp. 1162. New York, USA: Academic Press.

Fenwick, M. L. & Cooper, P. D. (1962). Early interactions between poliovirus and ERK cells: some observations on the nature and significance of the rejected particles. *Virology* **18**, 212-23.

Flanegan, J. B. & Baltimore, D. (1977). Poliovirus-specific primer-dependent RNA polymerase able to copy poly(A). *Proc Natl Acad Sci U S A* **74**, 3677-80.

Flanegan, J. B., Petterson, R. F., Ambros, V., Hewlett, N. J. & Baltimore, D. (1977). Covalent linkage of a protein to a defined nucleotide sequence at the 5′-terminus of virion and replicative intermediate RNAs of poliovirus. *Proc Natl Acad Sci U S A* **74**, 961-5.

Flint, S. J., Enquist, L. W., Racaniello, V. R. & Skalka, A. M. (2004). Principles of virology: molecular biology, pathogenesis and control of animal viruses, second edn, pp. 887. Washington, D.C.: ASM Press.

Fogg, M. H., Teterina, N. L. & Ehrenfeld, E. (2003). Membrane requirements for uridylylation of the poliovirus VPg protein and viral RNA synthesis in vitro. *J Virol* **77**, 11408-16.

Franco, D., Pathak, H. B., Cameron, C. E., Rombaut, B., Wimmer, E. & Paul, A. V. (2005). Stimulation of poliovirus synthesis in a HeLa cell-free in vitro translation-RNA replication system by viral protein 3CDpro. *J Virol* **79**, 6358-67.

Fricks, C. E. & Hogle, J. M. (1990). Cell-induced conformational change in poliovirus: externalization of the amino terminus of VP1 is responsible for liposome binding. *J Virol* **64**, 1934-45.

Fujimoto, T., Chikahira, M., Yoshida, S., Ebira, H., Hasegawa, A., Totsuka, A. & Nishio, O. (2002). Outbreak of central nervous system disease associated with hand, foot, and mouth disease in Japan during the summer of 2000: detection and molecular epidemiology of enterovirus 71. *Microbiol Immunol* **46**, 621-7.

Gamarnik, A. V. & Andino, R. (1997). Two functional complexes formed by KH domain containing proteins with the 5′ noncoding region of poliovirus RNA. *RNA* **3**, 882-92.

Gilbert, G. L., Dickson, K. E., Waters, M. J., Kennett, M. L., Land, S. A. & Sneddon, M. (1988). Outbreak of enterovirus 71 infection in Victoria, Australia, with a high incidence of neurologic involvement. *Pediatr Infect Dis J* **7**, 484-8.

Goldstaub, D., Gradi, A., Bercovitch, Z., Grosmann, Z., Nophar, Y., Luria, S., Sonenberg, N. & Kahana, C. (2000). Poliovirus 2A protease induces apoptotic cell death. *Mol Cell Biol* **20**, 1271-7.

Gomez Yafal, A., Kaplan, G., Racaniello, V. R. & Hogle, J. M. (1993). Characterization of poliovirus conformational alteration mediated by soluble cell receptors. *Virology* **197**, 501-5.

Gonzalez, J. M., Penzes, Z., Almazan, F., Calvo, E. & Enjuanes, L. (2002). Stabilization of a full-length infectious cDNA clone of transmissible gastroenteritis coronavirus by insertion of an intron. *J Virol* **76**, 4655-61.

Goodfellow, I., Chaudhry, Y., Richardson, A., Meredith, J., Almond, J. W., Barclay, W. & Evans, D. J. (2000). Identification of a cis-acting replication element within the poliovirus coding region. *J Virol* **74**, 4590-600.

Goodfellow, I. G., Polacek, C., Andino, R. & Evans, D. J. (2003). The poliovirus 2C cis-acting replication element-mediated uridylylation of VPg is not required for synthesis of negative-sense genomes. *J Gen Virol* **84**, 2359-63.

Gradi, A., Svitkin, Y. V., Imataka, H. & Sonenberg, N. (1998). Proteolysis of human eukaryotic translation initiation factor eIF4GII, but not eIF4GI, coincides with the shutoff of host protein synthesis after poliovirus infection. *Proc Natl Acad Sci U S A* **95**, 11089-94.

Griffin, D. E., Mullinix, J., Narayan, O. & Johnson, R. T. (1974). Age dependence of viral expression: comparative pathogenesis of two rodent-adapted strains of measles virus in mice. *Infect Immun* **9**, 690-5.

Gritsun, T. S. & Gould, E. A. (1995). Infectious transcripts of tick-borne encephalitis virus, generated in days by RT-PCR. *Virology* **214**, 611-8.

Gromeier, M., Alexander, L. & Wimmer, E. (1996). Internal ribosomal entry site substitution eliminates neurovirulence in intergeneric poliovirus recombinants. *Proc Natl Acad Sci U S A* **93**, 2370-5.

Gromeier, M., Bossert, B., Arita, M., Nomoto, A. & Wimmer, E. (1999). Dual stem loops within the poliovirus internal ribosomal entry site control neurovirulence. *J Virol* **73**, 958-64.

Haller, A. A., Stewart, S. R. & Semler, B. L. (1996). Attenuation stem-loop lesions in the 5′ noncoding region of poliovirus RNA: neuronal cell-specific translation defects. *J Virol* **70**, 1467-74.

Hamaguchi, T., Fujisawa, H., Sakai, K., Okino, S., Kurosaki, N., Nishimura, Y., Shimizu, H. & Yamada, M. (2008). Acute encephalitis caused by intrafamilial transmission of enterovirus 71 in adult. *Emerg Infect Dis* **14**, 828-30.

Harris, K. S., Hellen, C. U. & Wimmer, E. (1990). Proteolytic processing in the replication of picornaviruses. *Semin Virol* **1**, 323-333.

Harvala, H., Kalimo, H., Dahllund, L., Santti, J., Hughes, P., Hyypia, T. & Stanway, G. (2002). Mapping of tissue tropism determinants in Coxsackievirus genomes. *J Gen Virol* **83**, 1697-706.

Hashimoto, I. & Hagiwara, A. (1982a). Pathogenicity of a poliomyelitis-like disease in monkeys infected orally with enterovirus 71: a model for human infection. *Neuropathol Appl Neurobiol* **8**, 149-56.

Hashimoto, I. & Hagiwara, A. (1982b). Studies on the pathogenesis of and propagation of enterovirus 71 in Poliomyelitis-like disease in monkeys. *Acta Neuropathol* **58**, 125-32.

Hashimoto, I., Hagiwara, A. & Kodama, H. (1978). Neurovirulence in cynomolgus monkeys of enterovirus 71 isolated from a patient with hand, foot and mouth disease. *Arch Virol* **56**, 257-61.

Hayward, J. C., Gillespie, S. M., Kaplan, K. M., Packer, R., Pallansch, M., Plotkin, S. & Schonberger, L. B. (1989). Outbreak of poliomyelitis-like paralysis associated with enterovirus 71. *Pediatr Infect Dis J* **8**, 611-6.

He, Y., Bowman, V. D., Mueller, S., Bator, C. M., Bella, J., Peng, X., Baker, T. S., Wimmer, E., Kuhn, R. J. & Rossmann, M. G. (2000). Interaction of the poliovirus receptor with poliovirus. *Proc Natl Acad Sci U S A* **97**, 79-84.

Herold, J. & Andino, R. (2001). Poliovirus RNA replication requires genome circularization through a protein-protein bridge. *Mol Cell* **7**, 581-91.

Herrero, L. J. (2007). Cell attachment and entry of human group A enteroviruses. In *Discipline of Microbiology and Immunology*, pp. 234. Perth: University of Western Australia.

Herrero, L. J., Lee, C. S., Hurrelbrink, R. J., Chua, B. H., Chua, K. B. & McMinn, P. C. (2003). Molecular epidemiology of enterovirus 71 in peninsular Malaysia, 1997-2000. *Arch Virol* **148**, 1369-85.

Hirsch, M. S., Zisman, B. & Allison, A. C. (1970). Macrophages and age-dependent resistance to Herpes simplex virus in mice. *J Immunol* **104**, 1160-5.

Ho, M. (2000). Enterovirus 71: the virus, its infections and outbreaks. *J Microbiol Immunol Infect* **33**, 205-16.

Hogle, J. M. (2002). Poliovirus cell entry: common structural themes in viral cell entry pathways. *Annu Rev Microbiol* **56**, 677-702.

Hogle, J. M., Chow, M. & Filman, D. J. (1985). Three-dimensional structure of poliovirus at 2.9 A resolution. *Science* **229**, 1358-65.

Hosoya, M., Kawasaki, Y., Sato, M., Honzumi, K., Kato, A., Hiroshima, T., Ishiko, H. & Suzuki, H. (2006). Genetic diversity of enterovirus 71 associated with hand, foot and mouth disease epidemics in Japan from 1983 to 2003. *Pediatr Infect Dis J* **25**, 691-4.

Huang, C. C., Liu, C. C., Chang, Y. C., Chen, C. Y., Wang, S. T. & Yeh, T. F. (1999). Neurologic complications in children with enterovirus 71 infection. *N Engl J Med* **341**, 936-42.

Huang, S. C., Hsu, Y. W., Wang, H. C., Huang, S. W., Kiang, D., Tsai, H. P., Wang, S. M., Liu, C. C., Lin, K. H., Su, I. J. & Wang, J. R. (2008). Appearance of intratypic recombination of enterovirus 71 in Taiwan from 2002 to 2005. *Virus Res* **131**, 250-9.

Hurrelbrink, R. J., Nestorowicz, A. & McMinn, P. C. (1999). Characterization of infectious Murray Valley encephalitis virus derived from a stably cloned genome-length cDNA. *J Gen Virol* **80**, 3115-25.

Hyypia, T., Hovi, T., Knowles, N. J. & Stanway, G. (1997). Classification of enteroviruses based on molecular and biological properties. *J Gen Virol* **78**, 1-11.

Jacobson, M. F. & Baltimore, D. (1968). Morphogenesis of poliovirus. I. Association of the viral RNA with coat protein. *J Mol Biol* **33**, 369-78.

Janda, M., French, R. & Ahlquist, P. (1987). High efficiency T7 polymerase synthesis of infectious RNA from cloned brome mosaic virus cdna and effects of 5′ extensions on transcript infectivity. *Virology* **158**, 259-62.

Jee, Y. M., Cheon, D. S., Kim, K., Cho, J. H., Chung, Y. S., Lee, J., Lee, S. H., Park, K. S., Lee, J. H., Kim, E. C., Chung, H. J., Kim, D. S., Yoon, J. D. & Cho, H. W. (2003). Genetic analysis of the VP1 region of human enterovirus 71 strains isolated in Korea during 2000. *Arch Virol* **148**, 1735-46.

Jia, Q., Hogle, J. M., Hashikawa, T. & Nomoto, A. (2001). Molecular genetic analysis of revertants from a poliovirus mutant that is specifically adapted to the mouse spinal cord. *J Virol* **75**, 11766-72.

Johnson, K. L. & Sarnow, P. (1991). Three poliovirus 2B mutants exhibit noncomplementable defects in viral RNA amplification and display dosage-dependent dominance over wild-type poliovirus. *J Virol* **65**, 4341-9.

Johnson, R. T. (1964). The Pathogenesis of Herpes Virus Encephalitis. I. Virus Pathways to the Nervous System of Suckling Mice Demonstrated by Fluorescent Antibody Staining. *J Exp Med* **119**, 343-56.

Kandolf, R. & Hofschneider, P. H. (1985). Molecular cloning of the genome of a cardiotropic Coxsackie B3 virus: full-length reverse-transcribed recombinant cDNA generates infectious virus in mammalian cells. *Proc Natl Acad Sci U S A* **82**, 4818-22.

Kaplan, G., Lubinski, J., Dasgupta, A. & Racaniello, V. R. (1985). In vitro synthesis of infectious poliovirus RNA. *Proc Natl Acad Sci U S A* **82**, 8424-8.

Kapoor, M., Zhang, L., Mohan, P. M. & Padmanabhan, R. (1995). Synthesis and characterization of an infectious dengue virus type-2 RNA genome (New Guinea C strain). *Gene* **162**, 175-80.

Kauder, S. E. & Racaniello, V. R. (2004). Poliovirus tropism and attenuation are determined after internal ribosome entry. *J Clin Invest* **113**, 1743-53.

Kawamura, N., Kohara, M., Abe, S., Komatsu, T., Tago, K., Arita, M. & Nomoto, A. (1989). Determinants in the 5′ noncoding region of poliovirus Sabin 1 RNA that influence the attenuation phenotype. *J Virol* **63**, 1302-9.

Kennett, M. L., Birch, C. J., Lewis, F. A., Yung, A. P., Locarnini, S. A. & Gust, I. D. (1974). Enterovirus type 71 infection in Melbourne. *Bull World Health Organ* **51**, 609-15.

Khromykh, A. A. & Westaway, E. G. (1994). Completion of Kunjin virus RNA sequence and recovery of an infectious RNA transcribed from stably cloned full-length cDNA. *J Virol* **68**, 4580-8.

Klump, W. M., Bergmann, I., Muller, B. C., Ameis, D. & Kandolf, R. (1990). Complete nucleotide sequence of infectious Coxsackievirus B3 cDNA: two initial 5′ uridine residues are regained during plus-strand RNA synthesis. *J Virol* **64**, 1573-83.

Koike, S., Taya, C., Aoki, J., Matsuda, Y., Ise, I., Takeda, H., Matsuzaki, T., Amanuma, H., Yonekawa, H. & Nomoto, A. (1994). Characterization of three different transgenic mouse lines that carry human poliovirus receptor gene-influence of the transgene expression on pathogenesis. *Arch Virol* **139**, 351-63.

Koike, S., Taya, C., Kurata, T., Abe, S., Ise, I., Yonekawa, H. & Nomoto, A. (1991). Transgenic mice susceptible to poliovirus. *Proc Natl Acad Sci U S A* **88**, 951-5.

Komatsu, H., Shimizu, Y., Takeuchi, Y., Ishiko, H. & Takada, H. (1999). Outbreak of severe neurologic involvement associated with Enterovirus 71 infection. *Pediatr Neurol* **20**, 17-23.

Kraus, W., Zimmermann, H., Zimmermann, A., Eggers, H. J. & Nelsen-Salz, B. (1995). Infectious cDNA clones of echovirus 12 and a variant resistant against the uncoating inhibitor rhodanine differ in seven amino acids. *J Virol* **69**, 5853-8.

Kung, C. M., King, C. C., Lee, C. N., Huang, L. M., Lee, P. I. & Kao, C. L. (2007). Differences in replication capacity between enterovirus 71 isolates obtained from patients with encephalitis and those obtained from patients with herpangina in Taiwan. *J Med Virol* **79**, 60-8.

Kuo, R. L., Kung, S. H., Hsu, Y. Y. & Liu, W. T. (2002). Infection with enterovirus 71 or expression of its 2A protease induces apoptotic cell death. *J Gen Virol* **83**, 1367-76.

Kuss, S. K., Etheredge, C. A. & Pfeiffer, J. K. (2008). Multiple host barriers restrict poliovirus trafficking in mice. *PLoS Pathog* **4**, e1000082.

Kuyumcu-Martinez, N. M., Joachims, M. & Lloyd, R. E. (2002). Efficient cleavage of ribosome-associated poly(A)-binding protein by enterovirus 3C protease. *J Virol* **76**, 2062-74.

La Monica, N. & Racaniello, V. R. (1989). Differences in replication of attenuated and neurovirulent polioviruses in human neuroblastoma cell line SH-SY5Y. *J Virol* **63**, 2357-60.

Lai, C. J., Zhao, B. T., Hori, H. & Bray, M. (1991). Infectious RNA transcribed from stably cloned full-length cDNA of dengue type 4 virus. *Proc Natl Acad Sci U S A* **88**, 5139-43.

Lambert, C., Leonard, N., De Bolle, X. & Depiereux, E. (2002). ESyPred3D: Prediction of proteins 3D structures. *Bioinformatics* **18**, 1250-6.

Lawson, M. A. & Semler, B. L. (1991). Poliovirus thiol proteinase 3C can utilize a serine nucleophile within the putative catalytic triad. *Proc Natl Acad Sci U S A* **88**, 9919-23.

Le, S. Y., Siddiqui, A. & Maizel, J. V., Jr. (1996). A common structural core in the internal ribosome entry sites of picornavirus, hepatitis C virus, and pestivirus. *Virus Genes* **12**, 135-47.

Li, J. P. & Baltimore, D. (1990). An intragenic revertant of a poliovirus 2C mutant has an uncoating defect. *J Virol* **64**, 1102-7.

Li, M. L., Hsu, T. A., Chen, T. C., Chang, S. C., Lee, J. C., Chen, C. C., Stollar, V. & Shih, S. R. (2002). The 3C protease activity of enterovirus 71 induces human neural cell apoptosis. *Virology* **293**, 386-95.

Liebig, H. D., Seipelt, J., Vassilieva, E., Gradi, A. & Kuechler, E. (2002). A thermosensitive mutant of HRV2 2A proteinase: evidence for direct cleavage of eIF4GI and eIF4GII. *FEBS Lett* **523**, 53-7.

Lin, K. H., Hwang, K. P., Ke, G. M., Wang, C. F., Ke, L. Y., Hsu, Y. T., Tung, Y. C., Chu, P. Y., Chen, B. H., Chen, H. L., Kao, C. L., Wang, J. R., Eng, H. L., Wang, S. Y., Hsu, L. C. & Chen, H. Y. (2006). Evolution of EV71 genogroup in Taiwan from 1998 to 2005: an emerging of subgenogroup C4 of EV71. *J Med Virol* **78**, 254-62.

Liu, M. L., Lee, Y. P., Wang, Y. F., Lei, H. Y., Liu, C. C., Wang, S. M., Su, I. J., Wang, J. R., Yeh, T. M., Chen, S. H. & Yu, C. K. (2005). Type I interferons protect mice against enterovirus 71 infection. *J Gen Virol* **86**, 3263-9.

Lopez de Quinto, S. & Martinez-Salas, E. (1997). Conserved structural motifs located in distal loops of aphthovirus internal ribosome entry site domain 3 are required for internal initiation of translation. *J Virol* **71**, 4171-5.

Lum, L. C., Chua, K. B., McMinn, P. C., Goh, A. Y., Muridan, R., Sarji, S. A., Hooi, P. S., Chua, B. H. & Lam, S. K. (2002). Echovirus 7 associated encephalomyelitis. *J Clin Virol* **23**, 153-60.

Lum, L. C., Wong, K. T., Lam, S. K., Chua, K. B., Goh, A. Y., Lim, W. L., Ong, B. B., Paul, G., AbuBakar, S. & Lambert, M. (1998). Fatal enterovirus 71 encephalomyelitis. *J Pediatr* **133**, 795-8.

Lyle, J. M., Clewell, A., Richmond, K., Richards, O. C., Hope, D. A., Schultz, S. C. & Kirkegaard, K. (2002). Similar structural basis for membrane localization and protein priming by an RNA-dependent RNA polymerase. *J Biol Chem* **277**, 16324-31.

Macadam, A. J., Ferguson, G., Burlison, D., Stone, D. M., Skuce, R., Almond, J. W. & Minor, P. D. (1992). Correlation of RNA secondary structure and attenuation of Sabin vaccine strains of poliovirus in tissue culture. *Virology* **189**, 415-422.

Macadam, A. J., Pollard, S. R., Ferguson, G., Dunn, G., Skuce, R., Almond, J. W. & Minor, P. D. (1991). The 5′ noncoding region of the type 2 poliovirus vaccine strain contains determinants of attenuation and temperature sensitivity. *Virology* **181**, 451-8.

Madshus, I. H., Olsnes, S. & Sandvig, K. (1984). Requirements for entry of poliovirus RNA into cells at low pH. *EMBO J* **3**, 1945-50.

Mandl, C. W., Ecker, M., Holzmann, H., Kunz, C. & Heinz, F. X. (1997). Infectious cDNA clones of tick-borne encephalitis virus European subtype prototypic strain Neudoerfl and high virulence strain Hypr. *J Gen Virol* **78**, 1049-57.

Martin, A., Benichou, D., Couderc, T., Hogle, J. M., Wychowski, C., Van der Werf, S. & Girard, M. (1991). Use of type 1/type 2 chimeric polioviruses to study determinants of poliovirus type 1 neurovirulence in a mouse model. *Virology* **180**, 648-58.

Martin, A., Wychowski, C., Couderc, T., Crainic, R., Hogle, J. & Girard, M. (1988). Engineering a poliovirus type 2 antigenic site on a type 1 capsid results in a chimaeric virus which is neurovirulent for mice. *EMBO J* **7**, 2839-47.

Martino, T. A., Tellier, R., Petric, M., Irwin, D. M., Afshar, A. & Liu, P. P. (1999). The complete consensus sequence of coxsackievirus B6 and generation of infectious clones by long RT-PCR. *Virus Res* **64**, 77-86.

Masters, P. S. (1999). Reverse genetics of the largest RNA viruses. *Adv Virus Res* **53**, 245-64.

Mathews, D. H., Sabina, J., Zuker, M. & Turner, D. H. (1999). Expanded sequence dependence of thermodynamic parameters improves prediction of RNA secondary structure. *J Mol Biol* **288**, 911-40.

McKnight, K. L. & Lemon, S. M. (1998). The rhinovirus type 14 genome contains an internally located RNA structure that is required for viral replication. *Rna* **4**, 1569-84.

McMinn, P., Lindsay, K., Perera, D., Chan, H. M., Chan, K. P. & Cardosa, M. J. (2001a). Phylogenetic analysis of enterovirus 71 strains isolated during linked epidemics in Malaysia, Singapore, and Western Australia. *J Virol* **75**, 7732-8.

McMinn, P., Stratov, I., Nagarajan, L. & Davis, S. (2001b). Neurological manifestations of enterovirus 71 infection in children during an outbreak of hand, foot, and mouth disease in Western Australia. *Clin Infect Dis* **32**, 236-42.

McMinn, P. C. (2002). An overview of the evolution of enterovirus 71 and its clinical and public health significance. *FEMS Microbiology Reviews* **26**, 91-107.

Melnick, J. L. (1984). Enterovirus type 71 infections: a varied clinical pattern sometimes mimicking paralytic poliomyelitis. *Rev Infect Dis* **6 Suppl 2**, S387-90.

Melnick, J. L., Tagaya, I. & von Magnus, H. (1974). Enteroviruses 69, 70, and 71. *Intervirology* **4**, 369-70.

Mendelsohn, C. L., Wimmer, E. & Racaniello, V. R. (1989). Cellular receptor for poliovirus: molecular cloning, nucleotide sequence, and expression of a new member of the immunoglobulin superfamily. *Cell* **56**, 855-65.

Merovitz, L., Demers, A. M., Newby, D. & McDonald, J. (2000). Enterovirus 71 infections at a Canadian center. *Pediatr Infect Dis J* **19**, 755-7.

Mishin, V. P., Cominelli, F. & Yamshchikov, V. F. (2001). A 'minimal' approach in design of flavivirus infectious DNA. *Virus Res* **81**, 113-23.

Molla, A., Harris, K. S., Paul, A. V., Shin, S. H., Mugavero, J. & Wimmer, E. (1994). Stimulation of poliovirus proteinase 3Cpro-related proteolysis by the genome-linked protein VPg and its precursor 3AB. *J Biol Chem* **269**, 27015-20.

Morrison, L. A., Sidman, R. L. & Fields, B. N. (1991). Direct spread of reovirus from the intestinal lumen to the central nervous system through vagal autonomic nerve fibers. *Proc Natl Acad Sci U S A* **88**, 3852-6.

Moss, E. G. & Racaniello, V. R. (1991). Host range determinants located on the interior of the poliovirus capsid. *EMBO J* **10**, 1067-74.

Murray, K. E. & Barton, D. J. (2003). Poliovirus CRE-dependent VPg uridylylation is required for positive-strand RNA synthesis but not for negative-strand RNA synthesis. *J Virol* **77**, 4739-50.

Nagata, N., Iwasaki, T., Ami, Y., Tano, Y., Harashima, A., Suzaki, Y., Sato, Y., Hasegawa, H., Sata, T., Miyamura, T. & Shimizu, H. (2004). Differential localization of neurons susceptible to enterovirus 71 and poliovirus type 1 in the central nervous system of cynomolgus monkeys after intravenous inoculation. *J Gen Virol* **85**, 2981-9.

Nagata, N., Shimizu, H., Ami, Y., Tano, Y., Harashima, A., Suzaki, Y., Sato, Y., Miyamura, T., Sata, T. & Iwasaki, T. (2002). Pyramidal and extrapyramidal involvement in experimental infection of cynomolgus monkeys with enterovirus 71. *J Med Virol* **67**, 207-16.

Nagy, G., Takatsy, S., Kukan, E., Mihaly, I. & Domok, I. (1982). Virological diagnosis of enterovirus type 71 infections: experiences gained during an epidemic of acute CNS diseases in Hungary in 1978. *Arch Virol* **71**, 217-27.

Nathanson, N. & Bodian, D. (1961). Experimental poliomyelitis following intramuscular virus injection. I. The effect of neural block on a neurotropic and a pantropic strain. *Bull Johns Hopkins Hosp* **108**, 308-19.

Nathanson, N. & Langmuir, A. D. (1995). The Cutter incident. Poliomyelitis following formaldehyde-inactivated poliovirus vaccination in the United States during the Spring of 1955. II. Relationship of poliomyelitis to Cutter vaccine. 1963. *Am J Epidemiol* **142**, 109-40; discussion 107-8.

Neznanov, N., Kondratova, A., Chumakov, K. M., Angres, B., Zhumabayeva, B., Agol, V. I. & Gudkov, A. V. (2001). Poliovirus protein 3A inhibits tumor necrosis factor (TNF)-induced apoptosis by eliminating the TNF receptor from the cell surface. *J Virol* **75**, 10409-20.

Norder, H., Bjerregaard, L., Magnius, L., Lina, B., Aymard, M. & Chomel, J. J. (2003). Sequencing of 'untypable' enteroviruses reveals two new types, EV-77 and EV-78, within human enterovirus type B and substitutions in the BC loop of the VP1 protein for known types. *J Gen Virol* **84**, 827-36.

Nugent, C. I. & Kirkegaard, K. (1995). RNA binding properties of poliovirus subviral particles. *J Virol* **69**, 13-22.

Oberste, M. S., Maher, K., Kilpatrick, D. R. & Pallansch, M. A. (1999). Molecular evolution of the human enteroviruses: correlation of serotype with VP1 sequence and application to picornavirus classification. *J Virol* **73**, 1941-8.

Oberste, M. S., Maher, K., Kilpatrick, D. R. & Pallansch, M. A. (1999). Molecular evolution of the human enteroviruses: correlation of serotype with VP1 sequence and application to picornavirus classification. *J Virol* **73**, 1941-8.

Oberste, M. S., Penaranda, S. & Pallansch, M. A. (2004). Complete genome sequences of all members of the species Human enterovirus A. *J Gen Virol* **85**, 1597-1607.

Oberste, M. S., Maher, K., Nix, W. A., Michele, S. M., Uddin, M., Schnurr, D., al-Busaidy, S., Akoua-Koffi, C. & Pallansch, M. A. (2007). Molecular identification of 13 new enterovirus types, EV79-88, EV97, and EV100-101, members of the species Human Enterovirus B. *Virus Res* **128**, 34-42.

Oberste, M. S., Schnurr, D., Maher, K., Al-Busaidy, S. & Pallansch, M. (2001). Molecular identification of new picornaviruses and characterisation of a proposed enterovirus 73 serotype. *J Gen Virol* **82**, 409-16

Ohka, S. & Nomoto, A. (2001). The molecular basis of poliovirus neurovirulence. *Dev Biol (Basel)* **105**, 51-8.

Ohka, S., Yang, W. X., Terada, E., Iwasaki, K. & Nomoto, A. (1998). Retrograde transport of intact poliovirus through the axon via the fast transport system. *Virology* **250**, 67-75.

Ong, K. C., Badmanathan, M., Devi, S., Leong, K. L., Cardosa, M. J. & Wong, K. T. (2008). Pathologic characterization of a murine model of human enterovirus 71 encephalomyelitis. *J Neuropathol Exp Neurol* **67**, 532-42.

Palacios, G. & Oberste, M. S. (2005). Enteroviruses as agents of emerging infectious diseases. *J Neurovirol* **11**, 424-33.

Pallansch, M. A. & Roos, R. P. (2007). Enteroviruses: Polioviruses, Coxsackieviruses, Echoviruses, and Newer Enteroviruses. In *Fields Virology*, 5th edn, pp. 839-892. Edited by D. M. Knipe, P. M. Howley, D. E. Griffin, R. A. Lamb, M. A. Martin, B. Roizman & S. E. Straus: Lippincott Williams & Wilkins.

Parsley, T. B., Towner, J. S., Blyn, L. B., Ehrenfeld, E. & Semler, B. L. (1997). Poly (rC) binding protein 2 forms a ternary complex with the 5′-terminal sequences of poliovirus RNA and the viral 3CD proteinase. *RNA* **3**, 1124-34.

Paul, A. V. (2002). Possible unifying mechanism of picornavirus genome replication. In *Molecular Biology of Picornaviruses*. Edited by B. L. Semler & E. Wimmer. Washington, DC: ASM Press.

Paul, A. V., Cao, X., Harris, K. S., Lama, J. & Wimmer, E. (1994). Studies with poliovirus polymerase 3Dpol. Stimulation of poly(U) synthesis in vitro by purified poliovirus protein 3AB. *J Biol Chem* **269**, 29173-81.

Paul, A. V., Peters, J., Mugavero, J., Yin, J., van Boom, J. H. & Wimmer, E. (2003). Biochemical and genetic studies of the VPg uridylylation reaction catalyzed by the RNA polymerase of poliovirus. *J Virol* **77**, 891-904.

Paul, A. V., Rieder, E., Kim, D. W., van Boom, J. H. & Wimmer, E. (2000). Identification of an RNA hairpin in poliovirus RNA that serves as the primary template in the in vitro uridylylation of VPg. *J Virol* **74**, 10359-70.

Paul, A. V., van Boom, J. H., Filippov, D. & Wimmer, E. (1998). Protein-primed RNA synthesis by purified poliovirus RNA polymerase. *Nature* **393**, 280-4.

Perez, L. & Carrasco, L. (1993). Entry of poliovirus into cells does not require a low-pH step. *J Virol* **67**, 4543-8.

Pettersson, R. F., Ambros, V. & Baltimore, D. (1978). Identification of a protein linked to nascent poliovirus RNA and to the polyuridylic acid of negative-strand RNA. *J Virol* **27**, 357-65.

Pfister, T. & Wimmer, E. (1999). Characterization of the nucleoside triphosphatase activity of poliovirus protein 2C reveals a mechanism by which guanidine inhibits poliovirus replication. *J Biol Chem* **274**, 6992-7001.

Pilipenko, E. V., Blinov, V. M., Romanova, L. I., Sinyakov, A. N., Maslova, S. V. & Agol, V. I. (1989). Conserved structural domains in the 5′-untranslated region of picornaviral genomes: an analysis of the segment controlling translation and neurovirulence. *Virology* **168**, 201-9.

Pilipenko, E. V., Gmyl, A. P., Maslova, S. V., Svitkin, Y. V., Sinyakov, A. N. & Agol, V. I. (1992a). Prokaryotic-like cis elements in the cap-independent internal initiation of translation on picornavirus RNA. *Cell* **68**, 119-31.

Pilipenko, E. V., Maslova, S. V., Sinyakov, A. N. & Agol, V. I. (1992b). Towards identification of cis-acting elements involved in the replication of enterovirus and rhinovirus RNAs: a proposal for the existence of tRNA-like terminal structures. *Nucleic Acids Res* **20**, 1739-45.

Pilipenko, E. V., Poperechny, K. V., Maslova, S. V., Melchers, W. J., Slot, H. J. & Agol, V. I. (1996). Cis-element, oriR, involved in the initiation of (-) strand poliovirus RNA: a quasi-globular multi-domain RNA structure maintained by tertiary ('kissing') interactions. *EMBO J* **15**, 5428-36.

Plotch, S. J. & Palant, O. (1995). Poliovirus protein 3AB forms a complex with and stimulates the activity of the viral RNA polymerase, 3Dpol. *J Virol* **69**, 7169-79.

Podin, Y., Gias, E. L., Ong, F., Leong, Y. W., Yee, S. F., Yusof, M. A., Perera, D., Teo, B., Wee, T. Y., Yao, S. C., Yao, S. K., Kiyu, A., Arif, M. T. & Cardosa, M. J. (2006). Sentinel surveillance for human enterovirus 71 in Sarawak, Malaysia: lessons from the first 7 years. *BMC Public Health* **6**, 180.

Polo, S., Ketner, G., Levis, R. & Falgout, B. (1997). Infectious RNA transcripts from full-length dengue virus type 2 cDNA clones made in yeast. *J Virol* **71**, 5366-74.

Racaniello, V. R. (2007). *Picornaviridae*: The Viruses and Their Replication. In *Fields Virology*, 5th edn, pp. 795-838. Edited by D. M. Knipe, P. M. Howley, D. E. Griffin, R. A. Lamb, M. A. Martin, B. Roizman & S. E. Straus: Lippincott Williams & Wilkins.

Racaniello, V. R. & Baltimore, D. (1981). Cloned poliovirus complementary DNA is infectious in mammalian cells. *Science* **214**, 916-9.

Raleigh, E. A., Murray, N. E., Revel, H., Blumenthal, R. M., Westaway, D., Reith, A. D., Rigby, P. W., Elhai, J. & Hanahan, D. (1988). McrA and McrB restriction phenotypes of some *E. coli* strains and implications for gene cloning. *Nucleic Acids Res* **16**, 1563-75.

Reed, L. J. & Muench, H. (1938). A simple method of estimating fifty percent endpoints. *Am J Hyg* **27**, 493-7.

Ren, R. & Racaniello, V. R. (1992). Human poliovirus receptor gene expression and poliovirus tissue tropism in transgenic mice. *J Virol* **66**, 296-304.

Ren, R. B., Costantini, F., Gorgacz, E. J., Lee, J. J. & Racaniello, V. R. (1990). Transgenic mice expressing a human poliovirus receptor: a new model for poliomyelitis. *Cell* **63**, 353-62.

Rice, C. M., Grakoui, A., Galler, R. & Chambers, T. J. (1989). Transcription of infectious yellow fever RNA from full-length cDNA templates produced by in vitro ligation. *New Biol* **1**, 285-96.

Rice, C. M., Levis, R., Strauss, J. H. & Huang, H. V. (1987). Production of infectious RNA transcripts from Sindbis virus cDNA clones: mapping of lethal mutations, rescue of a temperature-sensitive marker, and in vitro mutagenesis to generate defined mutants. *J Virol* **61**, 3809-19.

Richards, O. C. & Ehrenfeld, E. (1998). Effects of poliovirus 3AB protein on 3D polymerase-catalyzed reaction. *J Biol Chem* **273**, 12832-40.

Richards, O. C., Spagnolo, J. F., Lyle, J. M., Vleck, S. E., Kuchta, R. D. & Kirkegaard, K. (2006). Intramolecular and intermolecular uridylylation by poliovirus RNA-dependent RNA polymerase. *J Virol* **80**, 7405-15.

Rieder, E., Paul, A. V., Kim, D. W., van Boom, J. H. & Wimmer, E. (2000). Genetic and biochemical studies of poliovirus cis-acting replication element cre in relation to VPg uridylylation. *J Virol* **74**, 10371-80.

Robbins, F. C., Enders, J. F., Weller, T. H. & Florentino, G. L. (1951). Studies on the cultivation of poliomyelitis viruses in tissue culture. V. The direct isolation and serologic identification of virus strains in tissue culture from patients with nonparalytic and paralytic poliomyelitis. *Am J Hyg* **54**, 286-93.

Rodriguez, P. L. & Carrasco, L. (1993). Poliovirus protein 2C has ATPase and GTPase activities. *J Biol Chem* **268**, 8105-10.

Rodriguez, P. L. & Carrasco, L. (1995). Poliovirus protein 2C contains two regions involved in RNA binding activity. *J Biol Chem* **270**, 10105-12.

Roos, R. P., Griffin, D. E. & Johnson, R. T. (1978). Determinants of measles virus (hamster neurotropic strain) replication in mouse brain. *J Infect Dis* **137**, 722-7.

Rossmann, M. G., Arnold, E., Erickson, J. W., Frankenberger, E. A., Griffith, J. P., Hecht, H. J., Johnson, J. E., Kamer, G., Luo, M., Mosser, A. G. & et al. (1985). Structure of a human common cold virus and functional relationship to other picornaviruses. *Nature* **317**, 145-53.

Rotbart, H. A., McCracken, G. H., Jr., Whitley, R. J., Modlin, J. F., Cascino, M., Shah, S. & Blum, D. (1999). Clinical significance of enteroviruses in serious summer febrile illnesses of children. *Pediatr Infect Dis J* **18**, 869-74.

Sabin, A. B. (1956). Pathogenesis of poliomyelitis; reappraisal in the light of new data. *Science* **123**, 1151-7.

Sambrook, J. & Russell, D. (2000). Molecular Cloning: A Laboratory Manual., Third edn. New York: Cold Spring Harbour Laboratory Press.

Samuda, G. M., Chang, W. K., Yeung, C. Y. & Tang, P. S. (1987). Monoplegia caused by Enterovirus 71: an outbreak in Hong Kong. *Pediatr Infect Dis J* **6**, 206-8.

Sandoval, I. V. & Carrasco, L. (1997). Poliovirus infection and expression of the poliovirus protein 2B provoke the disassembly of the Golgi complex, the organelle target for the antipoliovirus drug Ro-090179. *J Virol* **71**, 4679-93.

Sarnow, P. (1989). Role of 3′-end sequences in infectivity of poliovirus transcripts made in vitro. *J Virol* **63**, 467-70.

Scarpignato, C., Capovilla, T. & Bertaccini, G. (1980). Action of caerulein on gastric emptying of the conscious rat. *Arch Int Pharmacodyn Ther* **246**, 286-94.

Schlegel, A., Giddings, T. H., Jr., Ladinsky, M. S. & Kirkegaard, K. (1996). Cellular origin and ultrastructure of membranes induced during poliovirus infection. *J Virol* **70**, 6576-88.

Schmidt, N. J., Lennette, E. H. & Ho, H. H. (1974). An apparently new enterovirus isolated from patients with disease of the central nervous system. *J Infect Dis* **129**, 304-9.

Schwarz, R., Kasper, A., Seelig, J. & Kunnecke, B. (2002). Gastrointestinal transit times in mice and humans measured with 27Al and 19F nuclear magnetic resonance. *Magn Reson Med* **48**, 255-261.

Sean, P. & Semler, B. L. (2008). Coxsackievirus B RNA replication: lessons from poliovirus. *Curr Top Microbiol Immunol* **323**, 89-121.

Shafren, D. R., Bates, R. C., Agrez, M. V., Herd, R. L., Burns, G. F. & Barry, R. D. (1995). Coxsackieviruses B1, B3, and B5 use decay accelerating factor as a receptor for cell attachment. *J Virol* **69**, 3873-7.

Shafren, D. R., Dorahy, D. J., Ingham, R. A., Burns, G. F. & Barry, R. D. (1997). Coxsackievirus A21 binds to decay-accelerating factor but requires intercellular adhesion molecule 1 for cell entry. *J Virol* **71**, 4736-43.

Shi, P. Y., Tilgner, M., Lo, M. K., Kent, K. A. & Bernard, K. A. (2002). Infectious cDNA clone of the epidemic west nile virus from New York City. *J Virol* **76**, 5847-56.

Shih, S. R., Ho, M. S., Lin, K. H., Wu, S. L., Chen, Y. T., Wu, C. N., Lin, T. Y., Chang, L. Y., Tsao, K. C., Ning, H. C., Chang, P. Y., Jung, S. M., Hsueh, C. & Chang, K. S. (2000). Genetic analysis of enterovirus 71 isolated from fatal and non-fatal cases of hand, foot and mouth disease during an epidemic in Taiwan, 1998. *Virus Res* **68**, 127-36.

Shimizu, H., Utama, A., Onnimala, N., Li, C., Li-Bi, Z., Yu-Jie, M., Pongsuwanna, Y. & Miyamura, T. (2004). Molecular epidemiology of enterovirus 71 infection in the Western Pacific Region. *Pediatr Int* **46**, 231-5.

Shimizu, H., Utama, A., Yoshii, K., Yoshida, H., Yoneyama, T., Sinniah, M., Yusof, M. A., Okuno, Y., Okabe, N., Shih, S. R., Chen, H. Y., Wang, G. R., Kao, C. L., Chang, K. S., Miyamura, T. & Hagiwara, A. (1999). Enterovirus 71 from fatal and nonfatal cases of hand, foot and mouth disease epidemics in Malaysia, Japan and Taiwan in 1997-1998. *Jpn J Infect Dis* **52**, 12-5.

Singh, S., Chow, V. T., Chan, K. P., Ling, A. E. & Poh, C. L. (2000). RT-PCR, nucleotide, amino acid and phylogenetic analyses of enterovirus type 71 strains from Asia. *J Virol Methods* **88**, 193-204.

Singh, S., Chow, V. T., Phoon, M. C., Chan, K. P. & Poh, C. L. (2002). Direct detection of enterovirus 71 (EV71) in clinical specimens from a hand, foot, and mouth disease outbreak in Singapore by reverse transcription-PCR with universal enterovirus and EV71-specific primers. *J Clin Microbiol* **40**, 2823-7.

Skinner, M. A., Racaniello, V. R., Dunn, G., Cooper, J., Minor, P. D. & Almond, J. W. (1989). New model for the secondary structure of the 5′ non-coding RNA of poliovirus is supported by biochemical and genetic data that also show that RNA secondary structure is important in neurovirulence. *Journal of Molecular Biology* **207**, 379-92.

Sriburi, R., Keelapang, P., Duangchinda, T., Pruksakorn, S., Maneekarn, N., Malasit, P. & Sittisombut, N. (2001). Construction of infectious dengue 2 virus cDNA clones using high copy number plasmid. *J Virol Methods* **92**, 71-82.

Suhy, D. A., Giddings, T. H., Jr. & Kirkegaard, K. (2000). Remodeling the endoplasmic reticulum by poliovirus infection and by individual viral proteins: an autophagy-like origin for virus-induced vesicles. *J Virol* **74**, 8953-65.

Sumiyoshi, H., Hoke, C. H. & Trent, D. W. (1992). Infectious Japanese encephalitis virus RNA can be synthesized from in vitro-ligated cDNA templates. *J Virol* **66**, 5425-31.

Svitkin, Y. V., Cammack, N., Minor, P. D. & Almond, J. W. (1990). Translation deficiency of the Sabin type 3 poliovirus genome: association with an attenuating mutation C472U. *Virology* **175**, 103-9.

Takegami, T., Kuhn, R. J., Anderson, C. W. & Wimmer, E. (1983). Membrane-dependent uridylylation of the genome-linked protein VPg of poliovirus. *Proc Natl Acad Sci U S A* **80**, 7447-51.

Takimoto, S., Waldman, E. A., Moreira, R. C., Kok, F., Pinheiro Fde, P., Saes, S. G., Hatch, M., de Souza, D. F., Carmona Rde, C., Shout, D., de Moraes, J. C. & Costa, A. M. (1998). Enterovirus 71 infection and acute neurological disease among children in Brazil (1988-1990). *Trans R Soc Trop Med Hyg* **92**, 25-8.

Tan, E. L., Tan, T. M., Tak Kwong Chow, V. & Poh, C. L. (2007). Inhibition of enterovirus 71 in virus-infected mice by RNA interference. *Mol Ther* **15**, 1931-8.

Tershak, D. R. (1984). Association of poliovirus proteins with the endoplasmic reticulum. *J Virol* **52**, 777-83.

Teterina, N. L., Egger, D., Bienz, K., Brown, D. M., Semler, B. L. & Ehrenfeld, E. (2001). Requirements for assembly of poliovirus replication complexes and negative-strand RNA synthesis. *J Virol* **75**, 3841-50.

Tio, P. H., Jong, W. W. & Cardosa, M. J. (2005). Two dimensional VOPBA reveals laminin receptor (LAMR1) interaction with dengue virus serotypes 1, 2 and 3. *Virol J* **2**, 25.

Todd, S., Towner, J. S., Brown, D. M. & Semler, B. L. (1997). Replication-competent picornaviruses with complete genomic RNA 3′ noncoding region deletions. *J Virol* **71**, 8868-74.

Tosteson, M. T. & Chow, M. (1997). Characterization of the ion channels formed by poliovirus in planar lipid membranes. *J Virol* **71**, 507-11.

Towner, J. S., Ho, T. V. & Semler, B. L. (1996). Determinants of membrane association for poliovirus protein 3AB. *J Biol Chem* **271**, 26810-8.

Toyoda, H., Franco, D., Fujita, K., Paul, A. V. & Wimmer, E. (2007). Replication of poliovirus requires binding of the poly(rC) binding protein to the cloverleaf as well as to the adjacent C-rich spacer sequence between the cloverleaf and the internal ribosomal entry site. *J Virol* **81**, 10017-28.

Toyoda, H., Nicklin, M. J., Murray, M. G., Anderson, C. W., Dunn, J. J., Studier, F. W. & Wimmer, E. (1986). A second virus-encoded proteinase involved in proteolytic processing of poliovirus polyprotein. *Cell* **45**, 761-70.

Triantafilou, K., Fradelizi, D., Wilson, K. & Triantafilou, M. (2002). GRP78, a coreceptor for coxsackievirus A9, interacts with major histocompatibility complex class I molecules which mediate virus internalization. *J Virol* **76**, 633-43.

Triantafilou, M., Triantafilou, K., Wilson, K. M., Takada, Y., Fernandez, N. & Stanway, G. (1999). Involvement of beta2-microglobulin and integrin alphavbeta3 molecules in the coxsackievirus A9 infectious cycle. *J Gen Virol* **80**, 2591-600.

Tsai, H. P., Kuo, P. H., Liu, C. C. & Wang, J. R. (2001). Respiratory viral infections among pediatric inpatients and outpatients in Taiwan from 1997 to 1999. *J Clin Microbiol* **39**, 111-8.

Tu, P. V., Thao, N. T., Perera, D., Huu, T. K., Tien, N. T., Thuong, T. C., How, O. M., Cardosa, M. J. & McMinn, P. C. (2007). Epidemiologic and virologic investigation of hand, foot, and mouth disease, southern Vietnam, 2005. *Emerg Infect Dis* **13**, 1733-41.

van der Werf, S., Bradley, J., Wimmer, E., Studier, F. W. & Dunn, J. J. (1986). Synthesis of infectious poliovirus RNA by purified T7 RNA polymerase. *Proc Natl Acad Sci U S A* **83**, 2330-4.

Van Dyke, T. A. & Flanegan, J. B. (1980). Identification of poliovirus polypeptide P63 as a soluble RNA-dependent RNA polymerase. *J Virol* **35**, 732-40.

van Kuppeveld, F. J., Hoenderop, J. G., Smeets, R. L., Willems, P. H., Dijkman, H. B., Galama, J. M. & Melchers, W. J. (1997). Coxsackievirus protein 2B modifies endoplasmic reticulum membrane and plasma membrane permeability and facilitates virus release. *EMBO J* **16**, 3519-32.

Van Ooij, M. J., Vogt, D. A., Paul, A., Castro, C., Kuijpers, J., van Kuppeveld, F. J., Cameron, C. E., Wimmer, E., Andino, R. & Melchers, W. J. (2006). Structural and functional characterization of the Coxsackievirus B3 CRE(2C): role of CRE(2C) in negative- and positive-strand RNA synthesis. *J Gen Virol* **87**, 103-13.

Vance, L. M., Moscufo, N., Chow, M. & Heinz, B. A. (1997). Poliovirus 2C region functions during encapsidation of viral RNA. *J Virol* **71**, 8759-65.

Wang, J. R., Tuan, Y. C., Tsai, H. P., Yan, J. J., Liu, C. C. & Su, I. J. (2002). Change of major genotype of enterovirus 71 in outbreaks of hand-foot-and-mouth disease in Taiwan between 1998 and 2000. *J Clin Microbiol* **40**, 10-5.

Wang, S. M., Lei, H. Y., Huang, K. J., Wu, J. M., Wang, J. R., Yu, C. K., Su, I. J. & Liu, C. C. (2003). Pathogenesis of enterovirus 71 brainstem encephalitis in pediatric patients: roles of cytokines and cellular immune activation in patients with pulmonary edema. *J Infect Dis* **188**, 564-70.

Wang, S. M., Liu, C. C., Tseng, H. W., Wang, J. R., Huang, C. C., Chen, Y. J., Yang, Y. J., Lin, S. J. & Yeh, T. F. (1999). Clinical spectrum of enterovirus 71 infection in children in southern Taiwan, with an emphasis on neurological complications. *Clin Infect Dis* **29**, 184-90.

Wang, Y. F., Chou, C. T., Lei, H. Y., Liu, C. C., Wang, S. M., Yan, J. J., Su, I. J., Wang, J. R., Yeh, T. M., Chen, S. H. & Yu, C. K. (2004). A mouse-adapted enterovirus 71 strain causes neurological disease in mice after oral infection. *J Virol* **78**, 7916-24.

Wenner, H. A. & Kamitsuka, P. (1957). Primary sites of virus multiplication following intramuscular inoculation of poliomyelitis virus in cynomolgus monkeys. *Virology* **3**, 429-43.

Wessels, E., Notebaart, R. A., Duijsings, D., Lanke, K., Vergeer, B., Melchers, W. J. & van Kuppeveld, F. J. (2006). Structure-function analysis of the coxsackievirus protein 3A: identification of residues important for dimerization, viral rna replication, and transport inhibition. *J Biol Chem* **281**, 28232-43.

WHO (1998). Forty-sixth report World Health Organisation Tech. Rep. Ser. Expert Committee on Biological Standardisation, pp. 1-90. Geneva: WHO.

Wien, M. W., Curry, S., Filman, D. J. & Hogle, J. M. (1997). Structural studies of poliovirus mutants that overcome receptor defects. *Nat Struct Biol* **4**, 666-74.

Wong, K. T., Lum, L. C. & Lam, S. K. (2000). Enterovirus 71 infection and neurologic complications. *N Engl J Med* **342**, 356-8.

Wong, K. T., Munisamy, B., Ong, K. C., Kojima, H., Noriyo, N., Chua, K. B., Ong, B. B. & Nagashima, K. (2008). The distribution of inflammation and virus in human enterovirus 71 encephalomyelitis suggests possible viral spread by neural pathways. *J Neuropathol Exp Neurol* **67**, 162-9.

Wright, A. J. & Phillpotts, R. J. (1998). Humane endpoints are an objective measure of morbidity in Venezuelan encephalomyelitis virus infection of mice. *Arch Virol* **143**, 1155-62.

Wu, C. N., Lin, Y. C., Fann, C., Liao, N. S., Shih, S. R. & Ho, M. S. (2002). Protection against lethal enterovirus 71 infection in newborn mice by passive immunization with subunit VP1 vaccines and inactivated virus. *Vaccine* **20**, 895-904.

Wu, T. C., Wang, Y. F., Lee, Y. P., Wang, J. R., Liu, C. C., Wang, S. M., Lei, H. Y., Su, I. J. & Yu, C. K. (2007). Immunity to avirulent enterovirus 71 and coxsackie A16 virus protects against enterovirus 71 infection in mice. *J Virol* **81**, 10310-5.

Xiang, W., Harris, K. S., Alexander, L. & Wimmer, E. (1995). Interaction between the 5′-terminal cloverleaf and 3AB/3CDpro of poliovirus is essential for RNA replication. *J Virol* **69**, 3658-67.

Yamshchikov, V., Mishin, V. & Cominelli, F. (2001). A new strategy in design of +RNA virus infectious clones enabling their stable propagation in *E. coli*. *Virology* **281**, 272-80.

Yan, J. J., Su, I. J., Chen, P. F., Liu, C. C., Yu, C. K. & Wang, J. R. (2001). Complete genome analysis of enterovirus 71 isolated from an outbreak in Taiwan and rapid identification of enterovirus 71 and coxsackievirus A16 by RT-PCR. *J Med Virol* **65**, 331-9.

Yang, K. D., Yang, M. Y., Li, C. C., Lin, S. F., Chong, M. C., Wang, C. L., Chen, R. F. & Lin, T. Y. (2001). Altered cellular but not humoral reactions in children with complicated enterovirus 71 infections in Taiwan. *J Infect Dis* **183**, 850-6.

Yin, J., Paul, A. V., Wimmer, E. & Rieder, E. (2003). Functional dissection of a poliovirus cis-acting replication element [PV-cre(2C)]: analysis of single- and dual-cre viral genomes and proteins that bind specifically to PV-cre RNA. *J Virol* **77**, 5152-66.

Yu, C. K., Chen, C. C., Chen, C. L., Wang, J. R., Liu, C. C., Yan, J. J. & Su, I. J. (2000). Neutralizing antibody provided protection against enterovirus type 71 lethal challenge in neonatal mice. *J Biomed Sci* **7**, 523-8.

Yun, S. I., Kim, S. Y., Rice, C. M. & Lee, Y. M. (2003). Development and application of a reverse genetics system for Japanese encephalitis virus. *J Virol* **77**, 6450-65.

Zeichhardt, H., Otto, M. J., McKinlay, M. A., Willingmann, P. & Habermehl, K. O. (1987). Inhibition of poliovirus uncoating by disoxaril (WIN 51711). *Virology* **160**, 281-5.

Zeichhardt, H., Wetz, K., Willingmann, P. & Habermehl, K. O. (1985). Entry of poliovirus type 1 and Mouse Elberfeld (ME) virus into HEp-2 cells: receptor-mediated endocytosis and endosomal or lysosomal uncoating. *J Gen Virol* **66**, 483-92.

Zell, R., Sidigi, K., Bucci, E., Stelzner, A. & Gorlach, M. (2002). Determinants of the recognition of enteroviral cloverleaf RNA by coxsackievirus B3 proteinase 3C. *RNA* **8**, 188-201.

Zuker, M. (2003). Mfold web server for nucleic acid folding and hybridization prediction. *Nucleic Acids Res* **31**, 3406-15.

APPENDIX

Full length sequence HEV71-6F (DQ381846)

TTAAAACAGCCTGTGGGTTGCACCCACCCACAGGGCCTACTGGGCGCTAGCACTCTGGCACTGAGGTACC
TTTGTGCGCCTGTTTTGACTTCCCTTCCCCGAAGTAACTTAGAAGCTGTAAATCAACGATCAATAGTAGG
TGTGACACACCAGTCATATCTTGATCAAGCACTTCTGTTTCCCCGGACTGAGTATCAATAGGCTGCTCGC
GCGGCTGAAGGAGAAAACGTTCGTTACCCGACCAACTACTTCGAGAAGCTTAGTACCACCATGAACGAGG
CAGAGTGTTTCGTTCAGCACAACCCCAGTGTAGATCAGGCTGATGAGCCACTGCAACCCCCATGGGCGAC
CATGGCAGTGGCTGCGTTGGCGGCCTGCCCATGGAGAAATCCATGGGACGCTCTAATTCTGACATGGTGT
GAAGAGCCTATTGAGCTAGCTGGTAGTCCTCCGGCCCCTGAATGCGGCTAATCCTAACTGCGGAGCACAT
GCTCACAAACCAGTGGGTGGTGTGTCGTAACGGGCAACTCTGCAGCGGAACCGACTACTTTGGGTGTCCG
TGTTTCCTTTTATTCTTATATTGGCTGCTTATGGTGACAATCAAAGAATTGTTACCATATAGCTATTGGA
TTGGCCATCCGGTGTGCAACAGAGCAATTGTTTACCTATTTATTGGTTTTGTACCATTATCACTGAAGTC
TGTGATCACTCTCAAATTCATTTTGACCCTCAACACAACCAAATATGGGCTCACAGGTGTCCACACAACG
CTCCGGTTCGCATGAAAACTCTAACTCAGCTACCGAGGGTTCCACTATAAATTATACTACCATTAATTAC
TATAAAGACTCCTATGCCGCCACAGCAGGTAAACAGAGTCTCAAGCAAGACCCAGACAAGTTTGCAAATC
CCGTCAAAGACATCTTCACTGAAATGGCGGCGCCATTAAAATCTCCATCCGCTGAGGCATGTGGTTACAG
CGATCGGGTAGCACAATTAACTATTGGCAACTCTACCATCACTACACAAGAAGCAGCAAACATCATAGTT
GGCTATGGTGAGTGGCCTTCCTACTGCTCGGATTCTGACGCTACAGCGGTGGACAAACCAACGCGCCCAG
ATGTTTCGGTGAATAGGTTTTACACATTGGACACTAAACTGTGGGAGAAATCATCCAAGGGGTGGTACTG
GAAATTCCCGGATGTGTTAACTGAAACCGGGGTCTTTGGTCAAAATGCGCAGTTCCACTACCTCTATCGG
TCAGGGTTCTGCATTCACGTGCAGTGCAATGCTAGTAAGTTCCACCAAGGAGCACTCCTAGTCGCTGTCC
TCCCAGAGTATGTCATTGGGACAGTAGCAGGTGGCACAGGGACGGAGGATAGCCACCCTCCTTACAAGCA
GACTCAACCCGGTGCTGATGGCTTCGAGCTGCAACACCCGTACGTGCTTGATGCTGGCGTTCCAATATCA
CAATTAACAGTGTGCCCACATCAGTGGATTAATTTGAGGACTAACAATTGTGCCACAATAATAGTACCGT
ACATAAACGCACTACCCTTTGATTCTGCCTTGAACCATTGTAACTTTGGTCTGCTGGTTGTGCCTATTAG
CCCGTTAGATTATGACCAAGGTGCGACGCCAGTGATCCCCATTACTATCACCCTGGCCCCAATGTGTTCT
GAATTTGCAGGCCTTAGACAAGCAGTTACGCAAGGGTTTCCTACTGAGCTGAAACCTGGCACAAACCAAT
TTTTAACCACTGACGATGGCGTCTCAGCACCCATTCTGCCAAACTTCCACCCCACCCCGTGTATCCATAT
ACCCGGTGAAGTTAGAAACTTGCTAGAGCTATGCCAGGTGGAGACCATTTTAGAGGTCAACAATGTACCC
ACGAATGCCACTAGCTTAATGGAGAGATTGCGCTTCCCGGTCTCAGCCCAAGCCGGAAAAGGTGAATTAT
GTGCAGTGTTCAGAGCTGACCCCGGGCGAAGTGGACCATGGCAGTCCACCTTGTTGGGCCAGTTGTGCGG
GTACTACACCCAATGGTCAGGATCACTGGAAGTCACCTTCATGTTCACTGGGTCCTTTATGGCTACCGGC
AAGATGCTCATAGCATACACACCACCAGGAGGTCCCTTACCCAAGGACCGGGCGACCGCCATGTTGGGTA
CGCACGTCATCTGGGACTTTGGGCTGCAATCGTCTGTCACCCTTGTAATACCATGGATCAGCAACACTCA
CTACAGAGCGCACGCTCGAGATGGTGTGTTTGACTACTACACTACAGGTTTGGTTAGCATATGGTACCAG
ACGAATTACGTGGTTCCAATTGGGGCACCCAATACAGCCTATATAATAGCATTGGCGGCAGCCCAGAAGA
ATTTCACCATGAAGTTGTGCAAGGATGCTAGTGATATCCTACAGACAGGCACTATCCAGGGAGATAGGGT
GGCAGATGTGATTGAGAGTTCTATAGGGGACAGTGTGAGCAGAGCCCTCACCCGAGCTCTACCGGCACCT
ACAGGTCAAGATACGCAGGTAAGTAGCCATCGATTGGATACTGGTAAAGTTCCAGCACTCCAAGCCGCTG
AAATTGGAGCATCATCAAATGCTAGTGATGAGAGCATGATTGAGACGCGATGTGTTCTTAATTCACATAG
CACAGCTGAGACCACTCTTGATAGCTTCTTCAGCAGAGCAGGATTAGTTGGAGAGATAGACCTTCCTCTT
AAAGGCACAACCAACCCGAATGGGTATGCAAACTGGGACATAGACATAACAGGTTACGCGCAAATGCGTA
GAAAGGTGGAGTTGTTCACCTACATGCGTTTTGACGCAGAGTTCACCTTTGTTGCATGCACGCCTACCGG
GGAAGTTGTCCCGCAATTGCTCCAGTATATGTTTGTACCACCCGGAGCCCCCAAACCAGACTCCAGAGAA
TCTCTCGTATGGCAGACTGCCACTAATCCCTCAGTCTTTGTGAAGCTGTCAGACCCCCCAGCACAGGTTT
CAGTACCATTCATGTCACCTGCAAGCGCCTATCAATGGTTCTATGACGGGTATCCCACATTCGGTGAACA
CAAGCAGGAGAAAGACCTTGAATACGGGGCATGCCCAAATAACATGATGGGTACGTTTTCAGTGCGGACT
GTAGGAACCTCGAAGTCCAAGTACCCATTGGTGATCAGGATTTACATGAGGATGAAGCATGTCAGGGCGT
GGATACCTCGCCCAATGCGCAACCAAAACTATCTATTCAAAGCCAACCCAAATTATGCTGGCAACTCCAT
TAAACCAACTGGTGCCAGTCGCACAGCTATCACCACCCTCGGGAAATTTGGACAACAGTCCGGGGCCATC
TACGTGGGCAACTTCAGAGTGGTCAACCGCCATCTTGCTACTCATAACGACTGGGCAAACCTTGTTTGGG
AGGACAGCTCCCGCGATTTGCTCGTATCATCTACCACTGCCCAAGGTTGTGACACAATTGCTCGTTGCAA
TTGCCAGACAGGAGTGTACTATTGTAACTCAATGAGAAAACACTATCCTGTCAGTTTCTCGAAACCCAGC
TTGATCTTCGTAGAGGCCAGTGAGTATTACCCGGCTAGATACCAGTCACACCTCATGCTTGCAGTGGGTC
ACTCAGAACCAGGGGATTGCGGTGGCATTCTTAGATGCCAACACGGCGTCGTAGGGATAGTTTCCACCGG
GGGAAACGGCCTGGTGGGATTCGCCGATGTGAGGGATCTTCTGTGGTTGGATGATGAGGCTATGGAGCAG
GGCGTGTCTGATTACATCAAAGGGCTTGGAGATGCTTTTGGCATGGGGTTTACAGACGCAGTGTCAAGAG
AAGTTGAAGCATTAAAAAATCACTTGATCGGCTCAGAGGGTGCCGTGGAGAAGATTCTTAAGAACTTAGT
CAAACTCATCTCTGCGCTCGTCATTGTCATCAGGAGTGATTATGACATGGTCACATTAACGGCAACACTT
GCCCTGATCGGGTGCCACGGGAGCCCTTGGGCCTGGGTTAAATCGAAGACAGCATCAATTTTGGGCATAC
CGATGGCTCAGAAGCAGAGTGCCTCTTGGTTAAAGAAGTTCAACGATGCGGCGAGTGCCGCTAAGGGGCT

TGAGTGGATCTCCAACAAAATCAGCAAATTTATCGATTGGCTCAAGGAGAAAATCATTCCGGCTGCTAAA
GAGAAAGTCGAGTTTCTAAACAATCTAAAGCAACTCCCCTTATTGGAGAACCAAATTTCCAATCTCGAAC
AGTCAGCAGCTTCGCAGGAGGACCTTGAAGCGATGTTTGGCAACGTGTCTTATCTGGCCCACTTCTGCCG
CAAATTCCAACCCCTCTATGCCACAGAAGCGAAGAGGGTGTACGCCCTAGAAAAGAGAATGAATAATTAC
ATGCAGTTCAAGAGCAAACACCGTATTGAACCTGTATGCCTAATCATTAGAGGCTCGCCTGGTACTGGGA
AGTCCTTGGCAACAGGGATTATTGCTAGAGCTATAGCAGACAAGTACCACTCCAGTGTGTATTCCTTACC
TCCGGACCCAGACCACTTTGACGGATACAAACAACAGATCGTCACTGTTATGGACGACCTATGCCAAAAC
CCAGACGGGAAAGACATGTCACTATTTTGTCAGATGGTCTCCACAGTGGATTTTATACCGCCTATGGCAT
CTCTGGAGGAGAAGGGAGTCTCATTTACCTCCAAGTTTGTGATCGCCTCCACAAACGCCAGTAACATCAT
AGTGCCAACAGTCTCGGATTCAGATGCCATCCGTCGTCGGTTCTTTATGGACTGTGATATTGAGGTAACT
GATTCCTATAAGACAGAGCTGGGCAGGCTTGATGCAGGGAGAGCAGCTAGGCTGTGCTCTGAGAACAACA
CTGCTAACTTTAAACGGTGCAGTCCATTGGTCTGTGGGAAAGCAATCCAGCTTAGGGATAGGAAGTCCAA
GGTGAGATACAGTGTGGACACGGTAGTGAGTGAGCTTGTCAGGGAGTATAACAACAGATCAGTTATTGGG
AACACCATTGAAGCTCTTTTCCAAGGGCCCCCTAAATTTAGACCGATAAGGATTAGCCTAGAGGAGAAGC
CCGCACCTGATGCTATTAGTGACCTATTAGCTAGTGTCGATAGTGAAGAGGTTCGCCAATACTGTAGAGA
TCAGGGATGGATTGTACCTGACTCTCCCACCAACGTTGAGCGCCACTTAAACAGAGCTGTCTTGATTATG
CAATCTGTAGCCACCGTGGTAGCGGTTGTGTCCCTTGTTTACGTTATCTACAAGTTGTTCGCCGGTTTTC
AAGGAGCATACTCCGGCGCCCCCAAGCAAACACTCAAGAAACCAGTGCTGCGCACGGCAACTGTGCAGGG
GCCGAGCTTGGACTTCGCCCTATCTCTACTTAGGAGGAACATTAGGCAGGTCCAAACCGACCAGGGCCAC
TTTACAATGTTAGGAGTGCGAGACCATTTGGCTGTGCTCCCCAGGCACTCCCAACCAGGAAAGACCATCT
GGGTTGAACACAAGTTAGTGAAGGTCGTAGATGCTGTGGAGCTAGTAGATGAACAAGGGGTTAACCTAGA
GCTCACACTGGTAACGCTTGACACCAACGAAAAATTTAGAGACATCACAAGATTCATACCAGAAACAATT
AGTCCTGCTAGTGATGCCACTTTAGTTATAAATACTGAACATATGCCCAGTATGTTTGTGCCAGTTGGAG
ATGTGGTCCAGTATGGATTTTTGAACCTTAGTGGTAAGCCCACTCACAGGACTATGATGTACAATTTTCC
AACAAAAGCAGGACAGTGTGGTGGAGTTGTGACTGCCGTGGGTAAGGTGATTGGGATCCACATTGGTGGC
AACGGTAGGCAAGGTTTCTGCGCTGCCCTGAAGAGGGGATACTTTTGCAGTGAACAAGGTGAGATCCAAT
GGATGAAGCCCAACAAAGAAACTGGCAGGTTGAACATCAACGGACCTACTCGCACTAAGCTTGAACCAAG
TGTCTTTCACGATGTGTTCGAGGGCACTAAAGAGCCAGCAGTGCTGACTAGTAAAGACCCAAGGCTGGAA
GTTGACTTTGAACAGGCTCTTTTTTCAAAATACGTGGGAAACACGCTTCATGAACCCGACGAGTTTGTCA
AGGAGGCGGCCTTACATTATGCCAACCAACTCAAGCAGTTAGATATTAAGACCACCAAGATGAGCATGGA
GGATGCTTGTTACGGTACAGAGAACCTGGAAGCTATAGATCTTCACACAAGTGCAGGATATCCATATAGT
GCACTAGGCATCAAGAAAAGGGATATTTTGGACCCAACAACTCGTGATGTCAGCAAAATGAAATCCTACA
TGGACAAGTATGGGTTGGATCTACCGTACTCTACTTATGTTAAAGATGAACTCAGGGCCATCGACAAGAT
CAAGAAAGGAAAGTCTCGTCTCATAGAAGCAAGCAGTCTAAATGACTCAGTGTACTTGAGAATGACATTT
GGGCACCTTTATGAAGCCTTTCACGCCAATCCAGGTACAGTCACTGGTTCAGCTGTTGGATGCAACCCAG
ATGTGTTCTGGAGTAAGTTACCAATTCTACTTCCAGGATCGCTTTTTGCGTTTGACTACTCGGGGTATGA
CGCTAGTCTCAGCCCAGTGTGGTTCAGGGCGCTGGAGATAGTCCTGCGGGAAATTGGATACTCTGAGGAC
GCACTGTCTCTCATAGAAGGGATCAATCATACCCACCATGTGTACCGCAATAAAACTTATTGTGTTCTTG
GGGGAATGCCCTCAGGTTGCTCAGGCACCTCCATTTTCAACTCGATGATCAACAACATTATTATTAGGAC
ACTCCTGATTAAAACATTCAAAGGGATAGATCTAGATGAATTGAACATGGTGGCCTACGGGGATGATGTG
TTGGCTAGTTACCCCTTCCCAATTGACTGTCTAGAATTGGCGAGAACAGGCAAGGAGTATGGTTTAACTA
TGACCCCTGCCGACAAGTCACCCTGCTTTAATGAAGTCACATGGGAGAATGCCACTTTCTTGAAGAGAGG
ATTCTTGCCTGATCATCAATTCCCGTTCCTCATCCACCCTACGATGCCAATGAGGGAGATTCACGAGTCC
ATTCGTTGGACCAAAGATGCACGAAGTACCCAAGATCATGTGCGCTCCCTCTGCTTATTAGCATGGCACA
ACGGGAAAGAGGAGTATGAAAAATTTGTGAGTACAATCAGATCAGTTCCAATTGGAAAAGCATTGGCTAT
ACCAAATTTTGAGAACCTGAGAAGAAATTGGCTCGAATTGTTTTAAATTTACAGTTCATAACTGAACCCC
ACCAGTAATCTGGTCGTGTTAATGACTGGTGGGGGTAAATTTGTTATAACCAGAATAGC

Full length sequence of HEV71-26M (EU364841)

TTAAAACAGCCTGTGGGTTGCACCCACTCACAGGGCCCACGTGGCGCTAGCACTCTGATTCTACGGAATC
TTTGTGCGCCTGTTTTACAACCCCCCCCCAATTTGCAACTTAGAAGCAATACACAACACTGATCAACAGC
AGGCATGGCGCACCAGCCATGTCTTGATCAAGCACTTCTGTTTCCCCGGACTGAGTATCAATAGACTGCT
CACGCGGTTGAAGGAGAAAGCGTCCGTTATCCGGCTAACTACTTCGAGAAACCTAGTAGCACCATTGAAG
CTGCGGAGTGTTTCGCTCGGCACTTCCCCCGTGTAGATCAGGCCGATGAGTCACTGCAATCCCCACGGGC
GACCGTGGCAGTGGCTGCGCTGGCGGCCTGCCTATGGGGCAACCCATAGGACGCTCTAATGTGGACATGG
TGCGAAGAGTCTATTGAGCTAGTTAGTAGTCCTCCGGCCCCTGAATGCGGCTAATCCTAACTGCGGAGCA
CATGCCCTCAACCCAGAGGGTAGTGTGTCGTAACGGGCAACTCTGCAGCGGAACCGACTACTTTGGGTGT
CCGTGTTTCCTTTTATTCTTACATTGGCTGCTTATGGTGACAATCACAGAATTGTTACCATATAGCTATT
GGATTGGCCATCCGGTGTGCAATAGAGCTATTATACACCTATTTGTTGGCTTTGTACCACTAACCTTAAA
ATCTATAACCACCCTCAACTTTATATTAACTCTCAATACAGTCAAACATGGGCTCACAAGTGTCTACTCA
GCGATCCGGCTCCCACGAGAACTCCAATTCAGCTACGGAAGGCTCTACCATTAATTACACTACCATCAAC
TATTACAAAGACTCCTATGCTGCAACAGCAGGCAAACAGAGCCTCAAACAAGACCCTGATAAGTTTGCTA
ACCCTGTCAAGGATATTTTCACTGAAATGGCTGCGCCACTGAAGTCTCCATCCGCTGAAGCTTGTGGTTA
TAGTGATCGTGTGGCACAACTCACCATTGGAAACTCCACCATTACTACACAGGAGGCGGCAAACATCATA
GTCGGTTATGGTGAGTGGCCCTCATATTGCTCTGATGACGATGCTACAGCGGTGGATAAACCAACGCGCC
CAGATGTGTCAGTGAATAGGTTTTATACATTGGACACCAAACTGTGGGAAAAATCATCTAAGGGGTGGTA
TTGGAAGTTTCCTGATGTTTTGACTGAGACCGGAGTCTTTGGCCAGAACGCACAGTTTCACTATTTATAT
AGATCAGGGTTTTGCATTCATGTGCAATGTAATGCTAGCAAGTTCCATCAAGGAGCGCTGTTAGTCGCTA
TTCTTCCAGAGTATGTTATAGGGACAGTGGCAGGCGGCACAGGTACAGAGGACAGCCACCCTCCTTACAA
ACAAACGCAACCTGGCGCTGATGGTTTTGAGCTGCAGCACCCGTACGTGCTCGATGCTGGGATTCCTATA
TCACAACTGACGGTGTGCCCCCATCAATGGATTAATCTGCGGACCAATAACTGTGCCACGATAATAGTGC
CATATATGAACACACTGCCTTTCGACTCTGCCCTGAACCATTGCAATTTTGGGCTGTTGGTAGTGCCCAT
TAGCCCATTAGATTTTGACCAAGGGGCAACTCCGGTTATCCCTATTACAATCACTCTAGCTCCAATGTGC
TCTGAGTTTGCAGGTCTCAGACAGGCAGTCACTCAAGGCTTCCCTACTGAGCCAAAACCAGGAACAAATC
AATTTTTGACCACCGATGACGGCGTCTCAGCACCCATTCTACCAAATTTCCACCCCACTCCATGTATTCA
CATACCCGGTGAAGTCAGAAACCTGCTTGAGTTGTGTCAAGTGGAGACTATTCTTGAGGTTAACAACGTA
CCCACCAATGATACCAGTTTGATGGAAAGGCTACGATTCCCAGTGTCTGCGCAAGCGGGGAAAGGTGAAT
TGTGTGCCGTGTTTAGGGCCGACCCTGGAAGGGACGGTCCATGGCAATCAACAATGCTGGGCCAGCTGTG
TGGATACTACACCCAGTGGTCAGGGTCACTGGAGGTCACTTTTATGTTTACCGGGTCTTTTATGGCCACG
GGTAAAATGCTCATAGCCTATACACCTCCTGGTGGCCCCTTACCTAAAGACCGGGCCACAGCAATGCTGG
GCACGCATGTTATCTGGGATTTTGGGTTACAATCATCTGTCACCCTTGTGATACCATGGATCAGTAACAC
CCACTACAGAGCGCATGCCCGGGACGGAGTGTTCGATTACTATACCACAGGACTGGTCAGTATCTGGTAT
CAAACAAACTACGTAGTTCCAATTGGGGCACCCAATACAGCTTACATAATAGCACTAGCGGCAGCCCAGA
AGAACTTTACCATGAAACTGTGCAAAGACACTAGTCACATATTACAGACAGCCTCCATTCAGGGAGATAG
GGTGGCAGATGTGATCGAGAGCTCTATAGGAGATAGTGTGAGTAGAGCACTTACCCAGGCCCTGCCAGCA
CCCACAGGTCAAAACACACAGGTGAGCAGTCATCGACTAGACACTGGCGAAGTTCCAGCGCTTCAAGCTG
CTGAAATTGGGGCATCGTCAAATACTAGTGATGAGAGTATGATTGAAACACGGTGCGTTCTTAACTCACA
CAGCACAGCAGAAACCACCTTGGATAGCTTCTTCAGTAGGGCAGGTTTGGTAGGGGAGATAGATCTCCCT
CTTGAGGGTACTACTAATCCGAATGGTTATGCCAACTGGGATATAGACATAACTGGTTACGCACAGATGC
GCAGGAAAGTGGAGTTGTTCACCTACATGCGCTTTGATGCGGAATTCACTTTTGTTGCGTGCACTCCCAC
CGGCGGGGTTGTTCCACAATTACTCCAGTATATGTTTGTTCCCCCTGGTGCTCCCAAACCAGAATCTAGA
GAATCACTTGCTTGGCAAACAGCCACAAACCCCTCAGTTTTTGTCAAGTTGACTGATCCCCCAGCACAGG
TCTCAGTTCCATTCATGTCACCTGCGAGCGCTTACCAGTGGTTTTACGACGGGTACCCCACGTTTGGAGA
ACATAAACAGGAGAAAGACCTTGAATATGGAGCGTGTCCTAATAACATGATGGGCACTTTCTCGGTGCGA
AATGTGGGGTCATCAAAGTCCAAGTACCCTCTGGTTGTCAGAATATATATGAGAATGAAGCATGTCAGGG
CATGGATACCTCGCCCGATGCGCAACCAAAACTACTTGTTCAAAGCCAATCCGAACTACGCTGGCAACTC
CATTAAGCCGACCGGCACTAGCCGTACTGCCATTACTACCCTTGGAAAGTTCGGCCAGCAATCTGGGGCC
ATCTACGTGGGCAACTTCAGAGTGGTTAATCGTCACCTCGCTACTCATAATGACTGGGCGAATCTCGTCT
GGGAAGACAGCTCCCGCGACCTACTAGTGTCGTCTACCACTGCCCAGGGCTGTGATACAATTGCACGTTG
TGACTGTCAAACAGGAGTGTACTATTGTAATTCTAAGAGAAAGCACTATCCAGTCAGCTTCTCTAAACCT
AGCCTCATTTATGTGGAAGCTAGCGAGTATTACCCTGCTAGATACCAGTCTCATCTCATGCTTGCGGCGG
GCCATTCTGAACCAGGAGATTGTGGTGGCATCCTTAGGTGCCAGCACGGTGTTGTCGGCATTGTGTCCAC
TGGTGGCAATGGGCTTGTTGGCTTTGCAGATGTCAGGGATCTCCTATGGTTGGATGAAGAAGCAATGGAG
CAGGGTGTGTCCGACTACATTAAGGGACTTGGTGATGCGTTTGGAACTGGCTTCACCGATGCAGTTTCCA
GAGAAGTTGAGGCTCTTAAGAACCACCTTATTGGGTCTGAGGGAGCTGTCGAGAAGATCCTAAAGAATTT
GATCAAATTAATCTCTGCTTTAGTCATCGTGATTAGGAGTGATTATGACATGGTCACTCTCACAGCAACT
TTAGCTCTGATAGGGTGCCACGGTAGTCCCTGGGCATGGATTAAAGCAAAAACAGCTTCCATTCTAGGCA
TCCCTATTGCCCAGAAGCAAAGTGCGTCCTGGCTTAAAAAGTTTAACGATATGGCCAACGCCGCCAAGGG
GTTAGAGTGGATCTCCAGTAAGATTAGTAAATTCATCGATTGGCTCAAAGAGAAAATCATACCAGCGGCT
AGGGAGAAGGTGGAGTTTCTGAACAACTTAAAACAGTTGCCGTTGTTGGAGAATCAGATCTCAAATCTAG
AGCAGTCTGCTGCTTCACAAGAAGATCTTGAAGCCATGTTCGGAAATGTGTCGTACCTAGCTCACTTCTG
CCGCAAATTCCAACCACTGTACGCTACAGAAGCCAAAAGGGTCTATGCTTTGGAGAAAAGAATGAACAAC

TACATGCAGTTCAAGAGCAAACACCGAATTGAACCTGTATGTCTTATTATTAGGGGTTCTCCGGGCACCG
GGAAATCACTAGCAACTGGCATCATTGCTCGGGCAATAGCAGACAAGTATCACTCAAGTGTGTACTCACT
CCCACCAGACCCGGATCACTTTGATGGATACAAACAGCAGGTGGTCACGGTCATGGATGACTTATGTCAG
AATCCTGATGGCAAAGATATGTCATTGTTCTGCCAGATGGTGTCCACAGTGGATTTCATCCCACCAATGG
CTTCCCTAGAAGAGAAAGGAGTTTCTTTCACATCTAAATTTGTCATTGCATCTACCAATTCCAGCAACAT
CATAGTACCAACAGTGTCTGATTCTGATGCAATTCGCCGTAGGTTCTATATGGATTGTGATATCGAAGTC
ACGGATTCATATAAAACGGACTTGGGTAGGTTAGATGCTGGGCGAGCCGCCAAATTGTGCTCTGAGAATA
ACACAGCAAATTTCAAGCGTTGTAGCCCACTAGTGTGTGGGAAGGCCATTCAGCTGAGAGATAGAAAGTC
CAAGGTCAGGTACAGTGTGGACACGGTGGTTTCTGAGCTCATAAGGGAATACAACAACAGGTCTGCTATT
GGTAACACAATTGAAGCACTATTCCAAGGTCCGCCTAAGTTTAGACCCATAAGGATCAGTCTTGAAGAAA
AGCCAGCCCCAGACGCCATTAGTGACCTTCTTGCTAGTGTGGATAGCGAGGAGGTACGCCAGTACTGTAG
AGATCAAGGTTGGATCATACCAGAGACTCCTACAAATGTTGAACGGCACCTCAACAGAGCTGTGCTAGTC
ATGCAATCCATCGCTACAGTTGTGGCAGTCGTTTCACTGGTGTATGTCATCTACAAGCTCTTCGCTGGAT
TCCAAGGCGCGTACTCTGGTGCTCCCAAGCAGATACTTAAGAAACCCGTTCTCCGCACGGCAACAGTACA
GGGTCCAAGTCTCGATTTCGCTCTGTCTCTACTGAGGAGGAATATCAGGCAAGTGCAAACAGATCAAGGA
CATTTCACCATGCTGGGTGTCAGGGACCGTTTGGCTGTTCTTCCACGCCACTCCCAGCCCGGCAAAACAA
TCTGGGTAGAGCACAAACTCGTAAACATTCTGGACGCTGTTGAACTGGTGGATGAACAAGGGGTTAATTT
GGAGCTAACCCTAATCACCCTTGACACTAATGAGAAATTCAGAGACATTACTAAGTTCATCCCAGAGAGC
ATCAGCGCTGCAAGCGATGCTACCCTAGTGATCAACACAGAGCACATGCCCTCAATGTTTGTGCCGGTGG
GAGACGTTGTGCAATATGGTTTTCTCAACCTCAGTGGAAAGCCAACCCACCGTACCATGATGTACAACTT
TCCCACCAAGGCAGGGCAGTGTGGAGGGGTGGTGACATCAGTTGGAAAGGTCATTGGTATACACATAGGT
GGTAACGGCAGACAAGGTTTCTGTGCGGGACTTAAGAGGAGCTACTTCGCCAGCGAGCAAGGAGAGATCC
AGTGGGTCAAGCCCAATAAAGAAACTGGGAGACTCAACATCAATGGGCCAACTCGCACTAAGCTCGAACC
CAGTGTATTTCATGATGTTTTTGAGGGAAACAAGGAGCCAGCAGTTCTACACAGTAAAGATCCCCGCCTC
GAGGTGGATTTTGAGCAGGCTTTGTTCTCCAAGTACGTAGGGAATACACTATATGAGCCTGATGAGTACA
TTAAGGAGGCAGCTCTTCACTATGCAAATCAGTTGAAACAGCTAGACATTGACACCTCCCAGATGAGCAT
GGAGGAAGCCTGTTACGGCACTGAGAACCTTGAGGCCATTGACCTTCACACTAGTGCAGGCTACCCATAC
AGTGCTCTAGGAATAAAGAAAAGAGACATCCTAGATTCTACTACTAGGGATGTGAGCAAGATGAAATTTT
ATATGGACAAGTATGGCTTGGACCTTCCCTACTCCACCTATGTCAAGGATGAGCTACGCTCGATAGATAA
GATCAAGAAGGGGAAGTCTCGTTTGATTGAAGCCAGCAGCTTAAATGATTCTGTGTACCTTAGGATGACT
TTTGGGCACCTTTATGAAACCTTCCATGCAAACCCTGGAACTGTGACCGGCTCGGCCGTGGGATGCAATC
CGGATACATTCTGGAGTAAACTACCCATCTTACTCCCTGGCTCACTCTTTGCTTTCGACTATTCAGGATA
TGATGCTAGTCTTAGCCCTGTCTGGTTCAGAGCATTGGAATTAGTTCTTAGGGAAATAGGCTACAGTGAG
GAAGCAGTTTCACTTGTTGAGGGGATCAATCACACACACCATGTATACCGCAACAAAACTTACTGTGTGC
TTGGTGGCATGCCCTCTGGTTGCTCAGGAACATCCATATTCAATTCAATGATCAATAACATTATTATTAG
AGCACTGCTCATCAAAACGTTCAAGGGCATTGATTTAGACGAGCTCAACATGGTTGCCTACGGGGATGAT
GTGCTTGCCAGTTACCCTTTTCCAATTGACTGTTTGGAGTTGGCAAGAACGGGCAAGGAGTACGGTTTAA
CCATGACTCCTGCAGACAAATCCCCATGCTTCAATGAAGTCAATTGGGATAACGCAACCTTTCTCAAAAG
AGGCTTCTTGCCCGATGAACAATTTCCATTCCTTATCCACCCTACCATGCCAATGAAAGAAATCCACGAG
TCCATACGGTGGACCAAGGACGCGCGAAATACCCAAGATCACGTGCGGTCCTTGTGCCTTCTGGCATGGC
ACAATGGTAAACAGGAATATGAAAAGTTTGTGAGCGCAATTAGATCAGTACCAGTAGGAAAAGCATTGGC
TATTCCAAATTATGAGAATCTGAGACGCAATTGGCTCGAACTATTCTAGAGGTTAAGTATATACCTCAAC
CCCACCAGGAATCTGGTCGTGAACATGACTGGTGGGGGTAAATTTGTTATAACCAGAATAGC